

Cardiff School of Pharmacy and Pharmaceutical Sciences, Cardiff University



# Emulsion assisted nonsteroidal anti-inflammatory drug delivery system for the osteoarthritis treatment

A thesis submitted in accordance with the conditions governing candidates for the degree of

Doctor of philosophy in Cardiff University

Tahani Saeedi

Supervisors:

Dr. Polina Prokopovich

July 2023

## **Acknowledgements**

Thanks God Almighty for good health, peace of mind and the strength to finish this research despite the difficult situations.

I would like to express my deep sincere gratitude to my supervisor Dr Polina Prokopovich for giving me the opportunity to do the research and for her continuous support, guidance, teaching, enthusiasm and endless help throughout my PhD journey. The completion of this thesis could not have been possible without her valuable experience and support.

I am thankful to Taibah university (Saudi Arabia) for supporting this research. Without funding, this project with not be possible.

Big thanks to my mum (Hayat Laz), my husband (Sultan), my children (Layan, Khalid and Lolia), my sisters and my brother for their love, prayers, caring, patience, unconditional support, and encouragement in completing this research work.

I will never forget to thank my dad (Ali), who passed away, for his kindness, help, and support in joining the pharmacy school. He was proud of me and gave me the power to complete my studies and achieve my dream.

Finally, many thanks to my lab colleagues, all the members of Cardiff University, and all my family and friends who helped and encouraged me all the time. Also, I would like to thank the technical staff at the school of bioscience for providing the expertise and help with equipment used in this study.

## PhD output

1. Published first paper ‘‘ Saeedi, T. Alotaibi, H. and Prokopovich, P. (2020) ‘Polymer colloids as drug delivery systems for the treatment of arthritis’, *Advances in Colloid and Interface Science*, 285:102273. doi: 10.1016/j.cis.2020.102273.
2. Presented in 1<sup>st</sup> Eurasian International Workshop on Antimicrobial and Biosensing Nanotechnologies conference on 15th May 2021 at Nazarbayev University. Talk title ‘‘Emulsion assisted non-steroidal drug delivery system for osteoarthritis treatment’.
3. Published second paper ‘‘ Saeedi, T. and Prokopovich, P. (2021) ‘Poly beta amino ester coated emulsions of NSAIDs for cartilage treatment’, *Journal of Materials Chemistry B*, 9(29), pp. 5837-5847. doi: 10.1039/d1tb01024g.

## Abstract

Osteoarthritis (OA) is one of the considerable chronic health conditions worldwide. In the UK, 8.75 million people were receiving OA treatment. Currently, there are no disease-modifying drugs, and treatment relies on the management of pain associated with OA. The delivery of OA drugs is challenging because the cartilage is dense, avascular (i.e., has no blood vessels), and relies on diffusion to transport nutrients and drugs to the cells. Moreover, cartilage matrix is composed of anionic proteoglycans that can repel negatively charged drugs, making it difficult for OA drugs to penetrate through the matrix and reach the target cells. Additionally, most OA drugs are hydrophobic, so an appropriate technique is required to deliver them inside cartilage. A novel and efficient emulsion-based local delivery of OA drugs coated with poly beta-amino ester polymers (POLY-X) into cartilage was proposed.

In this project, nonsteroidal anti-inflammatory drugs as a model drug for OA treatment were examined. The characterization of the developed delivery system and its efficacy in native (non-treated) and glycosaminoglycan (GAG) depleted cartilage was assessed by measuring the zeta potential and size, amount of drug uptake and retention in the cartilage. In addition, the ability of the developed drug delivery system to inhibit cytokine (IL-1 $\alpha$ ) induced glycosaminoglycan and collagen degradation, as well as the loss of cell viability in cartilage explants were tested.

The data showed that the developed emulsion delivery system exhibited enhanced and prolonged drug localisation not only on non-treated cartilage tissues but also on GAG depleted sample resulting in a higher amount of drug uptake and retention in cartilage compared to the control, and the difference was statistically significant ( $p < 0.05$ ). Furthermore, the developed emulsion delivery system protects the viability of the chondrocyte cell and provides a significant increased ( $p < 0.01$ ) in glycosaminoglycan and collagen content compared to IL-1 $\alpha$  treated cartilage and similar to untreated control. The percentage of sGAG and collagen loss was 3 to 5 times higher in IL-1 $\alpha$  treated cartilage compared to the untreated and developed drug delivery system treated groups.

This study proved that modified emulsion-based therapy could provide a substantial improvement in the treatment of OA to maintain cartilage properties and improve OA outcomes.

## Contents

1.	Chapter one: General introduction .....	18
1.1.	Introduction .....	18
1.1.1.	Osteoarthritis.....	18
1.1.2.	Pathology of OA .....	18
1.1.3.	Stages of OA .....	24
1.1.4.	Statistics of OA .....	27
1.1.5.	OA risk factors .....	27
1.1.6.	Symptoms of OA .....	28
1.2.	Cartilage .....	28
1.2.1.	Composition and cartilage repair .....	28
1.3.	Treatment of OA .....	31
1.3.1.	Non-pharmacological treatment.....	32
1.3.2.	Pharmacological treatment.....	32
1.3.3.	Surgical treatment .....	43
1.3.4.	Tissue engineering .....	46
1.3.5.	Disease modifying agents .....	49
1.3.6.	Drug delivery systems.....	50
1.4.	Poly (beta-amino esters) polymer: .....	55
	Study aim.....	58
2.	Chapter two: Methodology.....	60
2.1.	Chemicals .....	60
2.1.1.	NSAIDs.....	60
2.1.2.	Oleic acid.....	60
2.1.3.	Polycations.....	60
	Buffer preparation .....	60
2.1.4.	Acetate buffer .....	60
2.1.5.	Citrate buffer.....	61
2.2.	NSAIDs preparation and coating methods.....	61
2.2.1.	Control preparation.....	61
2.2.1.1.	1 <sup>st</sup> control .....	61
2.2.1.2.	2 <sup>nd</sup> control.....	62
2.2.2.	Polycations preparation .....	62
2.2.3.	Emulsion preparation.....	67
2.2.4.	Oil droplet coating process (with POLYX).....	67
2.3.	Particle characterization .....	68

2.3.1. Zeta potential measurements .....	68
2.3.2. Size measurements.....	69
2.3.3. Determination of POLYX molecular weight and its degradation kinetics.....	69
2.4. Cartilage uptake experiments .....	71
2.4.1. Cartilage samples.....	71
2.4.2. Cartilage digestion.....	72
2.4.3. Drug uptake into cartilage .....	72
2.4.4. Drug retention into cartilage.....	73
2.5. Drug quantification.....	73
2.5.1. Calibration curves.....	73
2.5.1.1. Indomethacin .....	76
2.5.1.2. Ketorolac.....	76
2.5.1.3. Naproxen.....	77
2.5.1.4. Diclofenac sodium .....	77
2.6. Effect of the drug delivery system on IL-1 $\alpha$ treated cartilage.....	78
2.6.1. Fresh bovine cartilage harvest and culture .....	78
2.6.2. Treatment of cartilage with cytokine (IL-1 $\alpha$ ).....	78
2.6.3. Treatment of cartilage with NSAIDs emulsion coated with different types of PBAEs polymer.....	79
2.6.4. Quantification of glycosaminoglycan (GAG) .....	79
2.6.5. Collagen content determination assay .....	81
2.6.6. Live/dead staining and imaging.....	82
2.6.7. XTT assay:.....	83
2.6.8. Histological evaluation of cartilage tissues .....	84
2.7. Statistical analysis .....	85
3. Chapter three: Osteoarthritis (OA) ex vivo model development .....	86
3.1. Introduction.....	86
3.2. Materials and methods.....	90
3.2.1. OA model development.....	90
3.2.1.1. Early-stage OA .....	90
3.2.1.2. Post-traumatic OA .....	90
3.3. Results .....	90
3.3.1. Quantification of collagen and sGAG content in OA cartilage model.....	91
3.3.2. Amount of sGAG loss measurement in IL-1 $\alpha$ treated.....	92
cartilage.....	92
3.3.3. Collagen content determination in IL-1 $\alpha$ treated cartilage.....	93

3.3.4. Live/dead viability assay .....	94
3.4. Discussion .....	96
3.4.1. Trypsin treated (GAG depleted) ex vivo model .....	100
3.4.2. Catabolic ex vivo model, IL-1 $\alpha$ treated cartilage tissue .....	100
3.5. Conclusion.....	101
4. Chapter four: Developing of PBAEs and emulsion-based drug delivery system to deliver NSAID inside OA cartilage tissue .....	103
4.1. Introduction.....	103
4.2. Materials and methods .....	105
4.2.1. Emulsion diffusion in cartilage .....	105
4.3. Results.....	106
4.3.1. Polymer hydrolysis and MW determination .....	106
4.3.2. Zeta potential measurement.....	109
4.3.3. Size measurement.....	114
4.3.4. Stability study:.....	117
4.3.4.1. Zeta potential.....	118
4.3.4.2. Particle size analysis:.....	119
4.3.4.3. Visual observation of emulsion stability:.....	125
4.3.5. Amount of drug uptake measurement: .....	128
4.3.6. Drug retention inside cartilage .....	138
4.3.7. Emulsion diffusion through cartilage .....	147
4.4. Discussion: .....	148
4.4.1. Polymer degradation and mechanism of drug penetration inside cartilage tissue .....	148
4.4.2. Size and charge effects .....	149
4.4.3. Stability of emulsion droplets.....	151
4.4.4. Untreated and GAG depleted cartilage uptake and retention.....	152
4.5. Conclusion .....	154
5. Chapter 5: Assessing POLY-A5 coated ketorolac emulsion as drug delivery for post-traumatic osteoarthritis (PTOA).....	156
5.1. Introduction:.....	156
5.2. Materials and methods: .....	157
5.3. Results.....	157
5.3.1. Glycosaminoglycan (GAG) loss measurement .....	157
5.3.2. Collagen content determination.....	160
5.3.3. Live/dead viability imaging: .....	163
5.3.4. Histological analysis of cartilage explants .....	177
5.3.5. XTT assay.....	179

5.4. Discussion .....	180
5.4.1. Effect of the drug delivery system on the biochemical properties of the cartilage explants treated with IL-1 $\alpha$ .....	180
5.4.2. Viability of cartilage tissue over 20 days .....	184
5.5. Conclusion: .....	185
6. Chapter 6: Effect of different types of PBAEs on the efficacy of emulsion-based drug delivery system containing Ketorolac .....	186
6.1. Introduction.....	186
6.2. Materials and methods .....	186
6.3. Results.....	187
6.3.1. Zeta potential measurement.....	187
6.3.2. Size .....	190
6.3.3. Drug uptake measurement.....	191
6.3.4. Drug retention duration measurement.....	196
6.3.5. XTT .....	200
Bovine ex vivo model .....	201
6.3.6. Glycosaminoglycan (GAG) loss measurement .....	201
6.3.7. Collagen content determination.....	202
6.3.8. Live/dead viability assay .....	203
6.3.9. Histological analysis of cartilage explants .....	209
6.4. Discussion .....	211
6.4.1. Structure-function activity relationship of PBAEs.....	212
6.4.2. Uptake and retention of Ket inside the cartilage tissue:.....	212
6.4.3. XTT .....	213
6.4.4. IL-1 $\alpha$ assays.....	214
6.5. Conclusion .....	215
Study limitation:.....	216
Future perspectives. ....	216
References:.....	217

## List of figures:

- Figure 1-1 . Comparison of normal and OA knee joint. The osteoarthritis knee displays signs of joint degeneration, such as cartilage injury, bone exposure, and visible bony prominences (ostophytes)..... 19
- Figure 1-2. Osteoarthritis. The pathological changes in OA that cause cartilage loss, synovial inflammation (synovitis), subchondral bone alteration, osteophyte formation, and joint space narrowing. .... 20
- Figure 1-3. Pathophysiology of OA. Cartilage degradation products are released into the synovial fluid and exaggerate synovial inflammation. In addition, activated synovial cells produce catabolic and inflammatory mediators that cause cartilage breakdown by the production of the proteolytic enzyme. The inflammatory response then expands by activating synovial T cells, B cells and infiltrating macrophages. ....21
- Figure 1-4 : Role of inflammatory mediators such as IL-1 $\beta$ , TNF- $\alpha$ , IL-6, MMPs, neutrophil elastase and procathepsin-B in OA disease and progression. An excess of inflammatory mediators creates a chronic inflammatory environment causing decrease in synovial fluid content and thinning of cartilage .....22
- Figure 1-5 . Articular cartilage components. Chondrocyte in articular cartilage and the ECM which composed of proteoglycan and collagen. Proteoglycan consists of core protein and glycosaminoglycan (GAG) side chain that is directly attached to the link protein ..... 29
- Figure 1-6. Molecular organization of cartilage matrix. A variety of protein interactions stabilizes the cartilage ECM such as decorin, biglycan, fibromodulin and aggrecan .....31
- Figure 1-7 . Loss of homeostasis in cartilage. Cartilage destruction and finally OA results from a failing of chondrocytes to maintain a homeostatic equilibrium between matrix synthesis and degradation ..... 31
- Figure 1-8. Mechanism of action of non-steroidal anti-inflammatory drugs (NSAIDs) and arachidonic acid pathway. This pathway showing production of prostaglandins from membrane phospholipids in presence of cyclooxygenase (COX) enzymes which is inhibited by the NSAIDs. Prostaglandins H2 is converted by tissue specific isomerase to multiple prostanoids such as prostacyclin, thromboxane A2, prostaglandin F2, E2 and D2. .... 35
- Figure 1-9. The current clinical approaches to cell-based therapy for cartilage tissue engineering. Cell-based treatments such as stem and primary cells are more focused on cartilage regeneration and utilized to replace or repair OA-damaged tissues ..... 47
- Figure 1-10. Therapeutic window of administered drug. Repeated injection of drug lead to dose fluctuation between toxic and subtherapeutic ranges (solid line). Single injection of drug with drug delivery system (DDS) allowed drug to be within the required therapeutics range (dashed line) ..... 51
- Figure 2-1. Example of synthesis of poly beta amino ester polymer (PBAE) by reaction between 1,4 butanediol diacrylate (compound A) and dimethylamino-1-propylamine (compound 5) under addition of dichloro-methane for 48 hr at 50-55°C oil bath to form POLY-A5 polymer. .... 63
- Figure 2-2 . Schematic diagram of NSAID emulsion coated with PBAE polymer and graphical description of study design. Coated emulsion droplet with the positive charge PBAE polymer allow it to interact electrostatically with articular cartilage containing the negative charge GAG. Whereas uncoated emulsion cannot interact easily with GAG articular cartilage due to charge repulsion (both have negative charge)..... 68
- Figure 2-3. GPC calibration curve of polyethylene glycol (PEG) stander using HPLC. The x-axis represents the incubation time (min) and the y-axis represents PEG log MW. .... 70
- Figure 2-4. Image of cartilage extraction from bovine feet using 5mm diameter biopsy puncher..... 71

Figure 2-5. Indomethacin calibration curve using HPLC. The x-axis represents the concentration of indomethacin in $\mu\text{g/mL}$ , and the y-axis represents the response of the detector in mAU.....	76
Figure 2-6 . Ketorolac calibration cure using HPLC. The x-axis represents the concentration of ketorolac in $\mu\text{g/mL}$ , and the y-axis represents the response of the detector in mAU.....	76
Figure 2-7. Naproxen calibration curve using HPLC. The x-axis represents the concentration of naproxen in $\mu\text{g/mL}$ , and the y-axis represents the response of the detector in mAU. The regression equation is shown as a solid line, with the equation $y = 266.79x - 15.975$ and $R^2 = 0.9993$ indicated in the legend. ....	77
Figure 2-8. Diclofenac calibration curve using HPLC. The x-axis represents the concentration of diclofenac sodium in $\mu\text{g/mL}$ , and the y-axis represents the response of the detector in mAU.....	77
Figure 2-9 . Calibration curve of chondroitin sulphate using plate reader (Tecan Infinite 200 PRO) at 525 nm. The x-axis represents the concentration of chondroitin sulphate in $\mu\text{g/mL}$ , and the y-axis represents the optical density in nm. ....	80
Figure 2-10 . Calibration curve of hydroxyproline using plate reader (Tecan Infinite 200 PRO) at 570 nm. The x-axis represents the concentration of hydroxyproline in $\text{mg/mL}$ , and the y-axis represents the optical density in nm. ....	82
Figure 2-11. Principle of XTT assay: the enzymatic reduction of XTT to form the orange-coloured formazan derivative by viable cells. ....	84
Figure 3-1. Sulphated glycosaminoglycan (sGAG) and collagen content measurement. Percentage of sGAG in non-treated (untreated) and trypsin treated cartilage (45%) for 24 hours (A), and the percentage of collagen content in non-treated (untreated) and trypsin treated cartilage (51%) for 24 hours (B).. ....	91
Figure 3-2. Quantification of sulphated glycosaminoglycan (sGAG) in culture media from control (untreated cartilage, blue line) and IL-1 $\alpha$ treated explants (orange line) at day 1, 2, 4, 7,9,11,14 and 20 using the DMMB assay. ....	93
Figure 3-3. Collagen content determination on untreated (blue line) and IL-1 $\alpha$ treated (orange line) cartilage explants at day 1, 2, 4, 7,9,11,14 and 20 using hydroxyproline assay. ....	94
Figure 3-4. Images of fluorescently stained bovine explants using live/dead staining assay to evaluate chondrocyte viability on days 1,2,7, 14 and 20 in untreated and IL-1 $\alpha$ treated cartilage samples. Live cells were stained green by calcein and dead cells were stained red by ethidium homodimer. ....	95
Figure 4-1. MW and hydrolysis of POLY-A5 for 30 days at pH 5 (blue line) and pH 7.4 (orange line) using GPC. POLY-A5 degradation was faster at pH 7.4 than pH 5.....	107
Figure 4-2. Charge hydrolysis using Zeta potential (ZP) for POLY-A5 for 30 days at pH 5 (blue line) and pH 7.4 (orange line). POLY-A5 degradation was faster at pH 7.4 than pH 5. ....	108
Figure 4-3. MW and hydrolysis of POLY-B5 for 30 days at pH 5 (blue line) and pH 7.4 (orange line) using GPC. POLY-B5 degradation was faster at pH 7.4 than pH 5.....	108.
Figure 4-4. Charge hydrolysis using Zeta potential (ZP) for POLY-B5 for 30 days at pH 5 (blue line) and pH 7.4 (orange line). POLY-B5 degradation was faster at pH 7.4 than pH 5.....	109
Figure 4-5. Characterization of coated emulsion – measuring the zeta potential (mV) values for NSAIDs emulsion before and after adding POLY-A5 continuously until reach the saturation to complete coated the emulsion droplet with the positively charged POLY-A5.....	111

Figure 4-6. Characterization of coated emulsion – measuring the zeta potential (mV) values for NSAIDs emulsion before and after adding POLY-B5 continuously until reach the saturation to complete coated the emulsion droplet with the positively charged POLY-B5.....	113
Figure 4-7. Characterisation – measuring the hydrodynamic size distribution of indomethacin, ketorolac, naproxen and diclofenac before and after coated with PBAE polymer via DLS.....	115
Figure 4-8. Zeta potential (mV) values for stability of o/w emulsion before and after adding Ket/POLY-A5. Zeta potential was measured using a Zetasizer Nano ZS apparatus to determine emulsion stability as charge changing for 14 days.....	119
Figure 4-9. Size distribution of emulsion droplets before and after adding Ket/POLY-A5, as measured by dynamic light scattering (DLS) using a Zetasizer Nano ZS apparatus. The DLS measurements were taken at regular intervals over a period of 10 days to assess the stability of the o/w emulsion.....	121
Figure 4-10. Visual observation of emulsion stability. Emulsions (o/w emulsion before and after adding Ket/POLY-A5) were stored at room temperature and observed for 10 days.....	126
Figure 4-11. Comparison of indomethacin (Ind) uptake into cartilage for 10 minutes using P control (Ind in PBS), E control (Ind emulsion) and Ind emulsion saturated with POLY-A5 in both untreated cartilage (A) and GAG depleted cartilage (B).....	129
Figure 4-12. Comparison of ketorolac (Ket) uptake into cartilage for 10 minutes using P control (Ket in PBS), E control (Ket emulsion) and Ket emulsion saturated with POLY-A5 in both untreated cartilage (A) and GAG depleted cartilage (B).....	130
Figure 4-13. Comparison of naproxen (Nap) uptake into cartilage for 10 minutes using P control (Nap in PBS), E control (Nap emulsion) and Nap emulsion saturated with POLY-A5 in both untreated cartilage (A) and GAG depleted cartilage (B).....	131
Figure 4-14. Comparison of diclofenac sodium (DC) uptake for 10 minutes into cartilage using P control (DC in PBS), E control (DC emulsion) and DC emulsion saturated with POLY-A5 in both untreated cartilage (A) and GAG depleted cartilage (B).....	132
Figure 4-15. Comparison of indomethacin (Ind) uptake into cartilage for 10 minutes using P control (Ind in PBS), E control (Ind emulsion) and Ind emulsion saturated with POLY-B5 in both untreated (A) and GAG depleted cartilage (B).....	134
Figure 4-16. Comparison of ketorolac (Ket) uptake into cartilage for 10 minutes using P control (Ket in PBS), E control (Ket emulsion) and Ket emulsion saturated with POLY-B5 in both untreated (A) and GAG depleted cartilage (B).....	135
Figure 4-17 Comparison of naproxen (Nap) uptake into cartilage for 10 minutes using P control (Nap in PBS), E control (Nap emulsion) and Nap emulsion saturated with POLY-B5 in both untreated (A) and GAG depleted cartilage (B). The concentration of Nap that has penetrated the cartilage is expressed in $\mu\text{g}$ per mg cartilage. ....	136
Figure 4-18 Comparison of diclofenac sodium (DC) uptake into cartilage for 10 minutes using P control (DC in PBS), E control (DC emulsion) and DC emulsion saturated with POLY-B5 in both untreated (A) and GAG depleted cartilage(B). The concentration of DC that has penetrated the cartilage is expressed in $\mu\text{g}$ per mg cartilage. ....	137
Figure 4-19 Comparison of indomethacin (Ind) retention into cartilage for 180 minutes (3 hours) using P control (Ind in PBS), E control (Ind emulsion) and Ind emulsion saturated with POLY-A5 in untreated (A) and GAG depleted cartilage (B). The concentration of Ind that has penetrated the cartilage is expressed in $\mu\text{g}$ per mg cartilage. ....	139

Figure 4-20 Comparison of ketorolac (Ket) retention into cartilage for 180 minutes (3 hours) using P control (Ket in PBS), E control (Ket emulsion) and Ket emulsion saturated with POLY-A5 in untreated (A) and GAG depleted cartilage (B). The concentration of Ket that has penetrated the cartilage is expressed in $\mu\text{g}$ per mg cartilage. ....	140
Figure 4-21 Comparison of naproxen (Nap) retention into cartilage for 180 minutes (3 hours) using P control (Nap in PBS), E control (Nap emulsion) and Nap emulsion saturated with POLY-A5 in untreated (A) and GAG depleted cartilage (B). The concentration of Nap that has penetrated the cartilage is expressed in $\mu\text{g}$ per mg cartilage. ....	141
Figure 4-22 Comparison of diclofenac sodium (DC) retention into cartilage for 180 minutes (3 hours) using P control (DC in PBS), E control (DC emulsion) and DC emulsion saturated with POLY-A5 in untreated (A) and GAG depleted cartilage (B). The concentration of DC that has penetrated the cartilage is expressed in $\mu\text{g}$ per mg cartilage. ....	142
Figure 4-23 Comparison of indomethacin (Ind) retention into cartilage for 350 minutes (6 hours) using P control (Ind in PBS), E control (Ind emulsion) and Ind emulsion saturated with POLY-B5 in untreated (A) and GAG depleted cartilage (B). The concentration of Ind that has penetrated the cartilage is expressed in $\mu\text{g}$ per mg cartilage. ....	143
Figure 4-24 Comparison of ketorolac (Ket) retention into cartilage for 350 minutes (6 hours) using P control (Ket in PBS), E control (Ket emulsion) and Ind emulsion saturated with POLY-B5 in untreated (A) and GAG depleted cartilage (B). The concentration of Ket that has penetrated the cartilage is expressed in $\mu\text{g}$ per mg cartilage. ....	144
Figure 4-25 Comparison of naproxen (Nap) retention into cartilage for 350 minutes (6 hours) using P control (Nap in PBS), E control (Nap emulsion) and Nap emulsion saturated with POLY-B5 in untreated (A) and GAG depleted cartilage (B). The concentration of Nap that has penetrated the cartilage is expressed in $\mu\text{g}$ per mg cartilage. ....	145
Figure 4-26 Comparison of diclofenac sodium (DC) retention into cartilage for 350 minutes (6 hours) using P control (DC in PBS), E control (DC emulsion) and Ind emulsion saturated with POLY-B5 in untreated (A) and GAG depleted cartilage (B). The concentration of DC that has penetrated the cartilage is expressed in $\mu\text{g}$ per mg cartilage. ....	146
Figure 4-27. Examples of confocal images of Nile red fluorescently tagged oil emulsions (red) diffusion through cartilage chondrocyte cells countered stained with DAPI (blue). Nile red was dissolved into oleic acid to fluorescently tag the emulsions and confirm that the droplets diffuse through the cartilage tissue and not just adsorb onto the outer surface of the samples. ....	147
Figure 5-1. Quantification of sGAG in IL-1 $\alpha$ (1ng/mL) treated cartilage using DMMB assay. Using main samples (untreated (media only ) and IL-1 $\alpha$ treated samples) and different types of control (A), Ket emulsion coated with/without POLY-A5(B) and Dex emulsion coated with/without POLY-A5(C), the figures were separated for clarity. ....	159
Figure 5-2. Collagen content determination on IL-1 $\alpha$ treated cartilage using hydroxyproline assay. Using main samples (untreated (media only) and IL-1 $\alpha$ treated sample) and different types of control (A), emulsion Ket coated with/without POLY-A5(B) and Dex emulsion coated with/without POLY-A5(C), the figures was separated for clarity. ....	161
Figure 5-3. Examples of images of live/dead fluorescently stained bovine explants exposed to IL-1 $\alpha$ (1ng/mL) to evaluated chondrocyte viability on day 1. The cartilage explants were incubated with controls (pure media, IL-1 $\alpha$ , Ket, oleic acid emulsion with/without IL-1 $\alpha$ and POLY-A5). Live cells were stained green by calcein and dead cells were stained red by ethidium homodimer. ....	164

Figure 5-4. Examples of images of live/dead fluorescently stained bovine explants exposed to IL-1 $\alpha$ (1ng/mL) to evaluated chondrocyte viability on day 2. The cartilage explants were incubated with controls (pure media, IL-1 $\alpha$ , Ket, oleic acid emulsion with/without IL-1 $\alpha$ and POLY-A5). Live cells were stained green by calcein and dead cells were stained red by ethidium homodimer. ....	165
Figure 5-5. Examples of images of live/dead fluorescently stained bovine explants exposed to IL-1 $\alpha$ (1ng/mL) to evaluated chondrocyte viability on day 7. The cartilage explants were incubated with controls (pure media, IL-1 $\alpha$ , Ket, oleic acid emulsion with/without IL-1 $\alpha$ and POLY-A5). Live cells were stained green by calcein and dead cells were stained red by ethidium homodimer. ....	166
Figure 5-6. Examples of images of live/dead fluorescently stained bovine explants exposed to IL-1 $\alpha$ (1ng/mL) to evaluated chondrocyte viability on day 14. The cartilage explants were incubated with controls (pure media, IL-1 $\alpha$ , Ket, oleic acid emulsion with/without IL-1 $\alpha$ and POLY-A5). Live cells were stained green by calcein and dead cells were stained red by ethidium homodimer. ....	167
Figure 5-7. Examples of images of live/dead fluorescently stained bovine explants exposed to IL-1 $\alpha$ (1ng/mL) to evaluated chondrocyte viability on day 1. The cartilage explants were incubated with controls (pure media, IL-1 $\alpha$ , Ket emulsion with without IL-1 $\alpha$ and POLY-A5). Live cells were stained green by calcein and dead cells were stained red by ethidium homodimer. ....	169
Figure 5-8. Examples of images of live/dead fluorescently stained bovine explants exposed to IL-1 $\alpha$ (1ng/mL) to evaluated chondrocyte viability on day 2. The cartilage explants were incubated with controls (pure media, IL-1 $\alpha$ , Ket emulsion with without IL-1 $\alpha$ and POLY-A5). Live cells were stained green by calcein and dead cells were stained red by ethidium homodimer. ....	170
Figure 5-9. Examples of images of live/dead fluorescently stained bovine explants exposed to IL-1 $\alpha$ (1ng/mL) to evaluated chondrocyte viability on day 7. The cartilage explants were incubated with controls (pure media, IL-1 $\alpha$ , Ket emulsion with without IL-1 $\alpha$ and POLY-A5). Live cells were stained green by calcein and dead cells were stained red by ethidium homodimer. ....	171
Figure 5-10. Examples of images of live/dead fluorescently stained bovine explants exposed to IL-1 $\alpha$ (1ng/mL) to evaluated chondrocyte viability on day 14. The cartilage explants were incubated with controls (pure media, IL-1 $\alpha$ , Ket emulsion with without IL-1 $\alpha$ and POLY-A5). Live cells were stained green by calcein and dead cells were stained red by ethidium homodimer. ....	172
Figure 5-11. Examples of images of live/dead fluorescently stained bovine explants exposed to IL-1 $\alpha$ (1ng/mL) to evaluated chondrocyte viability on day 1. The cartilage explants were incubated with controls (pure media, IL-1 $\alpha$ , Dex emulsion with without IL-1 $\alpha$ and POLY-A5). Live cells were stained green by calcein and dead cells were stained red by ethidium homodimer. ....	173
Figure 5-12. Examples of images of live/dead fluorescently stained bovine explants exposed to IL-1 $\alpha$ (1ng/mL) to evaluated chondrocyte viability on day 2. The cartilage explants were incubated with controls (pure media, IL-1 $\alpha$ , Dex emulsion with without IL-1 $\alpha$ and POLY-A5). Live cells were stained green by calcein and dead cells were stained red by ethidium homodimer. ....	174
Figure 5-13. Examples of images of live/dead fluorescently stained bovine explants exposed to IL-1 $\alpha$ (1ng/mL) to evaluated chondrocyte viability on day 7. The cartilage explants were incubated with controls (pure media, IL-1 $\alpha$ , Dex emulsion with without IL-1 $\alpha$ and POLY-A5). Live cells were stained green by calcein and dead cells were stained red by ethidium homodimer. ....	175
Figure 5-14. Examples of images of live/dead fluorescently stained bovine explants exposed to IL-1 $\alpha$ (1ng/mL) to evaluated chondrocyte viability on day 14. The cartilage explants were incubated with controls (pure media, IL-1 $\alpha$ , Dex emulsion with without IL-1 $\alpha$ and POLY-A5). Live cells were stained green by calcein and dead cells were stained red by ethidium homodimer. ....	176

Figure 5-15. Histology sections of cartilage tissue stained with safranin O on day 14 that exposed to pure media, IL-1 $\alpha$ (1ng/mL), Ket emulsion coated with POLY-A5, Ket o/w emulsion +IL-1 $\alpha$ and Ket+IL-1 $\alpha$ . The reddish orange colour intensity indicates the amount of GAG in the sample. ....	178
Figure 5-16. Viability assessment of cartilage tissues over 20 days. XTT assay was used to assess the effects of Ket emulsion coated with/without POLY-A5 on cartilage samples that exposed to IL-1 $\alpha$ . The figure showed 80% reduced in XTT results from day 0 to 20 on cartilage that treated with IL-1 $\alpha$ . Conversely, cartilage treated with Ket emulsion coated with POLY-A5 exhibited approximately 20% reduced in XTT results up to day 20. ....	180
Figure 6-1. Zeta potential (mV) value of Ket emulsions during coating with 14 types of poly-beta amino ester polymers until reach the saturation (1 $\mu$ L of Ket emulsion +10 $\mu$ L of POLY-X) and change the emulsion charge to positive. ....	189
Figure 6-2. Comparison of Ket uptake into cartilage for 10 min using P control (Ket in PBS), E control (Ket o/w emulsion) and Ket o/w emulsion saturated with POLY-X in both untreated and GAG depleted cartilage. The concentration of Ket that has penetrated the cartilage is expressed in $\mu$ g per mg cartilage. ....	192
Figure 6-3. Comparison of Ket retention into cartilage for 300 min (5 hours) using P control (Ket in PBS), E control (Ket o/w emulsion) and Ket o/w emulsion saturated with POLY-X in untreated and GAG depleted cartilage samples. ....	196
Figure 6-4. Viability assessment of cartilage tissues treated with POLY-X over 20 days in culture. Cartilage cell was not affected by the presence of POLY-X on media compared to samples that were treated with IL-1 $\alpha$ . ....	200
Figure 6-5. Quantification of sGAG in IL-1 $\alpha$ treated cartilage using DMMB assay for 20 days. Using emulsion Ket coated with POLY-B5 and POLY-F3, IL-1 $\alpha$ , POLY-B5 and POLY-F3 with/without IL-1 $\alpha$ . ....	202
Figure 6-6. Collagen content determination on IL-1 $\alpha$ treated cartilage using hydroxyproline assay for 20 days. Using emulsion Ket coated with POLY-B5 and POLY-F3, IL-1 $\alpha$ , POLY-B5 and POLY-F3 with/without IL-1 $\alpha$ . ....	203
Figure 6-7. Examples of images of live/dead fluorescently stained bovine explants exposed to IL-1 $\alpha$ (1ng/mL) to evaluate chondrocyte viability on day 1. The cartilage explants were incubated with controls (pure media, IL-1 $\alpha$ , oleic acid emulsion with/without IL-1 $\alpha$ , POLY-B5 and POLY-F3). ....	204
Figure 6-8. Examples of images of live/dead fluorescently stained bovine explants exposed to IL-1 $\alpha$ (1ng/mL) to evaluated chondrocyte viability on day 2. The cartilage explants were incubated with controls (pure media, IL-1 $\alpha$ , oleic acid emulsion with/without IL-1 $\alpha$ , POLY-B5 and POLY-F3). ....	205
Figure 6-9. Examples of images of live/dead fluorescently stained bovine explants exposed to IL-1 $\alpha$ (1ng/mL) to evaluated chondrocyte viability on day 7. The cartilage explants were incubated with controls (pure media, IL-1 $\alpha$ , oleic acid emulsion with/without IL-1 $\alpha$ , POLY-B5 and POLY-F3). ....	207
Figure 6-10. Examples of images of live/dead fluorescently stained bovine explants exposed to IL-1 $\alpha$ (1ng/mL) to evaluated chondrocyte viability on day 14. The cartilage explants were incubated with controls (pure media, IL-1 $\alpha$ , oleic acid emulsion with/without IL-1 $\alpha$ , POLY-B5 and POLY-F3). ....	208
Figure 6-11. Histology sections of cartilage tissue stained with safranin O on day 20 that exposed to pure media, IL-1 $\alpha$ (1ng/mL), Ket o/w emulsion coated with POLY-B5 and POLY-F3. ....	210

## List of tables:

Table 1-1. Role and types of different cytokines during OA onset and progression. The columns show the types of cytokine, name, its role in OA disease progression. Abbreviations: IL (interleukin), IFN- $\gamma$ (Interferon gamma), TNF- $\alpha$ (tumour necrosis factor alpha), SDF-1 (stromal cell-derived factor 1), IGF(insulin-like growth factor) and TGF $\beta$ (Transforming growth factor beta) (Jayasuriya, 2013; Wojdasiewicz, Poniatowski and Szukiewicz, 2014) .....	23
Table 1-2 Stages of OA. The columns show the different stages of OA, the characteristics of each stage in term of bone protrusion, joint destruction, severity of pain and treatment options for each stage. (Sharma and Berenbaum, 2007; Aigner and Schmitz, 2011; Bliddal, Leeds and Christensen, 2014; Holland, 2017).....	25
Table 1-3 The dosage and route of administration of common types of NSAIDs used in OA treatment (Fendrick and Greenberg, 2009).....	36
Table 1-4 Advantages and disadvantages of using NSAIDs. ....	38
Table 1-5 Advantages and disadvantages of using corticosteroids. ....	39
Table 1-6: Surgical treatment for OA, their advantages, disadvantages, and candidate group for each type of surgical treatment. ....	45
Table 2-1 : Amount of acetic acid and sodium acetate (mL) which used to prepare acetate buffer at different pH. ....	61
Table 2-2 Name, chemical structure, and coding system of compounds used to prepare different types of poly beta amino ester polymers. ....	64
Table 2-3 Coding, yield and chemical structures of poly beta amino ester polymers which prepared using different types of acrylates, and amines.. ....	65
Table 2-4 The GPC parameters for the determination of poly beta amino ester polymer molecular weight..	71
Table 2-5 Calibration curve parameters of NSAIDs, their solubility in PBS and log P value. All the NSAIDs have a slight aqueous solubility as they have a positive log P value (range between 2.28-4.15) which indicating that they have affinity to oil/lipid phase (lipophilic). ....	75
Table 3-1 Advantages and disadvantages of different types of in vitro and ex vivo models used in OA research.....	87
Table 4-1 Zeta potential (mV) for POLY-A5, o/w emulsion and NSAIDS o/w emulsion before and after coated with POLY-A5 and the amount of POLY-A5 required to coat 1mL of the NSAIDS emulsion completely. ....	112
Table 4-2 Zeta potential (mV)for POLY-B5, o/w emulsion and NSAIDS o/w emulsion before and after coated with POLY-B5 and the amount of POLY-B5 required to coat 1mL of the NSAIDS emulsion completely. ....	114
Table 4-3 Size measurements ( $\mu\text{m}$ ) for POLY-A5, NSAIDS emulsion before and after coated with POLY-A5. ....	117
Table 4-4 Size measurements ( $\mu\text{m}$ ) for POLY-B5, NSAIDS emulsion before and after coated with POLY-B5. ....	117
Table 6-1 Characterisation of coated emulsion – zeta potential (mV) values for Ket emulsion before and after coating with POLY-X and the amount of each POLY-X which required to coat Ket emulsion completely ( $\mu\text{L}$ ).....	188

Table 6-2 Size measurements ( $\mu\text{m}$ ) for Ket emulsions coated with 14 different types of poly-beta amino ester polymers. The results show variations in size measurements of the coated emulsions among the different types of poly-beta amino ester polymers used..... 191

**List of schemes:**

Scheme 1-1: Synthesis and applications of PBAEs polymer.....57  
Scheme 2-2: Miscellaneous properties mark PBAEs an ideal drug delivery system .....57  
Scheme 2-1. schematic diagram illustrates the cartilage slices place in the cartilage disk  
.....83

## List of abbreviation:

OA	Osteoarthritis
IL	Interleukin
IFN- $\gamma$	Interferon gamma
TNF	Tumour necrosis factor
IGF	insulin growth factor
COMP	Cartilage oligomeric matrix protein
TGF	transforming growth factor
SDF	Stromal cell-derived factor
CXCR	chemokine receptor
MCL	medial collateral ligament
LCL	lateral collateral ligament
ACL	anterior cruciate ligament
PCL	posterior cruciate ligament
BMP	bone morphogenetic protein
FGF	fibroblast growth factor
PDGF	platelet-derived growth factor
PG	proteoglycans
CS	chondroitin sulphate
KS	keratan sulphate
ECM	Extracellular matrix
COX	cyclooxygenase
CNS	Central nervous system
GIT	Gastrointestinal tract
CV	Cardiovascular
NSAIDs	Non-steroidal anti-inflammatory drugs
MMPs	metalloproteinases
IA	Intra-articular
HA	Hyaluronic acid
TENS	Transcutaneous electrical nerve stimulation
ACI	Autologous chondrocytes implantation
MSCs	Mesenchymal stem cells
ESCs	embryonic stem cells
iPSCs	induced pluripotent stem cells
DMOADs	disease modifying osteoarthritis
DDSs	drug delivery systems
PIG NPs	polyethylene glycolate gelatine nanoparticles
Ind	indomethacin
Ket	ketorolac
Nap	naproxen
DC	diclofenac sodium.
PBS	Phosphate buffer saline
SOP	standard operation procedures
ADAMTS	A disintegrin and metalloproteinase with thrombospondin motifs
EDTA	ethylenediaminetetraacetic acid
DTT	dithiothreitol
GAG	Glycosaminoglycan
HPLC	high performance liquid chromatography
ZP	Zeta potential

# **1. Chapter one: General introduction**

## **1.1. Introduction**

### **1.1.1. Osteoarthritis**

Osteoarthritis (OA) is one of the considerable chronic health conditions around the world and the most common form of arthritis. It is characterised by difficulty in joint movement, stiffness and gradual loss of articular cartilage, and moderate to severe pain (Sharma and Berenbaum, 2007; WHO, 2013). In other words, it is a problem which is known globally as a degenerative joint disease that causes joints to become painful and rigid. In fact, it is considered a ‘wear and tear’ disease because of the strong association between age and OA; it results from the gradual breakdown and loss of cartilage in the joints over time. With age, joints and cartilage can become damaged or worn down as a result of normal movements and activities. This can cause the bones in the joint to rub against each other, leading to osteoarthritis (Berenbaum, 2013; Grassel and Aszódi, 2017). It can affect the knees, hands, hips, feet, fingers and many other different parts of the body (Kaplan and Laing, 2004; Sharma and Berenbaum, 2007).

### **1.1.2. Pathology of OA**

To begin with, it is essential to understand normal joint anatomy and function (Figure 1-1). Each joint is composed of subchondral bone, cartilage, ligaments and a joint capsule (Aigner and Schmitz, 2011). Cartilage absorbs shock to allow freedom of mobility while bones determine the overall shape and movement of joints (Sophia Fox, Bedi and Rodeo, 2009). In addition, bones provide support and stability, prevent injury or dislocation, and allow one to perform a wide range of activities and movements (Sophia Fox, Bedi and Rodeo, 2009). For example, the knee joint is formed by the femur (thigh bone) and the tibia (shin bone). The shape of these bones determines the movement of the knee joint, which allows for leg flexion and extension. The capsule and ligaments, meanwhile, maintain stability and control range of motion (Aigner and Schmitz, 2011). Furthermore, the synovial membrane, a fluid-filled space at the site where the articulating surfaces of the bones contact each other, contains a large amount of synoviocytes cells. These serve to provide nourishment to chondrocyte cells, a specialized cell type found in cartilage tissue (Grassel and Aszódi, 2017). The purpose of chondrocyte cells is to maintain a balance between the anabolic and catabolic processes in the cartilage cellular matrix molecules in order to ensure effective cartilage function during movement and lifetime absorption of biomechanical stress (Bertrand and Held, 2017). Moreover, synoviocytes produce a high quantity of the necessary mediators such as cytokines

(e.g., IL-4 and IFN- $\gamma$ ), lubricant factors such as synovial fluid, hyaluronic acid and lubricin/superficial zone protein, which together play an essential role in joint flexibility and lubrication capacity (Aigner and Schmitz, 2011). Collectively, all of these components are crucial in terms of structure and function of healthy joints, as well as facilitating free movement within the required range without pain or discomfort.

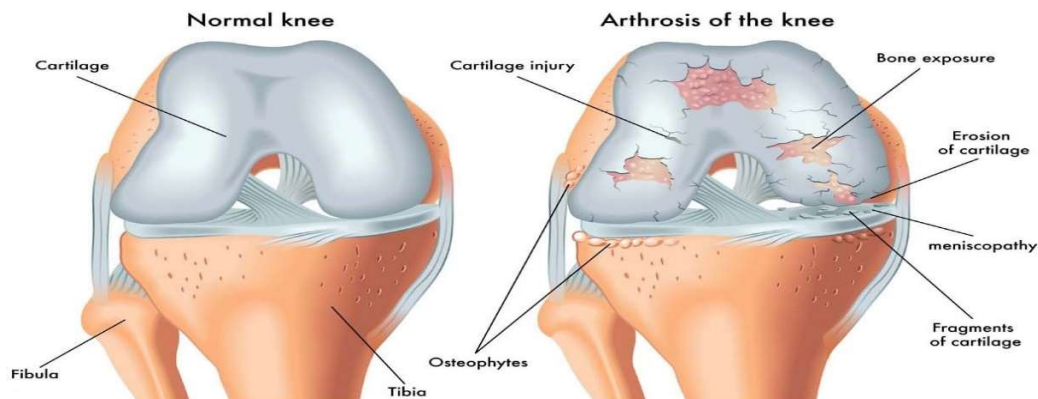


Figure 1-1 . Comparison of normal and OA knee joint. The osteoarthritis knee displays signs of joint degeneration, such as cartilage injury, bone exposure, and visible bony prominences (ostophytes) , adapted from (Blood-Smyth, 2015).

Typically, there is a balance between synthesis and degradation of cartilage by chondrocytes, but in OA cases equilibrium primarily assists degradation (Aigner and Schmitz, 2011). Until the late twentieth century, scientists believed that cartilage degradation or loss was the first sign of osteoarthritis (Sharma and Berenbaum, 2007). This led to an attempt to explain the mechanisms of cartilage degradation. Subsequently, approximately 50 years ago, it was suggested that subchondral bone alteration was the leading cause of OA (Radin and Paul, 1970). Since that time, many studies have investigated the leading causes of OA. More recently, researchers have convincingly demonstrated that the major common characteristic features of OA are cartilage loss, synovial inflammation or synovitis, and subchondral bone alteration (Figures 1-1 & 1-2) (Sharma and Berenbaum, 2007; Mobasher and Batt, 2016). Each of these features can in term lead to another condition; for example, bone change is a phenomenon secondary to the destruction of cartilage and cartilage loss has a role in synovial inflammation (Figure 1-2) (Saunders, 2003; Sharma and Berenbaum, 2007). Accordingly, it is clear that there is a correlation between articular cartilage loss, subchondral bone change and synovial inflammation. These can lead to joint space narrowing, osteophyte formation, and

ultimately to OA (Figure 1-2) (Saunders, 2003; Ashkavand, Malekinejad and Vishwanath, 2013).

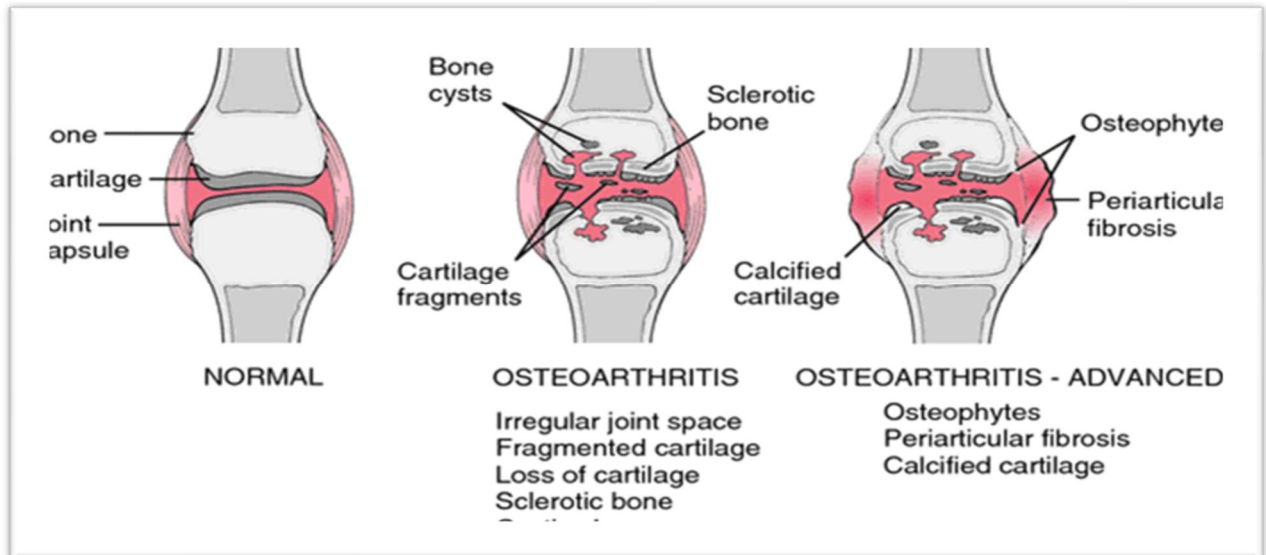


Figure 1-2. Osteoarthritis. The pathological changes in OA that cause cartilage loss, synovial inflammation (synovitis), subchondral bone alteration, osteophyte formation, and joint space narrowing. Adapted from (Saunders, 2003).

Cartilage acts as a protective layer for the end of each bone in the body to provide a smooth and easy joint motion, and also helps to prevent bone fracture (Sophia Fox, Bedi and Rodeo, 2009). In OA, this assisting layer breaks down, leading to inflammation, which in term results in characteristic and severe pain, stiffness, swelling and problems in moving the joint (Figure 1-2) (Saunders, 2003; Kidd, 2012). Additionally, cartilage contains one particular cell type, chondrocytes, responsible for making and maintaining cartilage (Grässel and Aszódi, 2017). On the other hand, bones and synovial membranes contain nerve cells that can signal inflammation factors in the synovial fluid and bones, causing the brain to translate these signals into pain (Kidd, 2012). Furthermore, the inflammation factors release prostaglandins and cytokines that encourage the further breakdown of cartilage, leading to development of new inflammatory reactions. Eventually, this can affect other joints via the bloodstream, causing simultaneous inflammation and osteoarthritis in affected area (Figures 1-3 & 1-4) (Kidd, 2012; Mathiessen and Conaghan, 2017).

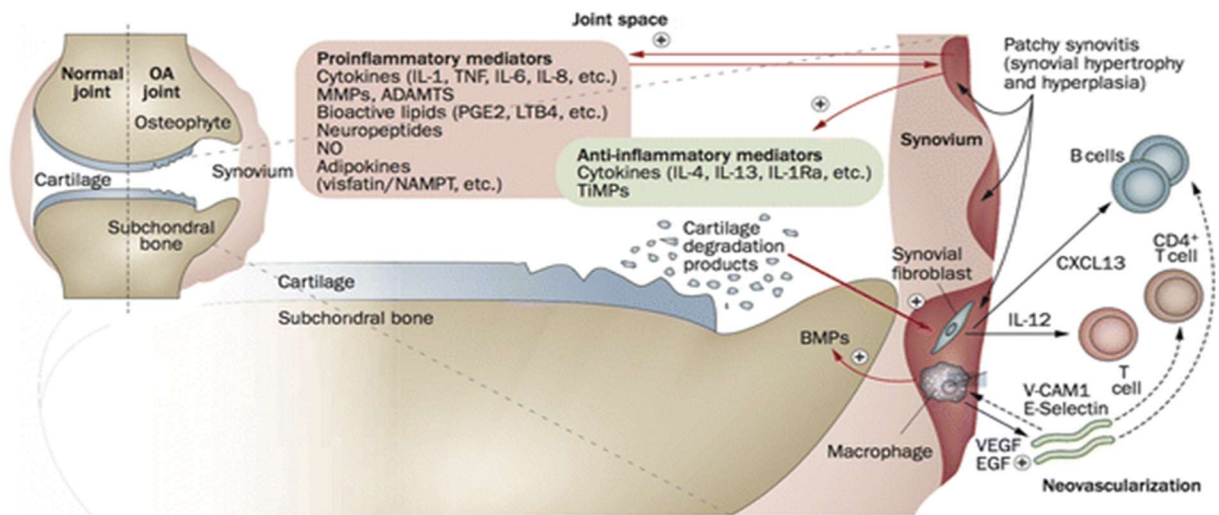


Figure 1-3. Pathophysiology of OA. Cartilage degradation products are released into the synovial fluid and exaggerate synovial inflammation. In addition, activated synovial cells produce catabolic and inflammatory mediators that cause cartilage breakdown by the production of the proteolytic enzyme. The inflammatory response then expands by activating synovial T cells, B cells and infiltrating macrophages. Moreover, synovium and cartilage produce anti-inflammatory cytokines. Adapted from (Sellam and Berenbaum, 2010).

In general, research has shown a relationship between joint inflammation and OA disease progression (Figures 1-3 & 1-4). Inflammatory mediators, together with mechanical and oxidative stress affect chondrocytes' activity, alter their normal functions and make them more sensitive to inflammatory and catabolic mediators (Mobasher and Batt, 2016). The main components of synovial infiltration in OA are macrophages, which are activated by T and B lymphocytes (Figure 1-3) (Wenham, McDermott and Conaghan, 2015).

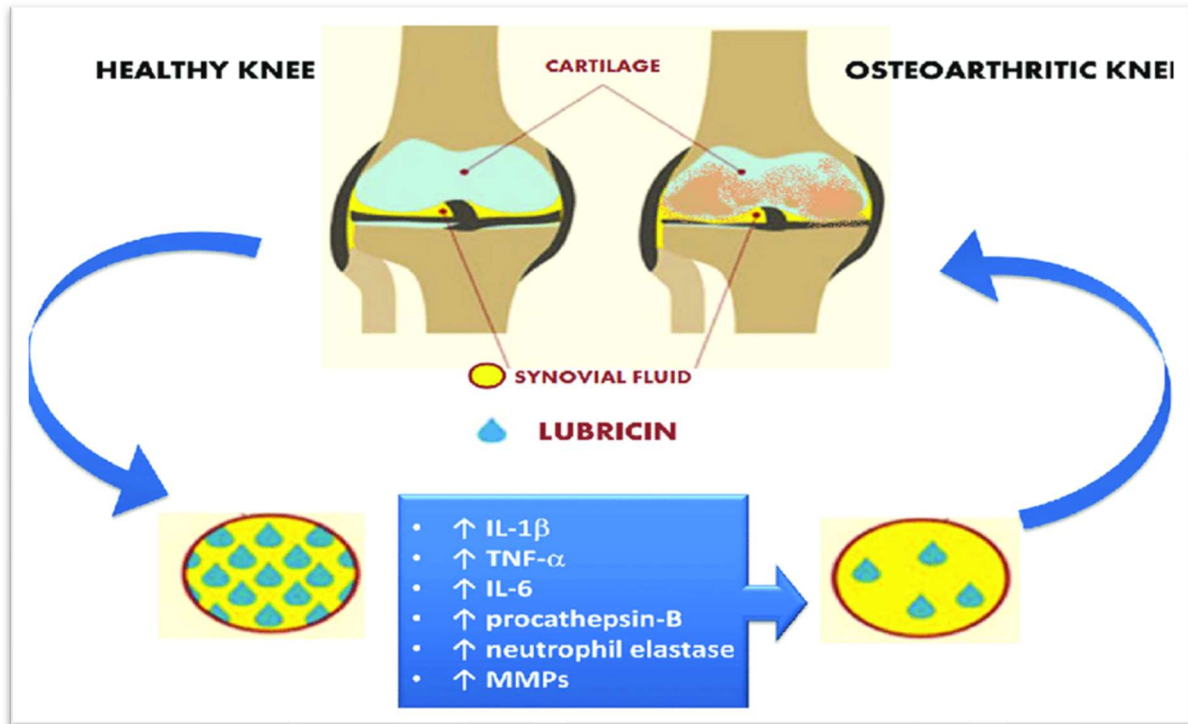


Figure 1-4. Role of inflammatory mediators such as IL-1 $\beta$ , TNF- $\alpha$ , IL-6, MMPs, neutrophil elastase and procathepsin-B in OA disease and progression. An excess of inflammatory mediators creates a chronic inflammatory environment causing decrease in synovial fluid content and thinning of cartilage, adapted from (Szychlinska et al., 2016).

Moreover, there are three different types of cytokines involved in the metabolism of articular cartilage: regulatory or enzyme inhibitory (IL-4, IL-6, IL-8, IL-10, IFN- $\gamma$ ); anabolic (growth factor, IGF, COMPs, TGF $\beta$ ) and catabolic (IL1 $\alpha$ , IL1 $\beta$ , TNF $\alpha$ ), (Table1-1) (Ashkavand, Malekinejad and Vishwanath, 2013; Berenbaum, 2013; Jayasuriya, 2013). In fact, there is normally a balance between these cytokines' inflammatory and catabolic mediators, with imbalance typically leading to OA. Many studies have shown an increase in cytokine levels in patients with OA (Table1-1) (Jayasuriya, 2013). It has also been accepted that there is a strong correlation between increased levels of IL-1, TNF- $\alpha$  and OA. Moreover, IL1- $\alpha$  and IL-1- $\beta$  levels are significantly elevated in osteoarthritic synovial fluids and considered to be fundamental during both early and late stages of OA (Van den Berg, 1999; Jayasuriya, 2013).

Table 1-1. Role and types of different cytokines during OA onset and progression. The columns show the types of cytokines, name, its role in OA disease progression. Abbreviations: IL (interleukin), IFN- $\gamma$  (Interferon gamma), TNF- $\alpha$  (tumour necrosis factor alpha), SDF-1 (stromal cell-derived factor 1), IGF(insulin-like growth factor) and TGF $\beta$  (Transforming growth factor beta) (Jayasuriya, 2013; Wojdasiewicz, Poniatowski and Szukiewicz, 2014)

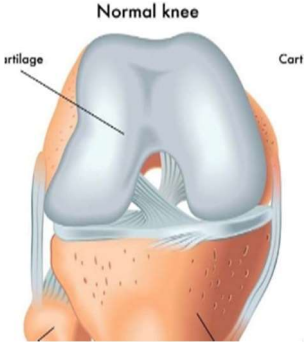
Types	Cytokines	Role in OA
Regulatory	IL-4	Decreases production of nitric oxide by OA associated inflammatory cytokines
	IL-10	Its level increases in OA as it acts mainly to inhibit the expression of IL-1 and TNF- $\alpha$
	IL-13	Inhibits the expression of IL-1 and TNF- $\alpha$ , while raising the expression level of IL-1Ra (IL-1 receptor antagonist)
	IFN- $\gamma$	Inhibits the catabolic effects of IL-1
	IL-6	The negative controller of chondrocyte proliferation and a biomarker for early diagnosis of OA. IL-1 $\beta$ and TNF- $\alpha$ increase production of IL-6.
	IL-8	The controller of chondrocyte hypertrophy. IL-1 $\beta$ and TNF- $\alpha$ increase production of IL-8.
Cytokines and chemokines suspected of tissue degradation (pro-inflammatory)	IL-1	Its level increases at early and late-stage OA; it enhances matrix metalloproteinases (MMP) production and inhibits cartilage anabolism
	IL-1 $\beta$	One of the most important proinflammatory cytokines in OA. High ability to release degenerative protease, such as MMPs and aggrecanases and generation of highly reactive oxygen species such as nitric oxide (NO); lead to cartilage tissue catabolism which progresses OA toward the later stages

	TNF- $\alpha$	A crucial player in proinflammatory cytokines in OA. Elevated during OA onset and promotes chondrocytes to produce a high level of nitric oxide and catabolic protease
	SDF-1	Elevated by three times in stages 1 and 2 of OA this leads to increasing the level of chondrocytes MMP-3, which has catabolic effects on the surrounding joint tissue by the release of tissue degrading proteases.
Anabolic (anti-inflammatory)	IGF	Stimulates ECM synthesis and decreases matrix catabolism
	TGF $\beta$	Maintain tissue haemostasis, stimulates the synthesis of ECM and decreases the catabolic activity of IL-1 and MMPs

### 1.1.3. Stages of OA

OA can be divided into five stages according to the severity of the illness. Stage 0 is considered to be healthy without any signs of OA or joint damage. At the opposite extreme, stage 4 is considered to be end-stage OA or including severe cases which cause severe pain, impair joint movement and result in disability (Table 1-2) (Sharma and Berenbaum, 2007; Aigner and Schmitz, 2011; Bliddal, Leeds and Christensen, 2014; Holland, 2017).

Table 1-2. Stages of OA. The columns show the different stages of OA, the characteristics of each stage in term of bone protrusion, joint destruction, severity of pain and treatment options for each stage. (Sharma and Berenbaum, 2007; Aigner and Schmitz, 2011; Bliddal, Leeds and Christensen, 2014; Holland, 2017)

Stages	Characteristic of joint	Joint destruction morphology	Severity of pain	General treatment
<p><b>0</b></p>  <p>Normal knee</p> <p>Cartilage</p> <p>Cart</p>	Normal	Healthy joint	No pain	No treatment was required for stage 0
<p><b>I</b></p> <p><b>Doubtful</b></p>  <p>Minimum disruption. There is already 10% cartilage loss.</p>	Minor protrusion of the bone on the joint area	No sign of cartilage loss, slight and superficially fibrillation.	No pain or any discomfort feeling.	Patients with risk factors have to start changing their lifestyle and glucosamine and chondroitin supplementation.
<p><b>II</b></p> <p><b>Mild</b></p>  <p>Joint-space narrowing. The cartilage to begin breaking down. Occurrence of osteophytes.</p>	“mild OA stage”. Greater bone protrusion but with normal space between the bone and a healthy level of synovial fluid for normal	Partial cartilage loss, middle zone fissures and lesions	Patients start pain experience, especially when walking, and symptoms of joint stiffness also start	Importantly lifestyle change and analgesics if required only.

	joint movement.		when sitting for a long time.	
<p>3</p> 	<p>“ moderate OA stage”.</p> <p>Distinct cartilage damage and narrowing of the space between the bone.</p>	<p>Partial cartilage loss, deep cartilage zone fissures and lesions</p>	<p>Persistent pain experience and joint swelling, especially during the activity and symptoms of joint stiffness also start when sitting for a long time.</p>	<p>Painkillers and cortisone injections are highly recommended. Viscosupplements of intra-articular injections of hyaluronic acid are also can be prescribed.</p>
<p>4</p> 	<p>“severe OA stage”.</p> <p>The joint space between bones is highly reduced.</p> <p>Cartilage is completely lost and severely decreased in the amount of synovial fluid, which leads to joint stiffness.</p>	<p>Complete cartilage loss</p>	<p>Severe pain and discomfort during the day.</p>	<p>Osteotomy, arthroplasty for severe knee OA,</p>

#### **1.1.4. Statistics of OA**

According to World Health Organization (WHO), OA is labelled as a priority disease because it is the leading cause of chronic disability around the world, especially for the elderly (> 70 years old) (Kaplan and Laing, 2004). In 2010, it was the eleventh most common cause of disability globally (Lozano *et al.*, 2010) but unfortunately, it is estimated to rise to ninth in the ranking by 2020 (Hermans *et al.*, 2012). Globally, 80% of OA patients had limitations in movement, while 25% had difficulty in proceeding with their main daily activities, representing a significant impact in terms of functional impairment and disability. In the UK, around one in 10 adults have been diagnosed clinically with symptomatic OA, and with 8.75 million people receiving treatment for osteoarthritis (60% female and 40% male) (Arthritis Research UK, 2018; Swain *et al.*, 2020). Recently, it has been estimated that treating osteoarthritis and rheumatoid arthritis is costing the UK economy £10.2 billion per year; worryingly, this figure is expected to reach around £118.6 billion by the next decade (Arthritis Research UK, 2018). Moreover, it represents one of the top five healthcare costs in Europe as a whole (Cross *et al.*, 2014). Clearly, OA represents a real and significant cost burden to global health and social care system.

#### **1.1.5. OA risk factors**

OA is a complex disease that can affect all ages; however, the effects are more pronounced in people older than 65 (Factors, 2000). In addition to age, OA is also associated with different risk factors, including obesity, joint injury and trauma, lack of activity or heavy exercise, occupational injury, genetic factors, diet and gender (Ashkavand, Malekinejad and Vishwanath, 2013; Mobasheri and Batt, 2016; Palazzo *et al.*, 2016). By way of illustration, women are twice as likely to suffer from OA as men, especially around the menopause, when estrogen levels decrease (Factors, 2000; Palazzo *et al.*, 2016). In fact, there is some debate among researchers as to the reasons for this; some suggest it is due to hormonal factors, while others believe it can be explained by the differences in muscle and bone strength between women and men (de Klerk *et al.*, 2009; Palazzo *et al.*, 2016). Moreover, excessive intake of carbohydrates and junk food could increase the risk, while antioxidants can help to protect against tissue injury (Ashkavand, Malekinejad and Vishwanath, 2013). Indeed, a daily supplement of vitamin C can provide threefold protection against the progression of OA because it acts as a strong antioxidant which can provide a protective function in terms of preventing oxidative stress-induced chondrocyte dysfunction from occurring in OA (Dunlap

Burton *et al.*, 2021). Vitamin D, meanwhile, plays a crucial role in healthy bone metabolism, so maintaining healthy vitamin D levels which is very important in protecting against the development and progression of OA (Factors, 2000). Normal bone metabolism is dependent on the presence of vitamin D, whereas low vitamin D tissue levels may impair the ability of bone to respond optimally to processes in osteoarthritis and indicate predisposition to progression of OA (Factors, 2000). Furthermore, genetic factors determine around half of hip, hand and knee OA instance (Ashkavand, Malekinejad and Vishwanath, 2013). Examples of common genes which are primarily responsible for the development of OA are the vitamin D receptor gene, insulin-like growth factor 1, cartilage oligomeric protein genes, type 2 collagen and growth differentiation factor 5 (Factors, 2000; Palazzo *et al.*, 2016). Moreover, obesity puts more load and pressure on joints, so there is a strong relationship between being overweight and the risk of OA (especially knee OA), this being significantly higher in females than in males (Factors, 2000; Palazzo *et al.*, 2016). According to the Framingham study, weight reduction by 5kg is likely to reduce the incidence of knee OA by 50% (Christensen *et al.*, 2007). Consequently, weight loss is a critical step in reducing the risk and progression of OA. In fact, all of the aforementioned risk factors contribute to increasing the severity of any joint disability.

### **1.1.6. Symptoms of OA**

Symptoms of OA vary depending on the severity of the disease (Table 1-2) and the type of joint affected. Generally, the knee, hip and small joint of the hand are more severely impacted than other joints. The most common symptoms of OA are pain and stiffness, followed by swelling, tenderness, and cracking sounds while moving the affected joints. Pain frequently occurs during activity, but night and rest pain can also occur. The symptoms become worse with the activity, which can affect impact the normal daily life by inhibiting performance of routine actions at work and at home. Moreover, the side effects of OA pain reduce the normal daily activities and medications side effects can also lead to adverse health effects, both directly and indirectly related to the joint disease (Sharma and Berenbaum, 2007; Kidd, 2012).

## **1.2. Cartilage**

### **1.2.1. Composition and cartilage repair**

Cartilage is a robust and flexible type of connective tissue which covers the surface of joints in order to absorb shock and to allow bones to move smoothly over each other with a low frictional coefficient (Sophia Fox, Bedi and Rodeo, 2009). There are three types of cartilage tissue in the human body: elastic cartilage (as found in the ear); fibrocartilage (in the

intervertebral disc) and hyaline cartilage (e.g., trachea and bronchi), which is the most widespread cartilage in the body (Patterson-Kane and Firth, 2014). Additionally, hyaline cartilage can be found in different parts of the body; this includes synovial joints, which are described as articular cartilage and represent a highly specialised connective tissue (Patterson-Kane and Firth, 2014). Articular cartilage consists of chondrocytes that make up about 5% of the tissue volume, alongside an extracellular matrix (ECM) which contributes the remaining 95% of the volume (Figure 1-5) (Neil, Caron and Orth, 2005; Firestein, 2013). Chondrocytes are mainly responsible for cartilage remodelling, by replacing broken macromolecules with newly synthesised ones (Miguel *et al.*, 2012). The function of chondrocytes is regulated by cytokines (Table 1-1) and growth factors (Van den Berg, 1999). Growth factors are a group of polypeptides that are generated by the body to stimulate cellular division, growth, and differentiation. In articular cartilage, growth factors work to regulate development and equilibrium of articular cartilage homeostasis over the human life span; examples include transforming growth factor- $\beta$ 1 (TGF-  $\beta$ 1), bone morphogenetic protein (BMP), insulin growth factor 1 (IGF 1), fibroblast growth factor (FGF) and platelet-derived growth factor (PDGF) (Fortier *et al.*, 2011). ECM is composed mainly of proteoglycans, collagens, and water (Darling and Athanasiou 2005). Importantly, collagen is the most prominent structural macromolecule in ECM contributing of 60% of the dry cartilage weight (Patterson-Kane and Firth, 2014). In general, 90% to 95% of the collagen is type II fibrils collagen, which helps to stabilise the cartilage matrix and provides shear, tensile stiffness, and strength to the tissue. Moreover, minor quantities of the other types of collagens (such as collagen I, IV, V, VI, IX and XI) are also present, helping to stabilise the type II collagen (Patterson-Kane and Firth, 2014).

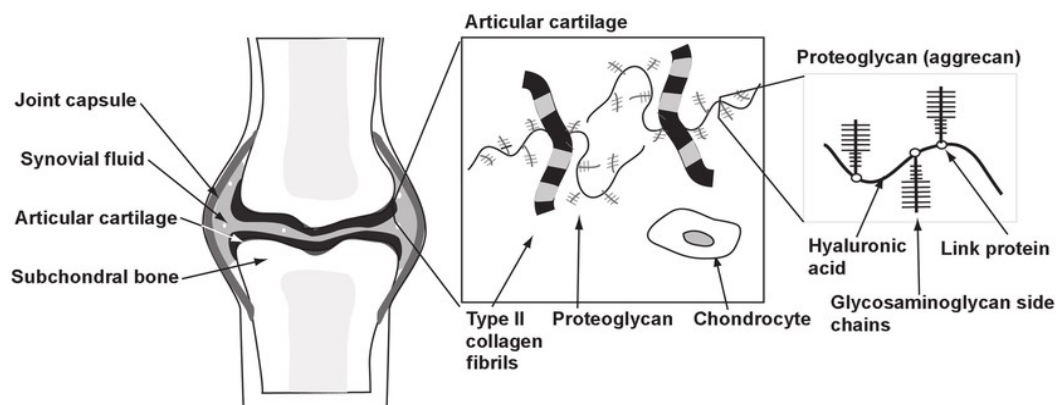


Figure 1-5. Articular cartilage components. Chondrocyte in articular cartilage and the ECM which composed of proteoglycan and collagen. Proteoglycan consists of core protein and glycosaminoglycan (GAG) side chain that is directly attached to the link protein, adapted form (Neil, Caron and Orth, 2005).

Turning to proteoglycans (PG), these are glycosylated protein monomers which are essential for normal cartilage function. In term of composition, they consist of decorin, biglycan, fibromodulin and aggrecan (Figure 1-6). Aggrecan account for the majority of PG content (approximately 50-85%), consisting of chondroitin sulphate (CS) and keratan sulphate (KS) side chain. It can interact with hyaluronan to form large PG aggregation along with protein links and fill the interfibrillar space of the cartilage ECM. Importantly, it maintains cartilage osmotic properties which are necessary for compressive loads resistance. Moreover, water and dissolved electrolytes represent the highest concentration within the cartilage accounting for 80%. Of the water, 30% is associated with collagen intrafibrillar space while the remainder is contained within the matrix pore space. The movement of water over the cartilage and articular surface helps to provide lubrication and carry nutrients to the chondrocyte. Furthermore, there exist a number of non-collagenous proteins and glycoproteins in the articular cartilage which are assumed to play a role in the organisation and maintenance of ECM structure (Miguel *et al.*, 2012; Firestein, 2013; Patterson-Kane and Firth, 2014). Therefore, cartilage is almost tending to be found in places where not only support and structure are needed but also a little flexibility as well. By its very nature, articular cartilage structure can tolerate and absorb repetitive and intensive shock and stress (of 2.5– to 5.0 times body weight) with only slight friction during daily walking. Nevertheless, it has a limited rate of complete self-repair following damage and lacks ability to heal after injury (Wang and Peng, 2015; Mobasheri and Batt, 2016). Consequently, the complex function and structure of articular cartilage can be affected by even a minor injury. In addition, destroyed chondrocyte function can affect the balance of synthesis and catabolism of the cartilage, leading to cartilage destruction (Figure 1-7), followed by OA (Sharma and Berenbaum, 2007).

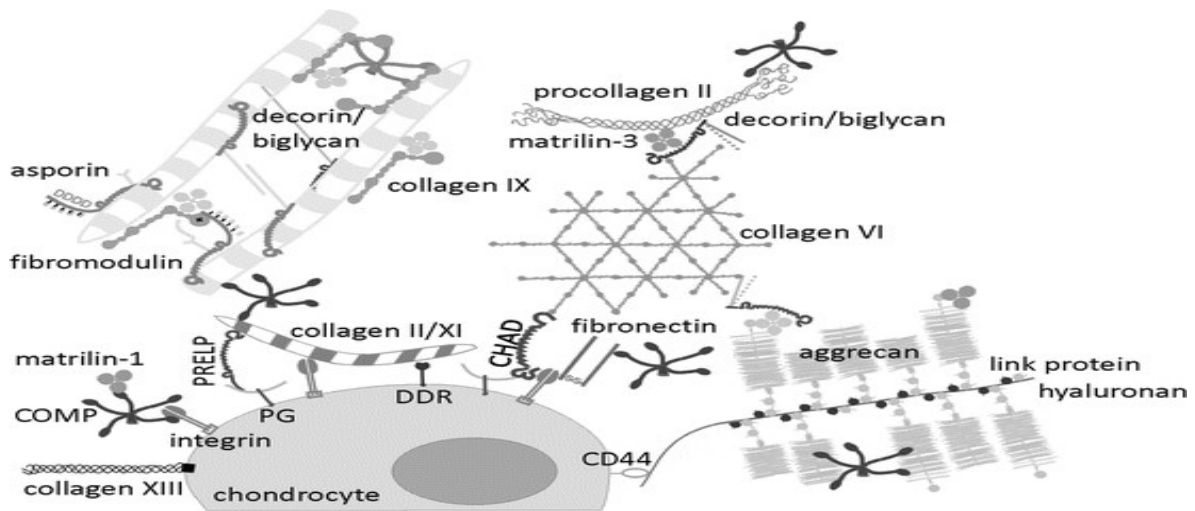


Figure 1-6. Molecular organization of cartilage matrix. A variety of protein interactions stabilizes the cartilage ECM such as decorin, biglycan, fibromodulin and aggrecan, adapted from (Grässel and Aszódi, 2017).

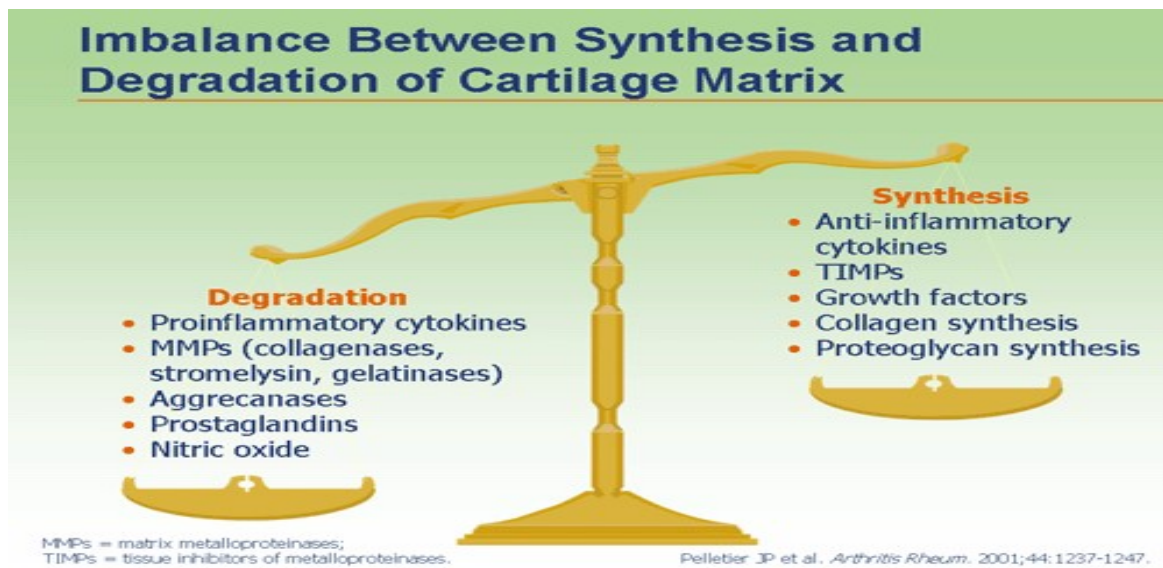


Figure 1-7. Loss of homeostasis in cartilage. Cartilage destruction and finally OA results from a failing of chondrocytes to maintain a homeostatic equilibrium between matrix synthesis and degradation, adapted from (Pelletier, Martel-Pelletier and Abramson, 2001).

### 1.3. Treatment of OA

There are different types and methods of OA treatment available. They predominantly aim to relieve symptoms, improve patient quality of life, and prevent OA complications and progression. The primary treatment modalities for OA include non-pharmacological (lifestyle changes), pharmacological (medications, supportive and nutritional supplements) and surgical

treatment (Bijlsma, Berenbaum and Lafeber, 2011). Non-pharmacological treatment is mainly appropriate for the early stages of OA, while surgical intervention is frequently used during the late or advanced stages. In contrast, pharmacological treatment is suitable for all stages of OA.

### **1.3.1. Non-pharmacological treatment**

Non-pharmacological modalities can improve patient lifestyle through helping to maintain healthy weight, while regular exercises is aimed at slowing the disease's progression and improving the patient health, especially in the early stages of OA (Mobasher and Batt, 2016). Generally, being overweight usually tends to worsen OA symptoms due to more pressure being placed on joints (especially the knee joint) thus exacerbating the disease. Accordingly, there is a strong relationship between obesity and OA development and progression (Bliddal, Leeds and Christensen, 2014). Exercise is generally recommended by medical professionals to improve mobility and joint function, and to increase muscle strength around OA joints (National Clinical Guideline Centre (UK), 2014). Moreover, exercise improves aerobic status and strengthens muscles both of which are beneficial for OA sufferers, particularly in cases affecting the hip or knee (Roddy, Zhang and Doherty, 2005). For example, aerobic walking, swimming, and muscle strength exercises are good for joint problems. In addition, exercising in a group can help to motivate patients to live more active daily lives. However, specific daily or weekly exercise targets must be agreed upon between patients and medical professionals, so as to achieve treatment goals while preventing any adverse reactions or worsening of OA symptoms (National Clinical Guideline Centre (UK), 2014).

In fact, regular exercise alongside healthy food such as antioxidants (e.g. fruits, vegetables, nuts, grains, poultry, fish, turmeric, ginger) or, food rich in vitamin C, vitamin D, or calcium (e.g. milk, cheese, yoghurt) is highly beneficial for losing weight, improving posture, reducing stress, strengthening joints, alleviating pain and other symptoms of OA (McAlindon *et al.*, 1996; Factors, 2000; Ashkavand, Malekinejad and Vishwanath, 2013; Bliddal, Leeds and Christensen, 2014). Patients should be encouraged to improve their life habits to achieve improved health and to avoid OA complications. Overall, modification of health behaviour through advice and education is positive way to improve patient quality of life.

### **1.3.2. Pharmacological treatment**

There are many types of medical treatment available for OA. Current treatment is only symptomatic, with no therapeutic treatment being sufficient to cure the disease.

### **1.3.2.1. Paracetamol**

Mild pain can be relieved simply by using analgesics such as paracetamol (4g/day for six weeks), which is recommended as the first-line therapy for OA as it is well-known for its safety and efficacy (Miceli-Richard *et al.*, 2004; Bijlsma, Berenbaum and Lafeber, 2011). Nevertheless, patients should be counselled to only take the prescribed dose and to avoid the risk of toxicity associated with taking a higher dose (Roberts *et al.*, 2016). Paracetamol acts by inhibiting prostaglandin synthesis in the central nervous system (CNS) by inhibiting the cyclooxygenase (COX) enzymes. However, it has a lower effect on COX in peripheral tissues, which accounts for its weak anti-inflammatory activity (Rang *et al.*, 2012). In spite of this, recent research has challenged the usefulness of paracetamol in the treatment of OA pain. In 2015, a systematic review and meta-analysis (involving 12 reports) was undertaken to evaluate its efficacy and safety for treatment of OA compared with placebos. It was concluded that paracetamol has a minimum effect on OA pain during short-term use (>2weeks but  $\leq$  three 3 months) (Machado *et al.*, 2015). Similarly, another large meta-analysis supports the finding that paracetamol does not achieve any important clinical difference in OA pain relief. The study assessed the effectiveness of paracetamol and non-steroidal anti-inflammatory drugs (NSAIDs) as analgesics for OA pain compared to a placebo. Data was collected from 74 randomised trials involving a total of 58,556 patients with osteoarthritis, and it was found that all of the analgesics improved pain symptoms compared with the placebo. Nevertheless, unlike NSAIDs, paracetamol failed to achieve the minimum clinically relevant difference (Moore *et al.*, 2016; Torjesen, 2016).

### **1.3.2.2. NSAIDs**

Generally, soluble mediators such as prostaglandins and cytokines play a significant role in the inflammation of joints by potentiating chondrocytes to produce metalloproteinases (MMPs) leading to synovitis and bone inflammation. Therefore, use of the anti-inflammatory medication can have a beneficial effect during treatment of OA (Berenbaum, 2013). NSAIDs (such as ketorolac, indomethacin, diclofenac, naproxen and ibuprofen) are more helpful and potent as analgesics for inflammatory incidents, particularly when paracetamol has been ineffective (Roberts *et al.*, 2016; Torjesen, 2016). NSAIDs act as analgesics and reduce inflammation by inhibiting the activity of cyclooxygenase in the CNS and peripheral tissue which is known to be the first step in the synthesis of prostaglandin (PG) from arachidonic acid (Figure 1-8). In the phospholipids of cell membranes, arachidonic acid is present and is released by the enzyme phospholipase A2 (Fendrick and Greenberg, 2009; Wang *et al.*, 2021). It then

catalyzes the production of prostaglandins and thromboxane via cyclooxygenase (COX) enzymes. COX enzymes exist in two isoforms, COX-1, and COX-2. COX-1 is expressed throughout the body and is present in most cells (such as stomach, platelet, kidney, endothelial cells and immune cells) to maintain normal body physiological processes. It is essential in the production of protective gastric mucosal secretions and regulation of gastric acid, promotion of platelet aggregation and the maintenance of renal blood flow. However, in some circumstances, such as inflammation, the expression of COX1 can be induced, producing pro-inflammatory prostaglandins that contribute to the pathophysiology of inflammatory conditions. Moreover, COX-2 is not expressed in tissue under normal circumstances, but rather is induced by pro-inflammatory stimuli commonly seen in cellular injuries (IL-1, TNF- $\alpha$ , and cytokines). Therefore, COX-2 acts as an inflammatory mediator which is produced in response to inflammation and pain initiation (Crofford, 1997; Fendrick and Greenberg, 2009).

Prostaglandins are physiologically active lipid compounds that can regulate fever and pain due to their homeostatic and inflammatory effects on the human body (Phillips, Contreras, and Oswald, 2020). They are the major mediators of inflammatory cascades resulting in peripheral sensitisation, inflammation, fever, and chronic pain. Prostaglandin H<sub>2</sub> (PGH<sub>2</sub>) is the main precursor for other prostaglandins (PGE<sub>2</sub>, PGI<sub>2</sub>, and PGF<sub>2</sub>) and thromboxane (Figure 1-8). PGE<sub>2</sub> is an important mediator of many biological functions, such as regulation of immune responses, blood pressure, and gastrointestinal (GI) integrity (Lippiello, 1981; Wang et al., 2021). Dysregulation or inhibition of PGE<sub>2</sub> synthesis has been associated with many pathological conditions such as peptic ulcer, hypertension, and GI bleeding. With regard to inflammation, PGE<sub>2</sub> is of particular importance because it is involved in all processes that lead to inflammation (including redness, oedema and pain). Moreover, PGE<sub>2</sub> causes arterial dilatation and increased microvascular permeability via increased blood flow into the inflamed tissue resulting in redness and swelling. Pain results from the effects of PGE<sub>2</sub> on peripheral sensory neurons as well as centrally within the spinal cord and the brain (Lippiello, 1981; Wang et al., 2021).

Additionally, PGD<sub>2</sub> is a major prostaglandin that is synthesised in CNS and in peripheral tissues that function in inflammatory, pain perception and homeostatic capacities. PGF<sub>2</sub> plays a significant part in renal function, contraction of arteries, myocardial dysfunction, and pain (Phillips, Contreras, and Oswald, 2020; Wang et al., 2021). Moreover, thromboxane and prostacyclin (PGI<sub>2</sub>) have important roles in terms of aggregation of blood platelets and blood clot formation. Indeed, this process is strongly stimulated by thromboxane and is inhibited by

PGI<sub>2</sub>. Prostacyclin is a potent vasodilator which is synthesised in the walls of blood vessels and serves the physiological function of preventing platelet aggregation. Furthermore, it is an important mediator of oedema and of pain associated with inflammation. In contrast, thromboxane is synthesised within platelets, in response to blood vessel injury, it causes platelet adhesion and aggregation to promote clot formation. Moreover, it causes smooth muscle contraction and proliferation, and activation of endothelial inflammatory responses (Phillips, Contreras, E, and Oswald, 2020; Wang et al., 2021). Overall, the synthesis of different types of prostaglandins (PG) from arachidonic acid is a tightly regulated process involving cyclooxygenase (COX) enzymes, which play critical roles in various physiological and pathophysiological processes in the body.

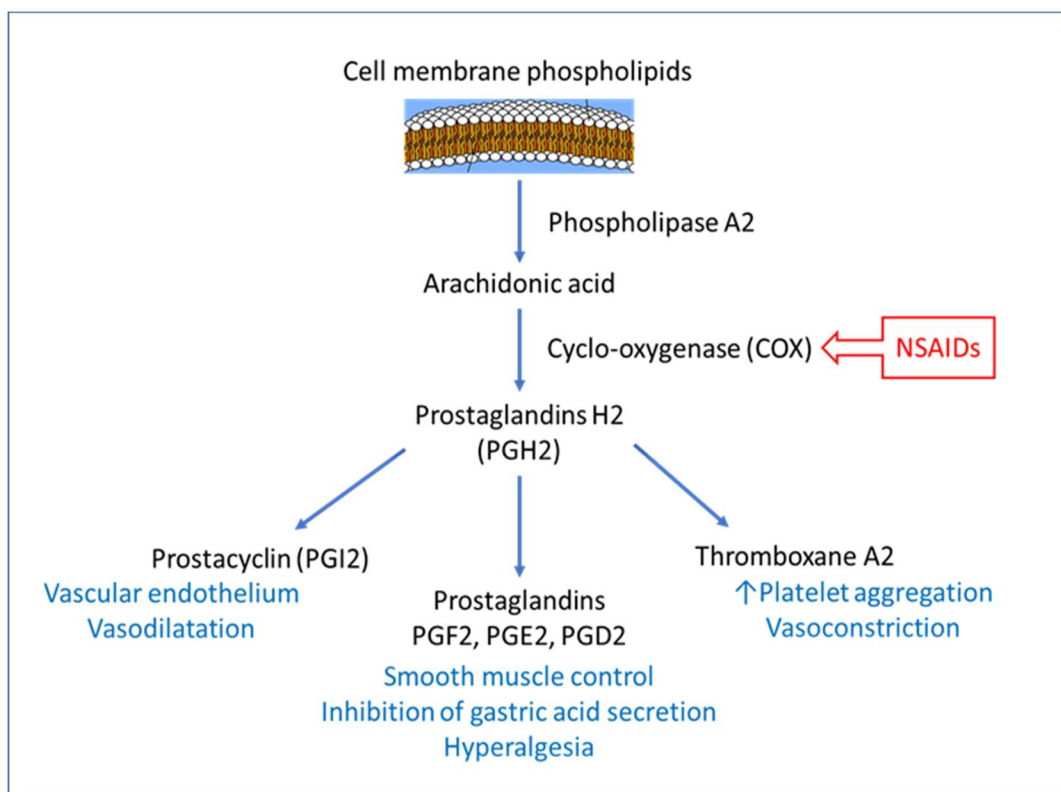


Figure 1-8. Mechanism of action of non-steroidal anti-inflammatory drugs (NSAIDs) and arachidonic acid pathway. This pathway showing production of prostaglandins from membrane phospholipids in presence of cyclooxygenase (COX) enzymes which is inhibited by the NSAIDs. Prostaglandins H<sub>2</sub> is converted by tissue specific isomerase to multiple prostanoids such as prostacyclin, thromboxane A<sub>2</sub>, prostaglandin F<sub>2</sub>, E<sub>2</sub> and D<sub>2</sub>. Adapted from (Rang *et al.*, 2012)

There are three types of NSAIDs; traditional or nonselective type (such as ibuprofen, naproxen, aspirin and diclofenac); COX-1 inhibitor selective type (such as indomethacin), and the COX-

2 inhibitor selective type (such as celecoxib and etoricoxib). The COX-1 selective types are mainly responsible for the gastrointestinal tract (GIT) side effects, such as GIT mucosa erosion, ulcers, bleeding, and GIT obstruction. COX-2 meanwhile leads to cardiovascular (CV) side effects such as hypertension, congestive heart failure, myocardial infarction and stroke (Patrignani *et al.*, 2011).

Table 1-3 The dosage and route of administration of common types of NSAIDs used in OA treatment (Fendrick and Greenberg, 2009).

NSAID	Route/dose
Indomethacin	Orally: 25mg BID or TID up to maximum 200mg/day. Extended release: 75-150 mg/day. Suppository: 50 to 200 mg rectally per day in divided doses
Ketorolac	Orally: 20 mg orally once followed by 10 mg every 4 to 6 hours when required. Parenteral injection: 30 mg IV/IM every 6 hours up to a maximum 120 mg/day. The maximum combined (oral and parenteral) duration of treatment is five days.
Naproxen	Orally: 250 -500 mg twice a day. Controlled release: 750 -1000 mg orally once a day. For the advanced stage of OA, the dose can be increased to 1500 mg orally once a day for a limited time up to 6 months
Diclofenac sodium	Orally: 50-75 mg, 2 or 3 times with maximum 150 mg daily. Extended-release tablets: 100 mg orally once a day. Topical: gel applies 2-4 g to the affected area 4 times daily with a maximum of 32 g/day over all affected joints.
Ibuprofen	Orally: 200-400mg every 4 -6 hours. Maximum 3200 mg orally per day in divided doses
Celecoxib	Orally: 200 mg once a day OR 100 mg orally twice a day
Meloxicam	Orally: 15 mg once daily (oral suspension) or 10 mg daily (oral capsule).
Etoricoxib	Orally: 30mg once a day, increase to a maximum of 60mg once a day if needed

In terms of administration, NSAIDs are available in oral, injectable and topical dosage forms, and all are effective in alleviating pain and inflammation. Table 1-3 shows the dosage and administration routes of NSAIDs in OA treatment. However, NSAIDs must be taken with caution by patients with GIT and CV medical conditions, such as peptic ulcer, angina, heart attack, myocardial infarction or stroke (Muller, 2018). In addition, concomitant drugs should generally be avoided because using a combination of NSAIDs has no impact (aside from increasing side effects), so the risk can actually be raised by increasing treatment (Pelletier *et al.*, 2016; Muller, 2018). It is also important to assess the desire of each patient for OA treatment and to weigh up the risks and rewards of using NSAIDs. To illustrate, reduction in ambulatory pain and alleviation of difficulty in doing daily activities are the most fundamental benefits for patients with no risk factors (Hochberg, McAlindon and Felson, 2000). Contrastingly, the risk of myocardial infarction and stroke are the most critical risk outcomes to be avoided for patients using NSAIDs, especially selective COX-2 inhibitors. Generally, choosing anti-inflammatory analgesic therapy has become complicated due to increased understanding of associated toxicities; it is absolutely essential to consider the presence of GIT and CV risk factors when NSAIDs are used. Accordingly, a patient suffering from GIT could be offered a proton pump inhibitor alongside oral NSAIDs to reduce the risk of GIT side effects. As touched upon above, NSAIDs are available in topical forms (such as creams, gels and solutions) that are applied directly to affected joints. They can be particularly useful for OA in the knees or hands to relieve pain and swelling in joints and may be preferred to oral NSAIDs due to their safety and efficacy profile (Rannou, Pelletier and Martel-Pelletier, 2016). Overall, the risks of GIT and cardiac toxicity limit the use of NSAIDs, with paracetamol being considered as a safe and effective alternative for mild pain conditions (Muller, 2018). Table 1-4 illustrate the advantages and disadvantages of NSAIDs.

Table 1-4. Advantages and disadvantages of using NSAIDs.

Advantages	Disadvantages
Effective in inflammation and pain control	Does not influence disease progression
Effective in swelling reduction Improve mobility and stiffness	GIT side effects (mainly COX 1 inhibitor and the non-selective NSAIDs): GIT mucosa erosion, bleeding and peptic ulcer.
Affordable cost Available in different routes of administration Improve the general quality of life	CV side effects (mainly COX 2 inhibitor): angina, heart attack, myocardial infarction, bleeding and stroke

### 1.3.2.3. Corticosteroids

Corticosteroids or steroids are a type of synthetic medication that mimics the body's natural hormone cortisol. When administered at a dose higher than physiological levels, they interact with steroid hormone receptors on nuclear membranes and act as corticosteroid hormone receptor agonists. They reduce inflammation, and inflammatory chemical production together with the activity of the immune system in order to decrease tissue damage. In addition, they decrease erythema, heat and swelling of inflamed body parts (Ayhan, 2014). Therefore, corticosteroids such as betamethasone, dexamethasone, triamcinolone acetonide and prednisolone are mainly used in the treatment of inflammatory conditions such as systemic vasculitis, gout, asthma, rheumatoid arthritis, multiple sclerosis, and OA. In relation to OA, they act by decreasing synovial inflammatory mediator expression (such as IL-1 $\beta$ , TNF- $\alpha$ , IL-8, MMP-3, basic fibroblast growth factor (b-FGF) and transforming growth factor B (TGF $\beta$ )), which leads to decreased inflammation (Huebner, Shrive and Frank, 2014). In addition, in OA they are commonly used via the intra-articular (IA) injections route due to their rapid anti-inflammatory and immunosuppressive effects (Wernecke, Braun and Dragoo, 2015). However, the effects of corticosteroids are not long-lasting (maximum 3 months) and repeated IA injections are required (Perkins, Whiting and Lee, 2017). With regards to long term usage, the benefits of corticosteroid injections are limited and can be accompanied by adverse effects (such as hot flashes, subcutaneous atrophy, risk of infection, skin depigmentation, muscle weakness, suppression of adrenal glands and growth retardation) (Hajjalilo *et al.*, 2016; Perkins, Whiting and Lee, 2017; Perni and Prokopovich, 2017). Table 1-5 illustrates the advantages and disadvantages of corticosteroids.

Table 1-5. Advantages and disadvantages of using corticosteroids.

Advantages	Disadvantages
Anti-inflammatory and immunosuppressive effects.	Dose not influence disease progression
Reduce erythema, heat and swelling at inflamed body parts.	Repeated injection leads to cartilage softening and the tendons weaken in the injected joint
Improve mobility and stiffness	
Fast acting and prolonged treatment effect	Hypercortisolism side effects
Improve the general quality of life	High risk for increased blood sugar level (caution for diabetic patients).

In 2014, Osteoarthritis Research Society International (OARSI) guidelines proposed intra-articular injection of corticosteroid for knee OA treatment (McAlindon *et al.*, 2014). They can be used to reduce swelling and pain (Wernecke, Braun and Dragoo, 2015; McAlindon *et al.*, 2017; Wehling *et al.*, 2017) and can provide pain relief for around 2 to 4 weeks (up to maximum of 3 months, as mentioned above) which is considered to be an advantage over painkiller medication. For example, injection of methylprednisolone acetate (10 mg - 80 mg depending on joint size) and triamcinolone (10 mg - 40 mg/mL injectable suspension depending on joint size) can be repeated every 3 months (albeit with no more than four injections per year) (Buyuk *et al.*, 2017). However, prolonged exposure to intra-articular corticosteroid injections can lead to side effects on articular cartilage which accelerates the progression of OA (Foster *et al.*, 2015; Wehling *et al.*, 2017). A recent study has shown that intra-articular corticosteroid causes a more significant loss in cartilage volume when compared with intra-articular saline (McAlindon *et al.*, 2017). In addition, another study has determined that chondrotoxicity is a significant side effect which is associated with exposure to a high dosage of intra-articular corticosteroid over a long period (Wernecke, Braun and Dragoo, 2015). Consequently, the use of corticosteroids (40 mg/dose) is limited to three to four intra-articular injections annually with at least a 3-month gap between them (Wernecke, Braun and Dragoo, 2015; He *et al.*, 2017).

#### 1.3.2.4. Opioid analgesics

Furthermore, opioid medications such as morphine, codeine, and tramadol, which are known to be strong painkillers, can be used in severe pain cases or when other analgesics are ineffective. They exert their major effects by interacting with opioid receptors in the CNS (e.g.,

thalamus, hypothalamus, and cortex in the brain and substantial gelatinosa in the spinal cord) and other anatomic structures, (e.g., gastrointestinal tract and urinary bladder). In addition, they cause hyperpolarisation of nerve cells, inhibition of nerve firing, and presynaptic inhibition of transmitter release (Rang *et al.*, 2012). Although they are very potent for pain relief and not prone to the GIT and CV complications associated with NSAIDs, they nevertheless have serious side effects which limit their use. The most common examples of opioid side effects are nausea, constipation, dizziness, confusion, withdrawal, and tolerance. Additionally, to achieve maximum pain relief, opioids may be combined with other types of analgesics, such as concomitant use of codeine and paracetamol. Sustained release (SR) formulation of tramadol produces prolonged plasma level effects while decreasing the incidence of opioid side effects and improving patients' tolerability. On the other hand, short-term treatment is preferred, and dose titration is important to minimise rapid drug discontinuations (Pelletier *et al.*, 2016). In general, opioids must be used in the short term under regular medical supervision to avoid adverse reactions (Muller, 2018).

### **1.3.2.5. Hyaluronic acid**

Hyaluronic acid (HA) is a complex glycosaminoglycan compound widely present in body tissues, with the highest concentration to be found in synovial fluid. It is one of the major components of the articular cartilage matrix (T.R. *et al.*, 2016). The primary function of HA is to provide viscoelasticity and lubricating properties to synovial fluid, allowing normal fluid flow, and joint motion alongside reduction of articular cartilage damage (Balazs and Denlinger, 1993; Goldberg and Goldberg, 2010). Furthermore, it prevents large plasma molecules from entering synovial fluid while facilitating small molecules to provide tissue nutrients (Goldberg and Buckwalter, 2005). The normal concentration of HA in synovial fluid is 297 mg per 100 mL which decreases in OA to 141 mg/100 mL (DECKER *et al.*, 1959). Therefore, the main objective treatment of OA with HA is to restore the viscoelastic properties of the synovial fluid. Hyaluronans (HAs) have recently been used for the treatment of painful OA and are known as a viscosupplementation treatment for OA (Balazs and Denlinger, 1993; Goldberg and Goldberg, 2010). The synthesis and levels of HA can be disrupted and decreased by increasing pro-inflammatory cytokines and protease in joints. Any abnormality in HA levels can potentiate cartilage damage and OA disease progression (Goldberg and Buckwalter, 2005; Goldberg and Goldberg, 2010). Therefore, the main goal of intra-articular HA injection is to restore metabolic homeostasis by improving joint function, reducing pain, promoting healing, improving lubrication, and stimulating the synthesis of nutritional and cartilage matrix

components (Goldberg and Buckwalter, 2005; Goldberg and Goldberg, 2010). HA injection (single dose 20 mg/2 mL) usually provides a long duration of action, typically around 6 months. On the other hand, it may cause transient pain, redness, tenderness at the site of injection, swelling, stiffness and difficulty in moving (Reinmüller, 2003). Generally, HA is an active agent in OA which reduces the side effects of oral medication, provides lubrication, and has anti-inflammatory and chondroprotective effects on the affected joint (Bowman *et al.*, 2018).

### **1.3.2.6. Nutritional supplements**

Symptomatic patients are sometimes prescribed a group of medications known as slow acting drugs for OA as a nutritional supplement (e.g., glucosamine sulphate and chondroitin sulphate). These represent a natural and major component of body cartilage and synovial fluid, with their function being to stimulate the anabolic process of the cartilage metabolism and they have instigated anti-inflammatory action in the cartilage. These two mechanisms delay the progression of cartilage damage and regenerate joint structure, thereby reducing pain, stiffness and increasing joint mobility (Jerosch, 2011). They can be used as a single supplement or as a combination to maximise their effects. However, there has been considerable controversy regarding glucosamine and chondroitin use. In fact, some researchers have indicated that glucosamine hydrochloride has no beneficial effects on OA (Bijlsma, Berenbaum and Lafeber, 2011; Vasiliadis and Tsikopoulos, 2017), while others have provided evidence for the symptomatic efficacy of glucosamine and chondroitin in the treatment of OA (McAlindon *et al.*, 2014; Zeng *et al.*, 2015; Vasiliadis and Tsikopoulos, 2017). In 2015, a clinical double-blind randomised placebo-controlled study was published, which assessed the efficacy of single and combined effects of glucosamine and chondroitin in knee OA (Fransen *et al.*, 2015). This study found that using a combination of glucosamine and chondroitin had a significant effect on reducing joint space narrowing in knee OA over the 2-year treatment period, whereas significant symptomatic differences between single and combination treatment above the placebo could not be detected over the study period (Fransen *et al.*, 2015). Overall, using both glucosamine (1500mg) and chondroitin (150 mg) for 3 months in the treatment of OA is assumed to be safe and could provide benefits in terms of disease modification. This goal can mainly be achieved through combined treatment rather than a single dose but there is currently no satisfactory information on the effectiveness of glucosamine and chondroitin on OA.

In addition, it has been stated that daily supplementation with omega-3 (fish oil) has significant clinical benefits in reducing OA inflammation (Rajaei *et al.*, 2015). It mainly acts by reducing arachidonic acid-binding to cell membranes, causing a corresponding decrease in inflammatory

markers (such as TNF- $\alpha$ ), decreased production of cytokines (such as IL-6), and cartilage-degrading enzymes (such as protease) (Rajaei *et al.*, 2015). Therefore, in addition to the health benefits to the human body of omega-3, such as maintaining brain health and lowering risk of heart disease, daily supplementation with 2.6 gm of omega 3 for 12 months can result in significant clinical benefits in term of OA pain and inflammation (Geusens *et al.*, 1994)

### **1.3.2.7. Supportive devices**

In addition to medical treatment, and to bypass side effects, the effectiveness of supportive devices as another method for OA pain control is well established. Transcutaneous electrical nerve stimulation (TENS) is one of the most common examples of a non-invasive modality used in physiotherapy to control both acute and chronic OA pain (Osiri *et al.*, 2009). It is a small battery-operated machine which is connected to electrodes that stick to the skin. When the machine is switched on, electrical impulses are delivered to affected body parts. These impulses or electric currents can stimulate nerve cells that diminish the transmission of pain signals that go to the brain and spinal cord thereby helping relieve pain and relax muscles. In addition, the production of endorphins in the body could be stimulated, acting as a natural pain killer that blocks the perception of pain (Jones and Johnson, 2009). Many studies into the effectiveness of TENS in OA pain have been conducted. Meta-analysis has assessed the efficacy of TENS and other devices in 1-2 week regimens in controlling knee OA, finding that TENS is a safe and clinically significant method for short-term knee OA pain relief (Bjordal *et al.*, 2007). Moreover, a sizable review study, undertaken in 2009 investigated the effectiveness of TENS in the treatment of OA (especially knee OA). This included assessment for pain relief, joint function and imaging changes, with different modes of TENS application being used. Eventually, it was concluded that TENS can be effective in terms of pain relief and decreased knee stiffness with at least 4 weeks duration of treatment (Osiri *et al.*, 2009). In addition, Maeda *et al.* (2017) have suggested that the use of TENS in combination with local heat application can relieve pain, and improve mobility and balance in patients with knee OA, when compared with TENS alone (Maeda *et al.*, 2017). On the other hand, one systematic review has suggested that TENS is not effective as an analgesic for knee OA pain (Rutjes *et al.*, 2009). These apparent contradictions stem from different study designs with different outcomes, and different types and methods of using TENS devices. Overall, it is an effective, safe, and inexpensive, short-term type of non-pharmacological pain relief.

Furthermore, there are different types of aids and devices which can help and support some OA patients, as they can feel more secure and stable when using them (such as walking sticks,

shoe insoles and braces). These kinds of joint assistance tools decrease pain by reducing weight and pressure on damaged joints, improving the ability of patients to move and walk comfortably (Van Raaij *et al.*, 2010; Carbone *et al.*, 2013).

### 1.3.3. Surgical treatment

The last treatment option is surgical management for patients with end-stage OA, when the joints are severely damaged and after all other types of pharmacological and non-pharmacological treatments have failed. Surgical treatment available include arthrodesis, arthroplasty, arthroscopy, osteotomy and mosaicplasty, (Table 1-6) (Hochberg, McAlindon and Felson, 2000; Stott, 2017). Arthrodesis is a joint fusion surgical procedure which is usually performed on the hand, foot, spine, ankle and wrist (Hochberg, McAlindon and Felson, 2000; Proffen *et al.*, 2013). In this procedure, two bones of the affected joint are fused together to become one solid bone. This can make the joint more stable and help to increase its weight tolerance. Nevertheless, despite alleviating pain, it is also associated with a loss of motion, thus it is not recommended for the upper and lower extremities (Hochberg, McAlindon and Felson, 2000). Meanwhile, arthroplasty is a total joint replacement procedure in which joints are replaced with metals or artificial plastic parts. It is mainly used for the hip, knee, and shoulder joints (glenohumeral joints) (Hochberg, McAlindon and Felson, 2000; Zachwieja, Perez and M, 2017). Nowadays, around seven million Americans are living with a hip or knee joint replacement and the number is estimated to increase over the coming years (Maradit Kremers *et al.*, 2015). In fact, it is the most effective medical procedure for the treatment of end stage OA, especially for elderly patients and lasts over 20 years (Hochberg, McAlindon and Felson, 2000; Zachwieja, Perez and M, 2017).

In contrast, arthroscopy was used widely in the past as a treatment option for the advanced stage of OA. This surgical procedure is performed in order to remove damaged cartilage and debris from affected joints, clean bone surfaces, and repair damaged tissue. It was often used on younger patients to prevent any disease progression. However, recently it has been replaced by other types of surgical treatment as its benefits and effectiveness are rather limited, especially when substantial joint-space narrowing is present (Hochberg, McAlindon and Felson, 2000; Felson, 2010; Zachwieja, Perez and M, 2017). Turning to osteotomy, this is mainly aimed at rearrangement of affected joints (primarily knee joints), by adding or removing a small section of bone to improve shape and function as well as alleviating pain. However, it is not a permanent procedure and further surgery may become necessary in the future, as it is performed

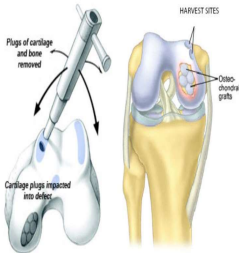
mainly to relieve symptoms and delay the rate of progression of the disease (Hochberg, McAlindon and Felson, 2000; Zachwieja, Perez and M, 2017).

Recently, mosaicplasty has been developed, consisting of osteochondral autografts which involve multiple cylindrical osteochondral grafts (cylindrical filling of bone and cartilage) transplanted into the drilled holes at the affected joint (Solheim *et al.*, 2013). In this surgical procedure, osteochondral graft plugs are harvested from the less weight-bearing areas (non-articulating regions of the joint surface) of the donor site; subsequently, cartilage repair occurs via natural healing processes (Wajid *et al.*, 2011; Solheim *et al.*, 2013). For example, in knee mosaicplasty, the most commonly used donor sites are the patellofemoral area and the edges of the medial and lateral femoral condyles as they are non-weight-bearing sites (Wajid *et al.*, 2011). In fact, using numerous small osteochondral cylinders instead of one large plug is preferable as multiple small ones can be placed next to each other to maintain articular surface curvature and cover articular defects. It is suitable for younger age patients (<50 years old) due to decreased repair capacity in older patient's age. Although it mainly targets the knee joint, it is also appropriate for elbow, ankle, and hip joints. Generally, it is a one stage procedure that is inexpensive (\$313.84 cost per point change). It is also relatively safe because use of a donor site on the patient's own body, means there is no risk of disease transmission or immunological reaction to the graft (Robert, 2011; Wajid *et al.*, 2011; Schrock *et al.*, 2017).

Overall, surgical treatment of OA is very effective and the best option for the late stage, as it completely relieves pain, and stiffness while improving motion and patient quality of life. Nevertheless, it is controversial due to its complications and cost. Generally, some operations are cost effective; for example, for arthroplasty the current cost burden to Medicare is US\$25,568 in patients with no complications (such as coagulopathy, congestive heart failure, and electrolyte imbalance) and \$50,648 for patients with complications (McLawhorn and Buller, 2017), while in the UK arthroplasty's is costly and its economic cost is estimated to be more than £850 million compared with around £1,34 million for arthroscopy (Chen *et al.*, 2012). In addition, complications include wound healing problems, infections, inflammation, OA in nearby joints due to overloading and postoperative instability (Stott, 2017; Zachwieja, Perez and M, 2017). Table 1-6 illustrates the major advantages and disadvantages together with the candidate group for each type of surgical treatment.

Table 1-6. Surgical treatment for OA, their advantages, disadvantages, and candidate group for each type of surgical treatment.

Surgical treatment types	Advantages	Disadvantages	Age group and candidates
<p>Arthrodesis (Joint fusion)</p> 	<p>Stabilize and strengthen the joints.</p> <p>Significantly relief OA pain.</p>	<p>Associated with loss of flexibility and motion.</p> <p>Not suitable for the upper and lower extremities.</p> <p>The possibility of wound-healing complications.</p>	<p>Any age groups.</p> <p>Mainly for hand, foot, spine, ankle, and wrist.</p>
<p>Arthroplasty (Total joint replacement)</p> 	<p>Most effective medical procedure for end stage OA.</p> <p>Last for over 20 years.</p> <p>Safely relief pain, improves joint movement and patient's quality of life.</p>	<p>Cost effective.</p> <p>Patients should follow regular exercise and rest regimen to avoid replaced joint weakness.</p> <p>The replaced joint may wear out after about 20 years or become loose.</p> <p>Surgery complications such as joint infection and blood clots.</p>	<p>Old patients (&gt; 70 years old).</p> <p>Mainly done for the hip, knee, and glenohumeral joints.</p>
<p>Arthroscopy</p> 	<p>Prevent disease progression.</p> <p>Small incision.</p> <p>Reduced hospital cost and complication rate.</p>	<p>Has limited benefits and effectiveness in case of joint-space narrowing.</p> <p>Joint infection can occur.</p>	<p>Young patients (&lt; 60 years old).</p> <p>Mainly for the knee, hip, shoulder, and hand.</p>
<p>Osteotomy</p> 	<p>Performed mainly to relieve pain and OA symptoms.</p> <p>Delay the rate of disease progression.</p>	<p>Not a permanent procedure.</p> <p>Further surgery may be necessary in the future.</p>	<p>Young patients (&lt; 60 years old).</p> <p>Mainly for the hip, knee, spine, and hand.</p>
<p>Mosaicplasty</p>	<p>One stage procedure.</p> <p>Reduce the risk of allergic or</p>	<p>Pain and swelling after the physical activity.</p> <p>Postoperative bleeding, crepitation and locking sensation.</p>	<p>Young patients (&lt; 50 years old).</p> <p>Mainly for Knee joint.</p>

	<p>immunological reactions.</p> <p>Low cost.</p>	<p>Limited donor site and high-quality graft in some cases.</p>	
---	--	---	--

### 1.3.4. Tissue engineering

Traditional OA therapy is mainly effective in reducing pain and inflammation but does not actually stop OA progression. Over the past two decades, tissue engineering has emerged as an auspicious biological treatment for OA (Hochberg, McAlindon and Felson, 2000). It is able to generate new ways for articular cartilage re-synthesis and repair to occur through developing biologically active cells and tissue substitutes that mimic damaged ones (Zhang, Hu and Athanasiou, 2009). In addition, as it uses a bright cell source (such as stem cells, signal molecules, biomatrix, emerging nanotechnology and chondrogenic factors), it offers a promising treatment for OA (Zhang, Hu and Athanasiou, 2009; Grässel and Lorenz, 2014). There exist a number of published pre-clinical and clinical studies in which tissue engineering has been used in the treatment of OA for chondral and osteochondral tissue repair (Zhang, Hu and Athanasiou, 2009; Luyten and Vanlauwe, 2012; Grässel and Lorenz, 2014). To illustrate, there are various different types of cell-based therapies in OA treatment (Figure 1-9) such as autologous chondrocytes implantation (ACI) and mesenchymal stem cells (MSCs) implantation (Zhang *et al.*, 2016). ACI is a regenerative procedure that involves harvesting biopsy from healthy cartilage with a low bearing load. The cell biopsy is then enzymatically treated for 3 to 5 weeks to obtain a sufficient number of chondrocyte cells (around 5 to 10 million cells) which are treated under conditions that preserve cell function and viability. The resulting chondrocytes are then injected into the patient's periosteum, where they grow and mature over time (Rodrigo, Jofré and Minguell, 2015). Minas *et al.* (2010) studied ACI on 135 patients with early-stage OA at a 5 year follow up; 95% of OA patients saw improvement in terms of functionality and pain, and the need for further surgical treatment was delayed. Overall, ACI results show that treatment enhances pain reduction, improves quality of life and leads to delaying the need for surgical joint replacement; however, it is mainly suitable for the young age group (< 45 years) (Rosenberger *et al.*, 2008). ACI is an effective and safe method of OA treatment but has some limitations including a requirement of multiple stages of surgical procedures, of finite cell availability and in vitro chondrocyte dedifferentiation (Zhang *et al.*, 2016).

Moreover, implantation of MSCs is considered to represent a promising cell source as it is immunosuppressive, has a high regeneration rate, and can be harvested from different tissues such as synovial membrane, bone marrow, umbilical cord blood, and adipose tissue (Zhang *et al.*, 2016). Additionally, intra-articular injection of MSCs is effective in reducing OA pain, improving ability to regenerate hyaline-like cartilage and reconstructing tissue function (Rodrigo, Jofré and Minguell, 2015). One particular study investigated the effectiveness of intra-articular injection of adipose tissue MSCs in knee OA. A cohort of 18 patients were involved in the study at 6 months follow up. The results show that intra-articular injection of MSCs leads to improved function, and reduced knee pain, and eliminates cartilage defects by regeneration of hyaline-like articular cartilage without causing significant side effects (Jo *et al.*, 2014). Furthermore, two types of stem cells were investigated embryonic stem cells (ESCs) from mammalian embryonic cells and induced pluripotent stem cells (iPSCs). Both types of stem cells have the pluripotent ability to distinguish into chondrocytes. ESCs can improve cartilage repair in animal models, and iPSCs generated from human OA chondrocytes have the ability to induce the cells into chondrocytes differentiation (Weil *et al.*, 2012; Zhang *et al.*, 2016). ESCs and iPSCs look promising as they can differentiate into human cartilage to treat OA; however, they can cause teratoma growth and immunogenicity (Weil *et al.*, 2012).

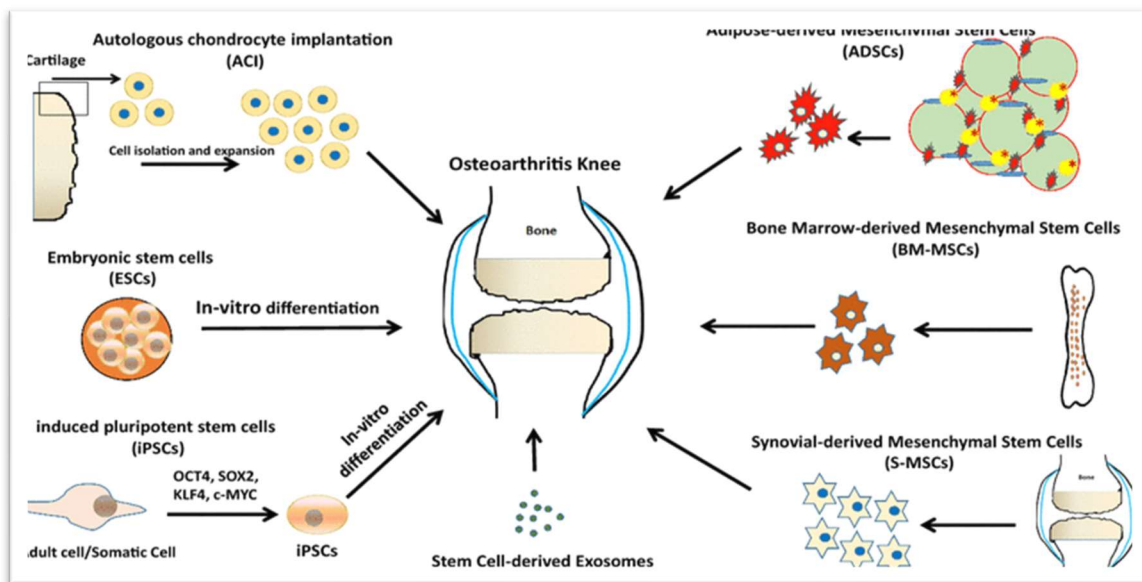


Figure 1-9. The current clinical approaches to cell-based therapy for cartilage tissue engineering. Cell-based treatments such as stem and primary cells are more focused on cartilage regeneration and utilized to replace or repair OA-damaged tissues, adapted from (Burke *et al.*, 2016).

A limitation of ACI and MSCs is that the cell proliferation capacity of chondrocytes in conjunction with low production of cell specific extracellular matrix leads to reduced use in regenerative treatment. Therefore, scaffold approaches have been developed to achieve the effective regeneration of hyaline cartilage (Rodrigo, Jofré and Minguell, 2015). Improved understanding of the structure and role of extracellular matrix components in cartilage has helped to develop scaffolds that mimic the cartilage microenvironment. Cell based scaffold can be used in ACI or any other form of cell therapy. As a result, there is cause for optimism with regard to treatment of chondral defects. For example, one study assessed the use of a tissue-engineering graft composed of autologous chondrocytes grown on a scaffold made of an esterified derivative of hyaluronic acid in knee OA. A total of 141 patients were enrolled, and after 8 months of follow up time it was apparent that more than 70 % of patients exhibited no pain or movement difficulty and histological analysis showed hyaline-like cartilage (Marcacci *et al.*, 2005). In another clinical trial, 18 patients suffering from knee OA with a mean age of 47 years underwent tibial osteotomy plus ACI using a collagen membrane scaffold. After 5 years of follow up, patients showed significant clinical improvement in their knee injuries and OA, albeit with minor side effects such as patellar tendinitis. On the other hand, cartilage infill and graft survival were poor (Bauer *et al.*, 2012). Nonetheless, the positive clinical results indicate clinical safety and effectiveness of using cell therapy scaffolds in the treatment of articular cartilage defects.

In addition, gene therapy allows for the control and synthesis of gene products located at the target cell. Therefore, the safety and efficacy of gene therapy have been confirmed in OA treatment (Chen, Deng and Li, 2012; Zhang *et al.*, 2016). TGF- $\beta$  gene therapy has been investigated, and it has been proven that the TGF- $\beta$  signaling pathway plays a vital role in chondrocytes, MSCs and synovial cells during OA progression. More specially, it drives chondrocytes toward hypertrophy, activating synovial lining cells growth and fibrosis, enhancing cell differentiation and angiogenesis in the subchondral bone (Shen, Li and Chen, 2014). The Tissue Gene-C technique was conducted using retrovirally transduced chondrocytes which overexpress TGF-  $\beta$  as a therapy for OA. Compared to placebo and control group, treatment recipients experienced reduced OA knee pain, improved sports activities, and higher quality of daily life (Cho *et al.*, 2017).

Overall, the results to date are promising, and tissue engineering therapy is showing signs of being a successful approach to curing cartilage disease. However, there are challenges and

numerous unexplained questions in relation to the clinical data, as these are still the early stages (Hochberg, McAlindon and Felson, 2000; Zhang, Hu and Athanasiou, 2009; Luyten and Vanlauwe, 2012; Grassel and Lorenz, 2014). Moreover, safety data for future results and side effects are still unclear. Therefore, an emphasis on progress in genetic profiling has taken priority in recent research efforts in the field.

### 1.3.5. Disease modifying agents

As part of a rapidly expanding field, disease modifying osteoarthritis drugs (DMOADs) and drug delivery systems (DDSs) that target joints represent an exciting and promising new strategy for OA treatment. DMOADs act as chondroprotective treatments as they are mainly focused on preventing the loss of articular cartilage as well as enhancing the regrowth or healing of damaged cartilage (Blanco and Ruiz-Romero, 2013). Methods of actions of DMOADs are based on the following pathological processes in OA: inhibition of inflammatory process, targeting subchondral bone change, targeting cartilage and growth factor (Davies *et al.*, 2013; Janssen *et al.*, 2014). DMOADs that inhibit or control inflammation and inhibit matrix degradation can also inhibit the progress of OA (Zhang *et al.*, 2016; Huang *et al.*, 2018). For instance, licofelone is an analgesic and anti-inflammatory agent for OA that acts by inhibiting COX and 5-lipoxygenase enzymes. In addition, it inhibits IL-1 $\beta$  synthesis in the synovium and decreases mRNA expression and protein synthesis of proteolytic enzymes involved in cartilage degradation (such as MMP-13, ADAMTS-5) (Gaur *et al.*, 2009). A clinical trial endorsed its protective effects on knee OA as it decreased knee cartilage volume loss within 12-24 months (Raynauld *et al.*, 2009). Moreover, inhibition of the major pro-inflammatory cytokines (IL-1 $\beta$  and TNF- $\alpha$ ) has a chondroprotective effect which can control the structural progression of OA. Infliximab, a monoclonal antibody that inhibits TNF- $\alpha$ , has been shown to have good efficacy and a tolerable symptomatic effect on erosive OA affecting the hand (Fioravanti *et al.*, 2009). Moreover, interleukin-10 (IL-10) is an anti-inflammatory cytokine that potently suppresses proinflammatory cytokine activity. It also has chondroprotective effects as it reduces production of matrix metalloprotease and inhibits chondrocyte apoptosis. Therefore, IL-10 could have potential benefits in OA management, both for pain improvement and suppression of cartilage-damaging processes. Currently, a phase-2b clinical trial is evaluating the safety and efficacy of a single injection of XT-150 (a plasmid DNA with a variant of human IL-10 transgene) in patients with knee OA (NCT04124042), and it estimated to be completed this year (in 2023) (John *et al.*, 2007).

Recently, all studies have shown that XT-150 offers long lasting pain relief and improvement of function in people suffering from knee osteoarthritis (Grigsby *et al.*, 2021).

Targeting the subchondral bone is another effective DMOAD approach to treating OA. Strontium ranelate, bisphosphonates and calcitonin are examples of DMOADs used for remodeling subchondral bone (Huang *et al.*, 2018). These drugs can be a potential treatment strategy as they shift the treatment aim from the cartilage to the subchondral bone. However, additional studies are needed to understand the disease-modifying effects (Zhang *et al.*, 2016). Furthermore, regulating cartilage catabolism and anabolism can be a powerful approach that modifies OA treatment. For instance, cartilage protease inhibitors, as MMPs inhibitors, and growth factors (fibroblast growth factor 18 (FGF-18) and bone morphogenetic protein-7 (BMP-7)) inhibitors are potential targets for the development of OA therapies. Generally, DMOADs seem to be an effective method of treatment as they inhibit disease deterioration and improve patients' symptoms and quality of life. However, they have a short life due to enzymatic degradation which can be solved by administration together with DDSs (Davies *et al.*, 2013; Janssen *et al.*, 2014). In addition, concurrent administration of DDSs, DMOADs and intra-articular injection can reduce the number of injections required, prolong drug retention time, and stabilise the concentration of drug within the therapeutics index hence decreasing toxic effects and enhancing patients' compliance (Shuid *et al.*, 2013).

### **1.3.6. Drug delivery systems**

In severe cases of OA where treatment with painkillers is inadequate for pain control, intra-articular injections are the best and most effective treatment method. Localising medication inside the inner space of the articular cartilage can improve treatment by working directly within the affected joints. It also, allow drugs to fall below the toxic level in plasma, thereby avoiding the systemic side effects associated with oral medications (He *et al.*, 2017). As discussed above, corticosteroids and hyaluronic acid are drugs widely used in clinics as intra-articular injections for OA treatment (He *et al.*, 2017).

On the other hand, physicians usually try to minimise the time between the injection to minimize potential side effects, risk of over-medication or joint damage and consider it to be from 2-12 weeks which may lead to ineffective treatment (Geiger, Grodzinsky and Hammond, 2018). Therefore, combining a drug delivery system with IA injections can provide effective treatment. Figure 1-10 shows the differences in release profiles between repeated intra-articular injection and single injection of administered drug using DDSs. Multiple injections can lead to

high dose fluctuation, ranging from toxic to subtherapeutic levels while a single injection plus DDSs falls within the required therapeutic level (dashed line) (Janssen *et al.*, 2014).

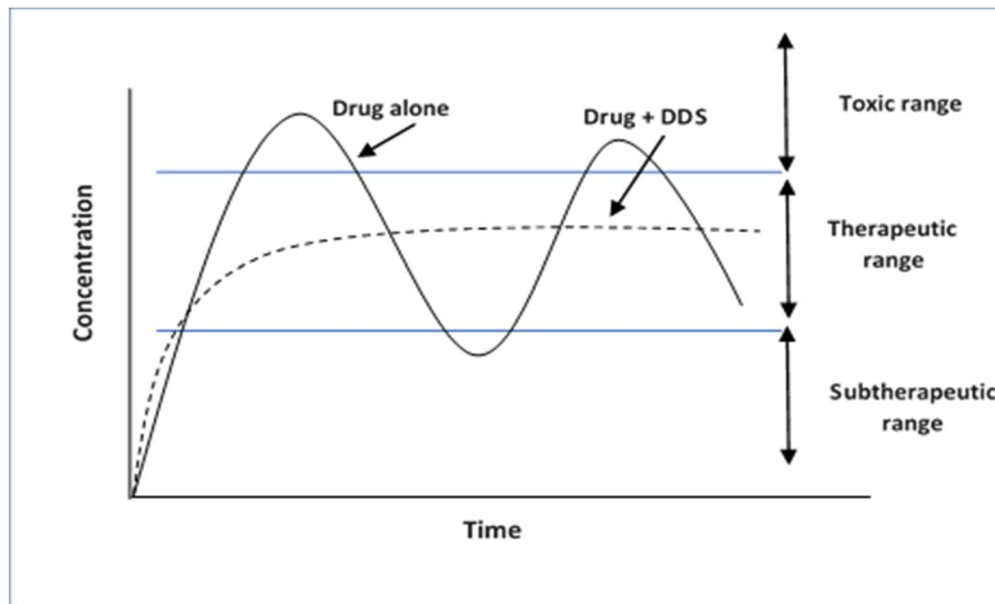


Figure 1-10. Therapeutic window of administered drug. Repeated injection of drug lead to dose fluctuation between toxic and subtherapeutic ranges (solid line). Single injection of drug with drug delivery system (DDS) allowed drug to be within the required therapeutics range (dashed line), adapted from (Janssen *et al.*, 2014)

In fact, the idea of DDSs was first recognised far back as the 1960s, when Judah Folkman found that a steady rate of drug delivery could be achieved by using silicone rubber tubes in rabbit anaesthesia (Hoffman, 2008). Subsequently, much research into effective methods for intra-articular DDSs has been undertaken, with many different carriers (ranging from macroparticles to nanoparticles) having been identified (Hoffman, 2008). In addition, projecting DDSs for intra-articular treatment of OA became an expanding area of concern from the late 1990s (Janssen *et al.*, 2014). Generally speaking, the fundamental problems with all OA therapies (including IA injections), are insufficient drug retention in pathological joints, rapid degradation, clearance of injected drugs, increased risk of complications, and systemic side effects (especially with oral drugs), as a result, fail to reach effective therapeutic levels (Huang and Zhang, 2012; Geiger, Grodzinsky and Hammond, 2018). This is mainly due to joint structure: when the drug enters the synovial fluid most of it is rapidly drained via blood vessels into the systemic circulation (Evans, Kraus and Setton, 2014). Therefore, it is cleared entirely from the affected joint within hours or days (exact duration is variable depending on molecular drug weight). In term of OA treatment, the target for most modifying drugs is the articular cartilage; however, drug penetration inside the cartilage is a challenge. This is mainly because

it is avascular (i.e., has no blood vessels), dense, has small pore size (<15nm), and has a highly anionic matrix as it is composed of negatively charged proteoglycans (Bajpayee *et al.*, 2016). Consequently, penetration of effective concentration of the drug into the cartilage occurs slowly and clears quickly. Significant efforts have been made to improve uptake, penetration, and retention time of OA drugs into the cartilage. The outcome of these investigations has contributed to a deeper understanding of the barriers and mechanisms involved in drug permeation in joints and has paved the way for the development of novel techniques for joint drug delivery.

DDSs are mainly aimed at enhancing specificity, improving activity, reducing toxicity and maximising treatment safety (Soussan *et al.*, 2009); they offer a useful method of treatment to target joints affected by OA. That being said, reducing drug joint clearance, and enhancing drug cartilage penetration need to be considered in order to conduct novel DDSs. Using a vehicle to sustain drug release inside joints over a long time is an effective approach to treatment (Janssen *et al.*, 2014). There are different types of vehicles that can facilitate drug delivery to affected joints and organs, such as matrix systems and vesicles. Carriers that depend on soft matter have principally interesting characteristics that consist of emulsions, micelles hydrogels, nanospheres, liposomes, dendrimers and solid lipid particles (Soussan *et al.*, 2009). Accordingly, various studies have been conducted and different DDSs created to try to optimize drug delivery. For example, nanocrystal-polymer particles have recently been adopted as an effective delivery system to treat OA for sustained periods with high dosage (Maudens *et al.*, 2018). Moreover, a liquid polymer formulation of corticosteroids has also been developed for extended treatment of OA (Rivera-Delgado *et al.*, 2018). In addition, using avidin as a nanocarrier to sustain delivery of dexamethasone inside cartilages has been proven to be an effective method for rapidly transporting drugs while minimising side effects (Bajpayee *et al.*, 2016).

It is clear that DDSs can offer a promising course of action to achieve avoidance of joint clearance and/or improvement of drug penetration in an effective concentration for treatment of OA. For instance, using biomaterials and hydrogels are different strategies for reducing drug clearance. Using microparticles to encapsulate the drug as a controlled release depot inside the joint is an effective method which increases the resident time of the drug in its intended location (Geiger, Grodzinsky and Hammond, 2018). FX-006 is an example of a polylactic-co-glycolic acid (PLGA) microparticle that encapsulates corticosteroids as intra-articular DDSs for OA. It

significantly reduces OA pain, and stiffness while heralding improved joint function within 12 weeks post-injection (Kumar et al., 2015). In common with microparticles, hydrogels are an effective reservoir for extending drug duration inside joints (Geiger, Grodzinsky and Hammond, 2018). These have been used to prolong the release of HA to enhance its analgesic and lubricative effects (He et al., 2017).

Despite the fact that such strategies are effective means of increasing drug exposure time inside joint space and alleviating OA pain, in isolation they do not cause drugs to interact with and penetrate cartilage cells. Therefore, further DDS strategies to achieve cartilage penetration and hinder joint clearance have been developed such as, using a small nanocarrier which binds to cartilage ECM (Geiger, Grodzinsky and Hammond, 2018). Rothenfluh *et al.* (2008) found that utilising a phage panned peptide (WYRGRL), which has strong affinity to type II collagen in ECM, was successful in increasing drug penetration to thin mouse cartilage to around 50  $\mu\text{m}$  for 4 days. Moreover, conjugating the drug with more WYRGRL peptide led to an increase in penetration depth and duration (Rothenfluh et al., 2008). In addition, a cationic peptide that forms an electrostatic interaction with the anionic glycoprotein in the cartilage can augment drug penetration and retention within the cartilage (Perni and Prokopovich, 2017; Geiger, Grodzinsky and Hammond, 2018). For example, avidin, (a protein that exhibits a positive charge of +20mV is able to penetrate 1000 $\mu\text{m}$  cartilage thick within 24 hours (Bajpayee et al., 2014). Similarly, poly beta-amino esters (PBAEs) polymers displaying a positive charge (+13 mV) also show effective performance uptake into cartilage (Perni and Prokopovich, 2017). Furthermore, nanoplex (a nanocarrier polyelectrolyte complex) that delivers growth factors (such as IGF-1), to deep the cartilage has been found to improve retention time for IGF-1 compared to using it alone (30 days, and 7 days, respectively) (Shah et al., 2016). In summary, it appears highly likely that a variety of safe and effective OA treatment options will be clinically available in the near future.

Moreover, all OA therapeutic agents naturally have small molecular sizes (i.e. diameter < 20nm) leading to rapid spread of porous sub-synovial capillaries and being subject to rapid metabolism and renal clearance (Janssen *et al.*, 2014). As previously discussed, to overcome these limitations many researchers and pharmaceutical companies have encapsulated chosen drugs and/or proteins in biocompatible and biodegradable polymers or lipid-based carriers in order to provide DDSs and to increase their molecular size (Evans, 2016). Overall, combining these drugs with effective DDSs has afforded significant progress in OA treatment. In addition,

targeting pain using medications such as NSAIDs, which are encapsulated in and released from DDSs, is likely to be more effective and clinically applicable in the future than relying on DMOADs (Janssen *et al.*, 2014).

In general, although NSAIDs are commonly used in OA treatment, their systemic side effects hinder long-term use and negatively affect patient compliance. The rationale for using them is that they effectively provide symptomatic OA pain relief, and minimise disease progression; importantly, they also have the ideal characteristics to be used via the intra-articular injection route alongside the oral route (Janssen *et al.*, 2014). Accordingly, many studies have incorporated them with a carrier in order to provide effective DDSs (Janssen *et al.*, 2014). For example, in one study ibuprofen sodium (1 mg/mL) was encapsulated in PEGylated gelatin nanoparticles (PIG NPs) to sustain its anti-inflammatory delivery effects for rheumatoid arthritis and chronic arthropathies. Based on the results of in vivo intravenous administration of PIG NAP's ibuprofen sodium to rats, it has been concluded that the formulation can provide controlled drug release over 4 days, compared with 2 days in unencapsulated form. This is mainly due to polyethylene glycol (PEG) successfully improving drug bioavailability by providing longer circulation duration for nanoparticles to achieve higher drug concentration within plasma (Narayanan *et al.*, 2013). Similarly, in vitro study has been conducted using PLGA nanoparticles containing diclofenac sodium to deliver the drug in a controlled manner and to reduce GIT side effects of diclofenac. The PLGA nanoparticle was effective to provide slow, and sustained release of diclofenac over 72 hours compared with 12 hours for non-glycolate nanoparticles (Cetin, Atila and Kadioglu, 2010). Meanwhile another study has found that intra-nasal or oral administration of meloxicam nanoparticles (polymerised form) in rats can lead to significantly higher plasma levels and better permeability than conventional ones (Kürti *et al.*, 2013). In addition, intra-nasal delivery has been showed preferable as it reduces GIT side effects (Kürti *et al.*, 2013).

As discussed above, many trials have been undertaken to develop clinically effective and safe treatment for OA; unfortunately, a truly optimal DMOAD is not yet available. This is mainly due to pharmacokinetics, which cause insufficient drug delivery within joints (Geiger, Grodzinsky and Hammond, 2018). Thus, there is great potential for superior drug delivery strategies to drive candidate therapeutics towards clinical fulfilment. Indeed, the search for the optimal OA drug for use alongside biocompatible and biodegradable DDSs has been the subject of extensive research (Janssen *et al.*, 2014). Such efforts have mainly focused on optimisation of DDSs and development of novel drugs to target and treat OA (Geiger, Grodzinsky and

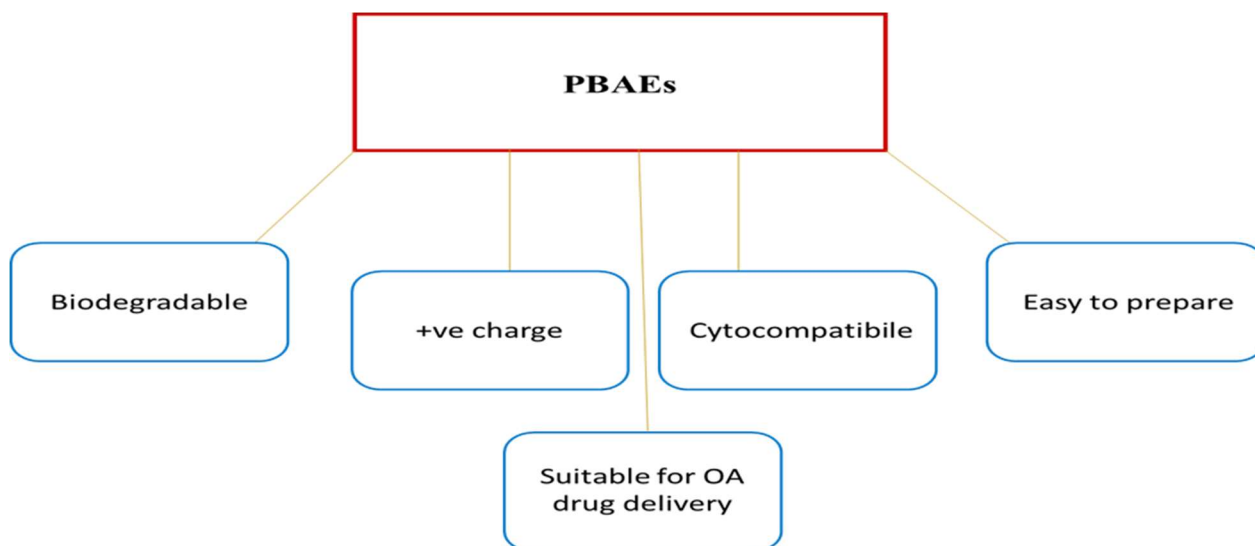
Hammond, 2018). This important work is still in progress, and positive developments may emerge in the near future.

#### **1.4. Poly (beta-amino esters) polymer:**

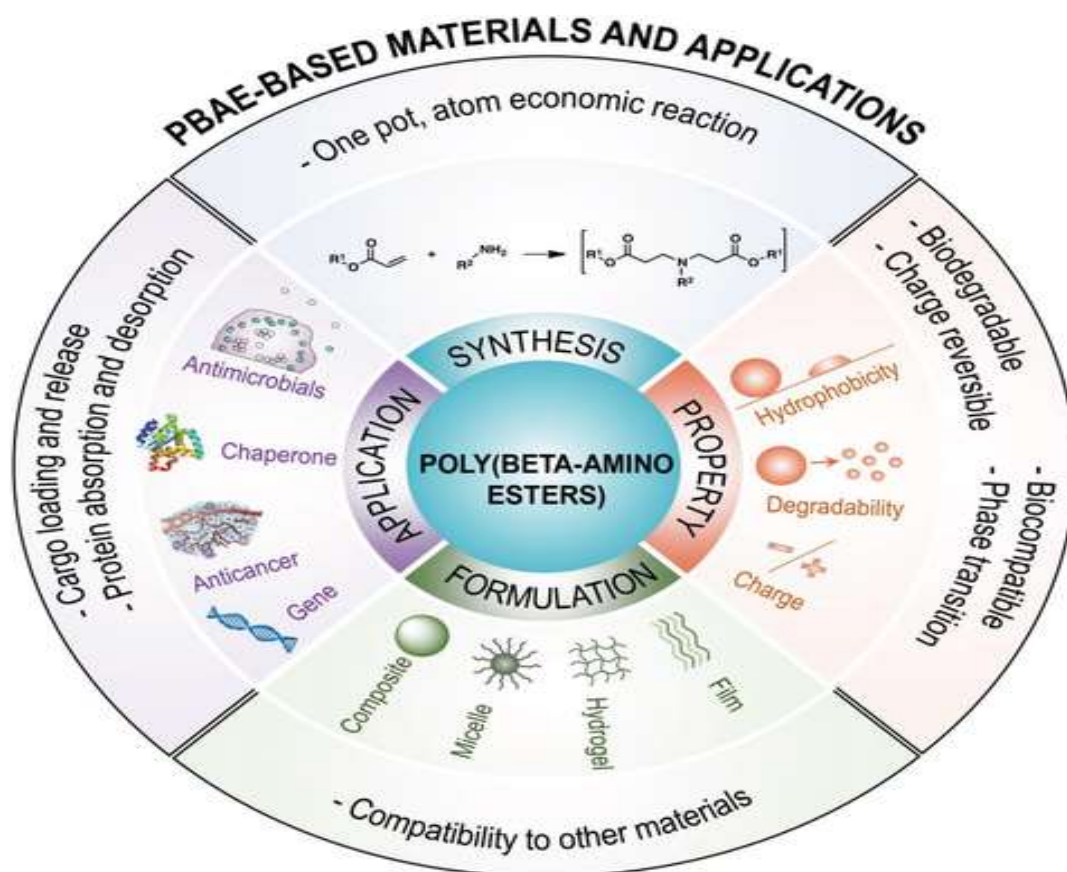
Polymers are an essential class of materials which are commonly used for medical applications, such as tissue engineering and drug delivery (Goldberg, Mahon and Anderson, 2008). They can be classified into natural polymers (such as chitosan, natural rubber, starch and protein) and synthetic polymers (such as polyethylene glycol, PLGA, poly L-lysine and polyester amides) (Goldberg, Mahon and Anderson, 2008; Janssen *et al.*, 2014). Historically, polymers have been widely used within drug delivery systems for OA treatment. For example, diclofenac sodium loaded albumin microspheres afford a considerable reduction in arthritis in vivo after 30 days (Tunçay *et al.*, 2000). In addition, poly (lactic acid) and polyethylene glycol have shown good biocompatibility in vivo and are able to control drug release (Liggins *et al.*, 2004; Bédouet *et al.*, 2013). However, the common problem with these polymers is initial burst release, which can lead to high, toxic drug concentration and acidic product breakdown, in turn affecting protein stability and decreasing drug release (Huang and Zhang, 2012; Janssen *et al.*, 2014). Therefore, use of bio-degradable material in polymer preparation offers a viable alternative as it provides improved control over degradation and release properties, and can readily degrade into non-toxic byproducts (example of such polymers include polyurethane, poly (4-hydroxy-L-proline ester) and polyester amines) (Lynn and Langer, 2000; Janssen *et al.*, 2014). The present study will focus on poly beta-amino esters as these are a particular interest of the researcher.

PBAEs are a group of polycationic polymers introduced by Lynn and Langer around two decades ago (Lynn and Langer, 2000). There exist more than 2500 different PBAE polymers which are mostly synthesised and used in gene and drug delivery (Lynn and Langer, 2000; Chen *et al.*, 2007; Liu *et al.*, 2019). They are synthesised via Michael addition through conjugate addition of an amine to acrylate monomers, without the production of side products or any precipitation in the subsequent addition reaction (Lynn and Langer, 2000; Liu *et al.*, 2019). Accordingly, this process enables one-step generation from commercially available materials of various structures of polyester containing amine in the backbone. Moreover, PBAEs can be formulated in different ways to suit many requirements in drug delivery, such as genes, anti-cancer drugs, osteoarthritis drugs and antimicrobial drug delivery (Lynn and Langer, 2000; Liu *et al.*, 2019). Furthermore, the PBAE approach provides a particularly attractive basis for use as an intra-articular drug delivery system for treatment of OA and other

diseases (Scheme 1-1): There are several reasons for this: 1) polymer contains necessary amines and easily degradable linkage; 2) its positive charge can bind to the negative charged glycosaminoglycan (GAG) inside cartilage tissue via electrostatic interaction; 3) it can be hydrolysed to biocompatible, non-toxic products; and 4) can be prepared easily and cheaply from inexpensive commercially available monomers (Lynn and Langer, 2000; Al Thaher *et al.*, 2018; Liu *et al.*, 2019). Finally, different formulations can be used for specific and targeted releases. One example, nanocomposite, in which cationic PBAEs can bind to negatively charged DNA strands via electrostatic interaction, leading to PBAE polymer being hydrolysed into biocompatible products allowing DNA release inside cells (Lynn and Langer, 2000; Green *et al.*, 2006; Goldberg, Mahon and Anderson, 2008; Perni and Prokopovich, 2017). In addition, films are usually formed through a layer by layer (LBL) technique, and are based on the deposition of alternatively counter charged polyelectrolytes onto substrata (Liu *et al.*, 2019). Furthermore, curcumin is a natural product with potent antioxidant and anti-inflammatory properties that are beneficial for osteoarthritis treatment (Crivelli *et al.*, 2019; Kang *et al.*, 2020). It was covalently incorporated into the backbone of PBAE polymers after which acid activatable curcumin polymer was self-assembled to form micelles leading to rapid release of curcumin under acidic conditions in OA joints (Kang *et al.*, 2020). Histological examination of knee joint osteoarthritis showed that acid activatable curcumin polymer micelles decreased inflammation by suppressing the two major inflammatory cytokines; tumour necrosis factor- $\alpha$  (TNF  $\alpha$ ) and interleukin  $1\beta$  (IL- $1\beta$ ) in a monoiodoacetic acid (MIA) induced osteoarthritis mouse model (Kang *et al.*, 2020). Moreover, this delivery system had excellent biocompatibility and allowed high drug content at the target joint. This is because it provided 95% of curcumin released at acidic media pH 6, compared to 25% at pH 7.4 (Kang *et al.*, 2020). Scheme 1-2 summarises the synthesis and application of PBAEs (Liu *et al.*, 2019).



Scheme 1-1. Miscellaneous properties mark PBAEs as an ideal drug delivery system for OA treatment.



Scheme 1-2. Synthesis, properties, different formulations and applications of PBAEs polymer, adapted from (Liu *et al.*, 2019)

## **Study aim**

OA drugs suffer from inadequate localisation, uptake and retention in target areas, mainly due to vasculature joint tissue which by nature causes rapid drug clearance from the tissue (Geiger, Grodzinsky and Hammond, 2018). Moreover, because these drugs are hydrophobic, an effective system of delivery to affected joints is required. Ongoing concurrent research into advanced arthritis treatments and delivery systems is showing promising signs, including discovery and synthesis of new biocompatible and biodegradable carriers (e.g., nanoparticles, liposomes, emulsions, cationic carriers, and hydrogels) alongside combination systems (composed of different carrier types) that aim to overcome the limitations of single drug delivery systems. Therefore, this study aims to develop a novel and efficient local delivery emulsion system which encapsulates NSAIDs in oleic acid emulsion and then coats the emulsion droplets with POLYX polymer (poly-beta amino ester polymer). As a result, enhanced drug uptake and retention in cartilage tissue are achieved, resulting in a reduction in toxicity and potentially an improvement in patient compliance and safety.

It is hypothesised that positively charged POLYX polymers will coat the negatively charged NSAIDs o/w emulsion (oleic acid-based emulsion), creating a positive charge formulation that will interact electrostatically with the negatively charged GAGs inside the joint cartilage, thus enhancing uptake of NSAIDs and prolonging retention duration inside the tissue.

To achieve this aims, this study's main objectives are to:

- A) Prepare oil in water emulsion using oleic acid to encapsulate NSAIDs (indomethacin, ketorolac, naproxen, and diclofenac sodium), which will then be coated with positively charged POLYX as the carrier.
- B) Measure emulsion droplets mobility and calculate zeta potential (ZP) at every stage of emulsion preparation to determine correct POLYX polymer amounts to be added to fully coat the emulsion and change its negative charge to positive
- C) Measure size distribution of emulsion droplets.
- D) Calculate DDSs' uptake abilities in untreated and GAG-depleted cartilage bovine ex -vivo models.
- E) Conduct drug retention experiments using untreated, and GAG depleted cartilage bovine ex vivo models.

F) Determine effects of the developed drug delivery system on IL-1 $\alpha$  treated cartilage using DMMB assay, hydroxyproline assay and XTT assay.

G) Perform live/dead viability assay using confocal microscopy to determine live and dead cells on cartilage tissues that was treated with/without IL-1 $\alpha$ , and the NSAIDs emulsion that encapsulated with POLYX.

H) Conduct histological analysis using safranin O staining methods of cartilage tissue treated with/without IL-1 $\alpha$  and NSAIDs emulsion encapsulated with POLYX to visualize and evaluate the damage to the cartilage by assessing GAG distribution inside the cartilage, as well as monitor the effectiveness of the developed formulation in promoting cartilage repair and regeneration.

## **2. Chapter two: Methodology**

This chapter describing the common methods used for the preparation of different polycations, emulsion, coating method, osteoarthritis models, and testing the properties of the prepared drug delivery system throughout this thesis.

### **2.1. Chemicals**

All chemicals were used as received and stored as recommended by the manufacturer.

#### **2.1.1. NSAIDs**

In this work, the model drugs were indomethacin (Sigma life science), ketorolac tris salt (Sigma life science), naproxen (Sigma Aldrich), and diclofenac sodium salt (Sigma life science). These drugs were named through the text as Ind for indomethacin, Ket for ketorolac, Nap for naproxen, and DC for diclofenac sodium.

#### **2.1.2. Oleic acid**

Oleic acid (Thorton & Ross) was used to create the oil-in-water emulsion for the NSAIDs, then coated with the polymer.

#### **2.1.3. Polycations**

The Patented POLYX (POLY-A, POLY-B, POLY-D, POLY-E and POLY-F) polymers (Table 2-2) were prepared from a specific acrylate and amine and used to coat oil droplets in the emulsion. Its preparation methods were explained later in this chapter.

### **Buffer preparation**

#### **2.1.4. Acetate buffer**

Acetate buffer (pH 3.6, pH 4 and pH 5) was prepared by mixing different amounts of acetic acid solution (5.8 mL of acetic acid glacial (Fisher) in up to 1 litre deionized water), and sodium acetate solution (13.6 g of sodium acetate trihydrate (Honeywell) in 1 litre deionized water) as in table 2-1 (Buffer, 2004). Along with acetonitrile (Fisher), buffer pH 3.6 were used as a mobile phase for indomethacin. In contrast, buffer pH 4 was used as a mobile phase for naproxen and diclofenac sodium to allow better elution of the drugs oil drops in the column. Buffer pH 5 was used to prepare and dissolve POLYX polymers. Additionally, in this slightly acidic buffer (pH 5), POLYX was charged positively because of the protonation of nitrogen from the amine ends ( $R-NH_3^+$ ); therefore, it was able to coat the emulsion (Kim, Sunshine and Green, 2014).

Table 2-1. Amount of acetic acid and sodium acetate (mL) which used to prepare acetate buffer at different pH.

pH	Acetic acid (0.1 M) mL	Sodium acetate (0.1M) mL
3.6	92.9	7.4
4	82	18
5	30	70

### 2.1.5. Citrate buffer

A pH 6 citrate buffer was prepared to be used for the hydroxyproline assay by mixing 46.12 g/L of citric acid, 119.7504 g/L of anhydrous sodium acetate trihydrate, 72.190184 g/L of anhydrous sodium acetate, 12 mL/L of acetic acid and 34 g/L of sodium hydroxide. The solution was left to be mixed with a magnetic stirrer for 5-10 min at 300 rpm until it dissolved completely. The buffer solution was then stored at room temperature for three months (Pratta *et al.*, 2003).

### 2.1.6. Phosphate buffer

A pH 6.8 phosphate buffer was used to make the cartilage digestion buffer solution. It was prepared by mixing 49 % sodium phosphate dibasic (71.7 g/L) (fisher) with 51 % of sodium phosphate monobasic (27.8 g/L) (sigma) (Kim, Sunshine and Green, 2014). The solution was left to be mixed with a magnetic stirrer for 5-10 min at 300 rpm until it dissolved completely. The buffer solution was then stored at fridge for three months.

## 2.2. NSAIDs preparation and coating methods

### 2.2.1. Control preparation

Two types of negative control which were used in this project were prepared as follows:

#### 2.2.1.1. 1<sup>st</sup> control

The first control group was prepared by dissolving 4 mg of the NSAIDs in 1 mL of phosphate buffer saline (PBS) (Oxoid), then was mixed with a magnetic stirrer at 300 rpm until it dissolved completely. Indomethacin and naproxen had slight solubility in PBS; therefore, they were left stirred in PBS for 48-72 hours to completely dissolved. While ketorolac and diclofenac were dissolved immediately in about 1-2 minutes, table 2-5 shows the solubility of NSAIDs in PBS buffer. This type of control was named through the text as P control.

### **2.2.1.2.2<sup>nd</sup> control**

The following steps was used to prepare the second control group; 40 mg/mL of NSAID powder in oleic acid was mixed with a magnetic stirrer at 300 rpm until it dissolved completely. Then, 10% of NSAIDs in the oleic acid emulsion were formulated by mixing 100  $\mu$ L of the previous solution with 900  $\mu$ L of PBS. Finally, it was vortex (SciQuip) until a milky consistency was achieved. This control was named through the text as E control.

### **2.2.2. Polycations preparation**

POLYX is a group of cationic polymers known as poly beta-amino ester (PBAE) polymer. It was synthesised according to Michael's addition (Al Thaher *et al.*, 2018; Liu *et al.*, 2019) polymerisation method by the copolymerization of a specific diacrylate monomer and a secondary or tertiary amine monomer in a 1:1.1 ratio. For example, to prepare POLY-A5 polymer, 792.88 mg (4mmol x MW (198.22)) from 1,4 butanediol diacrylate has been weighed first, then 449.592 mg of the dimethylamino-1-propylamine (4.4mmol x MW (102.18)) has been weighed too, then they were mixed in a tube. After that, 5 mL of dichloromethane (DCM) was added to the mixture to yield the polymer in 97 % yields (Figure 2-1). The polymerisation was performed and was kept in a 50-55°C oil bath for 48 hours (Perni and Prokopovich, 2017; Al Thaher *et al.*, 2018; Saeedi and Prokopovich, 2021). Then, approximately ten times the volume of diethyl ether (Fisher) was added (around 50 mL) to the mixture after it reached room temperature in order to recover the polymer through precipitation. After that, it was centrifuged at least three times for 5 minutes at 1300 rpm and washed with diethyl ether. The supernatant was removed every time, and finally, the polymer was dried using a rotatory evaporate method (Perni and Prokopovich, 2017; Al Thaher *et al.*, 2018; Saeedi and Prokopovich, 2021). The newly synthesised polymer was isolated as a clear viscous liquid (for POLY-A5, POLY-B5, POLY-D5, POLY-D1, and POLY-F1), yellowish sticky (for POLY-F3, POLY-F5, POLY-A3, POLY-D3, POLY-B3, and POLY-E3) ,white waxy block (for POLY-A1 and POLY-B1) or brown viscous liquid (for POLY-E5, and POLY-E1) which kept in the fridge for up to two weeks to maintain its freshness and effectiveness. Tables 2-2 & 2-3 illustrate the types of polymers used in this project, acrylates and amine monomers used, chemical structures, MW of each monomer and the percentage of yield after the polymerization reaction.

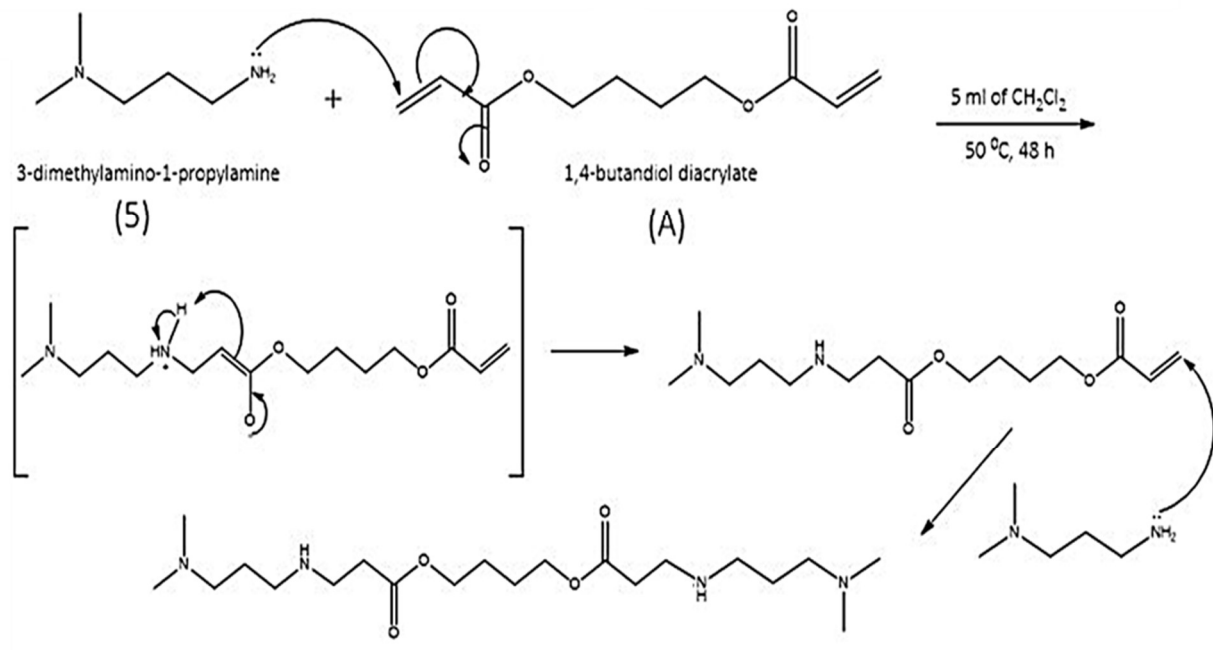
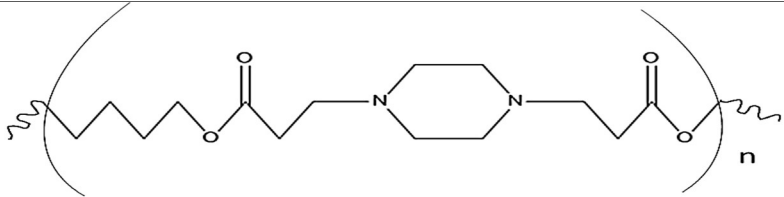
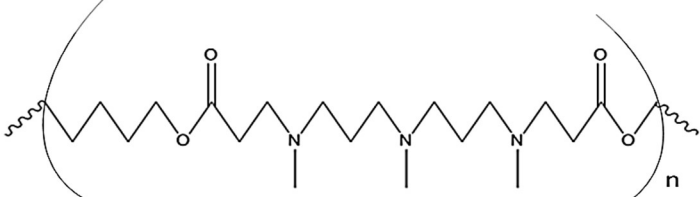
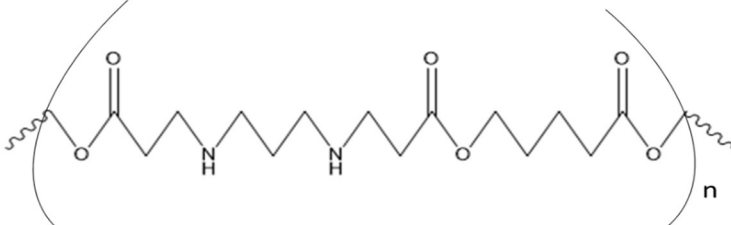
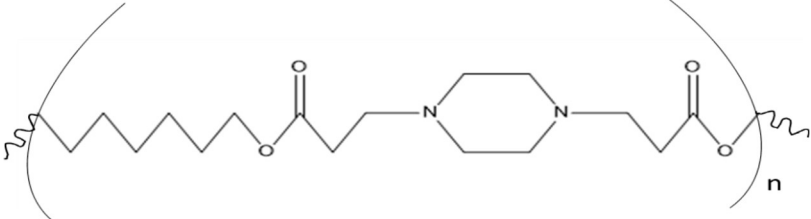
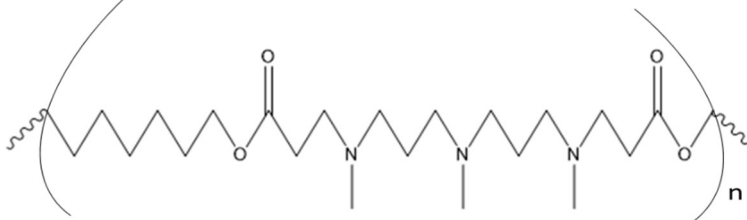
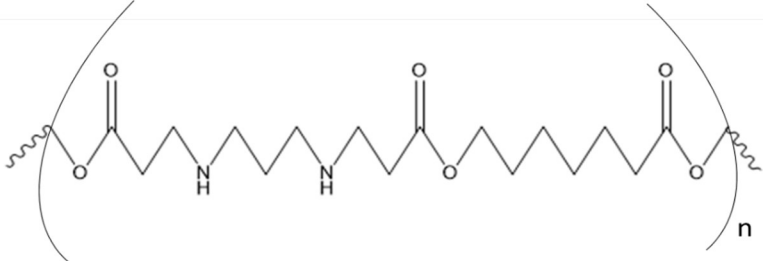


Figure 2-1. Example of synthesis of poly beta amino ester polymer (PBAE) by reaction between 1,4 butanediol diacrylate (compound A) and dimethylamino-1-propylamine (compound 5) under addition of dichloro-methane for 48 hr at 50-55 °C oil bath to form POLY-A5 polymer.

Table 2-2. Name, chemical structure, and coding system of compounds used to prepare different types of poly beta amino ester polymers.

Compounds name/(MW)	Coding system	Chemical structure
1,4 Butanediol diacrylate (198.22)	A	
1,6 Hexanediol diacrylate (226.27)	B	
Neopentyl glycol diacrylate (212.24)	D	
1,3 Butanediol diacrylate (226.27)	E	
Bisphenol A ethoxylate diacrylate (424.5)	F	
Piperazine (86.14)	1	
N, N Bis [3-(methylamino) propyl] methylamine (173.30)	3	
5 (Dimethyl amino)-1-propylamine (102.18)	5	

Table 2-3. Coding, yield and chemical structures of poly beta amino ester polymers which prepared using different types of acrylates, and amines.

Polymers coding	Yield (%)	Chemical structures
A1	93 %	
A3	98 %	
A5	97 %	
B1	96 %	
B3	99 %	
B5	96 %	

D1	94 %	
D3	95 %	
D5	96 %	
E1	97 %	
E3	94 %	
E5	97 %	
F1	98 %	

F3	99 %	
F5	98 %	

### 2.2.3. Emulsion preparation

First, 40 mg of NSAID powder were weighed. Then 1 mL of oleic acid was added, and the mixture was left stirred at 300 rpm with a magnetic stirrer until it dissolved completely. Finally, 10 % of NSAID in the oleic acid emulsion was formulated by mixing 100  $\mu$ L of the previous solution (40 mg/mL) with 900  $\mu$ L of PBS, then stirred at 300 rpm overnight or vortex (SciQuip) until a milky consistency was achieved (final NSAID concentration was 4 mg/mL). This emulsification technique encapsulated NSAID in oil drops, which were used in the following characterization experiments, cartilage penetration, cartilage retention experiments and IL-1 $\alpha$  assays. Throughout the text, this oil-in-water emulsion is referred to as an o/w emulsion.

### 2.2.4. Oil droplet coating process (with POLYX)

In acetate buffer (pH 5) prepared as described above, 2 mg/mL of POLYX was dissolved. After that, the electrophoretic mobility and the charge of the emulsion were determined by zeta potential (mV) at 25 °C using the Zetasizer Nano ZS apparatus (Malvern Instruments). The zeta potential of each type of POLYX and emulsion was measured separately. Then, a constant amount of POLYX (10  $\mu$ L) was added to 1 mL emulsion after the first sample (no POLYX added) until saturation of emulsion was achieved, which can be measured when observing a plateaued in charge (mV); it means the oil droplets was fully coated with POLYX. Figure 2-2 illustrates the study design and the ability of the POLYX coated emulsion droplet to interact with GAG in cartilage tissue compared to the uncoated droplet.

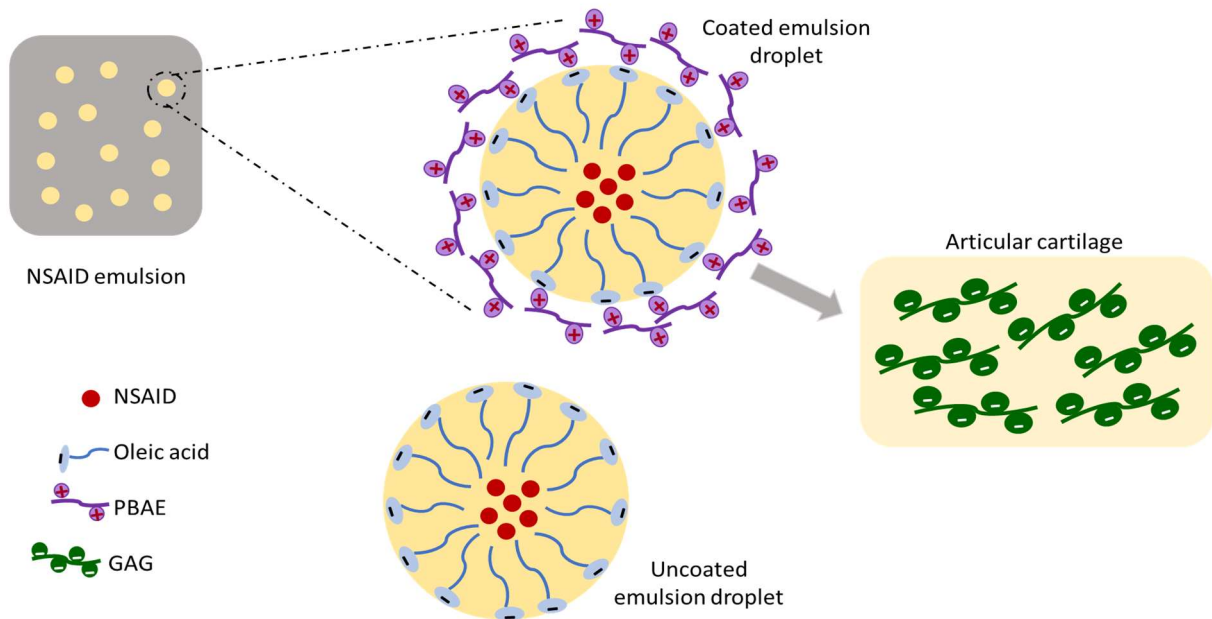


Figure 2-2 . Schematic diagram of NSAID emulsion coated with PBAE polymer and graphical description of study design. Coated emulsion droplet with the positive charge PBAE polymer allow it to interact electrostatically with articular cartilage containing the negative charge GAG. Whereas uncoated emulsion cannot interact easily with GAG articular cartilage due to charge repulsion (both have negative charge). Abbreviations: non-steroidal anti-inflammatory drug (NSAID), poly beta amino ester (PBAE), glycosaminoglycan (GAG).

## 2.3. Particle characterization

### 2.3.1. Zeta potential measurements

For all the emulsions, the charge changing, and electrophoretic mobility was determined by the Malvern Zetasizer nano ZS (Malvern Instruments Limited, UK). It is a dynamic light scattering technique that measures the electrophoretic mobility of particles and molecules, the zeta potential (ZP) of nanoparticles and colloids, size of particles and molecules in solution. Therefore, zeta potential is used in this work mainly for the determination of the charge on the surface of the emulsion droplets. In the electrophoresis method, ZP is calculated by placing fine particles in an electric field and measuring their mobility,  $vE$ . The mobility is then related to ZP at the interface and was calculated using the Smoluchowski equation (Equation 1) (Sze *et al.*, 2003).

$$vE=4\pi\epsilon_0\epsilon_r\zeta_6\pi\mu(1+\kappa r) \quad (1)$$

Where,  $\epsilon_0$  is the relative dielectric constant,  $\epsilon_r$  is the electrical permittivity of a vacuum (F/m),  $\mu$  is the solution viscosity,  $r$  is the particle radius (nm), and  $\kappa = (2n_0 z^2 e^2 / \epsilon_r \epsilon_0 k_B T)^{1/2}$  is the Debye–Hückel parameter (Sze *et al.*, 2003). The electrophoretic mobility is acquired by performing an electrophoresis experiment on the sample and measuring the particle velocity by using a laser as a light source (Laser Doppler Velocimetry (LDV)) (ZetaSizer nano user manual, v 5, August 2009). The following protocol was followed for each measurement: 1 mL of the NSAIDs o/w emulsion was added to capillary cell DTS1070 first, and then increased amount of 10  $\mu$ L polymer (2 mg/mL in phosphate buffer pH 5) was added until it reached the saturation. The total amount of polymer added was different for each type of polymer (Tables 4-1, 4-2 & 6-1). The dispersant for the o/electrolyte was phosphate buffer (1.05 viscosity and temperature 25°C), and the calculation was run for three measurements including three replicates. Finally, the data interpretation has been presented by the Zetasizer software under standard operation procedures (SOP).

### 2.3.2. Size measurements

Emulsion droplets particle size was measured by Dynamic light scattering (DLS) using Malvern Zetasizer Nano ZS (Malvern Instruments Limited, UK). It is a technique classically used for measuring the size of droplets dispersed in a solution or emulsion. Generally, it calculates size by measuring the Brownian movement of particles or molecules in a buffer or solvent (ZetaSizer nano user manual, v 5, August 2009). Using the Stokes-Einstein relationship (equation 2) (Coglitore *et al.*, 2017), this diffusion speed is converted into a size distribution.

$$D_h = k_B T / 3\pi\eta D_t \quad (2)$$

Where:  $D_h$  is the hydrodynamic diameter (m),  $D_t$  is the translational diffusion coefficient (J/K),  $k_B$  is Boltzmann's constant,  $T$  is the thermodynamic temperature (K), and  $\eta$  is dynamic viscosity (kg/m.s) (ZetaSizer nano user manual, v 5, August 2009). For the analysis, 1mL of the emulsion with/without the polymer was added to the cuvette cell and was measured, the experiment was run for three replicates and was conducted twice. The Zetasizer software measured the data interpretation under SOP.

### 2.3.3. Determination of POLYX molecular weight and its degradation kinetics

In a 15 mL test tube, a solution composed of 2 mg/mL of POLYX (POLY-A5 and POLY-B5) in acetate buffer pH 5 and another one in pH 7.3 was prepared and incubated at 37 °C to study POLYX molecular weight (MW), and its degradation kinetics. A Shimadzu model RID-20A

gel permeation chromatography (GPC) was used to determine the MW. GPC is an analytical technique that separates molecules in polymers by size diameter and presents the material molecular weight distribution. Its principle is that the large compounds ( $\geq 5 \mu\text{m}$ ) go around the GPC column particles made of gel material while the small compounds ( $< 5 \mu\text{m}$ ) go through the column particles porous (Beri, Hacche and Martin, 2000). Therefore, as the compound's size decreases, the elution time increases (Beri, Hacche and Martin, 2000). For the experiment, on day 0 (the first day of preparing the POLYX solution), a 1 mL of the sample from each buffer (pH 5 and pH 7.4) was collected and analysed for MW determination. After that, the sample was collected every 24 hours and immediately examined for over 30 days, (measurement was taken daily in the first 2 weeks and then every 5 days). For each sample, two replicates have been collected every time.

A calibration curve has been set up using polyethylene glycol (PEG) as a stander with known molecular weight (200-36000 Da) purchased from Fluka Chemie AG. First, a 1 mg from the polymer was diluted in 1 mL acetate buffer pH 5, then 1 mL was taken and determined using the GPC with 25 min running time. The mobile phase was acetate buffer pH 5, and the column used was Superdex 75 10/300GL (Table 2-4). The results were plotted on an Excel sheet, and the linear relationship between the MW (Da) and the time of peak appears as expected (figure 2-3). The calibration curve equation was equals to  $y = - 0.212x + 6.1465$  and  $R^2 = 0.987$ .

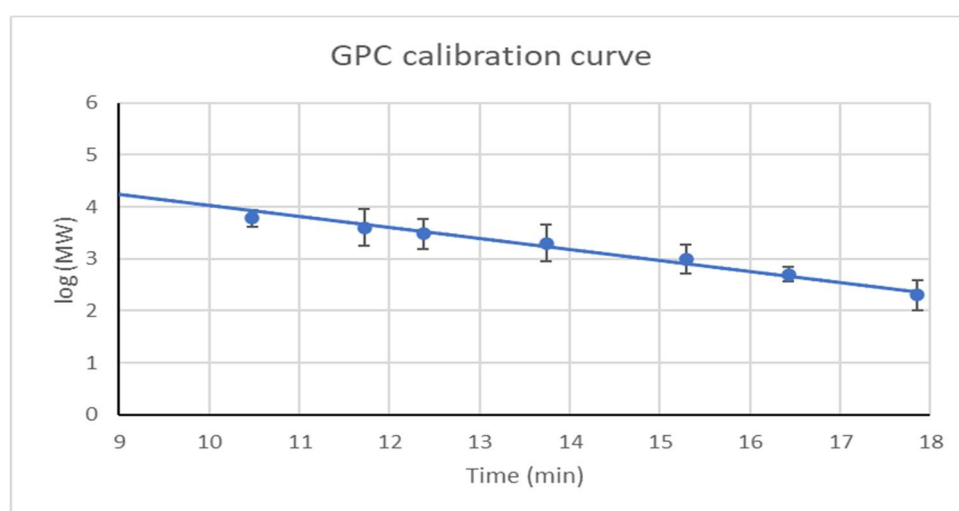


Figure 2-3. GPC calibration curve of polyethylene glycol (PEG) stander using HPLC. The x-axis represents the incubation time (min) and the y-axis represents PEG log MW. The regression equation is shown as a solid line, with the equation  $y = - 0.212x + 6.1465$  and  $R^2 = 0.987$ .

Table 2-4 The GPC parameters for the determination of poly beta amino ester polymer molecular weight

Mobile phase	100 % acetate buffer pH 5
Stationary phase (column)	Superdex™75,10/300 GL
Flow rate	1 mL/min
Injection volume	20 µL
Experimental time	25 min

In addition to the MW degradation, the polymer degradation kinetics was conducted using ZP calculation methods. To do that, approximately 700 µL of the polymer prepared in buffer pH 5 and pH 7.4 was added to capillary cell DTS1070 then the charge was measured once per day for 30 days. The dispersant for the polyelectrolyte was phosphate buffer (1.05 viscosity and temperature 25 °C), and the average value was calculated based on 3 measurements.

## 2.4. Cartilage uptake experiments

### 2.4.1. Cartilage samples

The cartilage extracted from 6 to 8 days old immature bovine steers feet purchased from local abattoirs (F DRURY & SONS LTD), which then washed and shaved using a sharp blade. After that, their metacarpophalangeal joints were exposed for gathering by using 5 mm diameter biopsy punchers (Kai medical) to be used for this project experimental work (Figure 2-4). A 5mm full-depth articular cartilage explants with thickness were maintained at approximately 0.5 mm. The explants were carried to a chilled box and stored in the freezer at -4 °C.

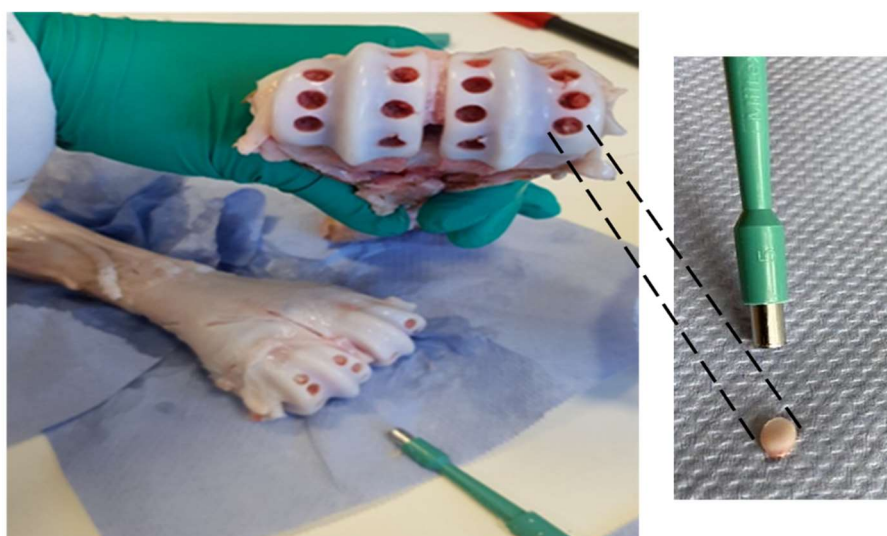


Figure 2-4. Image of cartilage extraction from bovine feet using 5mm diameter biopsy puncher.

Glycosaminoglycans (GAGs) depleted samples (simulating early OA stage) were prepared by digesting the cartilage disc in trypsin 1 mg/mL (1:250) powder (Gibco) in PBS (Oxoid). Cartilage discs were incubated in 500 $\mu$ L of trypsin solution for 24 hours at 37 °C.

### **2.4.2. Cartilage digestion**

A cartilage digestion buffer solution consisted of 300 mg of papain, 1mM ethylenediaminetetraacetic acid (EDTA) and 2mM dithiothreitol (DTT) which was added to 1 litre of the pH 6.8 phosphate buffer. A phosphate buffer of 0.2 M at pH 6.8 is used to neutralise the cartilage in the digestion and lower the mixture's viscosity. Papain is a digestive enzyme that mainly solubilizes GAGs by cleaving the core protein and chondrocyte DNA, and degrading nuclear binding proteins (Storer and Ménard, 2013). While EDTA is a chelation agent, it chelates toxic metal ions, decreases drug-related cytotoxicity, and decreases radical reaction and oxidation which are responsible for cell injury (Wolf and Gilbert, 1992). Moreover, DTT is a strong reducing agent used to reduce the disulphide bonds of proteins and to hinder the building of intramolecular and intermolecular disulphide bonds between cysteine residues of proteins (Li, 2003).

After conducting the uptake and retention experiments, the cartilage was incubated in 1 mL digestion buffer and incubated at 55 °C for 24 to 48 hours until the cartilage disc was completely dissolved. Then the drug concentration was determined using an HPLC instrument.

### **2.4.3. Drug uptake into cartilage**

96 well plate was used to study the uptake of the drug and its penetration level inside the cartilage tissue. Cartilage discs (5 mm diameter and approximately 0.5 mm thick) were weighed and fixed into the plate using a small amount of high vacuum grease facing the superficial layer (cartilage side) up. Each well was filled with 100  $\mu$ L of POLYX drug o/w emulsion and then placed inside an incubator at 37°C for the required time. The time starts at 30 seconds, then 1, 2, 3, 5, 7, 10, 15 and ends at 20 min. After that, each sample was removed, washed with an extensive amount of water to remove any debris, placed in an Eppendorf tube containing 1 mL of digestion buffer and incubated at 55 °C for 24 hours or until the cartilage dissolved completely. Experiments were performed 3 independent times with 4 replicates, while the samples were generated from 3 different bovine feet.

A comparison of the drug uptake was made between POLYX-NSAIDs o/w emulsion at a concentration of 4 mg/mL and NSAIDs prepared in P control and E control. The experiments

were performed on untreated cartilage and GAGs depleted cartilage (mimicking the early stage of OA cartilage).

#### **2.4.4. Drug retention into cartilage**

Cartilage samples were treated with NSAID solution in 96 well plates for 10 min (NSAID uptake was highest at 10 min for most of the cartilage sample; therefore, it was chosen for the retention experiment). Then, after washing with extensive amount of water, they were incubated at 37°C in Eppendorf containing 500µL of PBS at fixed intervals starting from 5 min then 15, 30, 60, 120, 150,180, 200, 300, up to 400 min. After that, cartilage was removed, washed with water, placed in 1 mL digestion buffer, and stored in an incubator at 55 °C for 24 to 48 hours until cartilage disc was dissolved completely. Finally, the sample was taken to measure the drug retention time using HPLC. Experiments were performed 3 independent times with 4 replicates, and samples were generated from 3 different bovine feet for both untreated and GAG depleted samples.

#### **2.5. Drug quantification**

Reverse phase- HPLC (Agilent 1220LC) was used to quantify the amount of NSAIDs in the cartilage. An Agilent serious HPLC system was used with a Teknokroma TRACE EXCEL 120 ODSB 5 µm while µBondapak® C18 10 µm 125A analytical columns was used for indomethacin at the 25 to30°C thermostat. The HPLC parameters used are the same as shown in table 2-5. The amount of drug retained in the cartilage was then expressed as the mass of drug per cartilage mass (µg/mg).

##### **2.5.1. Calibration curves**

It is the first and an important step for each drug in most measurement procedures which are used to understand the instrumental response to the compounds or drugs and calculate the concentration of an unknown sample in solution. Therefore, the reverse-phase high performance liquid chromatography (HPLC) was used in this project. The column used in the HPLC consists of an octadecyl-carbon chain (C18) bonded to silica nanoparticles; these columns withhold in the non-polar stationary phase, so this is ideal for the emulsion, while the mobile phase being pumped is an aqueous buffer with acetonitrile ( for ketorolac) or acetate buffer (for indomethacin, naproxen, diclofenac sodium) being used (table 2-5) as the polar organic modifier to allow better elution of NSAIDs emulsion in the column (Thorat and Jangle, 2013).

Generally, to set up the calibration curve a series of standard dilution samples were prepared at various concentrations starting from 1000  $\mu\text{g}/\text{mL}$  to 17 serial dilutions (1000  $\mu\text{g}$ , 500  $\mu\text{g}$ , 250  $\mu\text{g}$ , 125  $\mu\text{g}$ , 62.5  $\mu\text{g}$ , 31.25  $\mu\text{g}$ , 16  $\mu\text{g}$ , 8  $\mu\text{g}$ , 4  $\mu\text{g}$ , 2  $\mu\text{g}$ , 1  $\mu\text{g}$ , 0.976  $\mu\text{g}$ , 0.488  $\mu\text{g}$ , 0.244  $\mu\text{g}$ , 0.122  $\mu\text{g}$ , 0.061  $\mu\text{g}$ , 0.030  $\mu\text{g}$ ) that includes the sample of interest and then the HPLC response at each concentration is recorded. The solvent was dimethyl sulfoxide (DMSO) (organic liquid widely used as a chemical solvent). Firstly, a stock solution of NSAIDs in DMSO (1 mg/mL) was made, followed by 16 standard serial dilutions and the analysis was performed on 3 independent replicates for each dilution. The results were plotted on an Excel sheet and linear relationship between the concentration and the average area was expected. The response at each concentration was repeated 3 times for more accuracy and to understand the error. The data are then fit with a function so that unknown concentrations can be predicted. The following table (Table 2-5) shows the parameter for the different NSAIDs used in this project.

Table 2-5. Calibration curve parameters of NSAIDs, their solubility in PBS and log P value. All the NSAIDs have a slight aqueous solubility as they have a positive log P value (range between 2.28-4.15) which indicating that they have affinity to oil/lipid phase (lipophilic).

<b>NSAIDs</b>	<b>Mobile phase</b>	<b>Flow rate</b>	<b>UV spectrophotometer detector (nm)</b>	<b>Injection volume</b>	<b>Retention time</b>	<b>Solubility in PBS buffer</b>	<b>Log P</b>
<b>Indomethacin</b>	Acetonitrile and acetate buffer PH 3.6 (60:40)	1 mL/min	255	20 µL	5 min	0.734 mg/mL	3.4
<b>Ketorolac</b>	Acetonitrile, PBS and acetic acid glacial (26:70:4)	1 mL/min	315	20 µL	20 min	26 mg/mL	2.28
<b>Naproxen</b>	Acetonitrile and acetate buffer PH 4 (35:65)	1 mL/min	230	20 µL	10 min	1 mg/mL	3.18
<b>Diclofenac sodium</b>	Acetonitrile and acetate buffer PH 4 (42:58)	1 mL/min	276	20 µL	10 min	6.8 mg/mL	4.15

### 2.5.1.1. Indomethacin

The equation which has been got is equal to  $y = 40.815x + 11.897$  and  $R^2 = 0.9999$  (Figure 2-5).

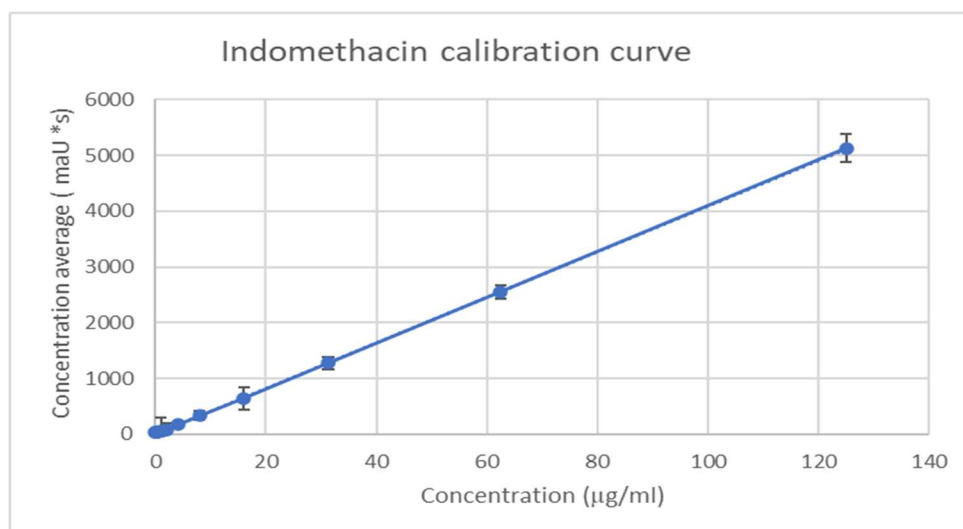


Figure 2-5. Indomethacin calibration curve using HPLC. The x-axis represents the concentration of indomethacin in µg/mL, and the y-axis represents the response of the detector in mAU. The regression equation is shown as a solid line, with the equation  $y = 40.815x + 11.897$  and  $R^2 = 0.999$  indicated in the legend.

### 2.5.1.2. Ketorolac

The equation which has been gained is equal to  $y = 51.295x + 329.97$  and  $R^2 = 0.9994$  (Figure 2-6).

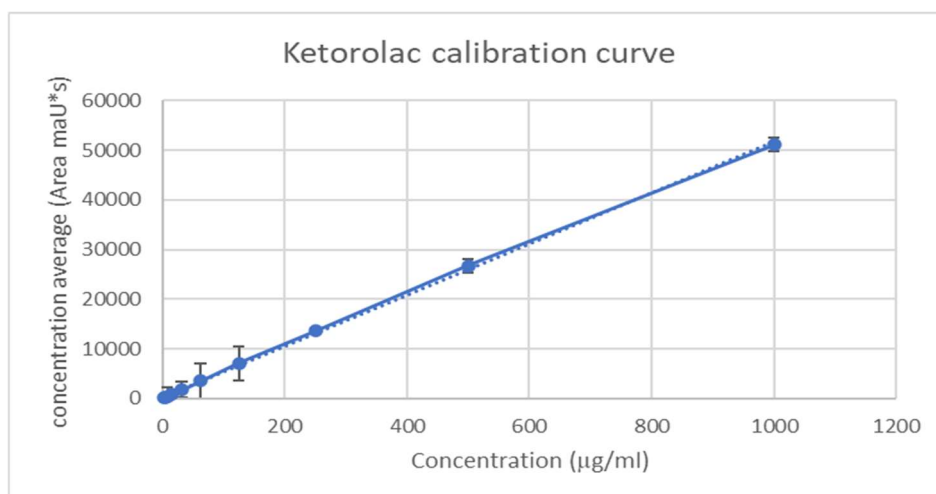


Figure 2-6 . Ketorolac calibration cure using HPLC. The x-axis represents the concentration of ketorolac in µg/mL, and the y-axis represents the response of the detector in mAU. The regression equation is shown as a solid line, with the equation  $y = 51.295x + 329.97$  and  $R^2 = 0.9994$  indicated in the legend.

### 2.5.1.3. Naproxen

Naproxen calibration curve equation is equal to:  $y = 266.79x - 17.471$  and  $R^2 = 0.9992$  (Figure 2-7).

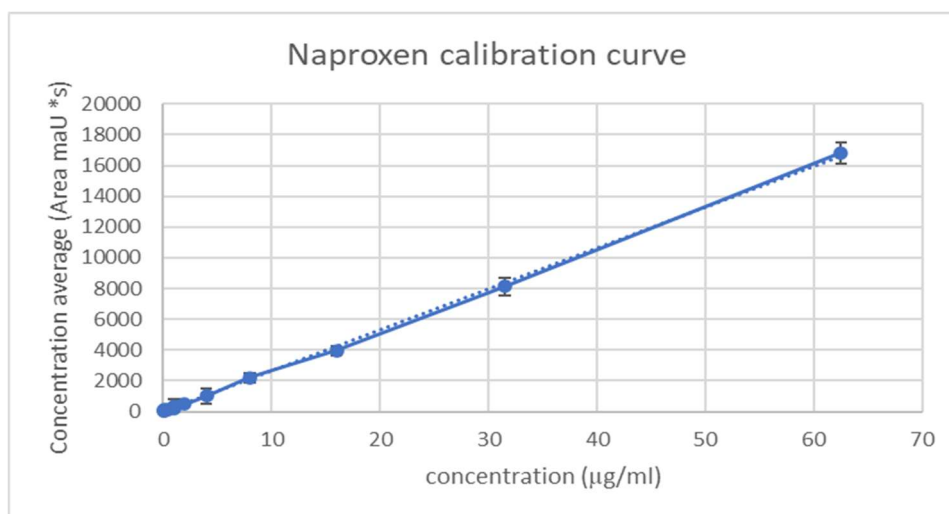


Figure 2-7. Naproxen calibration curve using HPLC. The x-axis represents the concentration of naproxen in  $\mu\text{g/mL}$ , and the y-axis represents the response of the detector in mAU. The regression equation is shown as a solid line, with the equation  $y = 266.79x - 17.471$  and  $R^2 = 0.9992$  indicated in the legend.

### 2.5.1.4. Diclofenac sodium

The final equation which got for the Diclofenac sodium is:  $y = 41.752x - 58.116$  and  $R^2 = 0.9996$  (Figure 2-8).

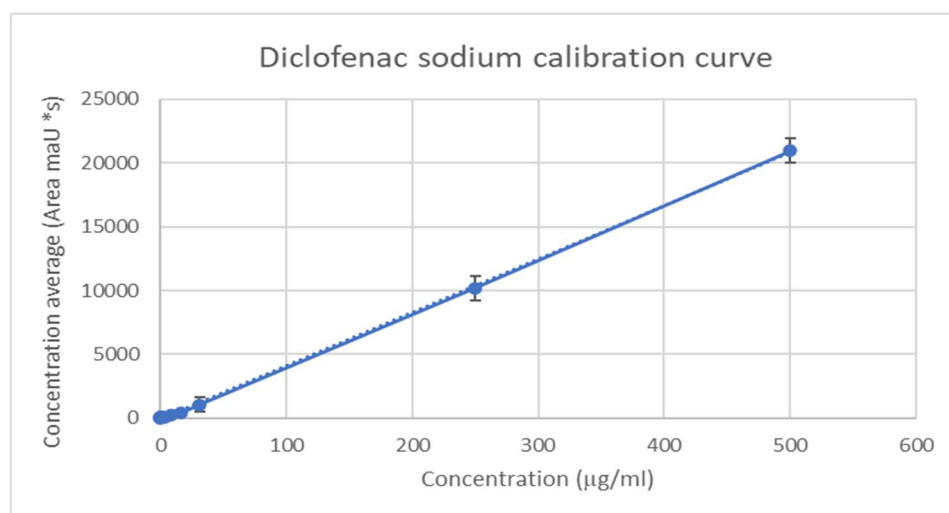


Figure 2-8. Diclofenac calibration curve using HPLC. The x-axis represents the concentration of diclofenac sodium in  $\mu\text{g/mL}$ , and the y-axis represents the response of the detector in mAU. The regression equation is shown as a solid line, with the equation  $y = 41.752x - 58.116$  and  $R^2 = 0.9996$  indicated in the legend.

## **2.6. Effect of the drug delivery system on IL-1 $\alpha$ treated cartilage**

The objective of this experiment was to test the ability of the DDS (Ket emulsion coated with POLY-X) to inhibit the effect of the inflammatory cytokine (IL-1 $\alpha$ ). It is aimed at preventing or decreasing GAG and collagen degradation and loss of cell viability in cartilage explants over two to three weeks after exposure to the DDS. The cartilage explants treated with IL-1 $\alpha$  (1ng/mL) were cultured with or without the DDS and then GAG, and collagen content was measured; the live/dead imaging and XTT assays were done on day1, 2, 4, 7, 9, 11, 14, and Safranin O staining assay was done in day 14 only for POLY-A5. For POLY-B5 and POLY-F3, all the experiments were done for 20 days. These experiments help to test the hypothesis that NSAIDs coated with POLYX can recover the effect in cytokine treated cartilage relevant to post-traumatic OA.

### **2.6.1. Fresh bovine cartilage harvest and culture**

Cartilage discs were extracted from fresh 6 to 8 days old immature bovine steers feet purchased from local abattoirs (F DRURY & SONS LTD) which then washed and shaved using a sharp blade. Using fresh cartilage samples, metacarpophalangeal joints were exposed for gathering using 5 mm diameter biopsy punchers, figure 2-4 (Kai medical). 5mm full-depth articular cartilage explants were extracted with thickness maintained at approximately 0.5 mm. Cartilage discs for all treatment groups were weighed to normalise the results. Cartilage discs were equilibrated in serum-free medium ( low-glucose DMEM, L-glutamine, 25 Mm HEPES, 110mg/l sodium pyruvate), supplemented with 5 mL 1% insulin-transferrin selenium, 5 mL (100X) Minimum essential medium nonessential amino acid (MEM NEAA) (all from gibco by life technologies), 4M proline (Aldrich), 20 mg/mL ascorbic acid (Fisher Scientific), 100 units/mL penicillin, 100  $\mu$ g/mL streptomycin and 250  $\mu$ g/mL amphotericin B (Sigma Aldrich) for three days prior to treatment in 37 °C, 5% CO<sub>2</sub> incubator. The serum-free medium formulation is essential to maintain cultured cartilage explant's mechanical and biochemical properties. After three days of equilibration the cartilage explants in such media, cartilage metabolism was found to be relatively stable during the experiment culture period (Liming Bian *et al.*, 2010).

### **2.6.2. Treatment of cartilage with cytokine (IL-1 $\alpha$ )**

Traumatic joint injury which leads to the development of post-traumatic OA, is characterized by increased concentration of pro-inflammatory cytokines such as IL-1 $\alpha$  and TNF $\alpha$  (Bajpayee *et al.*, 2016; Punzi *et al.*, 2016). In the present work, cartilage explants were treated with 1ng/mL of IL-1 $\alpha$  to mimic post-traumatic OA cartilage. Moreover, to create baseline

comparison for study the effectiveness of NSAIDs emulsion coated with POLY-X polymer, cartilage explants were first treated with/without IL-1 $\alpha$  (1 ng/mL) (Sigma Aldrich) for 20 days in the presence of the following conditions: (1) 4 mg/mL Dexamethasone or NSAIDs o/w emulsion, (2) 4 mg/mL dexamethasone or NSAIDs o/w emulsion coated with POLY-X polymer, (3) untreated cartilage, and (4) IL-1 $\alpha$  treated samples as a control group. During the 20-day culture period, the medium for all treatment groups was replenished every 2 to 3 days with dexamethasone and NSAIDs.

### **2.6.3. Treatment of cartilage with NSAIDs emulsion coated with different types of PBAEs polymer**

The experiments were done using ketorolac as a module of NSAID due to its high uptake and retention in cartilage, as reported in the results presented in chapter 4. Moreover, Dexamethasone (Dex) was used as a positive control which is widely used in the clinic as an intra-articular injection for OA treatment (Hochberg, McAlindon and Felson, 2000; Wehling *et al.*, 2017).

Initially, cartilage disc was equilibrated with 1 mL of culture medium in a 24-well plate for a period of three days. Then, the medium was replaced by 1 mL of fresh medium containing the treatment conditions with or without IL-1 $\alpha$  (1 ng/mL) as follows: (1) basal media, untreated control; (2) 1 ng/mL of IL-1 $\alpha$  alone; (3) Dex+IL-1 $\alpha$ ; (4) NSAIDs + IL-1  $\alpha$ ; (5) Dex alone; (6) NSAIDs alone; (7) o/w emulsion alone; (8) o/w emulsion+ IL-1  $\alpha$ ; (9) o/w emulsion + POLYX; (10) o/w emulsion+ IL-1  $\alpha$  + POLYX; (11) Dex o/w emulsion + POLYX; (12) Dex o/w emulsion+ POLYX+IL-1 $\alpha$ ; (13) NSAIDs o/w emulsion + POLYX; and (14) NSAIDs o/w emulsion+ POLYX+IL-1  $\alpha$ . An effective concentration of 4mg/ml of Dex, 4mg/ml of NSAIDs and 10 % of the o/w emulsion were used in all treatments. Moreover, the culture medium with the treatment condition was refreshed every 2-3 days, and at days 1, 2, 4, 7, 9, 11, 14, and 20 of the culture periods, the cartilage disc was collected to perform measurements of glycosaminoglycan (GAG) and collagen, imaging of viability through live/dead assays, the XTT assay, and histological assessment of the cartilage tissue.

### **2.6.4. Quantification of glycosaminoglycan (GAG)**

The negatively charged sulphated glycosaminoglycan (sGAG) side chain, which is mainly found on aggrecan, has been considered to play a significant role in cartilage homeostasis, since its negative charge attracts water into cartilage and led to create a high osmotic pressure (Elson *et al.*, 2015; Zheng and Levenston, 2015). Furthermore, this high negative charge density contributes to the tissue's structural stiffness and strength (Elson *et al.*, 2015; Zheng and

Levenston, 2015). Therefore, it is essential to measure sGAG quantity to assess cartilage integrity and strength. In this project, sGAG content in digested cartilage explants was measured using a dimethyl-methylene blue (DMMB) dye assay. DMMB is a simple colourimetric assay which widely used to quantify sGAG contents of tissues and fluids (Farndale, Buttle and Barrett, 1986; Zheng and Levenston, 2015). It is used mainly to estimate the amount of proteoglycan by measuring sGAG in the samples (Warren, 2000).

First, DMMB colour reagent was prepared following Farndale *et al.* procedure (Farndale, Buttle and Barrett, 1986), a 16 mg of DMMB was added to one litre of dH<sub>2</sub>O containing 3.04 g of glycine, 2.37 g of NaCl and 95 mL of 0.1M HCl. After that, calibration curve was performed using a different concentration of chondroitin sulphate stock solutions that ranged from 10 to 60 µg/mL prepared in dH<sub>2</sub>O (Figure 2-9). To generate the calibration curve, 40 µL of chondroitin sulfate at various concentrations was pipetted in triplicate onto 96-well plates, followed by the addition of 200 µL of DMMB reagent to each well. The colour density was measured immediately using a plate reader (Tecan, Infinite 200 PRO) at 525 nm.

For the experiment, cartilage explants (that were treated differently as described above) were removed from the media, washed with a sterile PBS to eliminate any debris, and placed in an Eppendorf tube containing 1ml of papain digestion buffer. Subsequently, the samples were incubated for a period of 24-72 hours at 55 °C until the cartilage dissolved completely. After that, 40 µL of the untreated digested cartilage (control), trypsin treated digested cartilage and 40 µL of the digested cartilage explants from each treatment type were added onto 96 well plates in 5 replicates, followed by addition of 200µL of DMMB reagent, then the colour density was measured immediately at 525 nm.

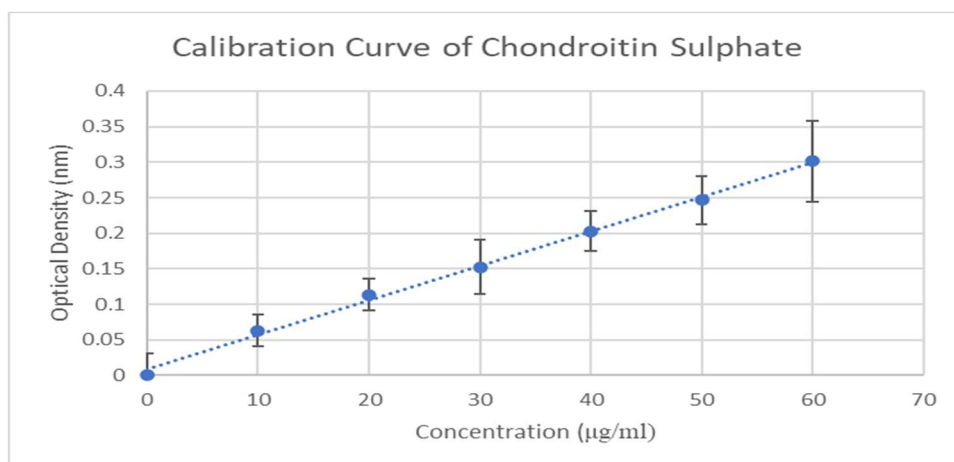


Figure 2-9 . Calibration curve of chondroitin sulphate using plate reader (Tecan Infinite 200 PRO) at 525 nm. The x-axis represents the concentration of chondroitin sulphate in µg/mL, and the y-axis

represents the optical density in nm. The regression equation is shown as a dotted line, with the equation  $y = 0.0049x + 0.0086$  and  $R^2 = 0.9969$  indicated in the legend.

### 2.6.5. Collagen content determination assay

Collagen content was measured using the hydroxyproline assay. Hydroxyproline is a major collagen component that stabilises its helical structure; therefore, its level was used as an indicator for collagen content in the sample (Lim, Choi and Park, 1999; Cissell *et al.*, 2017). Hydroxyproline assay is a broadly employed method of quantifying collagen in tissue based on the fact that collagen could be quantified indirectly through hydroxyproline content since this amino acid is primarily present in collagen (Cissell *et al.*, 2017). Different types of controls were prepared similarly to the sGAG quantification method. The hydroxyproline assay procedure is based on the acidic hydrolysis of the digested cartilage samples and the determination of the free hydroxyproline in hydrolysates. Chloramine-T was used to oxidise hydroxyproline to a pyrrole intermediate that reacts with N, N-dimethylbenzylamine to produce a chromophore with a peak absorption of light wavelength 570nm (Cissell *et al.*, 2017).

For the analysis, 100 $\mu$ L of the cartilage digest solution (following the same procedure of digestion of the cartilage as in sGAG quantification experiments) were aliquoted in Eppendorf's tubes and hydrolysed to individual amino acids including hydroxyproline using 500 $\mu$ L of 12N HCl (Sigma-Aldrich) at 100 $^{\circ}$ C oven for 18hour (Pratta *et al.*, 2003). After that, the tube was opened, and the hydrolysate was dried in the oven at 55  $^{\circ}$ C for 48-72 hour. Then, the residue was dissolved in 150 $\mu$ L dH<sub>2</sub>O, transferred to a 96 well plate and dried in a chemical hood for another 48-72 hour. Then using a 96 well plate, 60 $\mu$ L of dH<sub>2</sub>O was added to each well, followed by 20 $\mu$ L of assay buffer and 40 $\mu$ L of chloramine T solution (Sigma-Aldrich). The reagent was then left to react for 15 minutes at room temperature. Finally, to each well, 20 $\mu$ L of 1-propanol (Alfa Aesar), 30 $\mu$ L of perchloric acid (Sigma-Aldrich) and 30 $\mu$ L of N, N-dimethylbenzylamine (Sigma-Aldrich) were added, respectively. The plate was closed and left in a 70  $^{\circ}$ C oven for 20 minutes. Finally, after allowing the plate to cool down, the colour density of each well was measured at 570 nm using a plate reader (Tecan, Infinite 200 PRO) (Pratta *et al.*, 2003). Following the same methods, calibration curve was obtained using a different concentration of hydroxyproline solution ranging from 1-6 mg/mL) (Figure 2-10).

#### **Solution preparation:**

- **Assay buffer:** it was prepared by mixing 3 mL of 1-propanol (Alfa Aesar), 2 ml dH<sub>2</sub>O and 10 mL Ph 6 citrate buffer.

- **Chloramine T reagent:** it was prepared by combining 0.14g of chloramine T(Sigma-Aldrich), 500  $\mu$ L dH<sub>2</sub>O, 4 mL pH 6 citrate buffer and 500  $\mu$ L dH<sub>2</sub>O.

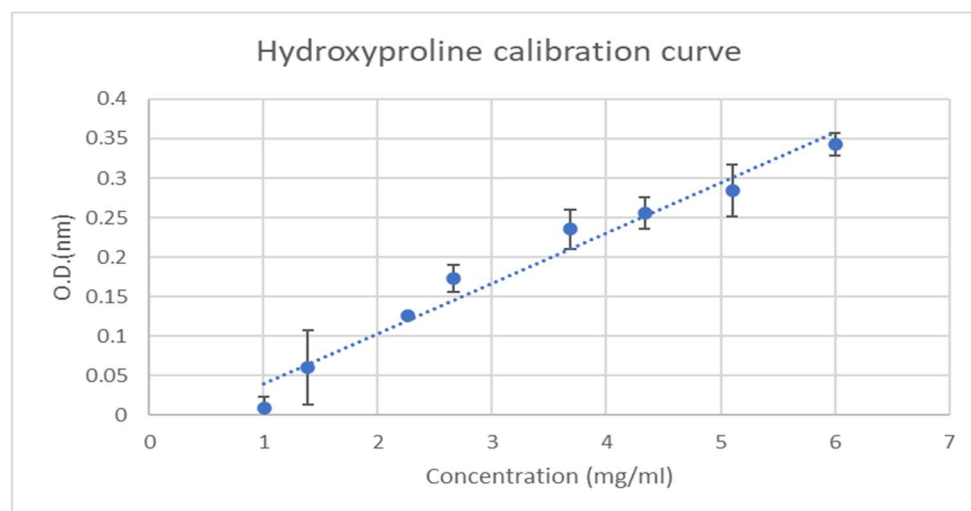


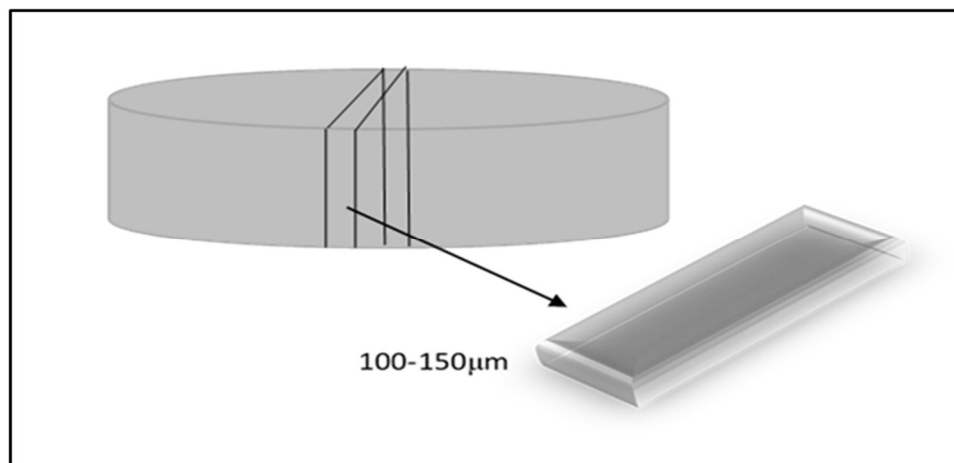
Figure 2-10 . Calibration curve of hydroxyproline using plate reader (Tecan Infinite 200 PRO) at 570 nm. The x-axis represents the concentration of hydroxyproline in mg/mL, and the y-axis represents the optical density in nm. The regression equation is shown as a dotted line, with the equation  $y=0.0636x+0.0243$  and  $R^2 = 0.9684$  indicated in the legend.

### 2.6.6. Live/dead staining and imaging

It is a method used to assess the viability of the cartilage tissue employing laser scanning confocal (LSM) microscopy (Zeiss LSM880). The live/ dead <sup>TM</sup> viability/cytotoxicity kit (LOT 206927, Invitrogen by Thermo fisher scientific) has been used which utilises calcein-AM (calcein acetoxymethyl ester) (green fluorescence) and ethidium homodimer-1 (red fluorescence). Calcein AM is a cell-permeable, non-fluorescent compound. After crossing the cell membrane, it is rapidly hydrolysed by cellular esterase inside live cells. This cleaves the AM group to allow converting the non-fluorescent calcein AM to a strongly green fluorescing calcein. Dead cells do not have active cytoplasmic esterase's, therefore, cannot convert calcein AM to calcein, and subsequently do not fluoresce green (Grogan *et al.*, 2001; Molecular-Probes, 2005). In contrast, ethidium homodimer-1 is a high-affinity nucleic acid stain which enters cells with the compromised cell wall and emits red fluorescence in dead cells after binding to the cell's DNA. It is excluded by the intact cell membrane of live cells (Grogan *et al.*, 2001; Molecular-Probes, 2005). These two compounds allow for quick and easy detection of metabolically active and dead cells in samples.

The live dead stain buffer was prepared by adding 5  $\mu$ L of calcein-AM and 20  $\mu$ L of ethidium homodimer-1 to 10 mL sterile PBS. The solution was prepared before use and used immediately as the calcein-AM is liable to hydrolysis when exposed to moisture.

On the day of the experiment, 100-150  $\mu\text{m}$  thick cartilage slices were cut from the centre of cartilage discs from each treatment type using a sharp-bladed (Scheme 2-1). Into 96 well plates, slices were immediately stained with 200 $\mu\text{l}$  live/dead staining solution for 30 minutes in the dark at room temperature. Slices were washed with PBS and imaged on 10 times objective lens using LSM (Zeiss LSM880) (calcein AM excitation/emission  $\sim 493\text{-}582\text{ nm}$  and ethidium homodimer1 excitation/emission  $\sim 582\text{-}741\text{ nm}$ ). Live cells were stained green with calcein-AM and dead cells were stained red with ethidium homodimer; the cells were imaged on days 1,2,4,7,9,11, 14 and 20 using confocal microscopy.



Scheme 2-1: The schematic diagram demonstrates the cutting position of the cartilage slices in the cartilage disc using a scalpel. Slice thickness around 100-150  $\mu\text{m}$  and 5mm depth.

### 2.6.7. XTT assay:

The XTT (2,3-bis-[2-methoxy-4-nitro-5-sulfophenyl]-2H-tetrazolium-5-carboxanilide tetrazolium salt) assay, which composed of a tetrazolium dye, is a widely employed method that is effective for evaluating cell proliferation and measuring cell viability. XTT is a negatively charged, colourless or faint yellow colour tetrazolium salt that turns to orange when it reduced to a soluble formazan dye (Figure 2-11). This colour change is due to the breaking apart the positively charged quaternary tetrazole ring. The extracellular reduction is occurred by electron transport across the plasma membrane of a living cell. As it proceeds by electron transport from outside the cell, the use of an intermediate electron acceptor such as phenazine methosulfate is required for complete reduction of XTT (XTT Cell Proliferation Assay Kit Instruction Manual, catalogue Number 30-1011K). The amount of XTT reduced is contributed to the cellular metabolic activity.

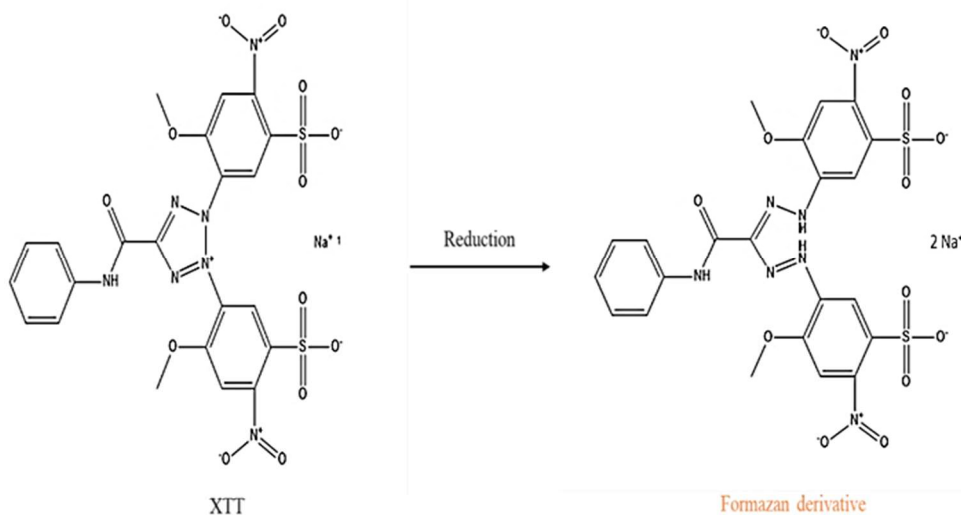


Figure 2-11. Principle of XTT assay: the enzymatic reduction of XTT to form the orange-coloured formazan derivative by viable cells.

Cartilage tissue viability was analysed using a cell proliferation assay kit II (XTT) (Roche) with a small adaptation to the company instruction (Roche). In brief, pre-weighed cartilage tissues were cultured in media (with /without IL-1  $\alpha$ ) for 20 days. Then, cartilage disc was cut using a scalpel into approximately 4-6 pieces and incubated in the XTT solution (1 mL) for a period of 4 hours at 37 °C. Then, XTT solution was removed and retained to be used later. After that, 0.5 mL of dimethyl sulfoxide (DMSO) was added to extract the tetrazolium product from the tissues and incubated for 1 hour. Prior to the absorbance reading, the XTT and DMSO solutions were mixed appropriately, and then the absorbance of the samples was measured using a microplate reader in triplicates at 450 nm and 690 nm (Tecan, Infinite 200 PRO) in a 96-well plate. Finally, the absorbances at 690 nm were subtracted from those at 450 nm, and XTT content was calculated per gram of tissue.

### 2.6. 8. Histological evaluation of cartilage tissues

The cartilage was sliced from the bone using a scalpel for histological evaluation. First, cartilage samples were fixed in 10 % (v/v) neutral buffered formalin (Sigma-Aldrich) for 48 hours. Then, it was dehydrated through increasing ethanol concentrations (70-96%) for 1 min, followed by xylene for 4 min and then embedded in paraffin wax for around 7 days. After that, serial sections (5  $\mu$ m) were rehydrated, and stained with Weigert's haematoxylin (Atom Scientific) for 3 min, differentiated in 1 % (v/v) acid alcohol (Sigma-Aldrich), stained with 0.02 % (w/v) aqueous fast green (Sigma-Aldrich) for 5 min and washed briefly in 1 % (v/v) acetic acid (APC pure) before staining with 0.1% safranin O (Sigma-Aldrich) for 5 min.

Finally, sections were dehydrated and mounted. Images were captured using a Leica DMRB photomicroscope controlled by Zen Pro software 2012 (Zeiss).

### **2.7. Statistical analysis**

After data were assessed for normality, statistically significant differences between the mean of NSAIDs uptake and retention ( $\mu\text{g}/\text{mg}$  cartilage) in untreated and GAG-depleted cartilage in comparison to NSAIDs uptake and retention in each type of control were tested using paired sample t-test or one way ANOVA with a Tukey's post hoc test ( $p < 0.05$ ). The statistical analysis was performed using IBM SPSS Statistics (Version 25).

### **3. Chapter three: Osteoarthritis (OA) ex vivo model development**

#### **3.1. Introduction**

When developing a drug delivery system as an intra-articular formulation for OA treatment, one of the main goals is to improve drug uptake and retention time inside the cartilage tissue. Therefore, selecting the right models is crucial for accurate outcome assessment, targeting effects, and decreasing traditional drug side effects (Salgado, Jordan and Allémann, 2021). Many in vitro or ex vivo models have been used to study the pathogenesis of OA at both tissue and cellular levels or to assess the effect of formulation/delivery system for OA treatment; however, no single model has proven to be the gold standard for OA research (Cope *et al.*, 2019; Salgado, Jordan and Allémann, 2021; Samvelyan *et al.*, 2021). It is mainly because of the variability in OA disease progression and the differences in anatomy and biomechanics between humans and animals, making it difficult to establish a standard animal model that accurately reflects human disease progression. Some animal models, such as mice and rats, can be expensive and require ethical approval surrounding the use of animals in research, limiting the use of these models. Moreover, developing new therapies for OA requires animal models that can accurately predict the efficacy and safety of the therapies in humans. Despite this, no animal model has been able to predict the outcome of human clinical trials (Cope *et al.*, 2019; Salgado, Jordan and Allémann, 2021; Samvelyan *et al.*, 2021).

An example of in vitro models which are currently used for the investigation of OA treatment are: monolayer culture; co-culture; an explant-based model; scaffold and scaffold-free systems. Monolayer culture, and co-culture are known as 2D cell models while the explant and scaffold/scaffold free are considered to be a 3D cellular model (Cope *et al.*, 2019; Salgado, Jordan and Allémann, 2021; Samvelyan *et al.*, 2021). Table 3-1 presents the advantages and disadvantages of each type of in vitro and ex vivo models.

Table 3-1 Advantages and disadvantages of different types of in vitro and ex vivo models used in OA research.

In vitro /ex vivo OA models	Advantages	Disadvantages
Monolayer	<p>High throughput.</p> <p>Inexpensive.</p> <p>Exposes cells to an equal amount of nutrients and growth factors.</p> <p>Permit the use of a single source of cells for multiple experimental treatments.</p>	<p>Cell may induce de-differentiation and changes in morphology.</p> <p>A large sample of cartilage is required to ensure enough cells are present to do an experiment.</p> <p>Furthest away from the in vivo tissue conditions.</p>
Co-culture	<p>Mainly used in studies of cell-to-cell interactions which are critical in regulating cell and tissue physiology.</p> <p>Allows to study the effects of specific compounds on cell phenotypes.</p>	<p>Different media are required for culturing each cell type.</p> <p>Expensive.</p> <p>Does not allow for growth in all directions, as in the 3D in vivo types.</p>
Explants	<p>Simply produce.</p> <p>Cheap.</p> <p>Allows for investigation of the cell-cell and cell-ECM interactions because it maintains tissue as a whole.</p>	<p>Cell death occurs at the explant edge.</p> <p>A limited number of cells can be extracted from a single source.</p> <p>High variability.</p>
Scaffold and scaffold-free systems	<p>Facilitates the study of cell-cell and cell-ECM interactions under disease phenotype.</p> <p>High similarity to in vivo tissue conditions.</p>	<p>Expensive.</p> <p>Difficult to maintain for a long time.</p> <p>Limited throughput.</p>

Generally, the size of the animal used as a model is significant. Small animal models of OA such as mice, rats, and rabbits are much easier to handle, quicker, and more readily available

to use than the larger animal models such as horses, pigs, dogs and bovines. They are commonly used to study the pathogenesis and physiology of the disease process. However, due to their smaller size, tissue samples extracted differ to a greater extent in their anatomical, physiological, and histological structure than humans (McCoy, 2015; Kuyinu *et al.*, 2016; Cope *et al.*, 2019). Therefore, large animal models offer many advantages over the small animal models in terms of their greater anatomical similarity to the human model and are therefore used mainly to study the effect of drugs or treatment before clinical studies in humans are carried out (McCoy, 2015; Kuyinu *et al.*, 2016; Cope *et al.*, 2019). Cartilage thickness is essential to select an appropriate animal model for OA research. A model with cartilage thickness similar to human cartilage may provide more reliable and accurate information regarding the treatment of OA in humans than a model with significant differences in cartilage thickness (Cope *et al.*, 2019). In addition, it can measure how approximately far the treatment can penetrate inside the cartilage and help researchers develop more effective treatments for OA. Moreover, measuring cartilage thickness in different animal models can help researchers to identify the factors that contribute to the development and progression of OA. For instance, it has been demonstrated in animal models that cartilage thickness is significantly decreased in weight-bearing joints, suggesting mechanical factors play a more prominent role in the development of OA in these joints. In contrast, a more widespread cartilage loss in an animal model may suggest a more systemic disease process (McCoy, 2015; Kuyinu *et al.*, 2016; Cope *et al.*, 2019). A bovine articular cartilage thickness, for example, is similar to that of humans; dogs cartilage thickness is less than half the size of that found in humans, whereas that of a mouse is a minimum of 70 times thinner than human cartilage; therefore, using bovine cartilage, for example, is advantageous due to its similarity to human cartilage. In addition, large animals have a longer life span than small animals, allowing for slower disease progression and, therefore, a longer time span to end-stage OA. Mice, rabbits, guinea pigs, dogs, sheep, bovines, and horses exhibited naturally occurring OA and were widely used as an OA model. Consequently, they are ideally suited to research as they offer opportunity to perform a wider range of tests (such as tissue culture, repeated synovial fluid collection, cartilage extraction, and imaging). Horse's articular cartilage is the most comparable to humans. They have been used to study articular cartilage repair and osteochondral defects as they provide a naturally occurring model for bone remodelling, cyst, and osteophyte formation. Additionally, the large size of horses allows for accessible tissue and fluid collection for imaging and OA treatment testing (McIlwraith, Frisbie and Kawcak, 2012; McCoy, 2015; Kuyinu *et al.*, 2016). Therefore, it could aid the development of treatment to encounter these

human changes, especially in PTOA (McIlwraith, Frisbie and Kawcak, 2012; Kuyinu *et al.*, 2016). In contrast, horse model is expensive, difficult to house and manage due to its large size and complexity (McIlwraith, Frisbie and Kawcak, 2012). Furthermore, it has been widely agreed that bovine OA models are one of the better suited to OA research than other small OA models (McCoy, 2015; Kuyinu *et al.*, 2016; Cope *et al.*, 2019). Cartilage explants provide an important and easy attainable method for studying the efficacy of arthritis drugs, the drug delivery system and assessing tissue remodelling in the cartilage extracellular matrix (McCoy, 2015; Kuyinu *et al.*, 2016; Remaut, 2019; Salgado, Jordan and Allémann, 2021).

In around 12% of people, joint trauma leads to post-traumatic arthritis and a long-term complication of OA (Lotz, 2010; Punzi *et al.*, 2016). Joint injury or trauma induces a number of local pathophysiological changes (such as disruption of the articular surface, synthesis of inflammatory cytokines, breakdown of the extra-cellular matrix cartilage components and the death of chondrocytes) (Punzi *et al.*, 2016; Grodzinsky *et al.*, 2017). These processes combine to bring the subsequent development of post-traumatic osteoarthritis (PTOA) and then chronic OA (Lotz, 2010; Punzi *et al.*, 2016). To prevent this from happening, it is necessary to inhibit these responses to injury and treat OA in the early stage, as injury may turn into an irreversible damage and cannot then be treated without surgical options (Lotz, 2010; Punzi *et al.*, 2016). Therefore, building PTOA model, testing the efficacy of drug or formulation on the reduction of disease progression and complication are important in the research of arthritis.

The aim of the research set out in chapter 3 was to build an early-stage OA and PTOA cartilage model using an *ex vivo* explant bovine cartilage to be used as an OA model and to test the effectiveness of DDSs in treating OA. Bovine cartilage has been commonly chosen as an experimental model by many researchers (Elsaid *et al.*, 2013; Bajpayee *et al.*, 2016; Perni and Prokopovich, 2017). Bovine cartilage explants are representative of the whole cartilage component, they have the advantage of being inexpensive, easy to extract, widely available, suitable for long-term culture, maintaining matrix integrity and homeostasis (D. *et al.*, 2013; Elsaid *et al.*, 2013; McCoy, 2015; Cope *et al.*, 2019). Building these models successfully helped in the study of drug formulation (later in this work). The objective of this chapter is to set out the following stages of this research: the careful extraction of the cartilage in the required thickness, performing an OA and PTOA models, measuring the sGAG and collagen content, and assessing the viability of the cartilage cell using OA models. All results are clearly presented in this chapter.

## **3.2. Materials and methods**

The details of the assay method are provided in chapter 2.

### **3.2.1. OA model development**

#### **3.2.1.1. Early-stage OA**

In OA cartilage, protease enzymes, including matrix metalloproteinases (MMPs) and aggrecanases, degrade cartilage ECM components by breaking down the structural proteins that make up the matrix, such as GAG and collagen, which in turn leads to cartilage weakening and thinning (Yoo *et al.*, 2011). These enzymes are produced by chondrocytes, and synovial cells, in response to various factors, such as mechanical stress, cytokines, and inflammation (Yoo *et al.*, 2011). In order to imitate the early onset of OA, cartilage was treated with 1 mg/ml trypsin in PBS for a period of 24 hours at 37 °C (Moody *et al.*, 2006; Perni and Prokopovich, 2017). Trypsin is a member of the protease family that cleaves aggrecan protein and reduces GAG and collagen levels in cartilage to mimic the early stages of OA. PBS pH is optimal for enzyme function, resulting in a reduction of GAG content of around 50% in the cartilage sample (Moody *et al.*, 2006; Yoo *et al.*, 2011; Perni and Prokopovich, 2017; Huang *et al.*, 2022). This method seemed to be effective as the OA model was prepared successfully in a simple and cost-effective way.

Following the extraction of the cartilage disc from the bovine joint, glycosaminoglycans (GAGs) depleted cartilage samples (simulating the early stage of OA) were prepared by digesting the cartilage in trypsin (Gibco). 1 mg of trypsin powder was measured and dissolved in 1 mL PBS (Oxoid) (1:250). Then, cartilage discs were incubated in 500 µL of trypsin/PBS solution for 24 hours at 37 °C.

#### **3.2.1.2. Post-traumatic OA**

PTOA is characterized by an increased concentration of pro-inflammatory cytokines such as IL-1 $\alpha$  and TNF $\alpha$ , primarily as a response to joint injury that helps the removal of debris in the joint and initiates tissue repair, which can develop into a chronic condition if not resolved on time (Wojdasiewicz, Poniatowski and Szukiewicz, 2014; Bajpayee *et al.*, 2016). In this study, the cartilage explants were treated with 1ng/ml of IL-1 $\alpha$  during the assay period (3 weeks) and incubated in 37 °C, 5 % CO<sub>2</sub> incubator to mimic PTOA cartilage. Therefore, it could be used to test the ability of the DDSs in inhibit IL-1 $\alpha$  induced cartilage degradation.

## **3.3. Results**

Bovine cartilage was extracted from 6 to 8 days old immature bovine steers feet for the development of an ex vivo OA cartilage model. Two models were prepared, as described

above, the difference in the amount of sGAG and collagen between the untreated and the OA model cartilage was measured, and the metabolic state of the tissue (live/dead staining) over three weeks was also studied. The results were as follows:

### 3.3.1. Quantification of collagen and sGAG content in OA cartilage model

An early OA simulated cartilage model (GAG depleted cartilage) was performed by adding trypsin directly to cartilage extract, as previously set out, (see section 3.2.1.1). For confirmation, DMMB and hydroxyproline assays were performed on untreated and GAG depleted cartilage; then, the percentage of sGAG and collagen in the samples were measured.

The results of trypsin treated (GAG depleted) cartilage for a 24-hour period presented approximately a 50% loss in sGAG and collagen content compared to untreated cartilage, which mimics the loss of sGAG and collagen content in the early stage of OA (Figure 3-1). Trypsin treated cartilage shows a significant (45%,  $p < 0.001$ ) loss of sGAG content and a (51%,  $p < 0.0001$ ) reduction in collagen content compared to the control (untreated cartilage).

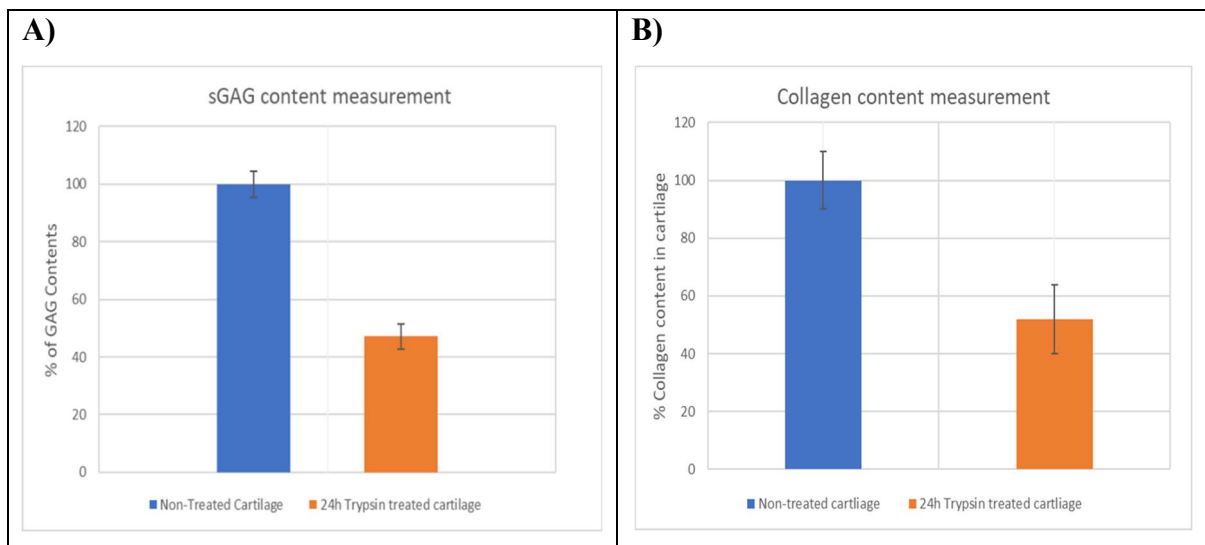


Figure 3-1. Sulphated glycosaminoglycan (sGAG) and collagen content measurement. Percentage of sGAG in non-treated (untreated) and trypsin treated cartilage (45%) for 24 hours (A), and the percentage of collagen content in non-treated (untreated) and trypsin treated cartilage (51%) for 24 hours (B). Half amount of sGAG and collagen was loss after 24hour of trypsin addition which is simulated early OA cartilage.

### **3.3.2. Amount of sGAG loss measurement in IL-1 $\alpha$ treated cartilage**

In addition to quantifying sGAG in cartilage tissue, the amount of sGAG loss in bovine cartilage and sGAG quantity was measured using DMMB assay. Cartilage explants were treated with/without IL-1 $\alpha$  for 20 days. After digestion of cartilage with papain and following the DMMB assay method, the optical density was measured at 525 nm, and the results were plotted as a percentage of sGAG loss by  $\mu\text{g}/\text{mg}$  cartilage weigh against the culture period (day) (Figure 3-2).

First, sGAG loss from the IL-1 $\alpha$  treated cartilage was faster during the first week (Figure 3-2). To illustrate, during period of 24-96 hours there was a 50% decrease of sGAG content compared to the untreated cartilage which reached 60% after one week of culture. After that, sGAG loss slightly increased to the end of the culture period (20 days), but the loss was still significantly higher than in the untreated cartilage ( $p < 0.01$ ). Overall, during this initial period of culture, there was a substantial rise in the percentage of sGAG loss in cartilage tissue. This trend was followed by consistent values or negligible sGAG loss from the samples up to day 20 (Figure 3-2). Such observations could be attributed to the fact that the explant cultures required a period of up to four days to adjust to the in vitro environment following harvesting. Additionally, the saturation of the cartilage samples, as the media and cells attained maximum density, may have resulted in decreased sGAG loss. Consequently, any further change in the cartilage tissue could not be detected. Nevertheless, the percentage of sGAG loss was three to five times higher in IL-1 $\alpha$  treated cartilage than in untreated samples (media only). In fact, a similar effect was shown in a study by Bajpayee *et al.* (2016) as IL-1 $\alpha$  treatment caused high (5 to 6 times) loss of sGAG compared to untreated control.

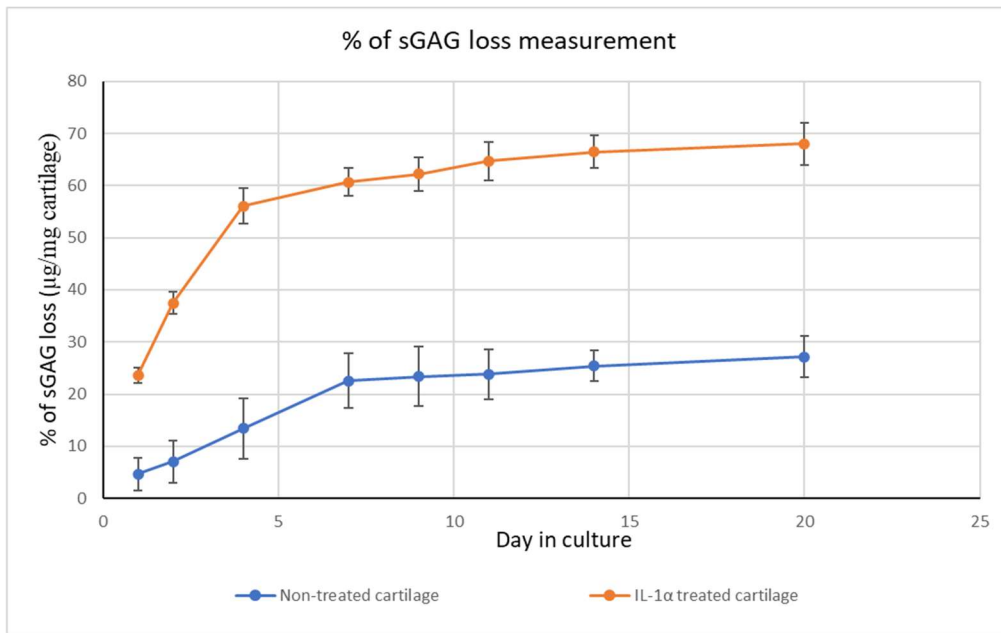


Figure 3-2. Quantification of sulphated glycosaminoglycan (sGAG) in culture media from control (untreated cartilage, blue line) and IL-1 $\alpha$  treated explants (orange line) at day 1, 2, 4, 7, 9, 11, 14 and 20 using the DMMB assay. More than 60% of sGAG loss in IL-1 $\alpha$  treated samples which was significantly higher than the untreated one ( $p < 0.01$ ).

### 3.3.3. Collagen content determination in IL-1 $\alpha$ treated cartilage

According to hydroxyproline assay results, collagen content dropped to around 60% during the first week after IL-1 $\alpha$  exposure, and then it decreased steadily for up to two weeks, which was considerably high ( $0.13 \pm 0.01$  mg) compared to untreated cartilage samples ( $0.63 \pm 0.05$  mg). Overall, collagen degradation product was significantly low following IL-1 $\alpha$  stimulation compared to that of the untreated cartilage ( $p < 0.05$ ) (Figure 3-3).

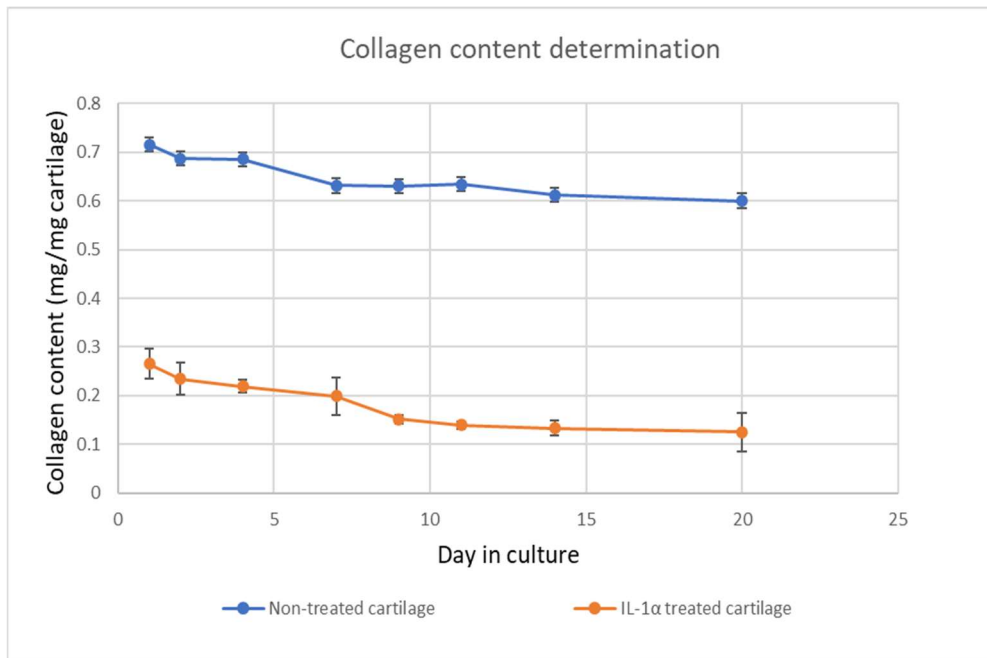
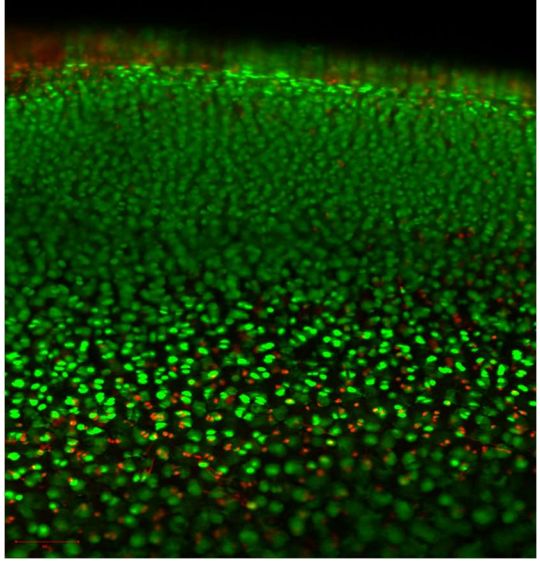
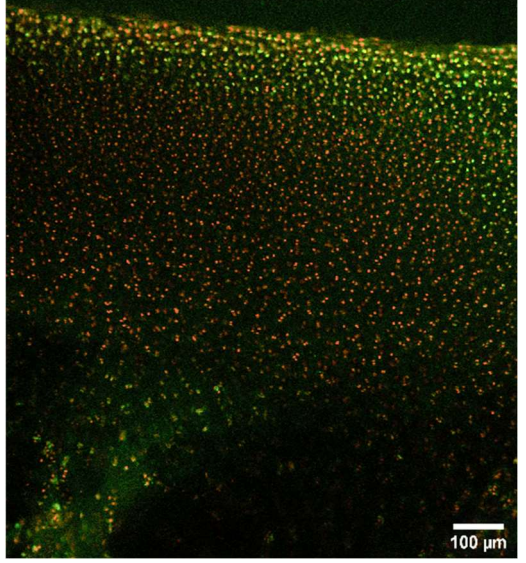
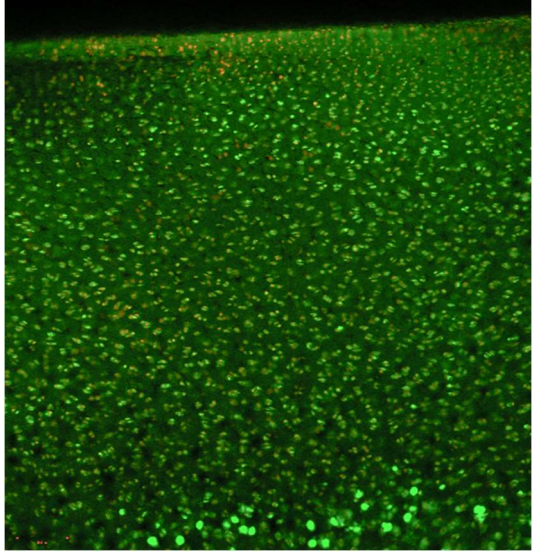
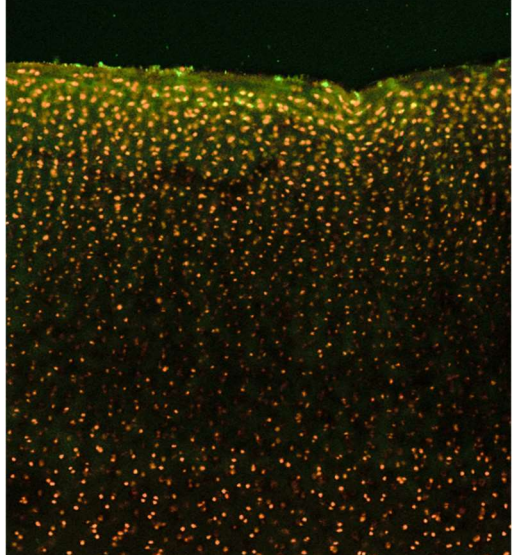
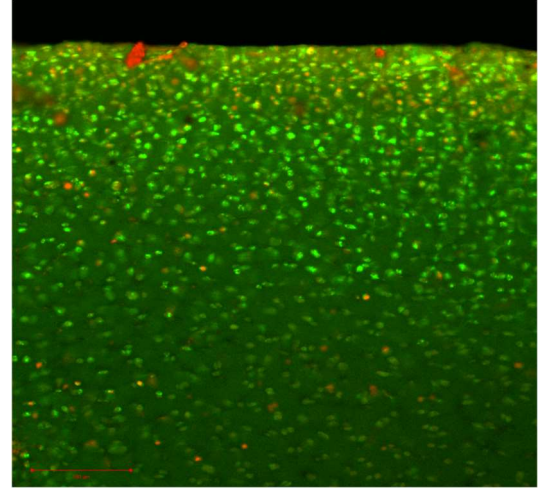
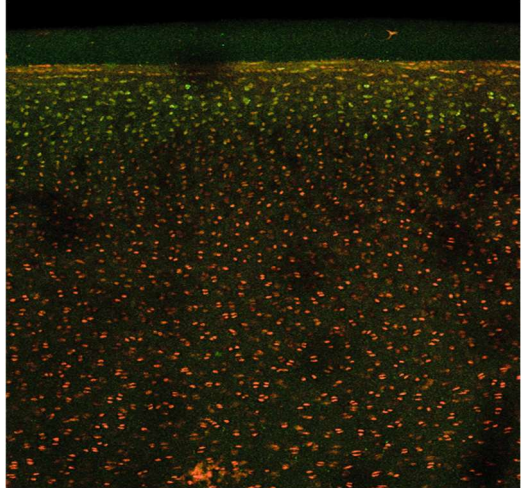


Figure 3-3. Collagen content determination on untreated (blue line) and IL-1 $\alpha$  treated (orange line) cartilage explants at day 1, 2, 4, 7, 9, 11, 14 and 20 using hydroxyproline assay. Collagen degradation product was significantly low following IL-1 $\alpha$  treated cartilage compared to the untreated cartilage samples ( $p < 0.05$ ).

### 3.3.4. Live/dead viability assay

The present experiment involved the treatment of cartilage explants with or without IL-1 $\alpha$  for a period of 20 days. Subsequently, this report presents images of the cartilage explants captured on days 1, 2, 7, 14, and 20, given the minimal discrepancy in the live/dead appearance of the cells following the first week.

Initially, 24 hours post-treatment, a considerable difference was observed between the untreated and IL-1 $\alpha$  treated cartilage with respect to chondrocyte viability, as the latter exhibited significantly suppressed cell viability in the cartilage explants compared to the former (Figure 3-4). The overall effect of treating cartilage with IL-1 $\alpha$  resulted in a great reduction in cell viability compared to the untreated control, which was observed until day 20 of the culture period.

Untreated cartilage (Day1)	IL-1 $\alpha$ treated cartilage (Day1)
	
Untreated cartilage (Day2)	IL-1 $\alpha$ treated cartilage (Day2)
	
untreated cartilage (Day7)	IL-1 $\alpha$ treated cartilage (Day7)
	

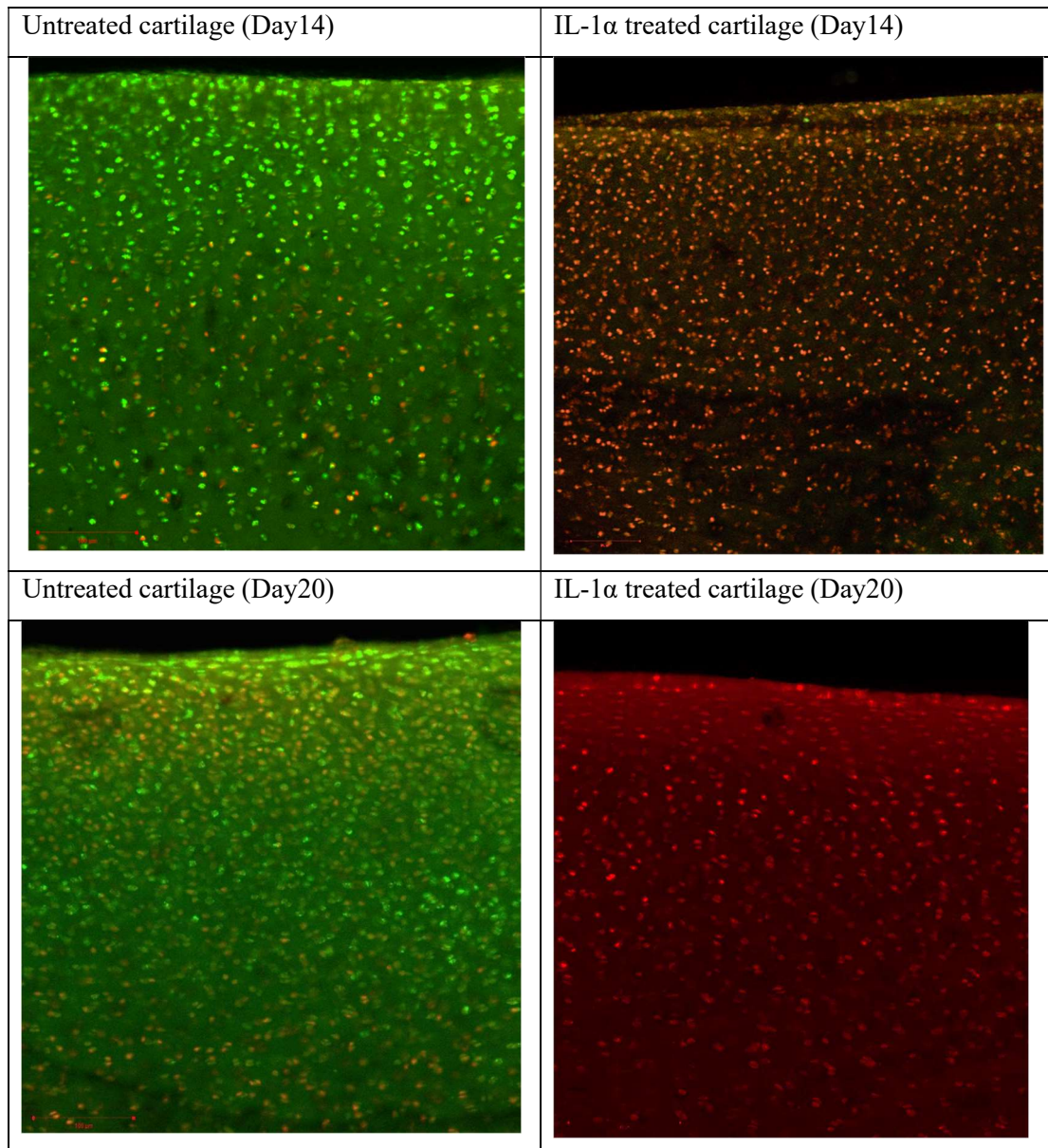


Figure 3-4. Images of fluorescently stained bovine explants using live/dead staining assay to evaluate chondrocyte viability on days 1,2,7, 14 and 20 in untreated and IL-1 $\alpha$  treated cartilage samples. Live cells were stained green by calcein and dead cells were stained red by ethidium homodimer. Scale bar 100 $\mu$ m.

### 3.4. Discussion

Ex vivo models are a fundamental way to study the effect of newly synthesised or improved drug formulations for the treatment of different types of diseases such as cancer, eye infection, arthritis, brain disorder, intestine disease and many other conditions (Steinstraesser *et al.*, 2010; Corzo-León, Munro and MacCallum, 2019; Remaut, 2019). They offer a controlled and simplified environment to study drug effects on specific cells or tissues, allowing for a more precise assessment of drug efficacy and safety without interference from other physiological processes in the body (Barré-Sinoussi and Montagutelli, 2015). In addition, they have noticeable anatomical and physiological similarities with humans which allows the researchers

to use them to investigate a large range of mechanisms and assess novel therapies before applying their discoveries to treat humans (Barré-Sinoussi and Montagutelli, 2015). They help in screening specific drug targets and reducing the systemic side effect of the drugs. They are widely used in research as a useful tool to verify the therapeutic effect of compounds, agents, or drugs. For example, ex-vivo skin was used to treat fungal infection (Corzo-León, Munro and MacCallum, 2019), and wound infection (Steinstraesser *et al.*, 2010). Additionally, an ex vivo eye model was used to study eye diseases such as hypertension and glaucoma (Mao *et al.*, 2011; Remaut, 2019), and cartilage explants were used to discover drug delivery system for the treatment of arthritis (Lu, Evans and Grodzinsky, 2011; Bajpayee *et al.*, 2016; Perni and Prokopovich, 2017). Ex vivo models maintain the architecture of the tissue closer to the in vivo system; they are easy, rapid, and cost-effective to use in the experiment before starting the in vivo assays (Cope *et al.*, 2019). However, use of these animal models are limited in that they need special hospitality to protect them from any other disease which may affect the study results. Modern methods allow the 3R principles that were developed in 1959 by Russell and Burch, which are useful models' tools and are widely recognized and accepted as a guiding framework for ethical animal research. The 3Rs stand for reducing, refining, and replacing animal experiments in research (Tannenbaum and Bennett, 2015). It involves replacing the use of animals with non-animal alternatives (such as cell cultures or tissue engineering techniques), reducing the number of animals used in experiments by improving the experimental design, and refining the experimental procedures to minimize any pain or distress that the animals may experience by using anaesthesia and analgesia during procedures, and providing enrichment to improve animals' health (Hartung, 2008; Tannenbaum and Bennett, 2015). Therefore, by implementing the 3R principle, researchers can save animals and obtain reliable and meaningful results (Hartung, 2008). Moreover, the implementation of an ex vivo bovine cartilage model in this project contributed to the 3Rs principle by serving as a partial replacement for the animal model, thereby reducing the number of animals required. This is due to the ability to extract approximately 15 cartilage discs from a single bovine leg for experimentation purposes. In addition, ex vivo models offer a greater anatomical similarity to the human model and have a long-life span, allowing for slower disease progression and, therefore, a longer time to end-stage OA. Availability of the tissue samples and easy control of experimental conditions, such as temperature and the surrounding media's composition, can help ensure the validity of results (McCoy, 2015; Kuyinu *et al.*, 2016; Cope *et al.*, 2019).

Post-traumatic OA accounts for 12% of all cases of OA (Lotz, 2010; Punzi *et al.*, 2016). Moreover, no specific measure exists to prevent OA; however, patients with PTOA are at a higher risk of developing this condition and thus are ideal for testing preventive and therapeutic measures (Lotz, 2010; Punzi *et al.*, 2016; Grodzinsky *et al.*, 2017). Early-stage OA and PTOA models were built successfully in this work and the length of time of the experiments after injury (adding IL-1 $\alpha$ ) was determined based on preventing the pathological changes that induced by injury becoming irreversible, which would lead to closing the opportunity for the prevention of PTOA and OA. Therefore, a period of 20 days was chosen in which to perform the experiments to ensure the effect of the DDSs could be assessed using the appropriate model.

Furthermore, synovial fluid (SF) is a naturally occurring lubricating fluid found in joints while culture media is an artificially created media to grow and study cell properties in a laboratory-based setting. Ex vivo studies on cartilage tissue necessitate the incubation of cartilage for long periods of time in appropriate tissue culture media ( 2 weeks to months) (Liming Bian *et al.*, 2010; Salgado, Jordan and Allémann, 2021). When cartilage tissue is incubated in culture media, the tissue metabolism remains relatively stable for the experiment as it is essential for supporting cell survival and growth by providing the cell with necessary components such as nutrients and growth factors. Therefore, the tissue continues to carry out its normal metabolic processes without significant changes or disruptions, allowing researchers to study the tissue properties and responses to experimental interventions in a controlled environment (Liming Bian *et al.*, 2010; Samvelyan *et al.*, 2021)

Generally, the results of experiments using culture media instead of SF can be affected in several ways. First, the composition of SF and culture media are different. Culture media is usually supplemented with different types of amino acids that support cell viability and protein synthesis. In addition, it contains antibiotics and antifungal to prevent cell contamination. On the other hand, SF contains a variety of biomolecules (such as endogenous proteases, hyaluronic acid, extracellular matrix components, negatively charged molecules and proteins) that are not found in culture media which could alter or decrease the penetration of the drugs into cartilage tissue when tested using in vivo models (Grässel and Aszódi, 2017). Therefore, the result of ex vivo experiments using culture media may not always accurately reflect the effects of experimental treatments on cartilage tissue using SF. However, ex vivo experiments using culture media can still provide valuable insights into the underlying mechanisms of cartilage metabolism, which can guide the development of new treatments for osteoarthritis (Grässel and Aszódi, 2017).

Second, physical properties of SF and culture media are different. SF is a viscous fluid that can provide mechanical support to cartilage which helps cells to regenerate and joints to move (Damiano and Bardin, 2010). Comparatively, culture media are designed to be less viscous, which allows nutrients and other molecules to diffuse better into the cells but does not provide the same level of mechanical support as SF (Damiano and Bardin, 2010; Poon, 2022). Although culture media can be adjusted according to the needs of the experiment, they generally have a lower viscosity than synovial fluids. Third, SF contain different types of cells such as synovial cells and immune cells that can play an important role in cartilage cells (chondrocytes) nourishment, growth and mechanical load which is typically not found in culture media (Grässel and Aszódi, 2017). Therefore, using culture media may not provide the same environment as SF and may lead to a difference in cell behavior and experimental results .

However, culture media can be used in laboratory experiments, rather than SF, for different reasons:

1. Culture media can be standardized and controlled more easily than SF which allows for more consistent and reproducible results.
2. The simplicity of culture media is advantageous, as it is easy to prepare, handle and store compared to SF.
3. It is cost effective; culture media is less expensive to obtain in large quantities compared to SF which is costly to process.
4. Culture media can be formulated to contain specific nutrient and growth factors which are needed for cartilage cells, allowing researchers to understand how different factors affect cartilage cells.
5. In vitro study using culture media allows for the study of cells and their behaviour towards different types of treatment outside the living organism, hence providing further understanding of the mechanism that regulates cartilage growth and repair.

Overall, culture media is a useful substitute for SF in many cartilage experiments but further in vivo study using SF is required to achieve more accurate results using real joint capsule. Nonetheless, based on the literature, they may no great effect would be expected when testing the DDSs using SF in vivo (Bajpayee *et al.*, 2016). For example, in vivo study using an IA injection of Avidin resulted in penetration from knee SF into the superficial zone and to the

full thickness of joint cartilages without being affected by SF components (Bajpayee et al., 2016).

In summary, this project established an ex vivo models to investigate the potential of DDSs to reduce the catabolic effect of cytokines and to measure NSAIDs uptake and retention inside the cartilage tissue. Consequently, assessment of the impact of DDS formulations ex vivo is typically carried out using appropriate culture media to evaluate the cartilage response to the developed DDS.

### **3.4.1. Trypsin treated (GAG depleted) ex vivo model**

In general, it has been reported that early-stage OA cartilage can exhibit a reduction in GAG content of up to 50% compared to healthy cartilage (Vignon *et al.*, 2003; Yoo *et al.*, 2011; Perni and Prokopovich, 2017). Trypsin-treated (GAG depleted) cartilage for 24 hours could mimic the GAG depletion observed in human OA because it showed around 50% loss of sGAG and collagen content compared to the control (untreated cartilage), Figure 3-1. Comparably, other studies used trypsin to reduce around 50% of GAG content in the cartilage sample (Yoo et al., 2011; Perni and Prokopovich, 2017). Therefore, the trypsin-treated OA model allowed to investigate the effects of GAG and collagen depletion on OA cartilage and to test potential therapeutic interventions to prevent or reduce cartilage degradation. GAG depletion can lead to a loss of cartilage hydration and swelling pressure, which in turn can affect the mechanical properties of the tissue and contribute to further damage (Bijlsma, Berenbaum and Lafeber, 2011; Grässel and Aszódi, 2017; Wu, 2018). In addition, GAG depletion causes increased collagen degradation, which leads to loss of cartilage integrity and function (Bijlsma, Berenbaum and Lafeber, 2011; Grässel and Aszódi, 2017; Wu, 2018). Overall, using a GAG depleted cartilage OA model can provide valuable insights into the mechanisms underlying osteoarthritis and be a useful model for testing potential therapeutic interventions.

### **3.4.2. Catabolic ex vivo model, IL-1 $\alpha$ treated cartilage tissue**

The ex vivo experiment is very important pre-in vivo study which could screen the efficacy of a drug before testing it directly on animals (in vivo) or humans. Ex vivo models as a 3D cellular model represent the inter cartilage tissue communication and its metabolic processes more closely to the in vivo situation (Barré-Sinoussi and Montagutelli, 2015; Cope *et al.*, 2019). Therefore, they are remarkably useful models available to OA researchers allowing them to present natural in vivo environments. Despite this, these models are more difficult to produce in terms of tissue volume and maintaining cell viability over extended periods of time (Barré-

Sinoussi and Montagutelli, 2015; Cope *et al.*, 2019). Some of the advantages, and disadvantages are summarized in table 3-1.

The objective of this study was to demonstrate the impact of IL- $\alpha$  on the loss of sGAG, collagen, and chondrocyte viability. IL-1 $\alpha$  is the classical inducer of catabolic responses in chondrocytes, and it is a potent inducer of prostaglandin (PG) synthesis in human chondrocytes (Hauser, 2010). Moreover, IL-1 $\alpha$  is one of the inflammatory cytokines that play an essential role in OA progression as its level increases at early, late-stage and PTOA, causing sGAG and collagen loss by enhancing MMP production, upregulating ADAMTS and inhibiting cartilage anabolism (Van den Berg, 1999; Jayasuriya, 2013; Wojdasiewicz, Poniatowski and Szukiewicz, 2014).

sGAG and collagen content are directly proportional to the ability of cartilage to tolerate compressive forces. Collagen provides tensile strength to prevent cartilage matrix stretching or tearing, while sGAG attract water, forming a gel-like substance with which cartilage is able to resist compression (Warren, 2000; Cissell *et al.*, 2017). Therefore, measuring its level is essential to determine the repair tissue properties (Warren, 2000). A fundamental test performed on the synovial fluid is DMMB assay, which is used to estimate the amount of proteoglycan by measuring sGAG. Additionally, as hydroxyproline is a primary sequence in collagen structure which is responsible for the stabilisation of its structure, hydroxyproline measurement was widely used as an indicator of collagen content (Warren, 2000).

The results for DMMB and hydroxyproline assays showed that in PTOA cartilage model, sGAG and collagen content were significantly reduced compared to untreated cartilage ( $p < 0.05$ ), (Figures 3-2&3-3). Additionally, the percentage of sGAG loss was three to five times higher in IL-1 $\alpha$  treated cartilage than in untreated samples (media only). Initially, the stimulation of cartilage with IL-1 $\alpha$  caused significantly more sGAG and collagen loss compared to untreated cartilage over the 20-day periods. In the post-traumatic OA (IL-1 $\alpha$  treated) cartilage model, there was a significant loss of cell viability compared to untreated cartilage extracts, as shown in live/dead assay results (Figure 3-4).

### **3.5. Conclusion**

Using *ex vivo* animal models is a useful tool with which to investigate in a more controlled environment, the complexity of the *in vivo* as they share some similarities with human tissue in anatomy and pathological processes. Larger animal models such as bovines are not only more comparable to humans physiologically but also in their progression of disease. Their

larger size also helps for the performance of a high range of analytical techniques and investigation. This work was successfully able to extract cartilage samples that are composed of 50% less sGAG and collagen content, which mimic an early stage of OA. Degradation of cartilage content was also achieved using IL-1 $\alpha$ , leading to a decrease in the viability of chondrocytes cells compared to the untreated cartilage which mimics the PTOA cartilage model. Therefore, these models were used at this study to test the effectiveness of the prepared formulations in treating OA compared to conventional treatment. The ex vivo culture platform allows for long-term culture of the cartilage explants while maintaining cartilage tissue content, structure, and mechanical properties.

## **4. Chapter four: Developing of PBAEs and emulsion-based drug delivery system to deliver NSAID inside OA cartilage tissue**

### **4.1. Introduction**

OA is a global disease and one of the most common causes of disability among adults (Grassel and Aszódi, 2017). Current treatment consists of physical therapy, lifestyle changes, oral medication, intra-articular injections, and surgical treatment, with main aim being to reduce pain, while improving function and quality of life (Bijlsma, Berenbaum and Lafeber, 2011). Nevertheless, effectively delivering therapeutics and agents directly to affected joint sites is challenging. Intra-articular (IA) administration of OA drugs can offer potential treatment benefits due to highly therapeutic effects on joints, and decrease in systemic bioavailability and certain side effects associated with oral administration; however, IA drugs have only a short retention time inside joints (hours to days) (Geiger, Grodzinsky and Hammond, 2018). Regarding potential clinical diligence, internalisation of drugs such as NSAIDs into DDSs, which may alleviate OA pain and inflammation for more extended periods, has displayed promise (Janssen *et al.*, 2014). In fact, articular cartilage structure by its nature sees a limited rate of complete self-repair following damage, and is unable to adequately heal after injury due to its aneural, avascular and alymphatic typical structure (Stoddart *et al.*, 2009; Mobasheri and Batt, 2016). In addition, the thick extracellular matrix characteristics of joints, highly negatively charged proteoglycans, and the porous and permeable vasculature of OA sub-synovium joints all influence the ability of small molecule drugs to localise into articular cartilage for long duration and accelerate clearance from affected joints (Chevalier, 2010; Bajpayee *et al.*, 2016).

Non-steroidal anti-inflammatory drugs are widely known to offer beneficial treatment for alleviation of pain and inflammation in OA patients (Edwards, 2011; Pelletier *et al.*, 2016; Zhang *et al.*, 2016). Indeed, NSAIDs are the preferred medicines for a variety of inflammatory diseases, including OA. Amongst the most commonly prescribed NSAIDs are indomethacin, ketorolac, naproxen, and sodium salt of diclofenac. Although NSAIDs have significant therapeutic outcomes, they also cause gastrointestinal and cardiovascular side effects which are mainly associated with the oral route of administration. In addition, frequent dosing is required with NSAIDs which may lead to patient noncompliance. Moreover, the dominant hydrophobic nature of these compounds leads to reduced residence time inside affected tissue and rapid diffusion into the systemic circulation (Fini, Fazio and Feroci, 1995; Huang and

Zhang, 2012). Table 2-1 shows the log P values for four different types of NSAIDs and reveals that they exhibit positive log P values ranging from 2.28 to 4.15, thus confirming their lipophilicity. Generally, log P is a constant that has negative values for hydrophilic compounds (higher affinity for the aqueous phase), positive values for lipophilic compounds (higher affinity for the lipid phase), and zero (0) values for compounds that partition equally between the lipid and aqueous phases (Lindsley, 2014). Additionally, log P value has a significant impact on compound solubility, meaning that compounds such as NSAIDs with positive log P values (2.28 to 4.15) tend to have low solubility in aqueous phase, consequently, limit bioavailability and decreased effectiveness in the body, resulting in inefficient drug distribution and reduced capability in reaching their site of action (Lindsley, 2014). Therefore, using NSAIDs in emulsion form has considerable impact on improving their solubility and bioavailability inside tissue, thereby increasing their therapeutic efficacy, and reducing side effects associated with higher doses or frequent dosing. In addition, polymers can encapsulate these hydrophobic drugs and effectively improve their solubility in water. Improving the solubility of NSAIDs as hydrophobic compounds and using PBAE polymers as drug delivery systems are essential when using them to target cartilage in OA joints. This is because NSAIDs may not be able to penetrate synovial fluid and interact with cartilage tissue, leading to poor drug efficacy and increased risk of side effects. Additionally, using PBAE polymers can help drugs to target specific joints, enhance drug bioavailability, and decrease drug clearance from cartilage tissue. Therefore, appropriate drug-delivery technologies are needed to reduce administration frequency and allow sustained drug release. Drug encapsulation is one of the delivery strategies known to effectively sustain drug release (Manjanna, Shivakumar and Kumar, 2010). This method reduces dosing, eliminates gastrointestinal and cardiovascular side effects, and prolongs drug retention time, thereby substantially improving patient compliance with OA pharmacotherapy.

Oleic acid is a natural plant oil that consists of a polar carboxylic acid head and a hydrophobic 18-carbon tail (Janke, Bennett and Tieleman, 2014). It is a type of monounsaturated omega-9 fatty acid that is well known for its health benefits, such as healing wounds, reducing the risk of coronary heart disease, and reducing inflammation in rheumatoid arthritis and OA (Sales-Campos *et al.*, 2013; Rajaei *et al.*, 2015; Pérez-Martínez *et al.*, 2016; Loef *et al.*, 2019). Encapsulating NSAIDs in oleic acid droplets leads to preservation longevity, and increases penetration of NSAIDs inside cartilage tissue because the acid acts as a penetration enhancer and helps in reducing inflammation at the injection site (Adamczak *et al.*, 2013).

POLY-A5 and POLY-B5 are members of the PBAE polymer class which have been developed for use as gene delivery systems as they bind to negatively charged strands of DNA, thereby allowing released into cells (Kim, Sunshine and Green, 2014). In term of OA treatment, they have shown positive results when used as DDSs by directly conjugating corticosteroids to the polymer through covalent bonding, with the polymers being tested layer-by-layer (Perni and Prokopovich, 2017). PBAE polymers have been chosen for use in the present study because of their proven biodegradability and biocompatibility from their hydrolysed monomeric products, compared to other cytotoxic cationic polymers such as poly-Lysine (Anderson, Lynn and Langer, 2003). In terms of present research, it is anticipated that, because POLY-A5 and POLY-B5 exhibit positive charges and have confirmed biocompatibility (Perni and Prokopovich, 2017), they could be used for delivering NSAIDs to OA cartilage via electrostatic interaction with negatively charged proteoglycans in cartilage tissue.

#### **Aim and objective of chapter 4**

- 1) Develop a novel DDSs composed of NSAIDs emulsion (oleic acid (oil) in water emulsion), then coated with POLY-A5 and POLY-B5 polymers.
- 2) Characterise the DDS in terms of polymer hydrolysis, size, charge, stability, uptake, and retention time inside the cartilage tissue while different types of NSAIDs emulsion (indomethacin, ketorolac, naproxen and retention) are coated with the polymers.

## **4.2. Materials and methods**

The details of the assay method are provided in chapter 2.

### **4.2.1. Emulsion diffusion in cartilage**

Nile red (Sigma Aldrich) was dissolved in oleic acid (2 µg/mL) and emulsion was prepared as described previously. Cartilage was placed in a 96 well plate with 100 µL of DAPI (Sigma Aldrich) solution (10 µg/mL in PBS); samples were stored for 10 min at room temp in darkness before washing three times in PBS. Cartilage samples were then placed in another 96 well plate with 100 µL of emulsion with Nile red (0.2 µg/mL) and incubated for 1 min; after washing in PBS, cartilage samples were placed on a glass slide and covered with a cover slip. Images were obtained using a confocal Zeiss LSM880 microscope with 20x lenses. 40 slices were then taken equally distributed from the superficial section to a depth of 130 µm.

### 4.3. Results

A novel drug delivery system was developed, encompassing a 10% emulsion of oleic acid-coated with POLY-A5 and POLY-B5 which encapsulated NSAIDs (Ind, Ket, Nap, DC) as the active ingredient/drug in the oil drops. The characterisation of the emulsion droplets of the drug delivery system and its efficacy in native (untreated) and GAG depleted cartilage were measured through zeta potential, size measurement, emulsion stability, amount of drug uptake, and retention in the cartilage.

#### 4.3.1. Polymer hydrolysis and MW determination

PBAEs were explicitly designed to degrade by aqueous hydrolysis of ester bonds in polymer backbones. Degradation occurred hydrolytically (requiring the incorporation of water into ester linkage) in acidic and alkaline media, to yield alcohol and biologically inert derivatives of small molecular weight *b*-amino acids (breakdown of esters into alcohol and carboxylic acid). Therefore, POLY-A5 degraded hydrolytically to yield 1,4-butanediol and *b*-amino acids while POLY-B5 degraded to yield 1,6-hexanediol and *b*-amino acids which are biologically inert derivatives (Lynn and Langer, 2000). In this project, polymer hydrolysis was recorded using GPC and zeta potential measurement. The degradation was monitored for 30 days using a 37°C incubator at buffered pH 7.4 and pH 5 to estimate the pH of the physiological and inflamed tissue.

Firstly, GPC was used for the purpose of determining the MW of POLY-A5 and POLY-B5 polymers and studying their hydrolysis in terms of polymer degradation. A measure of 2 mg/ml of each polymer was prepared in acetate buffer (pH 5 and pH 7.4) and incubated at 37°C for 30 days. Starting from day 0 (the first day of preparing the polymers), 1 mL of each buffer solution containing the polymer was taken and measured using GPC. The data reported in Figures 4-1 & 4-3 which shows the hydrolysis profile of POLY-A5 and POLY-B5 in pH 5 and pH 7.4 over 30 days.

Initially, the detected MW of POLY-A5 at pH 7.4 and pH 5 was equal to 1244 Da. After the first 24 hours, the MW almost halved (578.5 Da) at pH 7.4, then the curve pathway remained quite stable at around 126 Da for the remainder of the 30 days. Similarly, the MW of POLY-A5 at pH 5 lowered by half after 24 hours; it then degraded slowly up to day 12, after which it became stable at approximately 146 Da over the following days. As Figure 4-1 clearly shows, POLY-A5 degraded more rapidly at pH 7.4 than at pH 5 during the first 2 weeks.

Meanwhile, hydrolysis of POLY-B5 exhibited similar pattern to POLY-A5. Initially, the MW of POLY-B5 was equal to 1321 Da, which was slightly higher than POLY-A5, (Figures 4-1&4-3). After 1 day, the MW dropped to nearly half (536.5 Da) at pH 5, then the curve pathway decreased slightly until day 10 when it stood at 347.5 Da, after which it stabilised at 132 Da for the following days. At pH 7, the MW dramatically dropped by three quarters to 302 Da after 24 hours. It then decreased slightly before stabilising at 139 Da for the remind for the 30 days. In common with POLY-A5 described above, POLY-B5 also degraded more rapidly at pH 7.4 than at pH 5 during the first 2 weeks (see Figure 4-3).

Zeta potential was also used to assess the degradation of POLY-A5 and POLY-B5 polymers in terms of charge change. As shown in Figure 4-2, POLY-A5 hydrolysis charge changes in pH 5 and pH 7.4 were slightly different but this was not statistically significant ( $p > 0.5$ ); the initial charge was  $+12.6 \pm 0.9$  mV for both pH 5 and pH 7.4. After that, it dropped to  $-10.4$  mV after 24 hours at pH 7.4, then fluctuated before stabilising at  $-16.6 \pm 2.9$  mV on day 15. On the other hand, at pH 5 the initial positive charge decreased gradually to reach  $-1.1$  mV on day 5. After that, the charge degradation decreased steadily until it fell to  $-2.9 \pm 1.9$  mV. These zeta potential results confirm that POLY-A5 degradation was slower in the acidic pH buffer compared to the neutral pH buffer. As for POLY-B5 charge hydrolysis, the results show that charge degradation was faster in pH 7.4 than in pH 5 (Figure 4-4).

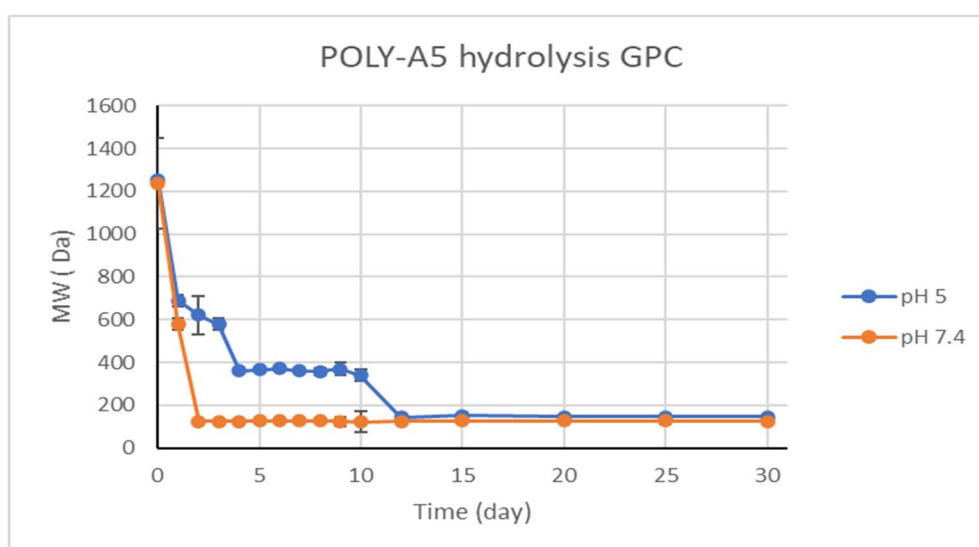


Figure 4-1. MW and hydrolysis of POLY-A5 for 30 days at pH 5 (blue line) and pH 7.4 (orange line) using GPC. POLY-A5 degradation was faster at pH 7.4 than pH 5.

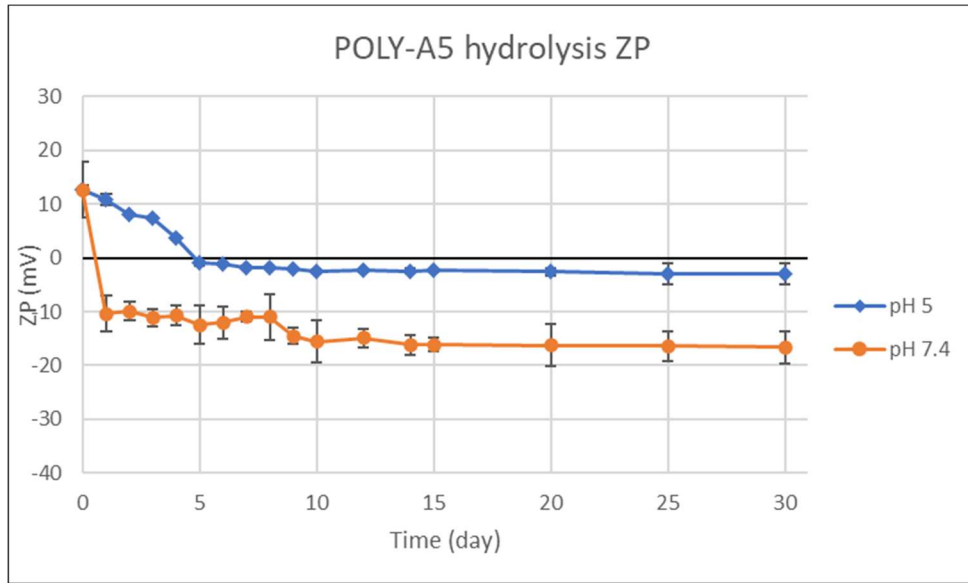


Figure 4-2. Charge hydrolysis using Zeta potential (ZP) for POLY-A5 for 30 days at pH 5 (blue line) and pH 7.4 (orange line). POLY-A5 degradation was faster at pH 7.4 than pH 5.

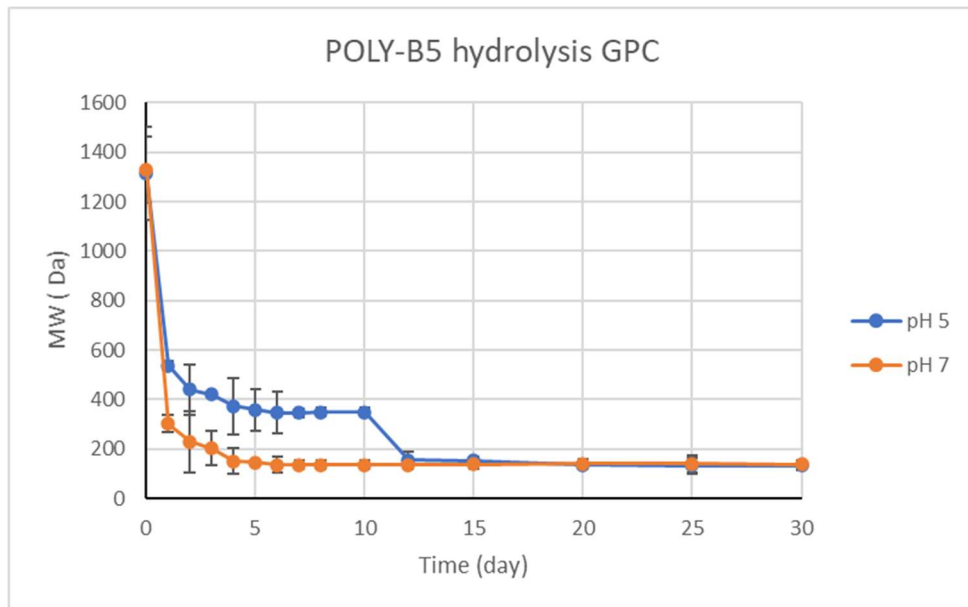


Figure 4-3. MW and hydrolysis of POLY-B5 for 30 days at pH 5 (blue line) and pH 7.4 (orange line) using GPC. POLY-B5 degradation was faster at pH 7.4 than pH 5.

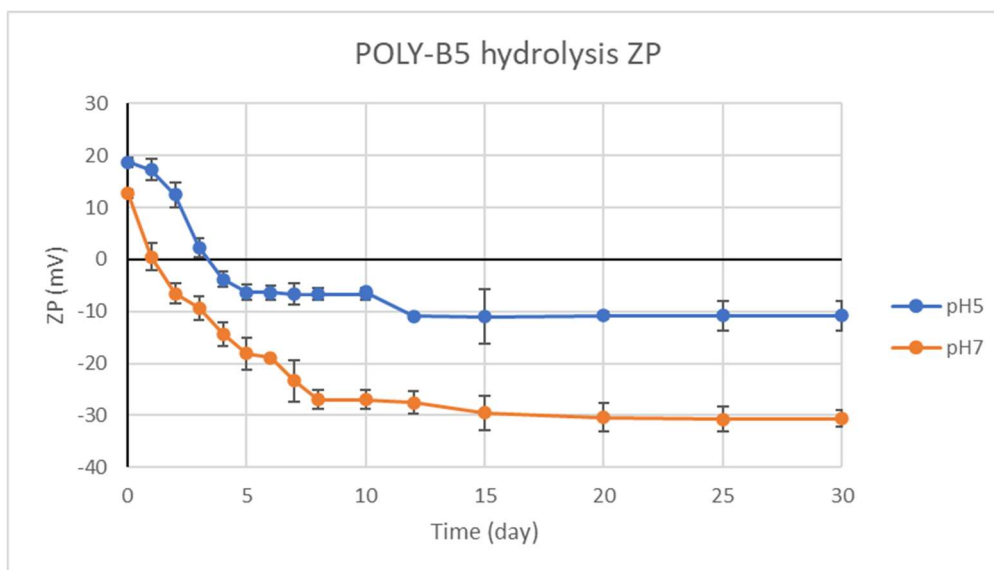


Figure 4-4. Charge hydrolysis using Zeta potential (ZP) for POLY-B5 for 30 days at pH 5 (blue line) and pH 7.4 (orange line). POLY-B5 degradation was faster at pH 7.4 than pH 5.

#### 4.3.2. Zeta potential measurement

Zeta potential (mV) was measured using Malvern Zetasizer Nano ZS (Malvern Instruments) to determine the interactions between positively charged POLY-A5, and POLY-B5 polymers and the negative charged NSAIDs o/w emulsion, and to calculate the amount of polymer required to coat the emulsion completely (Tables 4-2&4-4). In this context, four of the most common clinically used NSAIDs (Ind, Ket, Nap, DC) were examined. POLY-A5 and POLY-B5 characteristics were initially measured in acetate buffer (pH 5), then the characteristics of the NSAIDs o/w emulsion were also measured after adding a constant amount (10 $\mu$ l) of the polymer (see Figures 4-5 & 4-6); with respect to ZP (mV) where the X-axis was normalised, oleic acid density was 0.895 g/mL at 25 °C (O’Neil, 2013).

For NSAIDs to penetrate inside the full depth of joint cartilage and diffuse through it, the formulation must exhibit a positive charge to be able to bind with the cartilage’s negatively charged proteoglycans and allow the drug to penetrate inside the tissue. This change in the charge was clearly stated in the ZP graph (Figure 4-5&4-6). The mean initial charge of NSAIDs o/w emulsion was calculated each time then a constant amount of the polymers was added to the emulsion until saturation was reached (i.e., the point at which the charge plateaued, with little or no change in charge occurring). This meant that complete charge compensation on the surface was achieved, and the volume of polymer required to coat the emulsion completely could be predicted (Szczepanowicz et al., 2010). In fact, ZP measurement was necessary to

determine the actual volumes of POLY-A5 and POLY-B5 polymers that were required to be added to each emulsion.

Firstly, for POLY-A5, the ZP saturation method involving constant addition of 10 $\mu$ l of POLY-A5 to Ind, Ket and Nap o/w emulsions led to an increase in the emulsion charge and changed it to positive, as clearly shown in Table 4-1 & Figure 4-5. For Ind and Ket o/w emulsion, saturation was achieved after the addition of 160  $\mu$ L/mL of POLY-A5, while 190  $\mu$ L/mL of POLY-A5 was required for Nap o/w emulsion to be coated completely. On the other hand, DC o/w emulsion had a strong negative charge equalling -84.6 mV (Figure 4-5). Accordingly, a higher constant amount of POLY-A5 was added in order to achieve full coating and convert the high negative charge to positive. Consequently, 100  $\mu$ L/mL of POLY-A5 was added to achieve saturation of the emulsion droplets. Based upon this result, 1000  $\mu$ L/mL of POLY-A5 is needed to coat 1 mL of DC o/w emulsion completely and fundamentally change its charge to +5.5mV. To summarise, DC o/w emulsion exhibited the highest negative charge (-84.6 mV) followed by Ket, Nap and Ind o/w emulsion (Table 4-1). Accordingly, a higher amount of POLY-A5 was added to the DC o/w emulsion to change its highly negative charge to positive (1000  $\mu$ L/mL). In addition, after coating the NSAIDs o/w emulsions with the polymer, Nap conducted the highest positive charge (+26.6 mV), followed by Ind, Ket and DC (+18.4mV, +17.1mV, and +5.5 mV, respectively) (Table 4-1).

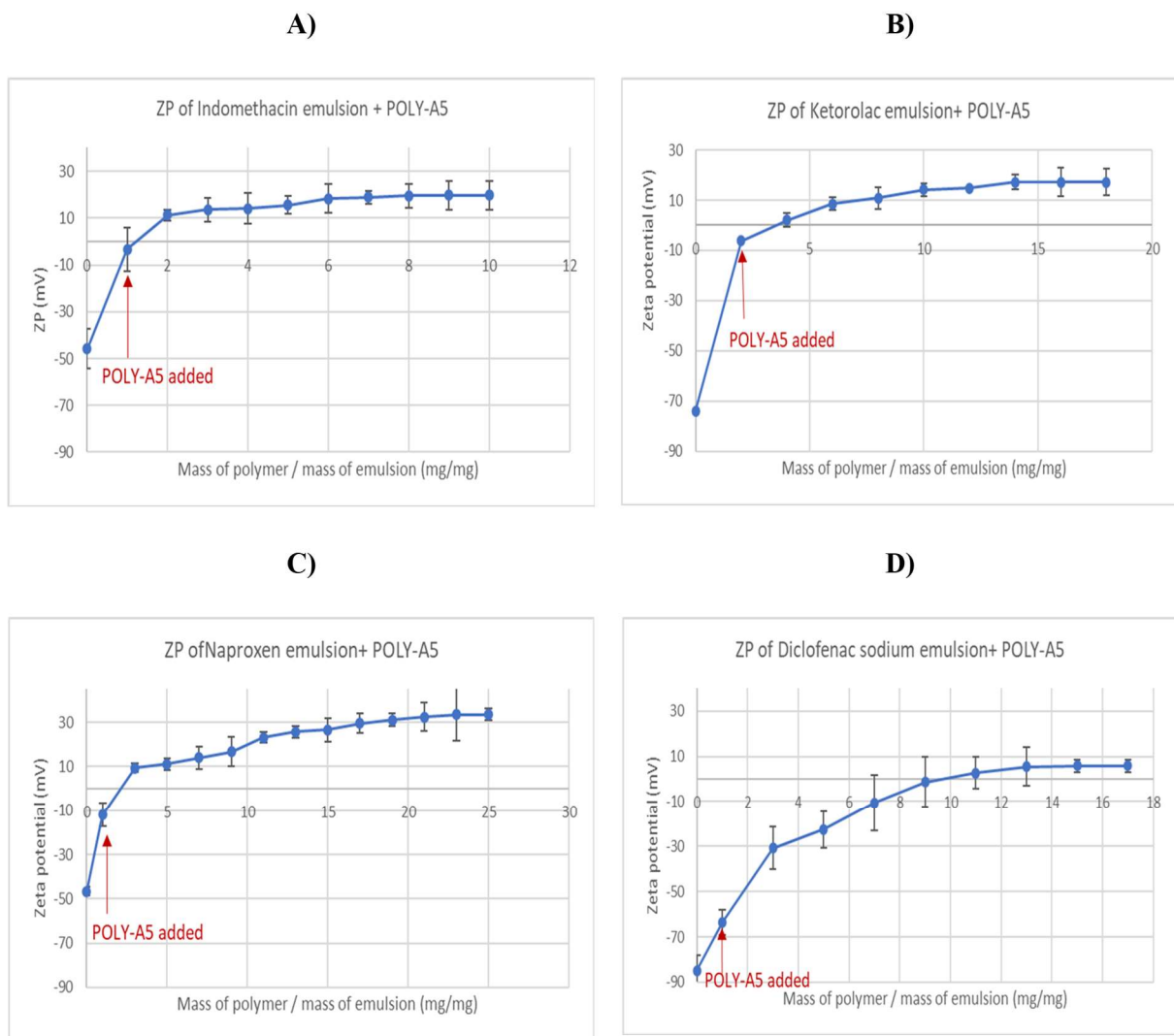


Figure 4-5. Characterization of coated emulsion – measuring the zeta potential (mV) values for NSAIDs emulsion before and after adding POLY-A5 continuously until reach the saturation to complete coated the emulsion droplet with the positively charged POLY-A5. Indomethacin emulsion (1 mL of the emulsion + 10  $\mu$ l POLY-A5) (A), ketorolac emulsion (1mL of the emulsion + 10  $\mu$ L POLY-A5) (B), naproxen emulsion (1mL of the emulsion + 10  $\mu$ l POLY-A5) (C), diclofenac sodium emulsion (1 mL of the emulsion + 100  $\mu$ L POLY-A5) (D).

Table 4-1 Zeta potential (mV) for POLY-A5, o/w emulsion and NSAIDs o/w emulsion before and after coated with POLY-A5 and the amount of POLY-A5 required to coat 1 mL of the NSAIDs emulsion completely.

NSAIDs emulsion	ZP for the drug alone (mV) before coating with the polymer	ZP for the drug in emulsion form (mV)	ZP (mV) for drug + POLY-A5 (2 mg/mL)	Amount of POLY-A5 (2mg/mL) added ( $\mu$ L)
POLY-A5	+12.6 $\pm$ 0.9			
o/w emulsion	-30.9 $\pm$ 1.8		+10.2 $\pm$ 0.2	<b>60</b>
Indomethacin	-34.5 $\pm$ 1.7	-45.8 $\pm$ 4.3	+18.4 $\pm$ 0.8	<b>160</b>
Ketorolac	-67.9 $\pm$ 6.3	-73.9 $\pm$ 0.5	+17.1 $\pm$ 1.9	<b>160</b>
Naproxen	-38.3 $\pm$ 6.5	-46.6 $\pm$ 0.4	+26.6 $\pm$ 1.4	<b>190</b>
Diclofenac sodium	-58.3 $\pm$ 9.5	-84.6 $\pm$ 3.4	+5.5 $\pm$ 4.3	<b>1000</b>

Secondly, for POLY-B5, the ZP saturation method was also followed by the constant addition of 10  $\mu$ L of POLY-B5 to Ind, Ket and Nap o/w emulsion, leading to an increase in the emulsion charge which changed it to positive (Table 4-2 & Figure 4-6). For Nap and Ind o/w emulsion, saturation was achieved after the addition of around 100  $\mu$ L/mL of POLY-B5, while 80  $\mu$ L/mL of POLY-B5 was added to Ket o/w emulsion for it to be coated completely. On the other hand, DC o/w emulsion had a stronger negative charge which was equal to -90 mV (Figure 4-6). Consequently, a higher constant amount of POLY-B5 was added to enable the DC o/w emulsion to be fully coated and to eventually change its high negative charge to positive. Therefore, 600  $\mu$ L/mL of POLY-B5 was needed to coat DC o/w emulsion completely and change its charge to +9.6 mV. To summarise, the highest amount of POLY-B5 was added to DC o/w emulsion to change its highly negative charge to positive followed by Nap, Ind, and Ket. In addition, after coating the NSAIDs o/w emulsion with the polymers, Nap (+26.3mV) conducted the higher positive charge, followed by Ind, Ket and DC (+21.8mV, +20.2mV and +9.7 mV, respectively) (Table 4-2).

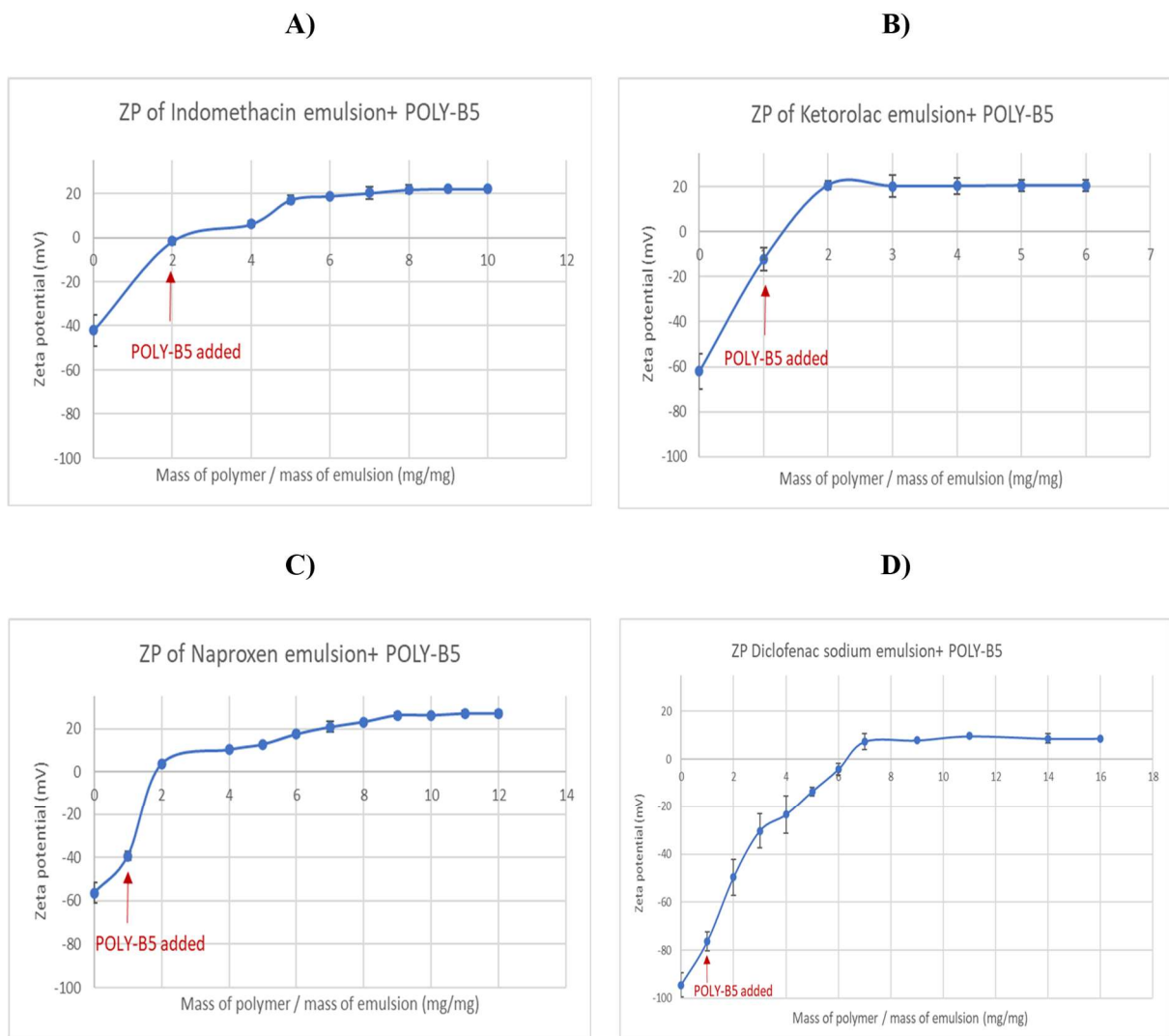


Figure 4-6. Characterization of coated emulsion – measuring the zeta potential (mV) values for NSAIDs emulsion before and after adding POLY-B5 continuously until reach the saturation to complete coated the emulsion droplet with the positively charged POLY-B5. Indomethacin emulsion (1 mL of emulsion + 10  $\mu$ L of POLY-B5 polymer) (A), ketorolac emulsion (1 mL of emulsion + 10  $\mu$ L of POLY-B5 of POLY-B5 polymer) (B), naproxen emulsion (1 mL of emulsion + 10  $\mu$ l of POLY-B5 polymer) (C), diclofenac sodium emulsion (1 mL of emulsion + 100  $\mu$ L of POLY-B5 polymer) (D).

Table 4-2 Zeta potential (mV) for POLY-B5, o/w emulsion and NSAIDs o/w emulsion before and after coated with POLY-B5 and the amount of POLY-B5 required to coat 1 mL of the NSAIDs emulsion completely.

NSAIDs emulsion	ZP for the drug alone (mV) before coating with the polymer	ZP for drug alone (mV)	ZP (mV) for drug + POLY-B5 (2 mg/mL)	Amount of POLY-B5 (2mg/mL) added ( $\mu$ L)
POLY-B5	+18.7 $\pm$ 0.9			
o/w emulsion	-33.5 $\pm$ 3.6		+16.2 $\pm$ 2.8	<b>60</b>
Indomethacin	-34.5 $\pm$ 1.7	-42.1 $\pm$ 6.9	+21.8 $\pm$ 1.9	<b>100</b>
Ketorolac	-67.9 $\pm$ 6.3	-62.1 $\pm$ 7.8	+20.2 $\pm$ 3.6	<b>80</b>
Naproxen	-38.3 $\pm$ 6.5	-56.3 $\pm$ 4.6	+26.3 $\pm$ 0.5	<b>110</b>
Diclofenac sodium	-58.7 $\pm$ 9.5	-90.5 $\pm$ 3.7	+9.7 $\pm$ 0.32	<b>600</b>

Finally, POLY-A5's charge was +12.6 mV while POLY-B5's charge was +18.7 mV, which supports the expectation that POLY-A5 and POLY-B5 are types of polycation POLYX (Perni and Prokopovich, 2017). POLY-A5 and POLY-B5 both possessed positive charges, mainly because of the presence of amine groups in their structure (5-dimethylamino-1-propylamine). POLY-B5 exhibited a higher positive charge (+18.7 mV) than POLY-A5 (+12.6 mV), which could be because polymer net charge can vary depending on the structures of acrylates and amine; POLY-B5 (1,6 hexanediol diacrylate) has a more elongated acrylate structure than POLY-A5 (1,4 butanediol diacrylate). This leads to a decrease in the amount of added polymer needed to fully coat NSAIDs emulsion and change its charge to positive. For example, to fully coat Ind just 100  $\mu$ l of POLY-B5 was added, whereas as much as 160  $\mu$ l of POLY-A5 was required. As for Ket, only 80  $\mu$ l of POLY-B5 was needed before it to be fully encapsulated, but 160  $\mu$ l of POLY-A5 was necessary to change its charge to positive (Tables 4-1&4-2, & Figures 4-5&4-6).

#### 4.3.3. Size measurement

The size distribution of POLY-A5, POLY-B5 polymers, and NSAIDs o/w emulsion (with/without polymer coating) were measured using dynamic light scattering (DLS) as shown in Tables 4-3&4-4. Quantities of 1 mL of NSAIDs o/w emulsion, both with and without polymers, were added to cuvette cells, then hydrodynamic size distribution was measured. The application of the polymer coating resulted in around twenty-fold increase in the particle size of the drug (Figure 4-7). The particle sizes of POLY-A5 and POLY-B5 were measured first

and were equal to  $0.21 \pm 0.02 \mu\text{m}$  and  $0.28 \pm 0.02 \mu\text{m}$ , respectively; this was mainly dependent on polymer chain length and self-arrangement within the chains (Tables 4-3&4-4).

NSAI Ds	DLS of drug before coating with the polymer	DLS of drug emulsion after coating with the POLY-A5
Ind	<p style="text-align: center;">Size distribution of indomethacin</p>	<p style="text-align: center;">Size Distribution of indomethacin emulsion coated with PBAE polymer</p>
Ket	<p style="text-align: center;">Size distribution of Ketorolac</p>	<p style="text-align: center;">Size distribution of Ket emulsion coated with PBAE polymer</p>
Nap	<p style="text-align: center;">Size distribution of naproxen</p>	<p style="text-align: center;">Size distribution of naproxen emulsion coated with PBAE polymer</p>

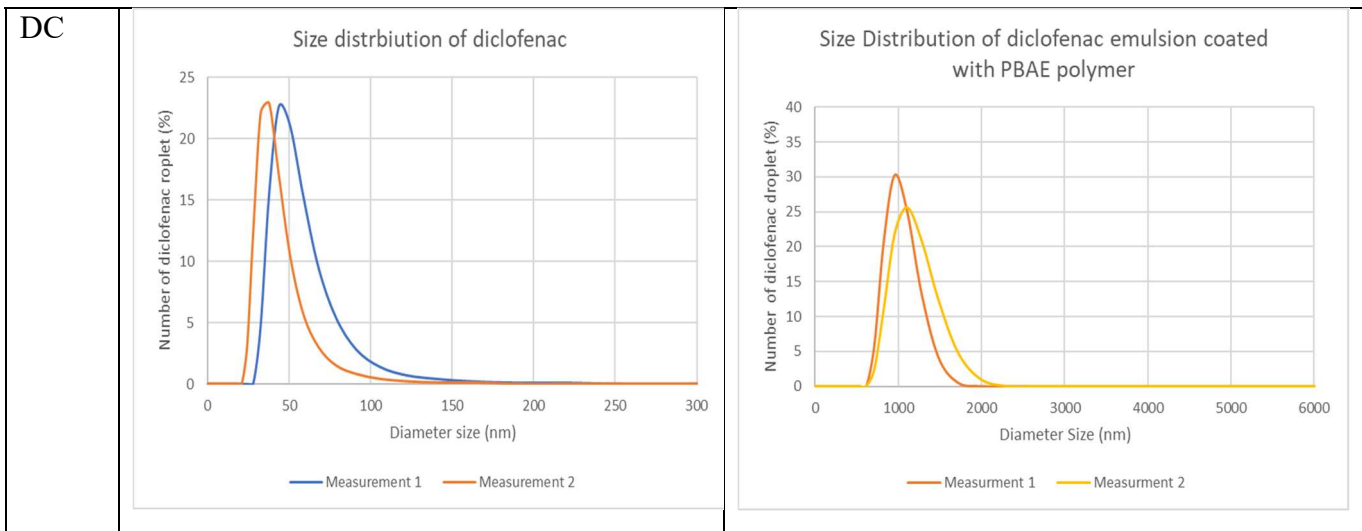


Figure 4-7. Characterisation – measuring the hydrodynamic size distribution of indomethacin, ketorolac, naproxen, and diclofenac before and after coated with PBAE polymer via dynamic light scattering (DLS). The particle size of the drug was increased around twentyfold after coated with the polymer.

Table 4-3 & Figure 4-7 shows that coating the NSAIDs with POLY-A5 remarkably increased the diameters of drug droplets. For example, upon being coated with POLY-A5, the size of DC o/w emulsion particles exhibited an approximate twenty-fold increase, as evidenced by an increase from  $0.05 \pm 0.03 \mu\text{m}$  to  $1.10 \pm 0.05 \mu\text{m}$ . Moreover, the original  $0.06 \pm 0.02 \mu\text{m}$  diameter size of the Ind o/w emulsion particles grew to  $1.01 \pm 0.33 \mu\text{m}$  after being coated with POLY-A5, more than tenfold increase compared with Ind o/w emulsion without the polymer. At the same time, Ket o/w emulsion droplets increased in size from  $0.09 \pm 0.02 \mu\text{m}$  to  $2.00 \pm 0.08 \mu\text{m}$  with POLY-A5 coating. Additionally, there was a slight increase in diameter of Nap o/w emulsion particles ( $0.05 \pm 0.03 \mu\text{m}$ ). Overall, Ket o/w emulsion particles saw the largest growth when coated with POLY-A5, followed by DC and Ind emulsion which exhibited approximately the same particle size. In comparison, Nap o/w emulsion coated with POLY-A5 had the smallest size change among the four NSAIDs. The reason for the variance in particle sizes among the drugs could be due to differences in electrostatic forces of attraction between the oil droplets and POLY-A5, causing the particles to move closer together and to interact in several ways, leading to which gives distinct sizes.

POLY-B5 also increased the distribution size of NSAIDs in the same manner as POLY-A5 (Table 4-4). Specifically, coating DC o/w emulsion with POLY-B5 led to an increase in droplet diameter size of more than 30 times. While it caused a twentyfold size increase in Ket, Ind and Nap particles (Table 4-4). Therefore, as with POLY-A5, Ket o/w emulsion coated with POLY-B5 displayed the largest particle size growth, followed by DC and Ind while Nap saw the

smallest size change. In summary, the sizes of all drug droplets were considerably increased after being coated with either POLY-A5 or POLY-B5 (Tables 4-3&4-4 & figure 4-7).

Table 4-3 Size measurements ( $\mu\text{m}$ ) for POLY-A5, NSAIDS emulsion before and after coated with POLY-A5.

<b>NSAIDs emulsion</b>	<b>NSAIDs droplets size (<math>\mu\text{m}</math>) before POLY-A 5 added</b>	<b>NSAIDs emulsion droplets size (<math>\mu\text{m}</math>) after POLY-A5 added</b>
POLY-A5	0.21 $\pm$ 0.02	
Indomethacin	0.06 $\pm$ 0.02	<b>1.01 <math>\pm</math>0.33</b>
Ketorolac	0.09 $\pm$ 0.02	<b>2.0 <math>\pm</math> 0.08</b>
Naproxen	0.05 $\pm$ 0.03	<b>0.98<math>\pm</math>0.04</b>
Diclofenac Sodium	0.05 $\pm$ 0.03	<b>1.10<math>\pm</math>0.05</b>
Emulsion only (o/w)	1.50 $\pm$ 0.02	<b>1.70 <math>\pm</math>0.01</b>

Table 4-4 Size measurements ( $\mu\text{m}$ ) for POLY-B5, NSAIDS emulsion before and after coated with POLY-B5.

<b>NSAIDs emulsion</b>	<b>NSAIDs emulsion droplets size (<math>\mu\text{m}</math>) before POLY-B 5 added</b>	<b>NSAIDs emulsion droplets size (<math>\mu\text{m}</math>) after POLY-B5 added</b>
POLY-B5	0.29 $\pm$ 0.02	
Indomethacin	0.06 $\pm$ 0.02	<b>1.21 <math>\pm</math>0.35</b>
Ketorolac	0.09 $\pm$ 0.02	<b>2.30<math>\pm</math>0.40</b>
Naproxen	0.05 $\pm$ 0.03	<b>1.11<math>\pm</math>0.04</b>
Diclofenac Sodium	0.05 $\pm$ 0.03	<b>1.80<math>\pm</math>0.35</b>
Emulsion only (o/w)	1.50 $\pm$ 0.02	<b>1.70 <math>\pm</math>0.01</b>

#### 4.3.4. Stability study:

Emulsion systems consist of at least two immiscible liquid phases, one of which is dispersed as droplets of microscopic or ultramicroscopic size, in the other (Kahar *et al.*, 2021). As mentioned above, in this project a preparation of oil (oleic acid)-in-water (o/w) (in which, the dispersed phase is oil the and external phase is water); was prepared to coat the NSAIDs. Emulsion stability was analysed by measuring charges and droplet sizes, alongside visual

observation. The stability of an emulsion refers to its ability to resist changes in its properties over time (Tadros, 2004; Saleh *et al.*, 2005). Emulsion instability causes changes in the spatial distribution and structural organization of molecules (Tadros, 2004; Saleh *et al.*, 2005). For the purposes of stability study, Ket o/w emulsion coated with POLY-A5 was prepared, in addition to the following control samples: o/w emulsion alone, o/w emulsion with Ket only and o/w emulsion with POLY-A5 only. Ket was chosen as a model example of NSAIDs, with POLY-A5 selected to exemplify PBAEs.

#### **4.3.4.1. Zeta potential**

ZP is the electrical potential of double layers that can be determined by measuring the velocity of charged particles moving towards electrodes across sample solutions, in the presence of external electric fields (Sze *et al.*, 2003). It is used in this chapter to characterise emulsion droplets with regards to their stability. Ket emulsion coated with POLY-A5 (the developed DDS) was prepared and ZP was calculated; this was then compared with the ZP values of o/w emulsion, Ket emulsion and emulsion coated with POLY-A5 without Ket as a control. The results show that Ket emulsion coated with POLY-A5 can be considered to be a cationic emulsion: its ZP was initially positive ( $+17.1 \pm 1.9$  mV) before dropping to  $-1.1$  mV (Figure 4-8) on day 7 due to polymer hydrolysis (as discussed above). These decreases in charge in the emulsion coated demonstrate that the polymer was hydrolysed and depleted over time, thereby decreasing emulsion stability. Comparing ZP results for Ket o/w emulsion coated with POLY-A5 with o/w emulsion alone, the charge of the former decreased slightly over 14 days whereas in the latter case it fell dramatically from  $-30.9 \pm 1.8$  mV to  $-38.6 \pm 0.8$  mV after 24 hours, which could accelerate instability of the emulsion (Figure 4-8). Moreover, both the Ket o/w emulsion and Ket alone samples had low zeta potential ( $-65.5 \pm 1.7$  mV and  $-69.9 \pm 6.3$  mV, respectively) compared with the other tested emulsions which plateaued after 3 days (Figure 4-8). This was mainly because oleic acid and Ket registered high negative charges, leading to electrostatic repulsive forces occurring between the droplets and maintaining the high negative charge for long time. Generally, Figure 4-8 shows that a decrease in charge indicates decrease in emulsion stability, as the oil droplets adsorb onto the surface or form one big oil droplet meaning the emulsion becomes less stable and more separated over time. However, this instability was delayed when POLY-A5 was used to coat the emulsion.

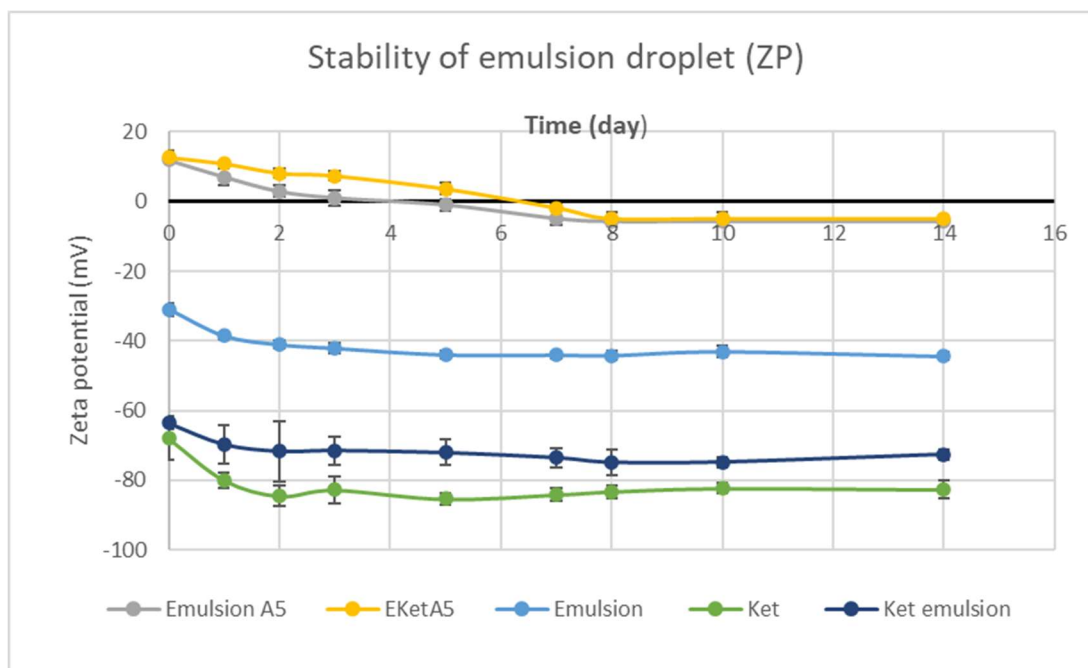


Figure 4-8. Zeta potential (mV) values for stability of o/w emulsion before and after adding Ket/POLY-A5. Zeta potential was measured using a Zetasizer Nano ZS apparatus to determine emulsion stability as charge changing for 14 days. The figure shows that emulsion with high zeta potential which containing POLY-A5 were the more stable emulsion.

#### 4.3.4.2. Particle size analysis:

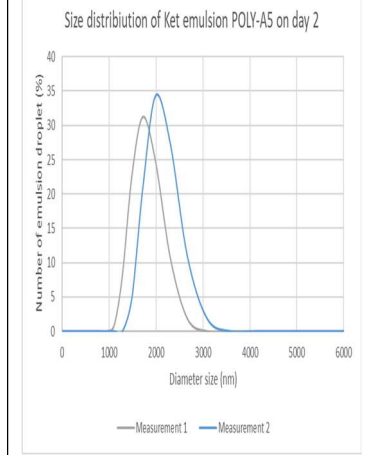
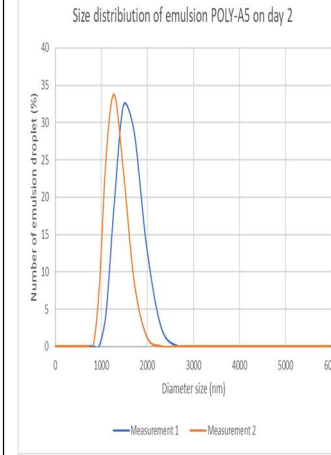
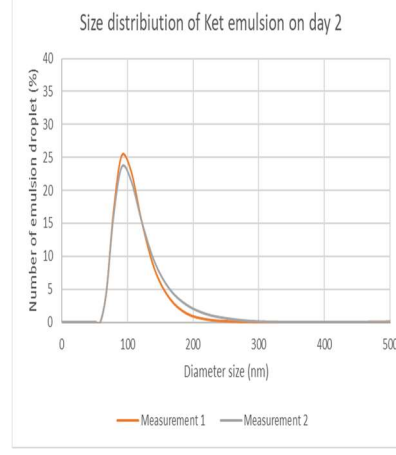
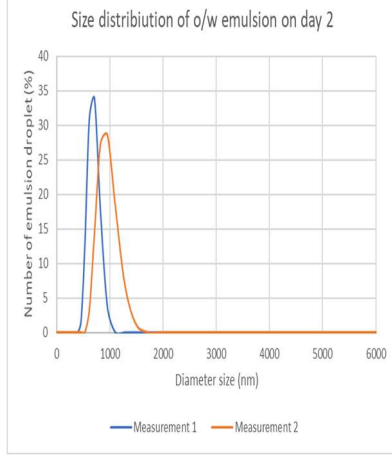
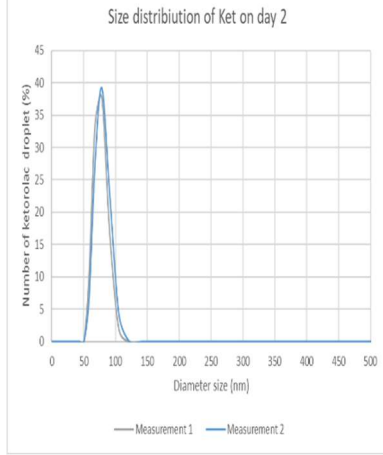
Measurement of droplet sizes in nano scaled emulsions is very important to evaluate their stability, since a dramatic change in droplet size over time can be directly attributed to internal droplet aggregation or coalescence (Tadros, 2004). The particles must be small and homogeneously distributed to allow a film to form around the droplets in the dispersed phase, resulting in a more stable emulsion. However, excessively small particles can be removed faster from the interface and so lead to emulsion instability (Tadros, 2004). In this work, the droplet sizes were measured using DLS at regular intervals (daily) over 14 days (Figure 4-9) (the Figures for days 0, 1,2,3,4,5,7 and 10 are presented, as there was no change in size distribution after 10 days). According to the size distribution results showed in Figure 4-9, emulsion particle sizes ranged from 0.10  $\mu\text{m}$  to 2  $\mu\text{m}$  (100-2000 nm). Ket emulsion coated with POLY-A5 (the developed DDS) exhibited larger particle sizes (2  $\mu\text{m}$ ) than the controls, while Ket alone presented the smallest sized droplets (0.10  $\mu\text{m}$ ). Generally, it has been shown that most commercial emulsion formulations used in drug delivery have particle diameters sized between 0.1  $\mu\text{m}$  to 10  $\mu\text{m}$  (Sarker, 2005; Islam, Islam and Hossain, 2018). In this project, the developed DDS fell within this range as well (its droplet size was 2  $\mu\text{m}$ ), thus maintaining stability and settling under the influence of gravity (when compared to the control emulsion) (Figure 4-9).

In addition, it exhibited optimal droplet size to decrease the possibility of the drug being washed out from the joints (the mean diameter of individual synovium capillaries is up to 0.03  $\mu\text{m}$  maximum), and increased drug penetration and retention inside cartilage tissue (Haywood and Walsh, 2001; Janssen *et al.*, 2014; Geiger, Grodzinsky and Hammond, 2018).

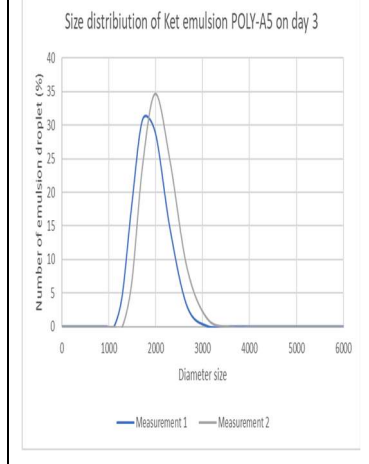
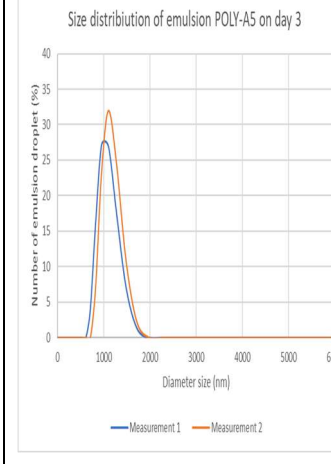
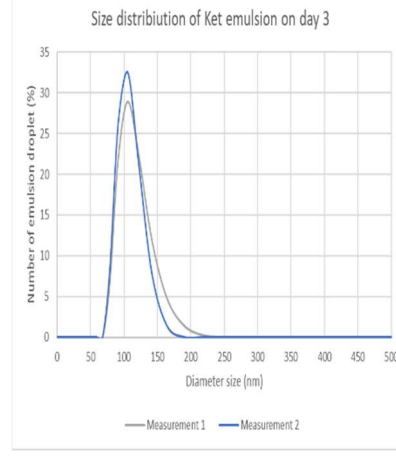
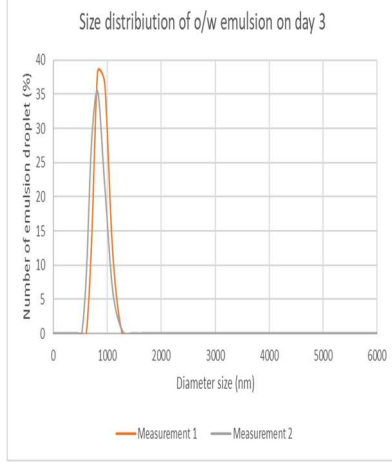
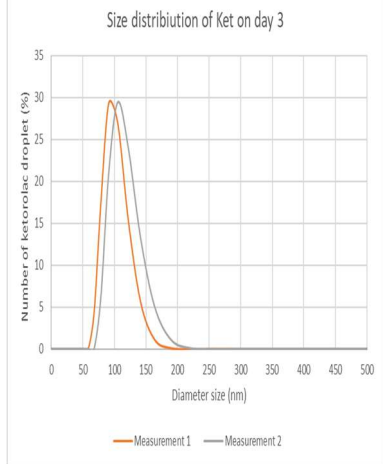
The results presented in Figure 4-9, showed that mean droplet size for the emulsion coated with POLY-A5 remained relatively stable over the first 7-day period, at around 1  $\mu\text{m}$  to 2  $\mu\text{m}$  (2000-1000 nm). However, a slight decreased in the size of the emulsion droplets was observed after 7 days due to polymer hydrolysis, with a final mean size of 0.60  $\mu\text{m}$  (600 nm). On the other hand, the mean droplet size decreased over the 10-day period, from an initial mean size of 1  $\mu\text{m}$  (1000 nm) to a final mean size of 0.10  $\mu\text{m}$  (100 nm) for emulsion or Ket alone (without polymer coating), which led to emulsion instability and phase separation (as in Figure 4-10). In general, it can be observed from this work that particle size decreases as sampling time increases. Furthermore, these results showed that the emulsion was able to maintain its stability over a period of 7 days, which is likely to be due to the presence of POLY-A5.

	Ket alone	Emulsion alone	Ket emulsion	Emulsion POLY-A5	Ket emulsion POLY-A5
Day0	<p>Size distribution of Ket on day 0</p>	<p>Size distribution of o/w emulsion on day 0</p>	<p>Size distribution of Ket emulsion on day 0</p>	<p>Size distribution of emulsion POLY-A5 on day 0</p>	<p>Size distribution of Ket emulsion POLY-A5 on day 0</p>
Day1	<p>Size distribution of Ket on day 1</p>	<p>Size distribution of o/w emulsion on day 1</p>	<p>Size distribution of Ket emulsion on day 1</p>	<p>Size distribution of emulsion POLY-A5 on day 1</p>	<p>Size distribution of Ket emulsion POLY-A5 on day 1</p>

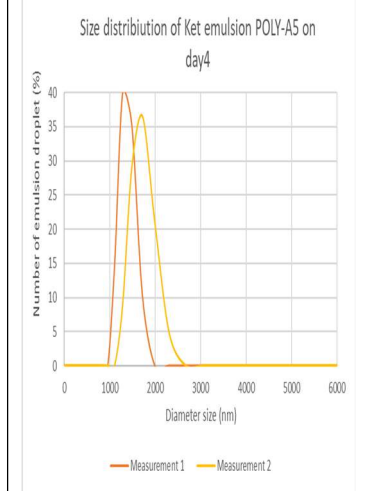
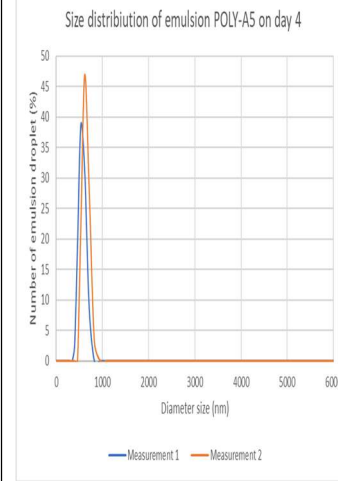
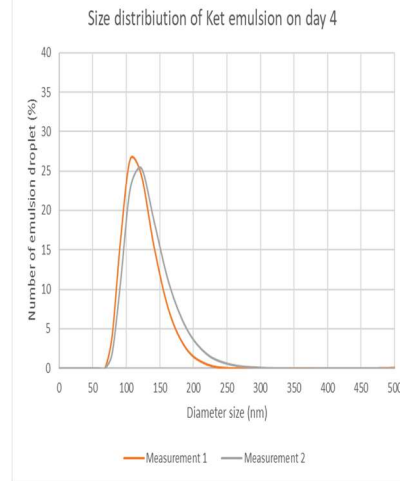
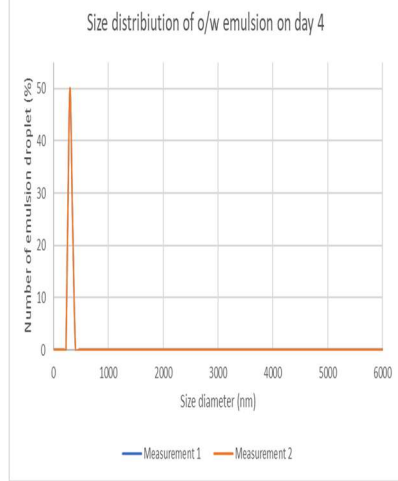
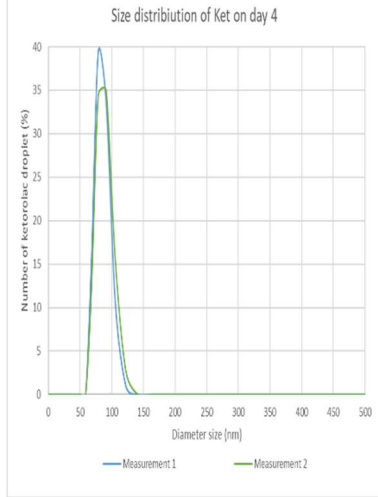
Day2



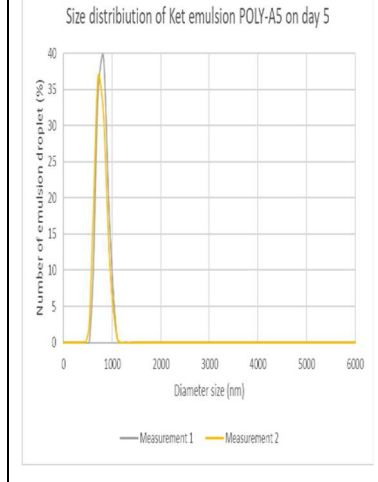
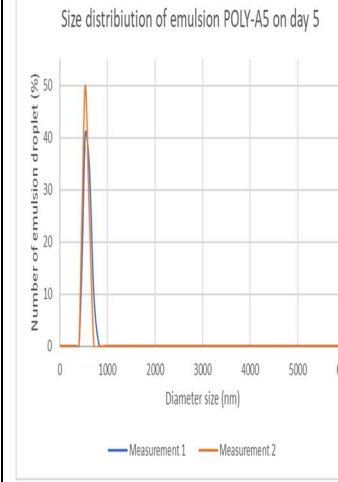
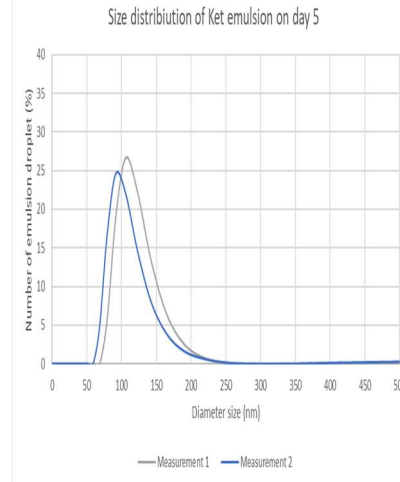
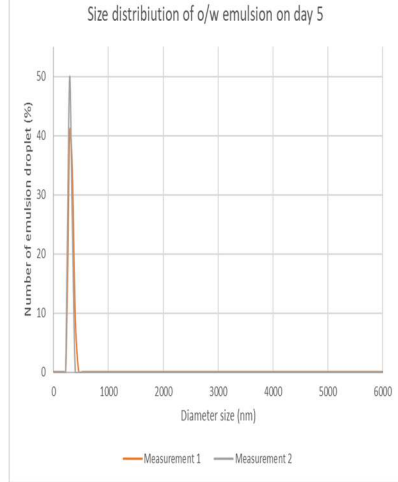
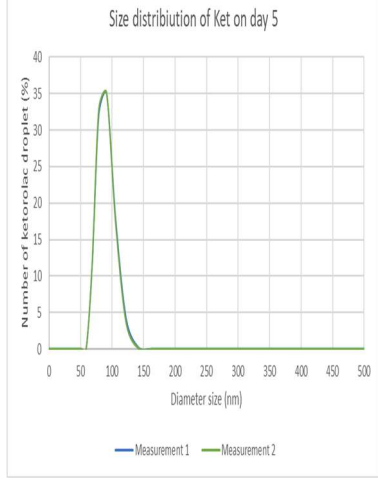
Day3



Day4



Day5



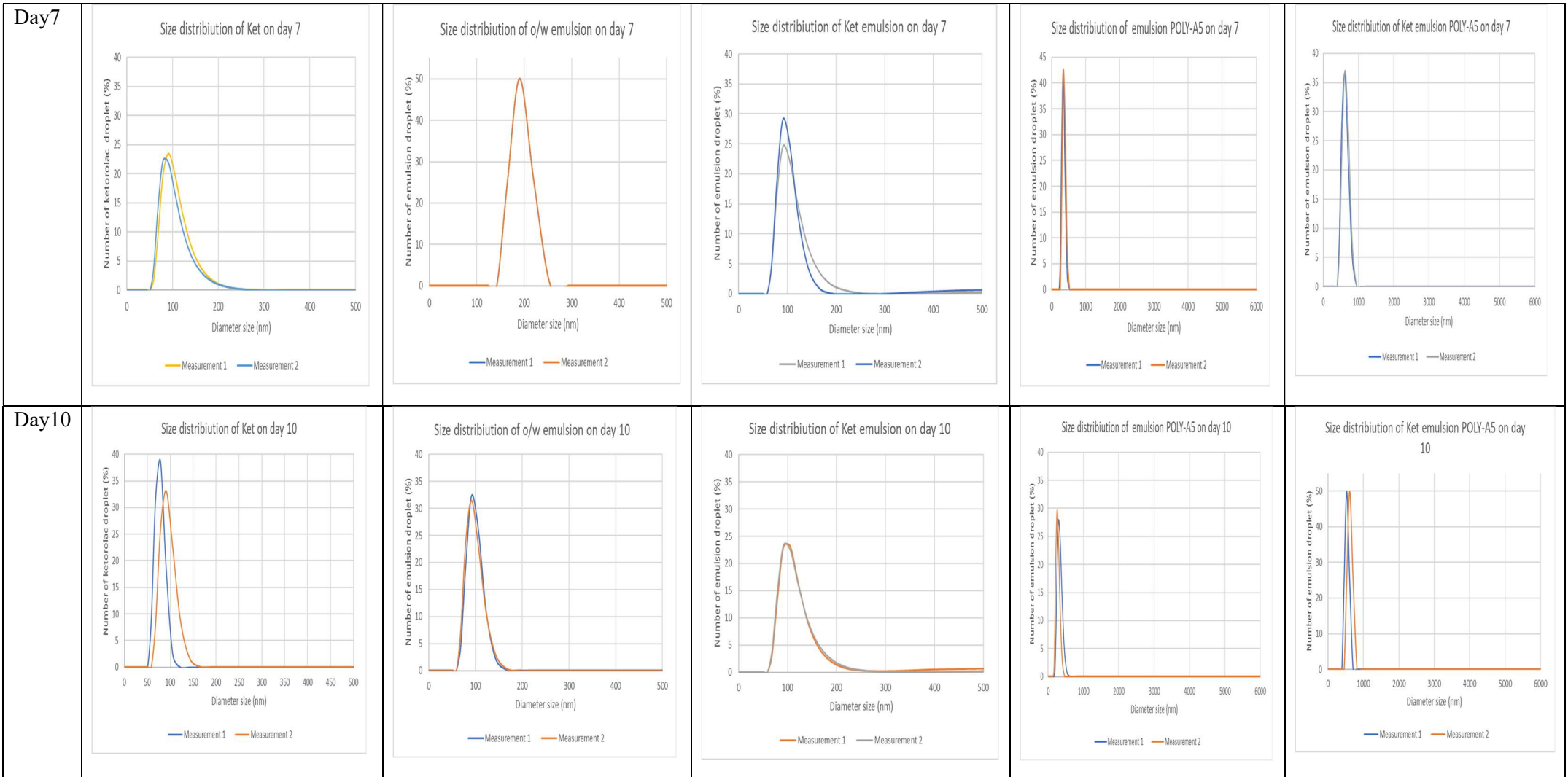
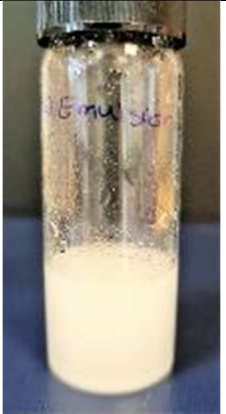
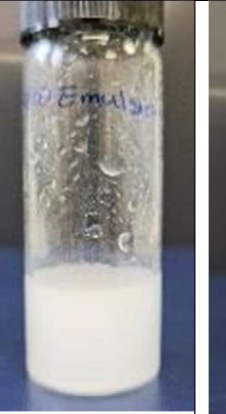
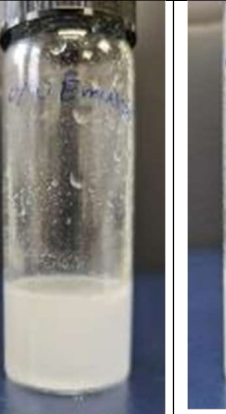
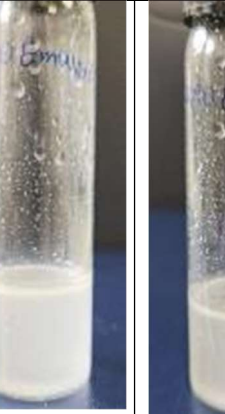
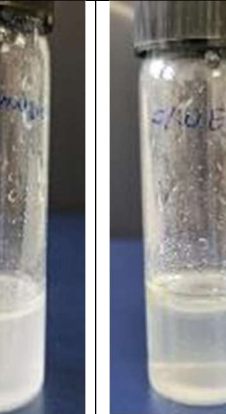
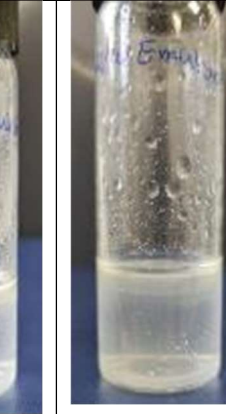
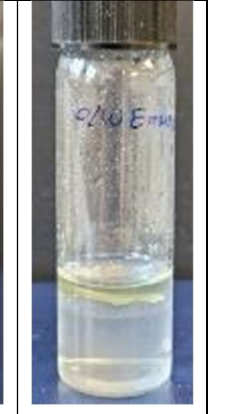
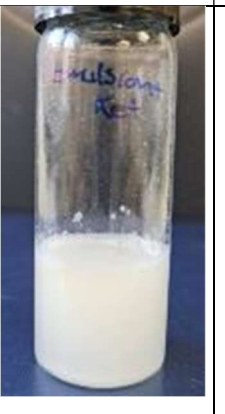
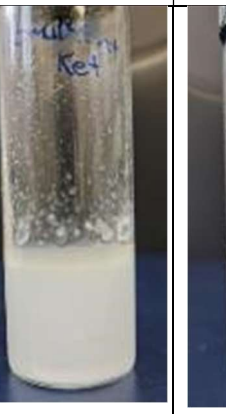
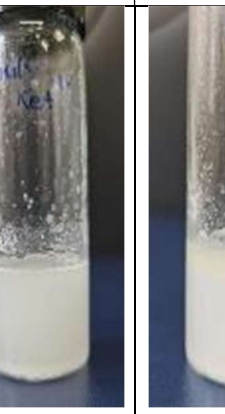
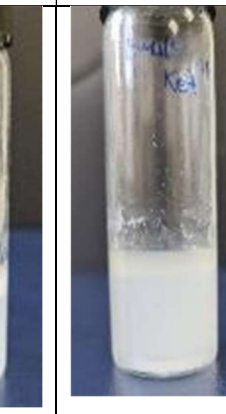
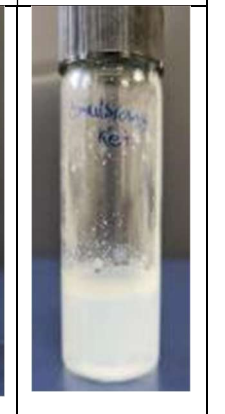


Figure 4-9. Size distribution of emulsion droplets before and after adding Ket/POLY-A5, as measured by dynamic light scattering (DLS) using a Zetasizer Nano ZS apparatus. The DLS measurements were taken at regular intervals over a period of 10 days to assess the stability of the o/w emulsion. The x-axis represent the particle diameter size (nm), while the y-axis represents the number of particles droplets (%). Emulsion diameter size was decrease slightly due to emulsion instabilities. The figure shows that emulsion which containing POLY-A5 with size were the more stable emulsion as a clear decrease in diameter size were seen after 7 days.

#### 4.3.4.3. Visual observation of emulsion stability:

The emulsions were prepared in clear glass bottles, then homogenised using high speed vortex 2700 rpm (Scientific Industries Vortex-Genie®) for 5-10 min before being stored at room temperature. The varying stabilities of different emulsions over 14 days are illustrated in Figure 4-10 (the Figures for days 0, 1,2,3,4,5, 6,7 and 10 are presented, as there was no change in size distribution after 10 days). According to the results, phase separation between the oil and aqueous phases occurred quickly (after 2 days) in the emulsions with smaller particle sizes ( $<0.2\mu\text{m}$ ), namely the o/w emulsion and Ket o/w emulsion. In contrast, Ket emulsion coated with POLY-A5 with  $2\mu\text{m}$  particle sizes was more stable than the smaller ones which showed oil and aqueous phase separation in around 7 days. During the first 2 days the emulsions had a cloudy appearance. After that, the o/w emulsion system underwent breakdown, followed by phase separation, which is a sign of emulsion destabilisation being prolonged to around 7 days using emulsion coated with POLY-A5 (Figure 4-10).

It has been shown that lipid based nanoparticles with high ZP values are able to maintain system stability and are less prone to form aggregates or suffer instability (Samimi *et al.*, 2018). In addition, protonated amines, are much more stable at a low pH value. The ZP of Ket emulsion coated with POLY-A5 was  $+17.1\text{ mV}$  and around pH 5. It was charged positively in this slightly acidic buffer (pH 5), because of the protonation of nitrogen from the amine ends ( $\text{R-NH}_3^+$ ) (Kim, Sunshine and Green, 2014; Perni & Prokopovich, 2017), thus providing a stable emulsion for around one week. Generally, at low pH, there is a high concentration of  $\text{H}^+$  ions in the solution, which makes it more likely for the amino group to pick up an  $\text{H}^+$  ion and become protonated (Kim, Sunshine and Green, 2014). The positively charged ammonium ion can form strong electrostatic interactions with negatively charged molecules such as water in the solution. The electrostatic interactions help to prevent the two phases from separating and allow the emulsion to remain stable over time. Therefore, using POLY-A5 to coat the emulsion was shown to be ideal for maintaining stability and decreasing emulsion destabilisation.

	Day0	Day1	Day2	Day3	Day4	Day5	Day6	Day7	Day10
O/W emulsion									
Ket o/w emulsion									

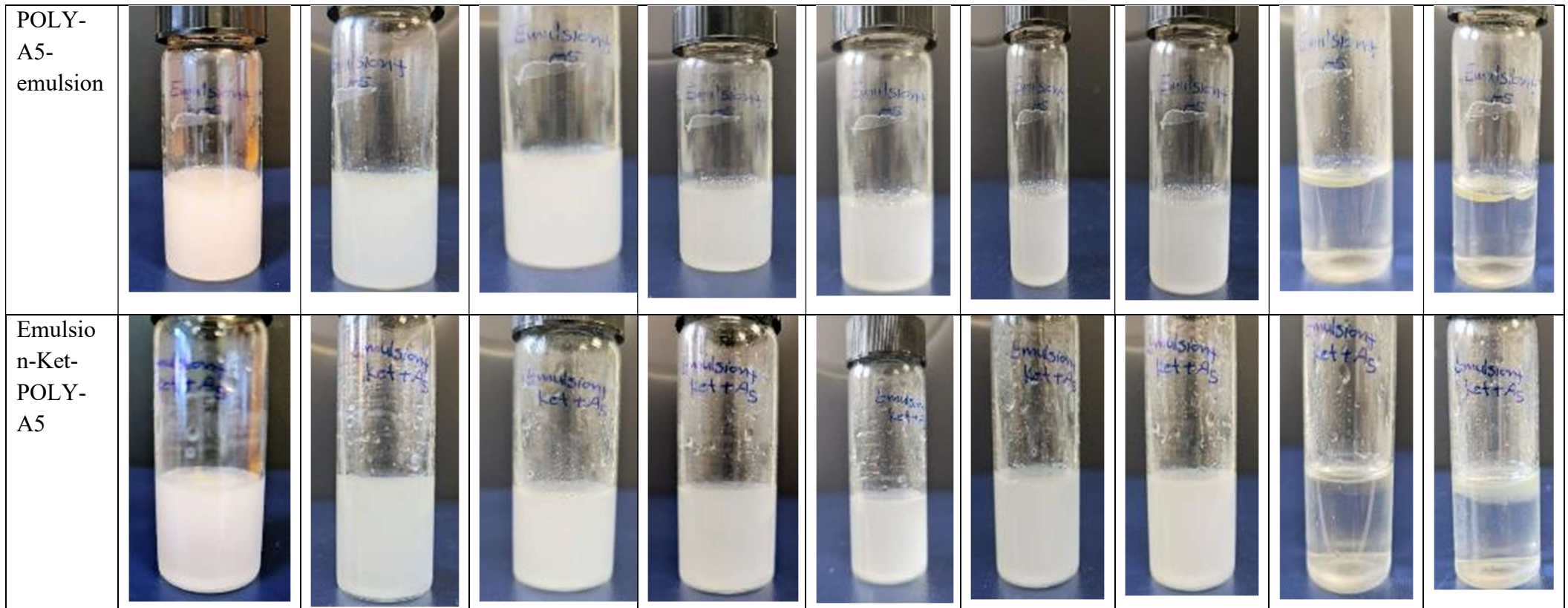


Figure 4-10. Visual observation of emulsion stability. Emulsions (o/w emulsion before and after adding Ket/POLY-A5) were stored at room temperature and observed for 10 days. The stability of emulsion is represented by cloudy appearance of the solution in homogeneous mixture. The stability was decrease over the time which represented as oil and water phase separation after 2 days for the emulsion without POLY-A5 and 7 days for the coated emulsion with POLY-A5.

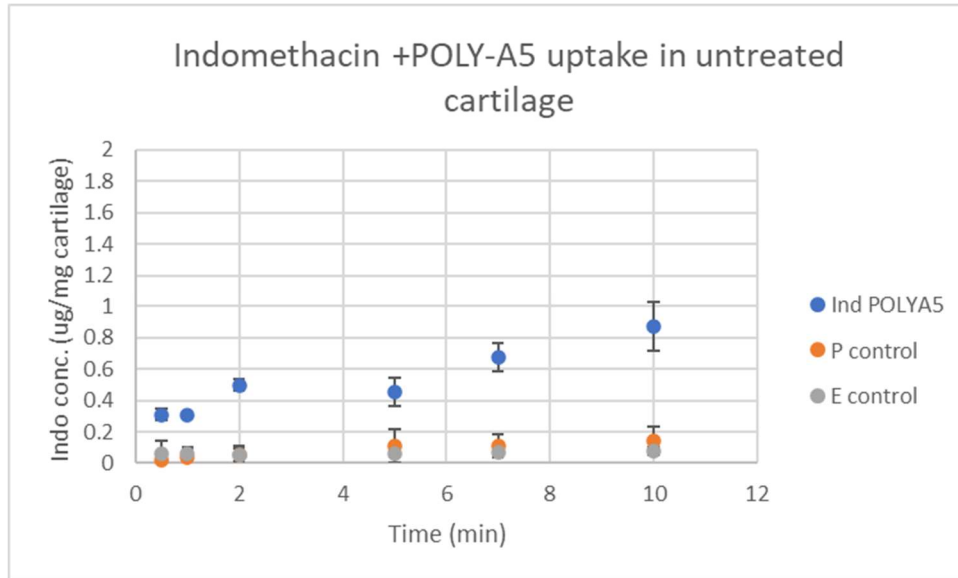
#### **4.3.5. Amount of drug uptake measurement:**

Cartilage penetration experiments were performed to test the efficacy of the drug delivery system. These proceeded with untreated and GAG depleted cartilage samples which were treated with P control, E control and NSAIDs o/w emulsion coated with POLY-A5 and POLY-B5.

For both the untreated and GAG depleted cartilage samples, it was observed that in most cases, there was a positive correlation between uptake duration and drug uptake amount inside cartilage. Generally, as incubation duration increased there was a steady increase in NSAIDs uptake until saturation at 10 min (as clearly shown in Figures 4-11 to 4-18). Furthermore, after each time point, NSAIDs emulsion coated with POLY-A5 showed a higher level of the drug uptake in cartilage compared to each control type, with the difference being statistically significant ( $p < 0.05$ ). Generally, the amount of drug uptake by cartilage was higher in untreated cartilage than in GAG depleted cartilage. This is because a higher amount of GAG allowed for greater electrostatic interaction between the positively charged polymers and the negatively charged GAG. Therefore, meaning a volume of drug was delivered to the cartilage tissue. This was clearly apparent in Ind, Nap and DC (Figures 4-11,4-13&4-14). On the other hand, the amount of uptake was higher in GAG depleted cartilage in Ket o/w emulsion than in the untreated one (Figure 4-12). This could be because GAG depleted cartilage displays a higher hydraulic permeability than normal cartilage; accordingly, it allows a better flow of drug delivery systems towards it (Nia *et al.*, 2015).

Similarly, POLY-B5 exhibited some of the same behaviours as POLY-A5. Firstly, the amount of drug uptake increased gradually in tandem with increased incubation time. Nap uptake in untreated cartilage was higher than in GAG depleted cartilage whereas Ind and Ket uptakes were higher in GAG depleted than untreated cartilage (Figures 4-15, 4-16 &4-17). In contrast, DC emulsion coated with POLY-B5 had a lower amount of uptake compared to the controls, which could be due to its high negative charge (-90.5 mV) potentially affecting the penetration efficacy of the formulation even after successful coating with POLY-B5 (Figure 4-18).

A)



B)

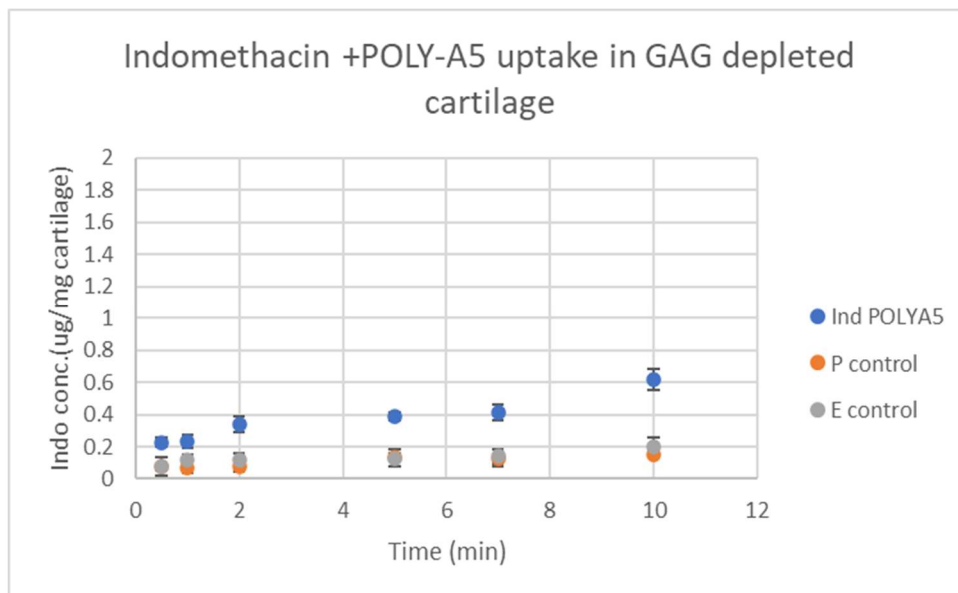
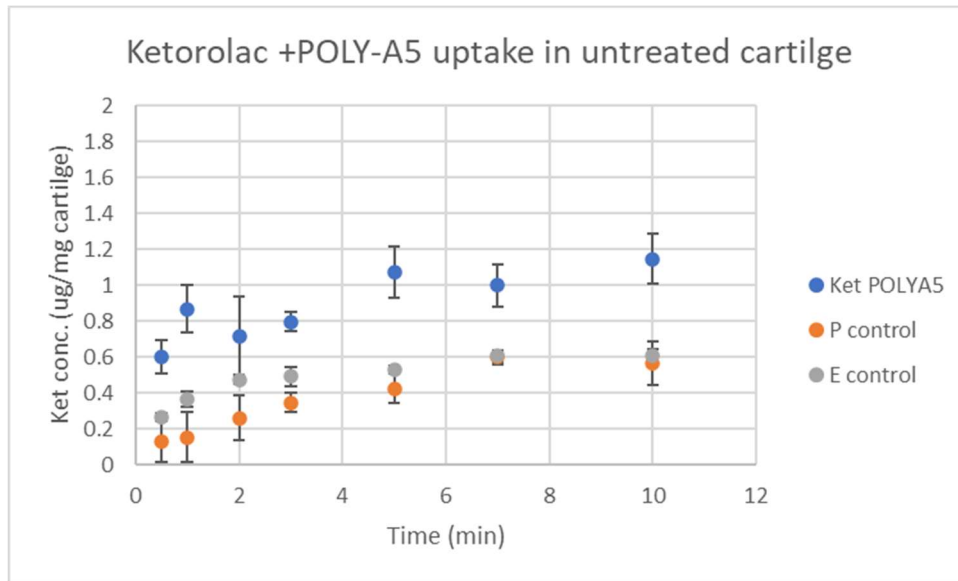


Figure 4-11. Comparison of indomethacin (Ind) uptake into cartilage for 10 minutes using P control (Ind in PBS), E control (Ind emulsion) and Ind emulsion saturated with POLY-A5 in both untreated cartilage (A) and GAG depleted cartilage (B). The concentration of Ind that has penetrated the cartilage is expressed in  $\mu\text{g}$  per mg cartilage. The amount of Ind uptake was higher in untreated cartilage compared to GAG depleted cartilage.

A)



B)

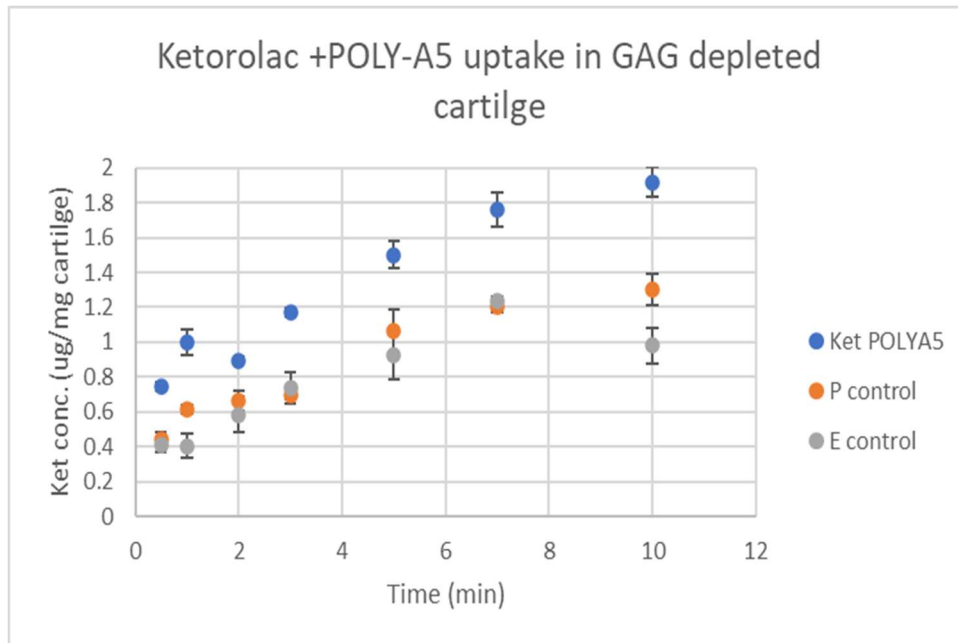
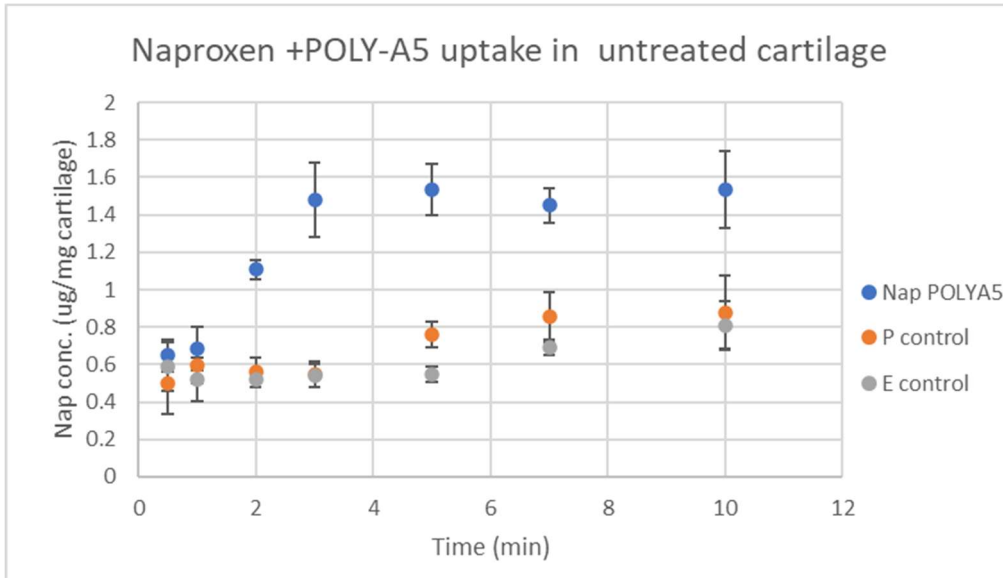


Figure 4-12. Comparison of ketorolac (Ket) uptake into cartilage for 10 minutes using P control (Ket in PBS), E control (Ket emulsion) and Ket emulsion saturated with POLY-A5 in both untreated cartilage (A) and GAG depleted cartilage (B). The concentration of Ket that has penetrated the cartilage is expressed in  $\mu\text{g}$  per mg cartilage. The amount of Ket uptake was higher in GAG depleted cartilage compared to untreated cartilage.

A)



B)

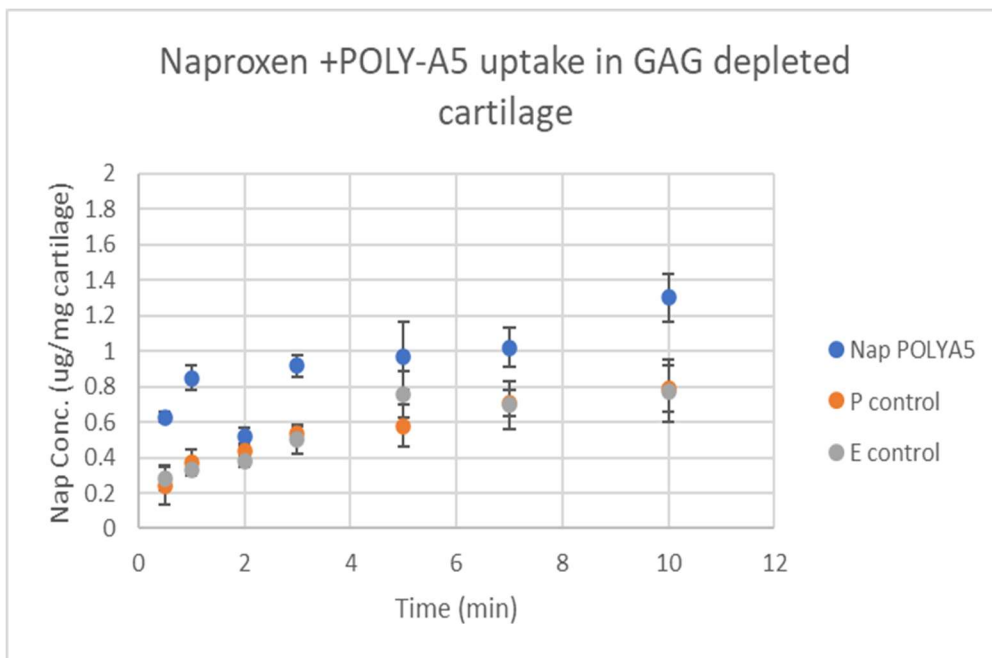
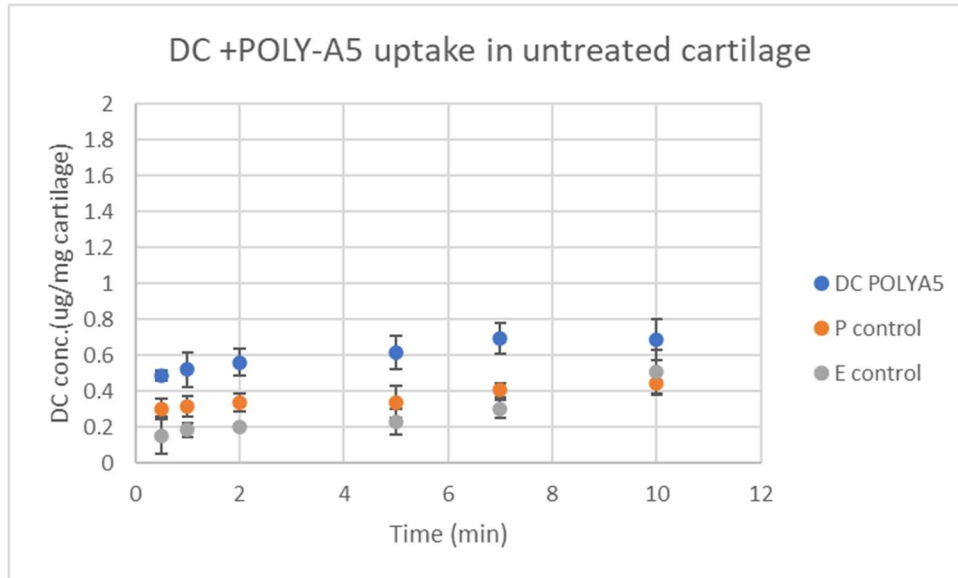


Figure 4-13. Comparison of naproxen (Nap) uptake into cartilage for 10 minutes using P control (Nap in PBS), E control (Nap emulsion) and Nap emulsion saturated with POLY-A5 in both untreated cartilage (A) and GAG depleted cartilage (B). The concentration of Nap that has penetrated the cartilage is expressed in  $\mu\text{g}$  per mg cartilage. The amount of Nap uptake was higher in untreated cartilage compared to GAG depleted cartilage.

A)



B)

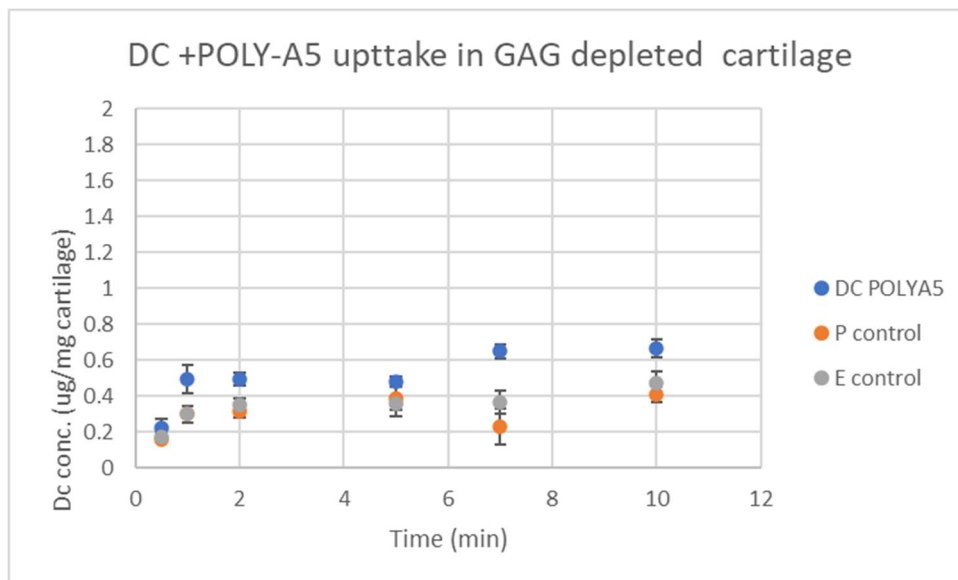
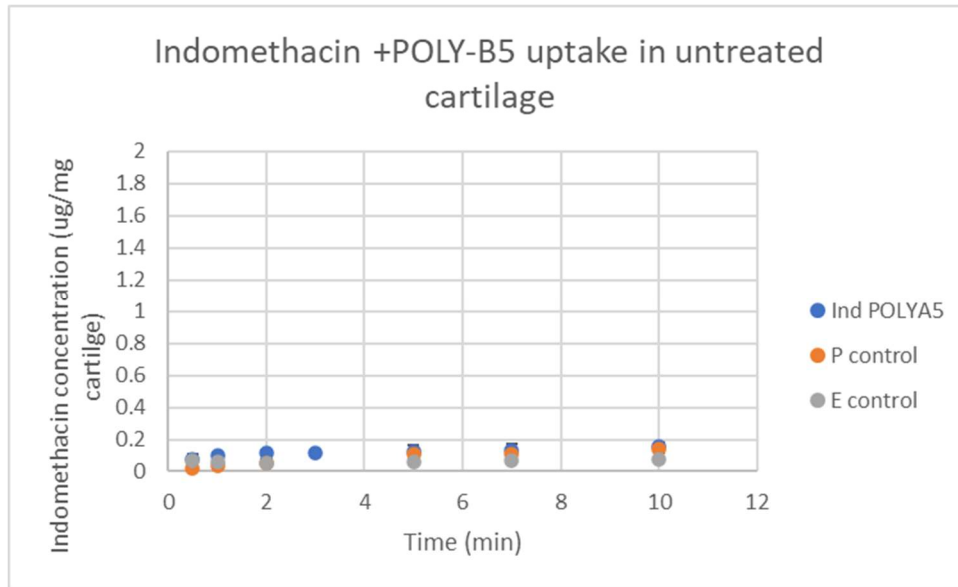


Figure 4-14. Comparison of diclofenac sodium (DC) uptake for 10 minutes into cartilage using P control (DC in PBS), E control (DC emulsion) and DC emulsion saturated with POLY-A5 in both untreated cartilage (A) and GAG depleted cartilage (B). The concentration of DC that has penetrated the cartilage is expressed in  $\mu\text{g}$  per mg cartilage. The amount of DC uptake was higher in untreated cartilage compared to GAG depleted cartilage.

The use of POLY-A5 and POLY-B5 resulted in gradual increases in Ind, Ket, Nap and DC uptake until the 10 min point. Accordingly, NSAIDs uptake was highest at 10 mins for most of the cartilage samples. In fact, this means that saturation occurred at 10 min; a similar effect was also reported in a previous study with cartilage uptake saturation being reached at 10 min for a POLYX polymer that conjugated Dex (Perni and Prokopovich, 2017). A possible reason for this is that the amount of drug that had penetrated inside the cartilage tissue could not be held for longer than 10 min and the drug potentially diffused out of the cartilage to the 96 well plates.

Overall, the uptake of NSAIDs emulsion coated with POLY-A5 was higher than POLY-B5. The difference was statistically significant for Ind, Ket, Nap and DC ( $p < 0.01$ ,  $p < 0.001$ ,  $p < 0.01$  and  $p < 0.01$ , respectively), However, for Nap emulsion on untreated cartilage, the difference was not statistically significant ( $p > 0.5$ ).

A)



B)

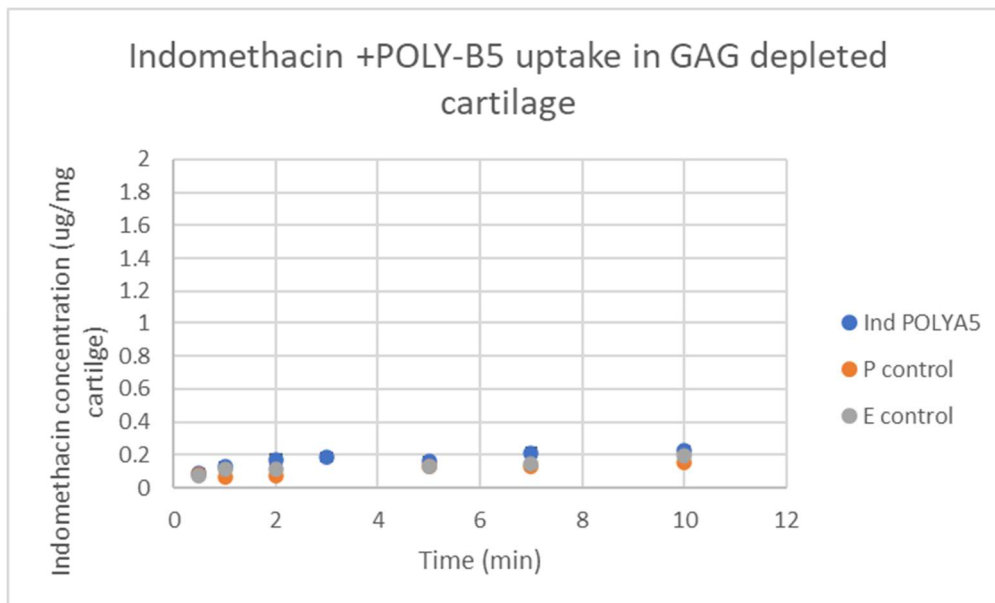
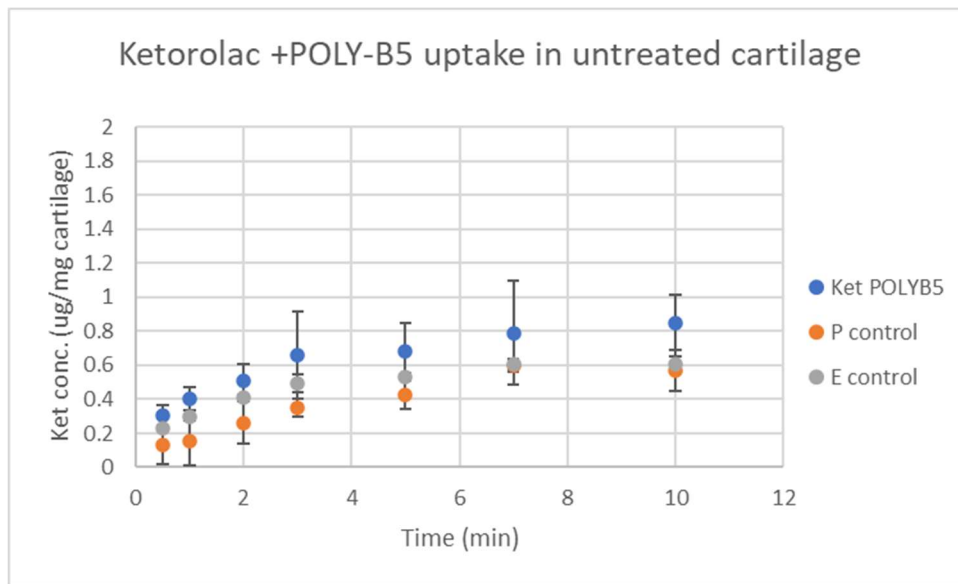


Figure 4-15. Comparison of indomethacin (Ind) uptake into cartilage for 10 minutes using P control (Ind in PBS), E control (Ind emulsion) and Ind emulsion saturated with POLY-B5 in both untreated (A) and GAG depleted cartilage (B). The concentration of Ind that has penetrated the cartilage is expressed in  $\mu\text{g}$  per mg cartilage. The amount of Ind uptake was higher in GAG depleted cartilage compared to untreated cartilage.

A)



B)

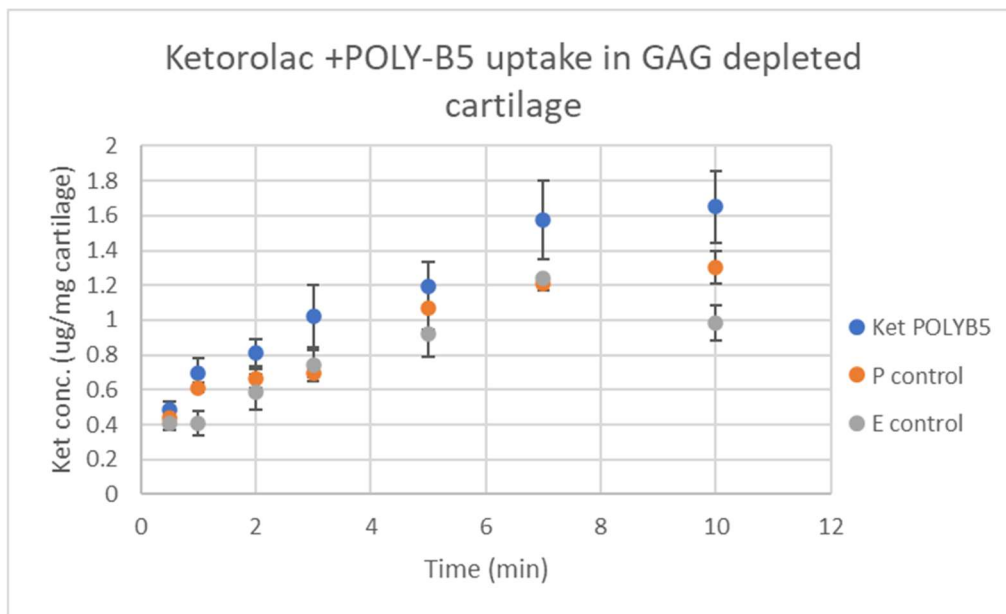
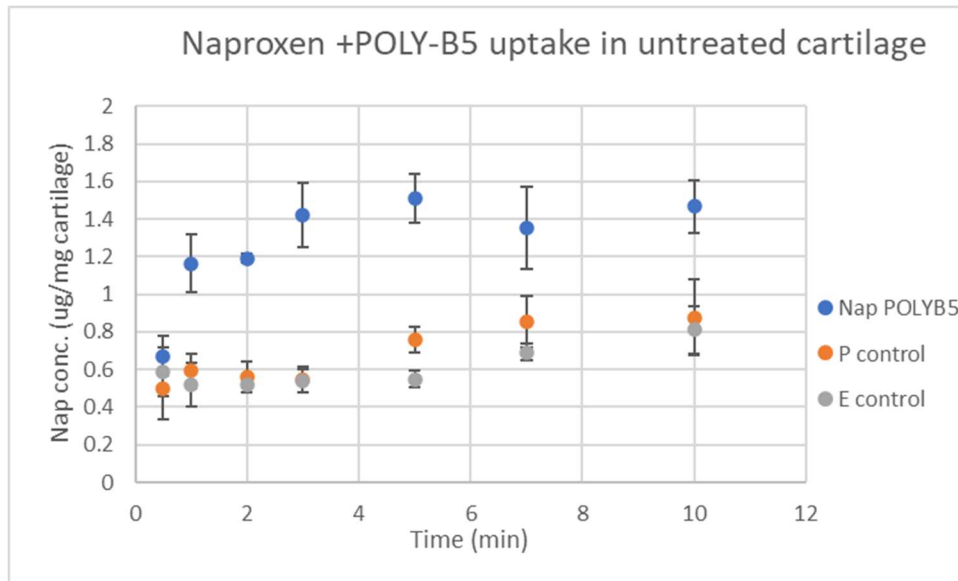


Figure 4-16. Comparison of ketorolac (Ket) uptake into cartilage for 10 minutes using P control (Ket in PBS), E control (Ket emulsion) and Ket emulsion saturated with POLY-B5 in both untreated (A) and GAG depleted cartilage (B). The concentration of Ket that has penetrated the cartilage is expressed in  $\mu\text{g}$  per mg cartilage. The amount of Ket uptake was higher in GAG depleted cartilage compared to untreated cartilage.

A)



B)

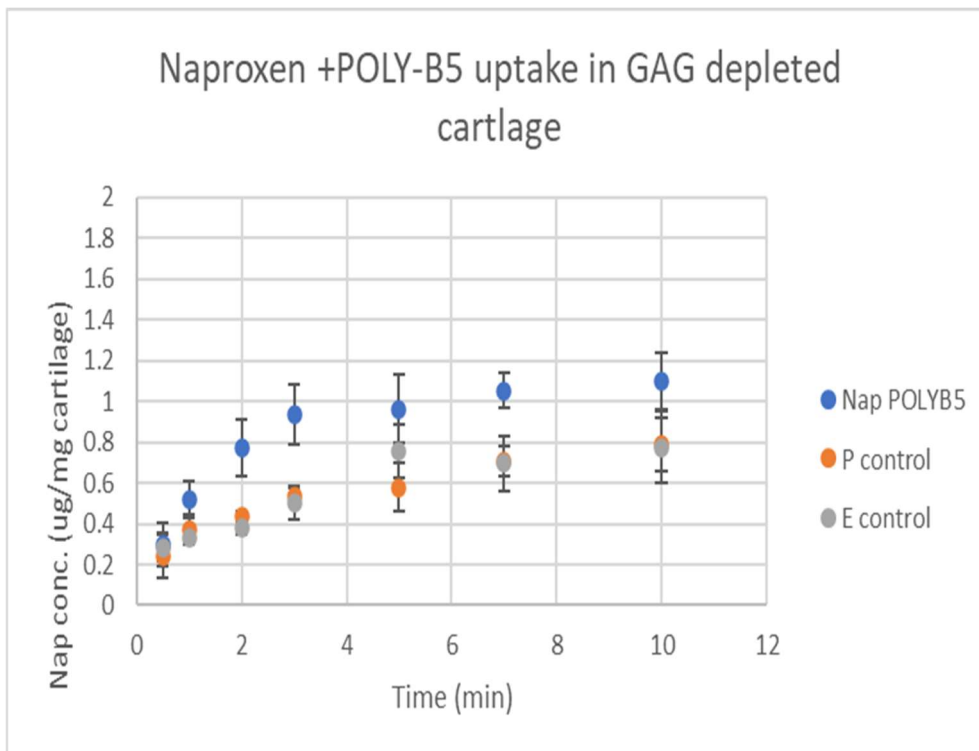
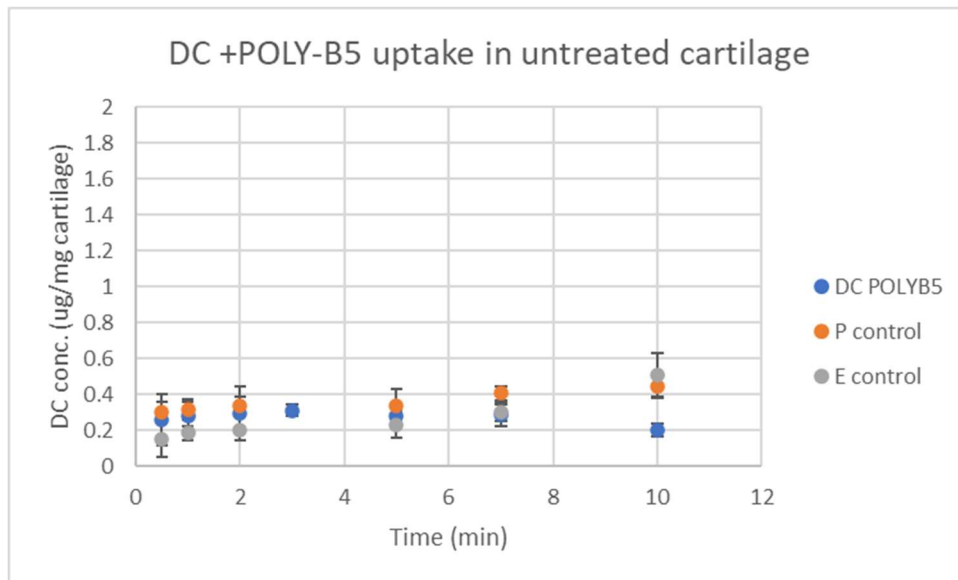


Figure 4-17 Comparison of naproxen (Nap) uptake into cartilage for 10 minutes using P control (Nap in PBS), E control (Nap emulsion) and Nap emulsion saturated with POLY-B5 in both untreated (A) and GAG depleted cartilage (B). The concentration of Nap that has penetrated the cartilage is expressed in  $\mu\text{g}$  per mg cartilage. The amount of Nap uptake was higher in untreated cartilage compared to GAG depleted cartilage.

A)



B)

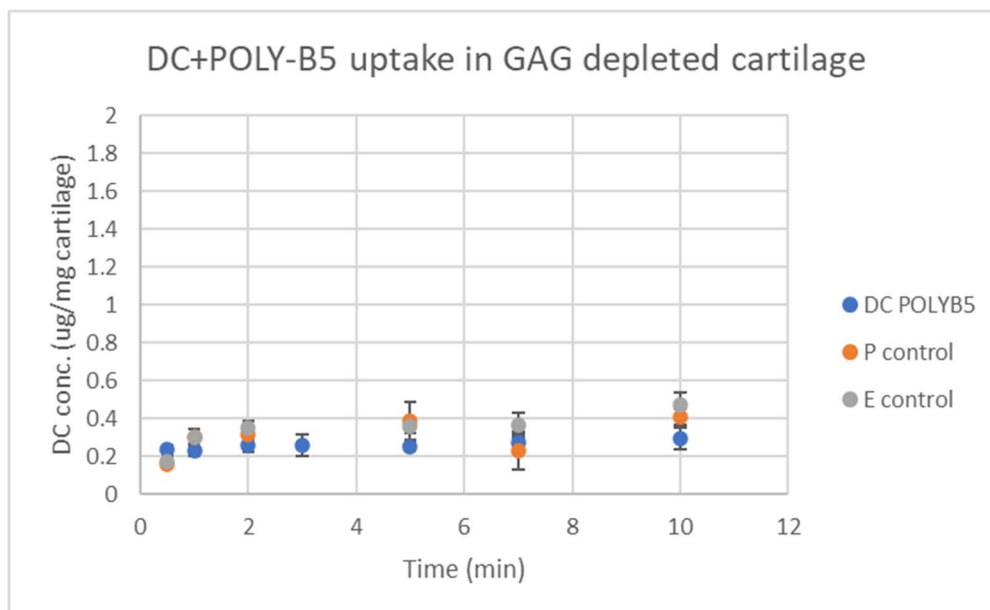


Figure 4-18 Comparison of diclofenac sodium (DC) uptake into cartilage for 10 minutes using P control (DC in PBS), E control (DC emulsion) and DC emulsion saturated with POLY-B5 in both untreated (A) and GAG depleted cartilage(B). The concentration of DC that has penetrated the cartilage is expressed in  $\mu\text{g}$  per mg cartilage. The amount of DC uptake was higher in GAG depleted cartilage compared to untreated cartilage.

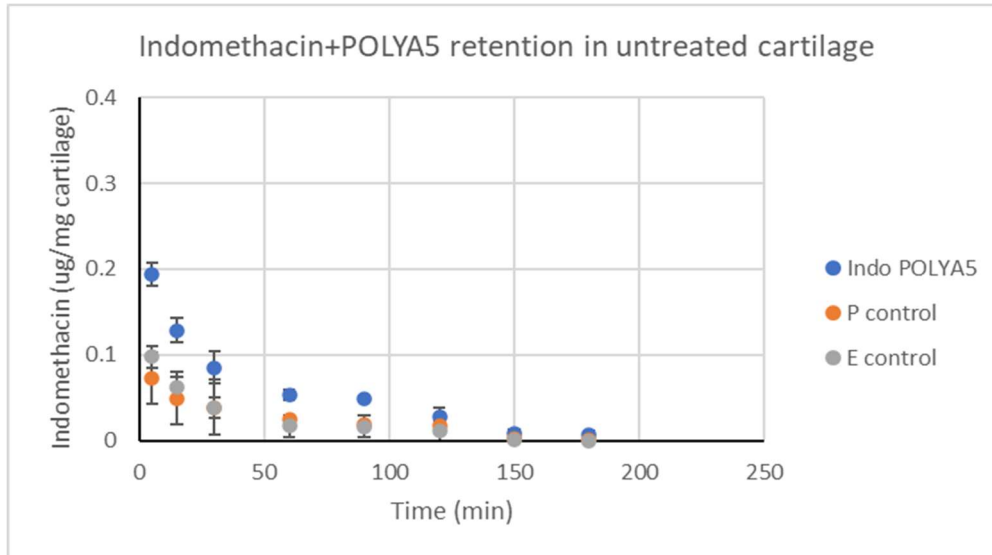
#### 4.3.6. Drug retention inside cartilage

Drug retention time for the P control, E control and emulsion coated with POLY-A5 and POLY-B5 were determined at 5, 15, 30 minutes, and at 1, 2, 2.5, 3, 3.5, 4, 5, and 8 hours. Increasing the retention duration of the drugs in the affected joints was necessary to control their release and improve their efficacy. In this work, the highest level of NSAIDs o/w emulsion uptake, in both untreated and GAG depleted cartilage, were seen after 10 min; therefore, retention time was measured after incubating the drug on cartilage tissue for 10 min. The retention experiment results are shown in Figures 4-19 to 4-26).

Generally, retention of NSAIDs in cartilage decreased continuously as the incubation time increased, with a great majority of the drug being released from the cartilage within the first 60 min after uptake (Figures 4-19 to 4-26). As for the untreated and GAG depleted samples, release of Ind, Nap, Ket and DC in the P and E controls was quicker than in the POLY-A5 and POLY-B5 coated emulsion samples, as the drug was not detected after 2 hours in the control group. When POLY-A5 was utilised, the drugs were still detectable even after 3 hours. Overall, using POLY-A5 resulted in the amount of NSAIDs remaining in the tissue being the same in both untreated, and GAG depleted cartilage (Figures 4-19 to 4-22). Furthermore, the amount of Nap and Ket remaining in the tissue when delivered through emulsion-POLY-A5 was higher than for the P and E controls throughout, with the difference between the DDSs and the control groups being statistically significant ( $p < 0.05$ ).

In addition, coating NSAIDs emulsion with POLY-B5 showed a prolonged retention time of the drug compared to POLY-A5. Specifically, when, using untreated cartilage extract models, most of the Nap was released from the samples in around 8 hours, followed by Ind which was released in 7 hours, and finally DC and Ket which were retained in the cartilage for 3-4 hours (Figures 4-23 to 4-26). In contrast, when using GAG depleted cartilage models the retention time of Ket was prolonged to 7 hours compared to untreated cartilage samples but shortened to 3 hours using Ind and DC emulsions.

A)



B)

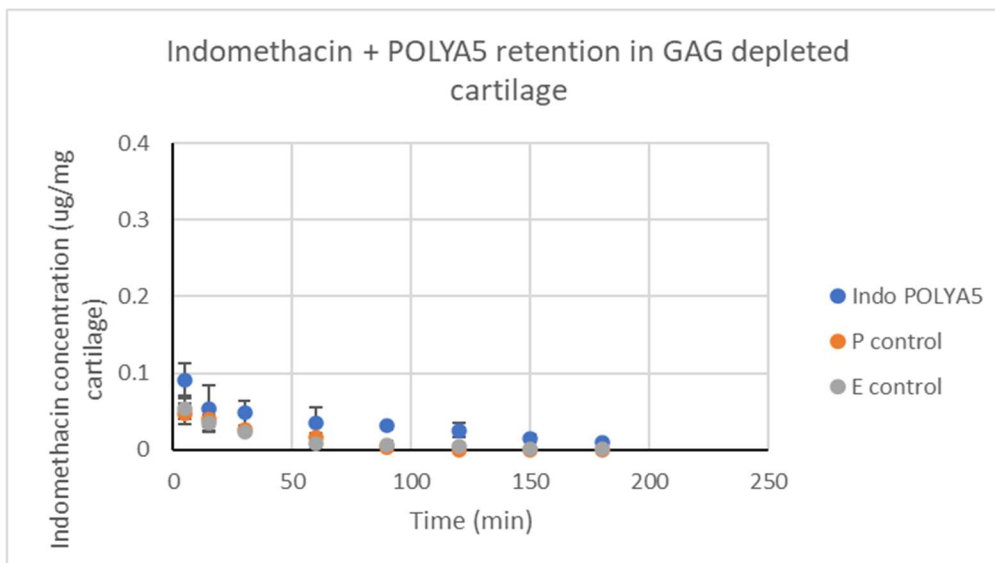
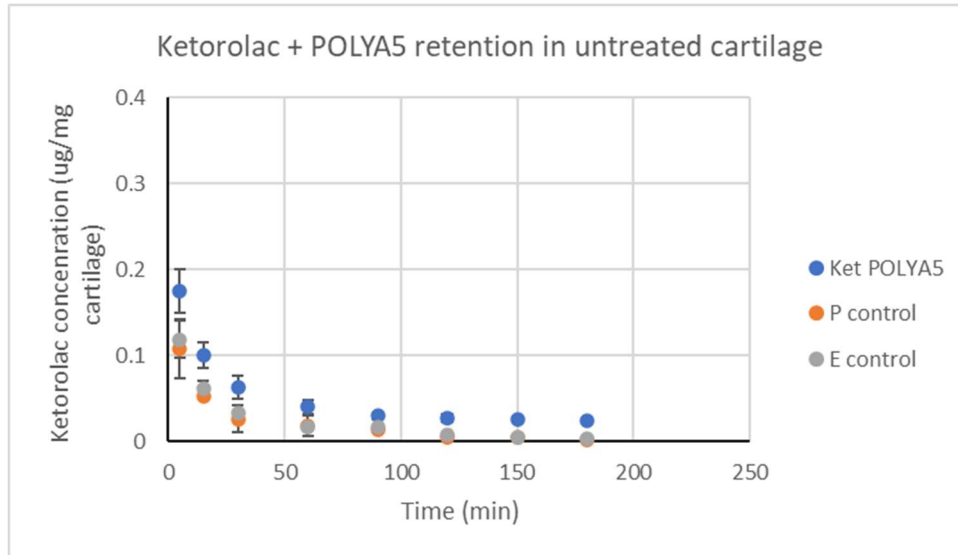


Figure 4-19 Comparison of indomethacin (Ind) retention into cartilage for 180 minutes (3 hours) using P control (Ind in PBS), E control (Ind emulsion) and Ind emulsion saturated with POLY-A5 in untreated (A) and GAG depleted cartilage (B). The concentration of Ind that has penetrated the cartilage is expressed in  $\mu\text{g}$  per mg cartilage. Ind retention time was prolonged using coated emulsion with POLY-A5 compared to the control in both untreated cartilage and GAG depleted cartilage.

A)



B)

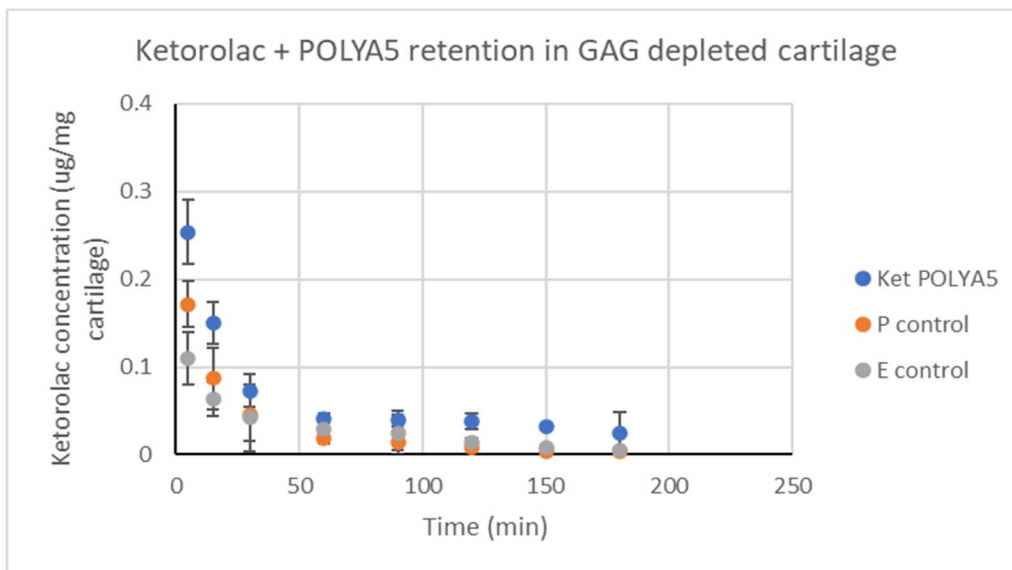
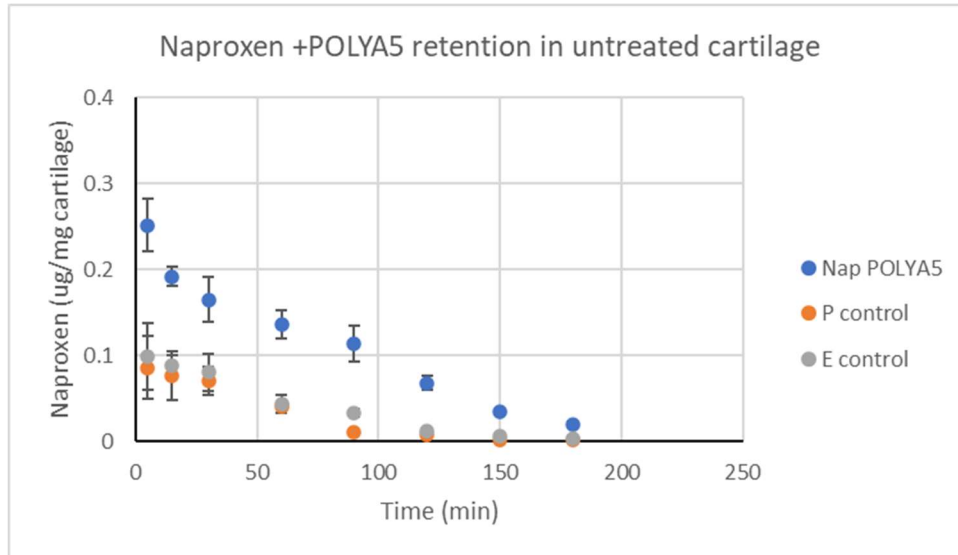


Figure 4-20 Comparison of ketorolac (Ket) retention into cartilage for 180 minutes (3 hours) using P control (Ket in PBS), E control (Ket emulsion) and Ket emulsion saturated with POLY-A5 in untreated (A) and GAG depleted cartilage (B). The concentration of Ket that has penetrated the cartilage is expressed in  $\mu\text{g}$  per mg cartilage. Ket retention time was prolonged using coated emulsion with POLY-A5 compared to the control in both untreated cartilage and GAG depleted cartilage.

A)



B)

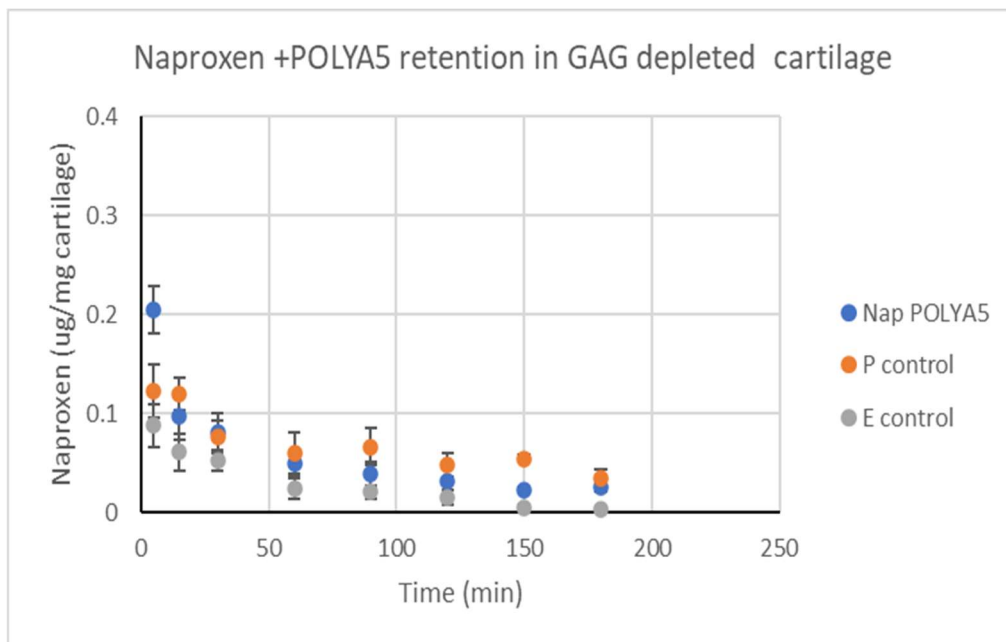
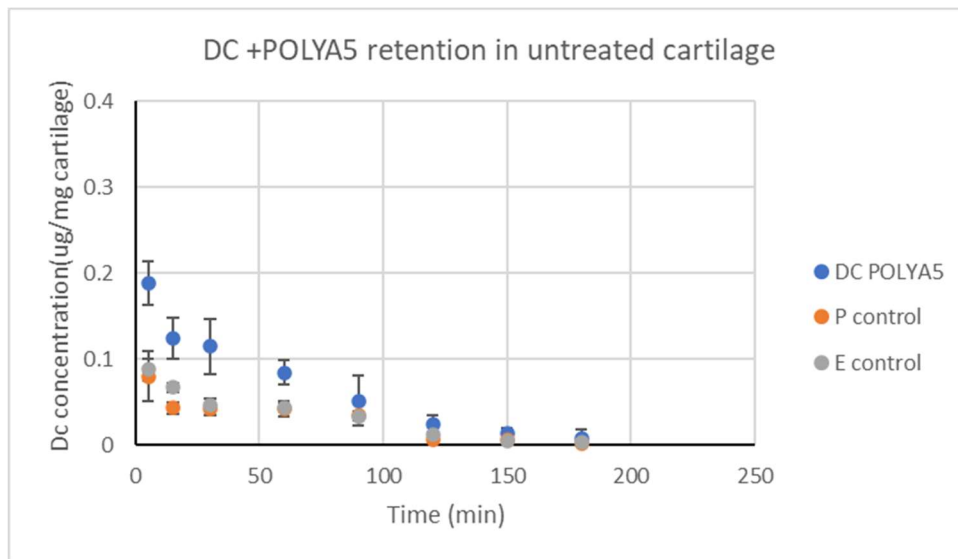


Figure 4-21 Comparison of naproxen (Nap) retention into cartilage for 180 minutes (3 hours) using P control (Nap in PBS), E control (Nap emulsion) and Nap emulsion saturated with POLY-A5 in untreated (A) and GAG depleted cartilage (B). The concentration of Nap that has penetrated the cartilage is expressed in  $\mu\text{g}$  per mg cartilage. Nap retention time was prolonged using coated emulsion with POLY-A5 compared to the control in untreated cartilage.

A)



B)

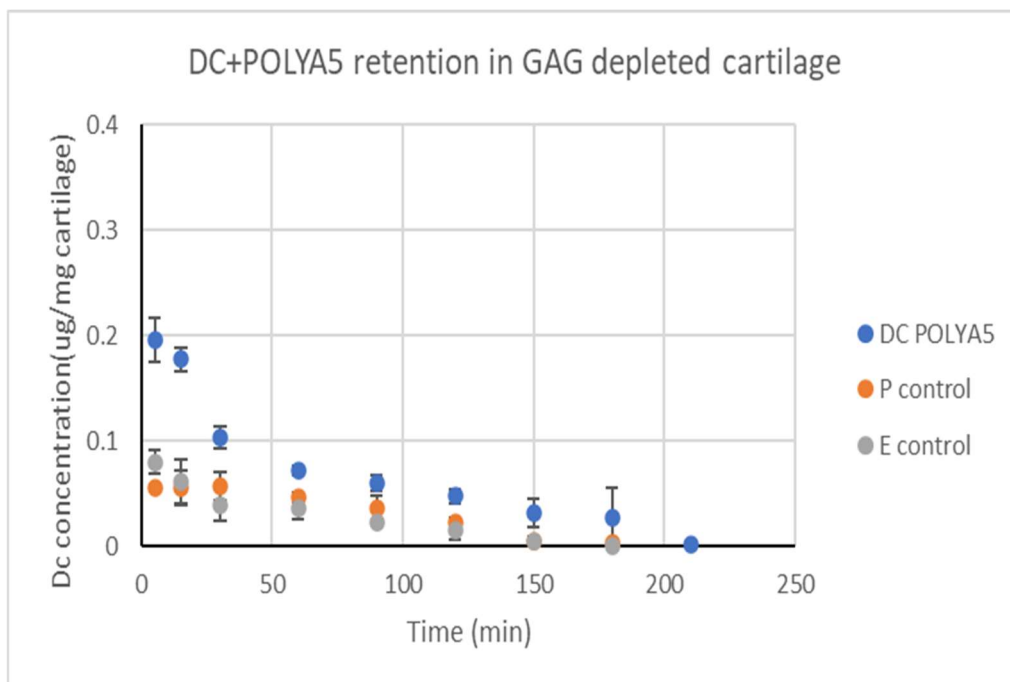
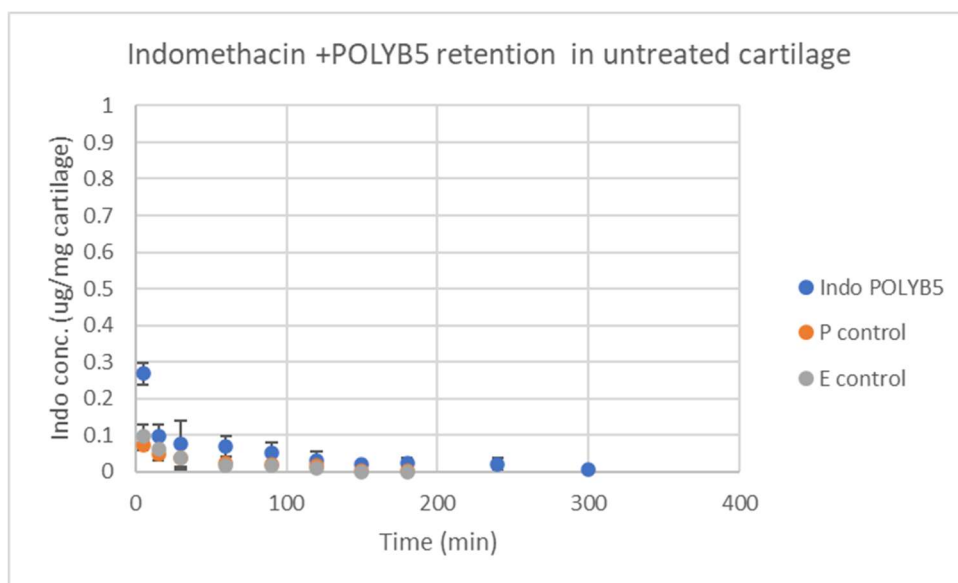


Figure 4-22 Comparison of diclofenac sodium (DC) retention into cartilage for 180 minutes (3 hours) using P control (DC in PBS), E control (DC emulsion) and DC emulsion saturated with POLY-A5 in untreated (A) and GAG depleted cartilage (B). The concentration of DC that has penetrated the cartilage is expressed in  $\mu\text{g}$  per mg cartilage. DC retention time was prolonged using coated emulsion with POLY-A5 compared to the control in both untreated cartilage and GAG depleted cartilage.

Overall, the NSAIDs emulsion coated with POLY-B5 had a prolonged retention time inside the cartilage tissue compared to the emulsion coated with POLY-A5. Ind and Nap retention duration in untreated cartilage and Ket retention duration in GAG depleted cartilage coated with POLY-B5 were two times longer than when coated with POLY-A5. In addition, DC emulsion retention lasted for 2 hours longer when coated with POLY-B5 rather than POLY-A5.

A)



B)

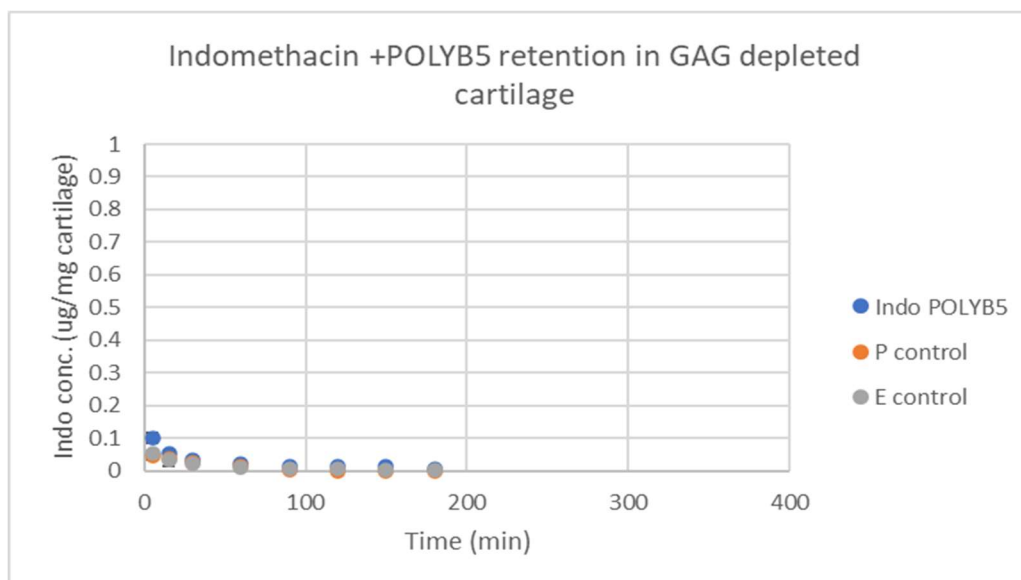
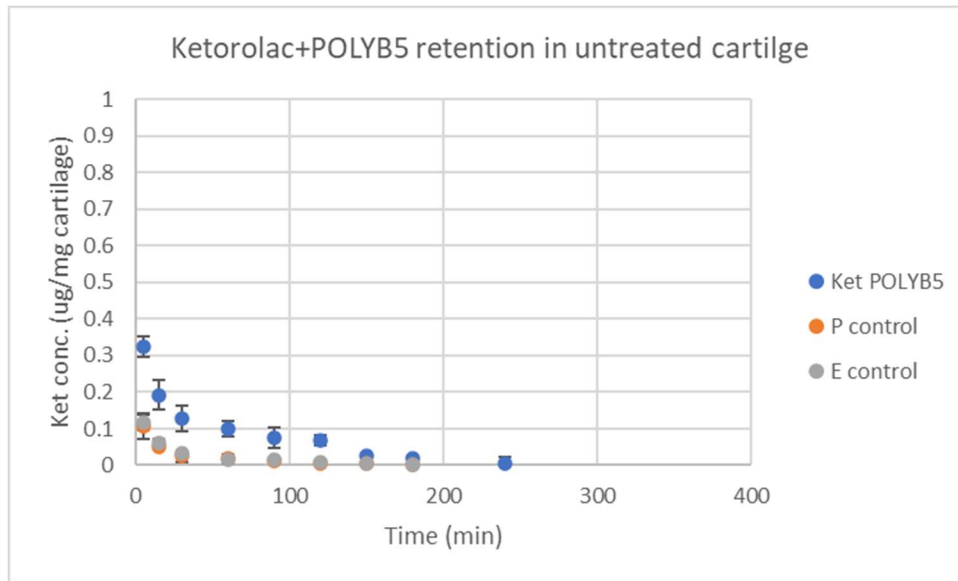


Figure 4-23 Comparison of indomethacin (Ind) retention into cartilage for 350 minutes (6 hours) using P control (Ind in PBS), E control (Ind emulsion) and Ind emulsion saturated with POLY-B5 in untreated (A) and GAG depleted cartilage (B). The concentration of Ind that has penetrated the cartilage is expressed in  $\mu\text{g}$  per mg cartilage. Ind retention time was prolonged using coated emulsion with POLY-B5 compared to the control in untreated cartilage.

A)



B)

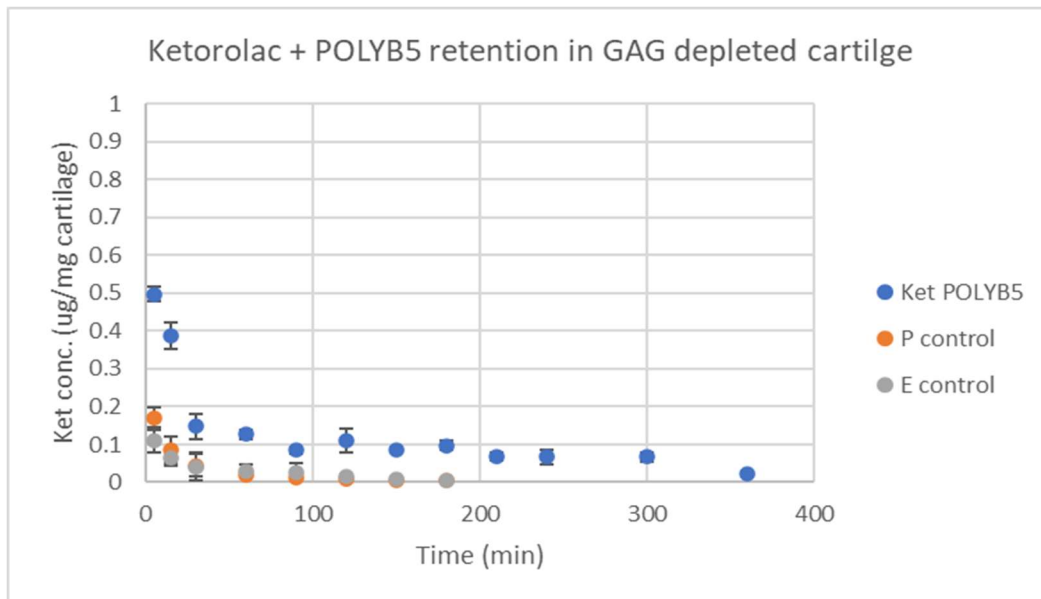
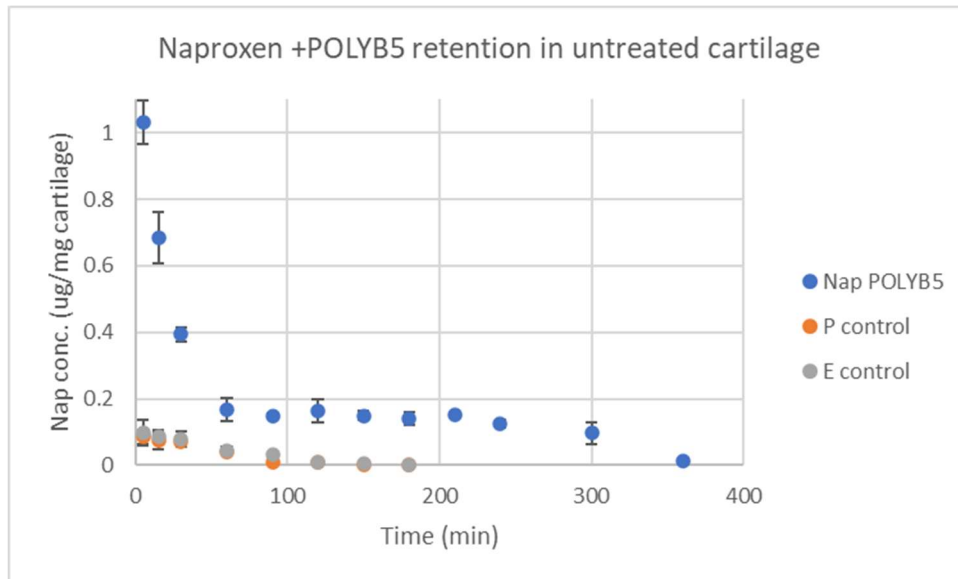


Figure 4-24 Comparison of ketorolac (Ket) retention into cartilage for 350 minutes (6 hours) using P control (Ket in PBS), E control (Ket emulsion) and Ind emulsion saturated with POLY-B5 in untreated (A) and GAG depleted cartilage (B). The concentration of Ket that has penetrated the cartilage is expressed in  $\mu\text{g}$  per mg cartilage. Ket retention time was prolonged using coated emulsion with POLY-B5 compared to the control in both untreated cartilage and GAG depleted cartilage.

A)



B)

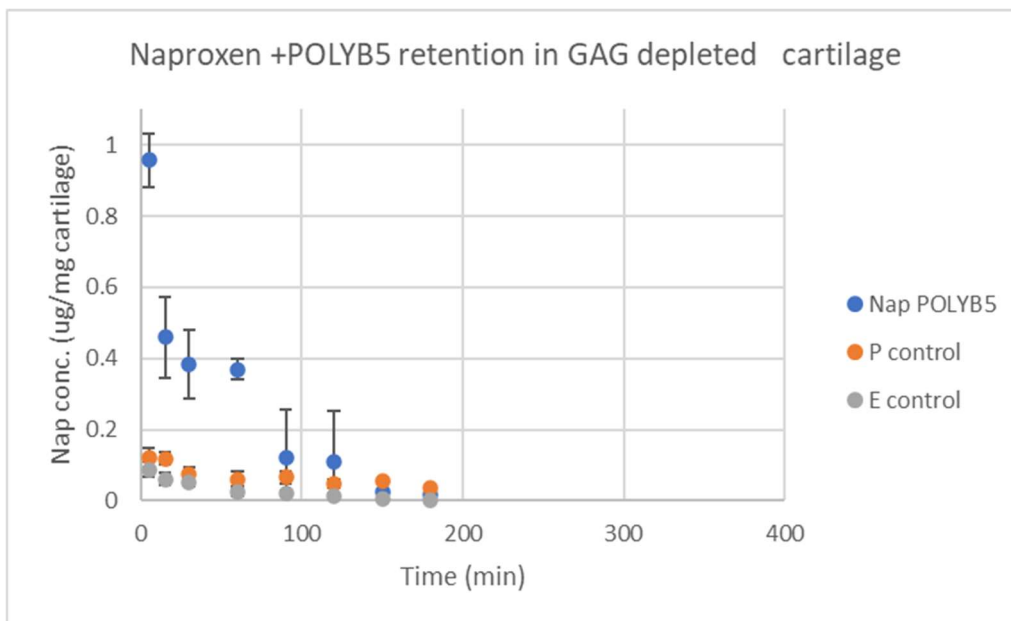
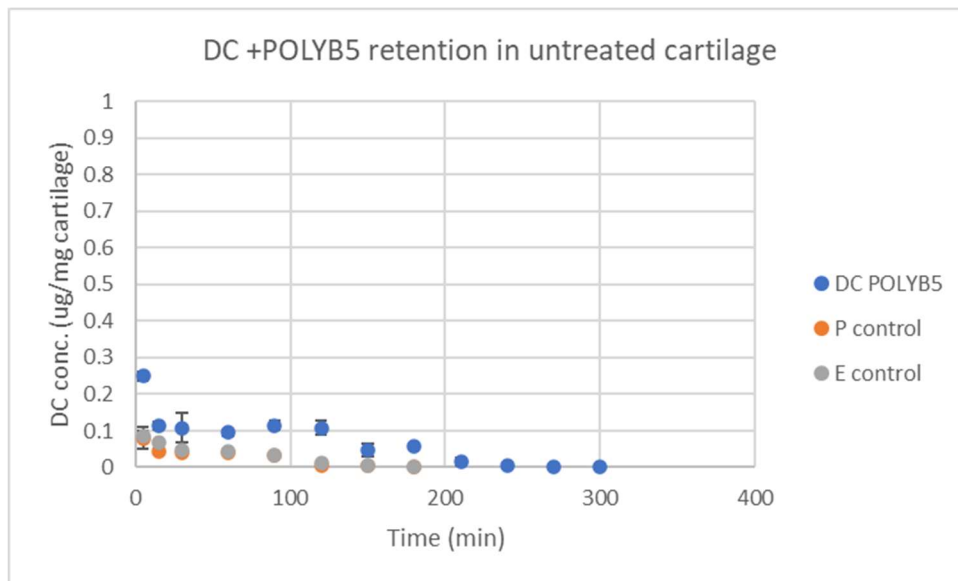


Figure 4-25 Comparison of naproxen (Nap) retention into cartilage for 350 minutes (6 hours) using P control (Nap in PBS), E control (Nap emulsion) and Nap emulsion saturated with POLY-B5 in untreated (A) and GAG depleted cartilage (B). The concentration of Nap that has penetrated the cartilage is expressed in  $\mu\text{g}$  per mg cartilage. Nap retention time was prolonged using coated emulsion with POLY-B5 compared to the control in untreated cartilage.

A)



B)

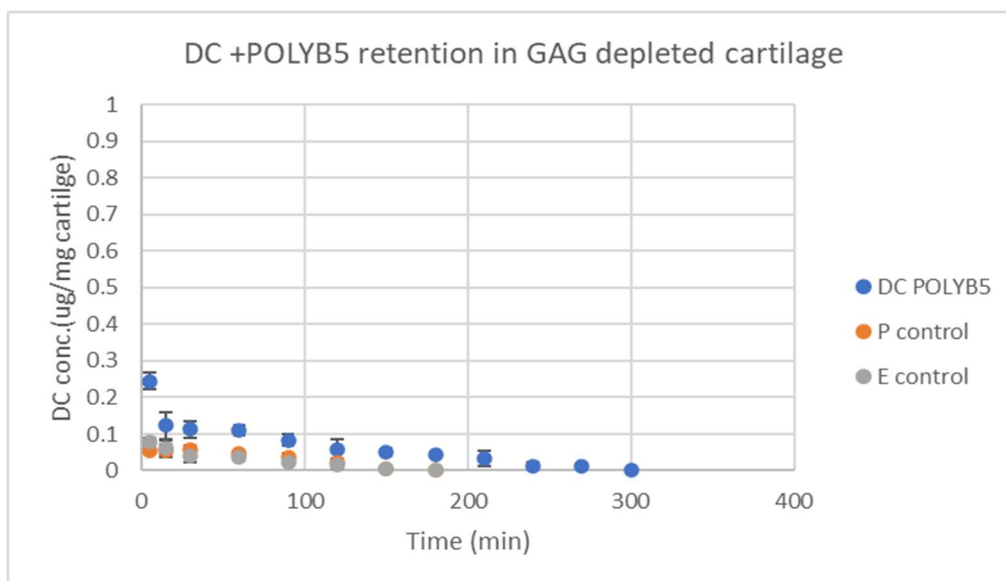


Figure 4-26 Comparison of diclofenac sodium (DC) retention into cartilage for 350 minutes (6 hours) using P control (DC in PBS), E control (DC emulsion) and Ind emulsion saturated with POLY-B5 in untreated (A) and GAG depleted cartilage (B). The concentration of DC that has penetrated the cartilage is expressed in  $\mu\text{g}$  per mg cartilage. DC retention time was prolonged using coated emulsion with POLY-B5 compared to the control in both untreated cartilage and GAG depleted cartilage.

To conclude, POLY-B5 had a higher positive charge (+18.7 mV) and size (0.29  $\mu\text{m}$ ) and it also retained NSAIDs for a longer time inside the cartilage tissue, around 6 hours, compared to POLY-A5 (+12.6 mV, 0.21  $\mu\text{m}$ ) which retained the drugs for only around 3 hours (Figures 4-19 to 4-26). However, using POLY-A5 helped to increase drug uptake more than POLY-B5. Therefore, according

to these results, it appears that charge and size are important parameters that affect NSAIDs penetration inside cartilage tissue.

#### 4.3.7. Emulsion diffusion through cartilage

Oil droplets were detectable inside chondrocyte cells, as both DAPI (tagging cells) and Nile red (tagging oil droplets) emissions overlapped in the images observed (Figure 4-27). Based on the findings, oil droplets containing Nile red were detected not only on the surface of the cartilage samples, but also at least 130  $\mu\text{m}$  deep after 1 min of incubation.

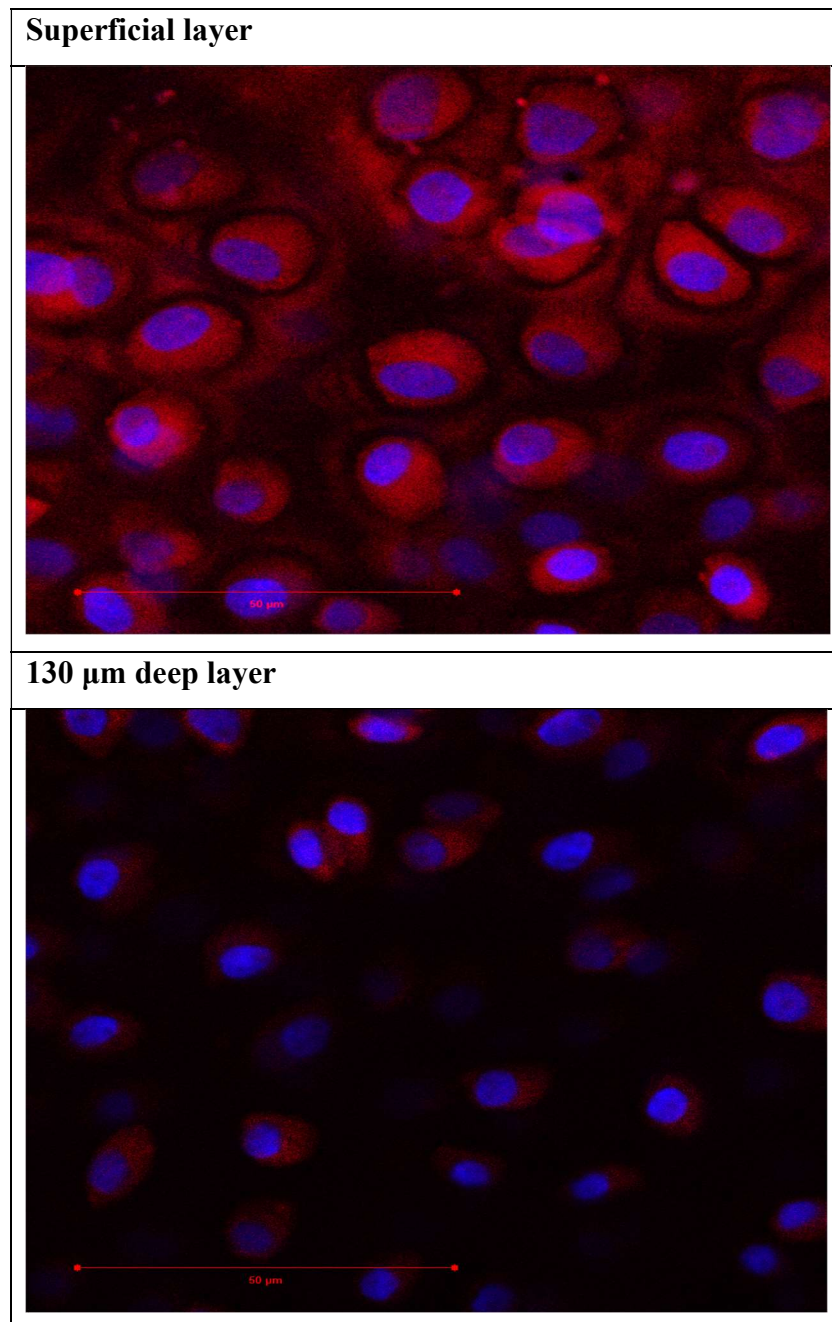


Figure 4-27. Examples of confocal images of Nile red fluorescently tagged oil emulsions (red) diffusion through cartilage chondrocyte cells countered stained with DAPI (blue). Nile red was dissolved into oleic acid to fluorescently tag the emulsions and confirm that the droplets diffuse through the cartilage tissue and not just adsorb onto the outer surface of the samples.

#### **4.4. Discussion:**

This chapter has been demonstrated that oleic acid-based o/w emulsion coated with POLY-A5 or POLY-B5 provides an effective delivery system for NSAIDs for OA treatment/management. This delivery system promotes uptake of NSAIDs and enable longer retention (6 hours) in cartilage tissue compared to P and E controls (2.5 hours); this is due to electrostatic attraction between the negatively charged GAG in the articular cartilage and the positively charged POLY-A5 or POLY-B5 polymer emulsion coating.

##### **4.4.1. Polymer degradation and mechanism of drug penetration inside cartilage tissue**

In this work, the degradation of PBAEs was studied at pH 5 and pH 7.4 using charge and MW degradation methods. Generally, a decrease in physiological pH from pH 7.4 to around pH 5 has been recorded on cartilage surfaces of OA patients (Bajpayee *et al.*, 2016). In OA, oxygen consumption is increased by inflammatory cells, such as synoviocytes, leading to a decrease in oxygen levels and reduced delivery of oxygen to synovial fluid due to joint capsule fibrosis and subchondral bone sclerosis (Collins *et al.*, 2013). Consequently, this oxygen deficiency causes changes in the physical environment through the release of inflammatory mediators and acidosis, which are likely to have important effects on chondrocyte function and cartilage integrity (Collins *et al.*, 2013).

Polyesters containing amine degrade more rapidly in basic solutions than in acidic solution (Chen *et al.*, 2007). Therefore, degradable polymers such as PBAEs are attractive materials for use in design of drug delivery systems as they provide favourable controlled drug release and degradation behaviour (Nazila *et al.*, 2016). Amine protonation in an acidic solution inhibits the intramolecular/intermolecular nucleophilic attack of amine to an ester, which causes a decrease in the degradation rate. Accordingly, the degradation rate of poly (beta-amino esters) is highly dependent on the pH of the solution, and the degradation rate increases in line with the pH value (Chen *et al.*, 2007). In fact, similar results have been published previously with it being demonstrated that PBAE degraded faster at pH7.4 than at pH 5.1 (Lynn and Langer, 2000). Moreover, another study found degradation kinetics of PBAEs to be dependent on the pH of the buffer. For example, the neutral buffer, was shown to be faster than the acidic buffer, with the half-lives lasting 48hours for pH 7, 14 days for pH 6 and 65 days for pH 5.

The movement of drug from coated oil droplets occurs by a combination of two extreme cases; the first is hydrolysis of the polymer, while the second is diffusion of the drug out of the emulsion throughout the matrix of cartilage tissue (Lynn and Langer, 2000; Kim, Sunshine and Green, 2014; Al Thaher *et al.*, 2018). In addition, the electrostatic interactions between PBAEs and cartilage protoglycan result in reversible binding of PBAEs within the tissue, thereby creating a drug reservoir

and providing sustained delivery to chondrocyte cells and ECM targets (Bajpayee and Grodzinsky, 2017; Karlsson *et al.*, 2021). They are then hydrolysed into biocompatible products that are alcohol and biologically inert derivatives of small molecular weight *b*-amino acids (For example, POLY-A5 degraded hydrolytically to yield 1,4-butanediol and *b*-amino acids), which are directly influenced by the medium pH (Figures 4-1 to 4-4). Indeed, pH level controls the polyelectrolyte level of protonation, which affects the electrostatic interactions between oppositely charged polymers and cartilage ECM, thus diffusing the drug through the tissue. The drug molecule may be more protonated and positively charged at a low pH, leading to stronger electrostatic interactions with the negatively charged cartilage ECM. Therefore, the drug diffuses through the tissue slowly and reaches its intended target gradually (Lynn and Langer, 2000; Kim, Sunshine and Green, 2014). On the other hand, at a high pH, the drug molecule may be less protonated and negatively charged, weakening the electrostatic interactions, and allowing the drug for faster diffusion through the tissue. Moreover, hydrolysis of PBAE inside the joint has been the only mechanism hypothesised, to date, for controlling drug release (Al Thaher *et al.*, 2018). Water molecules inside the joint can penetrate the PBAE polymer and break down the ester bonds, causing the polymer to break down into small fragments, which then releases the drug molecules inside the tissue. In this project, hydrolysis of PBAEs was compared at pH 5 (slow hydrolysis) simulate inflammation conditions and pH 7.4 (fast hydrolysis) simulate normal physiological conditions in order to test the validity of this hypothesis. The results confirm that PBAEs degradation occurs more slowly in acidic pH buffer than neutral pH buffer (Figures 4-1 to 4-4). Therefore, hydrolysis will be slower at the OA joint (acidic pH), allowing release of the drug in a controlled manner and decreasing its burst release in the cartilage tissue. Subsequently, diffusion of NSAIDs occurs throughout the cartilage thickness from the emulsion, resulting in painkilling and anti-inflammatory effects (Bajpayee and Grodzinsky, 2017). Overall, drug diffusion can be affected by drug solubility, droplet size, and charge. As mentioned above, solubility of NSAIDs was improved by forming emulsion droplets coated with PBAEs polymer. This created droplets with optimal sized to diffuse through the cartilage ECM and be retained for a longer duration than the uncoated drug (Figures 4-19 to 4-26). Moreover, the structure of PBAE polymer exhibited a positive charge to be able to form electrostatic interaction with cartilage GAG to improve drug uptake and diffuse inside the cartilage tissue (Figures 4-11 to 4-18).

#### **4.4.2. Size and charge effects**

Zeta potential (charge) and oil droplet sizes are mainly dependent on the drug being encapsulated in the oil phase. NSAIDs encapsulated within emulsion have a tendency to result in more negative ZP than pure oleic acid emulsion, due to the deprotonation of the carboxylic group at the oil/water interface (Saeedi and Prokopovich, 2021). Diclofenac showed more negative ZP which could be due to the positive charges of the secondary nitrogen present in its structure. The addition of

polyelectrolytes with positive charges (PBAEs) gradually saturated the negative charges present on the oil droplet surfaces and switched the ZP to a positive charge.

The characteristics of POLY-A5 and POLY-B5 were measured separately in acetate buffer (pH 5), as presented in Tables 4-1 & 4-2. They both exhibited positive charges (+12.6 mV for POLY-A5 and + 18.7 mV for POLY-B5), thus supporting the expectation that POLY-A5 and POLY-B5 are types of polycations that protonate amine ends (R-NH<sub>3</sub><sup>+</sup>) at appropriate pH levels and gain a positive charge (Perni and Prokopovich, 2017). The differences in zeta potential observed between POLY-A5 and POLY-B5 can be attributed to the different acrylates used in their polymeric chains because 1,4-butanediol diacrylate has MW 198.22 g/mol while 1,6-hexanediol diacrylate has MW 226.27 g/mol. In addition, coating the negatively charged NSAIDs o/w emulsion with POLY-A5 and POLY-B5 considerably changed their charges to positive (Figures 4-5&4-6 & Tables 4-1&4-2). Eventually, using the saturation method to fully coat NSAIDs with cationic POLY-A5 and POLY-B5 polymers represents an effective drug delivery strategy to accelerate drug penetration into the anionic cartilage and to augment retention time (Geiger, Grodzinsky and Hammond, 2018). Meanwhile, another study has suggested that the optimal volume of polycation is when the drug's nano capsule/emulsion ZP value is approximately equal to the free-floating polymers measured separately in the solution (Adamczak *et al.*, 2012). Nonetheless, as discussed previously, saturation was recorded in this study when the charges plateaued (i.e., little or no changes in charge occurred). This means that complete saturation of emulsion droplets with the polymers was achieved, thereby predicting the correct polymer volumes required for completely coating the emulsion (Szczepanowicz *et al.*, 2010). Emulsion oversaturation can cause the polymers to enter the cartilage and block the entry of the drug from the oil droplets; for that reason, ZP measurements were necessary to determine the optimal polymer volume per emulsion.

In fact, the mean diameter of individual synovium capillaries is up to 0.03 µm maximum (Haywood and Walsh, 2001). It is known that small particle sizes can easily be phagocytised by synoviocytes and /or cleared quickly from joints (Janssen *et al.*, 2014; Geiger, Grodzinsky and Hammond, 2018). Therefore, particle size dramatically affects the ability of the drug to penetrate and be retained inside the joint. As mentioned above, the size of POLY-A5 was 0.21 µm, with POLY-B5 being 0.29 µm; this indicates that these polymers were relatively large in term of particle size and had considerable uptake and retention performance. Similarly, Perni and Prokopovich (2017) have found that larger polymers (0.29 µm) result in preferable uptake and retention in joints than smaller ones (0.15 µm). In addition, particle size is an important factor in intra-articular drug delivery. According to Dong *et al.* (2013) the larger the particle sizes the greater the retention of the drug at the injection site; in their

study, liposome with a diameter of (4.98  $\mu\text{m}$ ) were considered to be optimal for intra-articular delivery.

Varying droplet sizes of DDSs result in different cartilage drug uptake levels and different retention and release kinetics (Janssen *et al.*, 2014). In the present study, coated NSAIDs o/w emulsion led to an increase in drug size (Figure 4-9). Maeda *et al.* (1994) report that the optimal molecular size for DDSs is 40 kDa or larger, so as promote both penetration and retention effects. When looking at NSAIDs' molecular masses (MW) we can see that these are very small; for example, naproxen's molecular mass is 252.25 g/mol or 0.2522 kDa, while indomethacin's is 357.8g/mol or 0.3578 kDa (Takada *et al.*, 2004). Therefore, increasing the particle sizes of small molecule drugs such as NSAIDs through coating with a polymer or encapsulating with oil should allow retention in the tissue for longer durations (Janssen *et al.*, 2014). The reason for this variance in particle sizes between drugs could be due to differences in electrostatic forces of attraction between the oil droplets and polymers, making the particles to move closer together and interact in different ways and thus leading to differences in size. Such larger positive sized particles can be used for drug delivery as they bind with cartilage proteoglycans, after which the polymer becomes gradually degraded allowing release of the drug, which could then be diffused within the cartilage over time (Bajpayee *et al.*, 2016). Accordingly, encapsulating small molecular sized NSAIDs with POLY-A5 or POLY-B5 leads to a large increase in drug particle sizes, offering an optimal drug delivery system to enhance both penetration and retention effects.

#### **4.4.3. Stability of emulsion droplets**

In the present work, calculating ZP of different emulsions, measuring their size distributions, and visually observing them were important steps which assisted in anticipating possible instabilities. The results suggest that PBAEs could stabilise emulsion structure, with the stability of the emulsion decreasing with decreasing particle sizes over 14 days. In addition, a rapid decrease in emulsion charges also accelerated emulsion instability (Figures 4-8&4-9). Stability of visual appearance declined with decreased particle sizes and reduced zeta potential (Figure 4-10). Ket emulsion coated with PBAEs showed a gradual decrease in ZP charges due to polymer hydrolysis properties, which is compatible with the hydrolysis results in Figure 4-2, which show a constant decrease in polymer charges due to polymer degradation at pH 5 and pH 7.4. Generally, it has been demonstrated that polyelectrolyte (such as PBAEs) stabilised emulsions are important in the field of nanomedicine and, in order to function properly, any drug delivery system must be biocompatible and biodegradable (De Geest *et al.*, 2009). PBAE polymers fulfil these requirements ( it is a known type of biocompatible and biodegradable polycation polymer), and thus can be used as capsules with emulsion inside. Oil in water emulsions is currently used as safe solvents for vaccines, which use polyelectrolytes to

stabilise emulsions and increase shelf life of vaccines (Saleh et al., 2005). Furthermore, PBAE polymers can help to reduce surface tension between the two immiscible phases and form protective layers around the oil droplets that are suspended in the water phase. Therefore, droplets are prevented from coalescing and causing emulsion breakage (Saleh et al., 2005). Moreover, if the entire surface of each of the oil droplets is coated or covered by emulsifier, the emulsion will be stable (Saleh et al., 2005). The advantage of using PBAEs is that they can coat emulsion droplets completely and behave as an emulsifier to decrease emulsion destabilisation as it leads to prolonged emulsion stability compared to uncoated emulsion with PBAEs (Figure 4-10). This has been done by ZP, firstly, the coating steps has been created, then complete saturation of emulsion droplets with the polymer was achieved and finally, predicted the volume of polymer required for coating the emulsion completely (as discussed earlier in this chapter). The size of the droplets in the emulsion, also known as the droplet size distribution, plays a crucial role in determining the stability of the emulsion. As described above, in this study it was observed decrease in droplet size and the broadening of the droplet size distribution over time which are indicative of a decrease in emulsion stability. One possible mechanism for decreasing droplet size is creaming. This is a process whereby two or more droplets come into contact and merge to form a larger droplet that moves upwards, causing oil and water phase separation. This can lead to a decrease in the number of droplets present in the emulsion and an overall decrease in average droplet size. However, this process was delayed by using PBAE polymers which prolonged emulsion stability. Overall, the results of this experiment demonstrate that a decrease in droplet size over time can lead to emulsion instability (Figure 4-9). This instability is likely caused by a combination with a decrease in the zeta potential of the droplets. These findings highlight the importance of maintaining narrow droplet size distribution and high zeta potential to ensure the stability of o/w emulsions and demonstrate that using PBAEs can improve emulsion stability. However, one of this study's limitations is that emulsion stability needs to be further improved in the future. As a result, non-ionic surfactants can provide enhanced stability, for example, polysorbates (such as Tween 20 and Tween 80) (Tadros, 2004; Szczepanowicz *et al.*, 2010; Kahar *et al.*, 2021). Furthermore, cationic surfactants can be used as an emulsifier to increase emulsion stability. These include cetyltrimethylammonium bromide (CTAB) and hexadecyl pyridinium chloride (HPC). Oil-in-water emulsions can also be stabilized using anionic surfactants such as sodium dodecyl sulfate (SDS), sodium lauryl sulfate (SLS), and sodium oleate (Tadros, 2004; Szczepanowicz *et al.*, 2010; Kahar *et al.*, 2021).

#### **4.4.4. Untreated and GAG depleted cartilage uptake and retention**

The early degeneration of articular cartilage in OA is due to a decrease in GAG content from the matrix. In order to mimic this early stage of OA, cartilage explants from bovine joints were digested with trypsin dissolved in PBS. PBS pH is optimal for the enzyme function, which was reduced by

around 50 % of GAG content in the cartilage sample (Yoo *et al.*, 2011; Perni and Prokopovich, 2017) (Yoo *et al.*, 2011; Perni and Prokopovich, 2017). Bajpayee *et al.* (2016) conducted a study using chondroitinase ABC enzyme to directly reduce GAG content in aggrecan. The DDSs presented in this work are dependent mainly on electrostatic interaction between positively charged POLY-A5, or POLY-B5 and negatively charged GAGs to increase uptake and retention of the drug inside the cartilage (Perni and Prokopovich, 2017). Therefore, it was expected that there would be a decrease in the efficiency of the DDSs in the GAG depleted cartilage; the results of this study clearly show such outcome, especially with regards to Ind, Nap and DC (Figures 4-11 to 4-18). Similarly, A1 and A2 uptakes were significantly higher in untreated cartilage than in GAG depleted cartilage (Perni and Prokopovich, 2017). On the other hand, drug uptake was higher in GAG depleted cartilage in the case of Ket; this could mainly be due to GAG depleted matrices displaying higher hydraulic permeability than normal matrices, accordingly, allowing improved flow of drug delivery systems towards them (Nia *et al.*, 2015; Saeedi and Prokopovich, 2021). Similarly, Elsaid *et al.* (2013) found that GAG depleted cartilage enhances drug-loaded micelle uptake into the tissue. Furthermore, another study identified a higher uptake of dexamethasone (a drug of choice in intra-articular injection for OA treatment) in GAG depleted cartilages than untreated cartilage (Elsaid *et al.*, 2013; Perni and Prokopovich, 2017). That being said, the prepared DDS seemed to be effective as there was an uptake in cartilage even when using GAG depleted cartilage from the matrix. In addition, reducing the amount of GAG in the sample did not prevent the uptake of the drug into the cartilage. Moreover, drug uptake was significantly higher ( $p < 0.01$ ) in NSAIDs emulsion coated with POLY-A5 or POLY-B5 than in any type of control. Accordingly, it can assertively be stated that these two polymers were effective not only in untreated cartilage but also in GAG depleted cartilage.

In addition, to validate the effectiveness of the newly developed drug delivery system in penetrating deep into the cartilage tissue, Nile red was dissolved in oleic acid and used to confirm that the droplets could diffuse through the cartilage tissue and not adhere to the outer surface of the samples (Figure 4-27). Nile red has been extensively used to label lipid droplets in research applications, particularly cell biology and biochemistry (Kurtz and Lawson, 2019). In addition, Nile red has been used to study lipid metabolism, lipid droplet release and distribution, lipid-related diseases such as obesity and atherosclerosis and lipid-based drug delivery formulations (Rumin *et al.*, 2015; Kurtz and Lawson, 2019). In the diffusion experiments, Nile red penetrated the cartilage tissue down to a depth of 130 $\mu$ m in 1 min, which confirms the ability of the DDS to diffuse inside the cartilage tissue. Indeed, after uptake of the drug in cartilage tissue via the developed DDS, it diffused deeply through the cartilage ECM where it was retained (for around 4-6 hours as in Figure 4-20 & 4-24) to produce the required anti-inflammatory and pain relief effects.

In addition to the drug uptake, drug retention determines the therapeutic range with which a drug concentration is above the minimum required to deliver its biological effects (Soussan *et al.*, 2009). As the same factors affecting drug uptake also control retention, it was expected that the emulsions coated with PBAEs would not only enhance drug localisation but also prevent release (Saeedi and Prokopovich, 2021). In addition, a drug's half-life in joints is around a few hours; therefore, treatment efficacy is related to that washout time (Perni and Prokopovich, 2017; Geiger, Grodzinsky and Hammond, 2018). Increasing drug retention duration is integral to providing effective DDSs (Soussan *et al.*, 2009). This study has shown that the vast majority of NSAIDs coated with POLY-A5 were still detected in the cartilage samples even after 3 hours of incubation in PBS for both untreated and GAG depleted cartilage, while the drugs coated with POLY-B5 were detected in the tissue for more than 8 hours (Figures 4-19 to 4-26). On the other hand, the drug washed out of the cartilage samples after only 2 hours in the cases of the P and E control groups. The results of this study also highlight the likely impact of polymer structure, as POLY-A5 exhibited lower retention performance and greater drug uptake in cartilage tissue despite being smaller than POLY-B5 (Figures 4-19 to 4-26).

Generally, the decline in retention can be explained as follows: firstly, the NSAIDs o/w emulsion penetrated the superficial zone of the cartilage from the oil drops and dispersed across the whole cartilage tissue depth until exiting the deep zone and then returning to the 96 well plates; and secondly, cartilage samples were incubated for different time intervals in PBS, where more drug particles naturally diffused from the cartilage into the PBS as duration increased (Tonge, 2018). To summarise, this work has provided an overview of an effective (candidate) drug delivery system that is necessary for OA treatment. Using NSAIDs as model drugs, PBAEs constitute effective drug delivery system for cartilage based upon the electrostatic attraction between GAGs and PBAEs. PBAEs could provide a useful delivery system for the localisation of drugs in cartilage through higher uptake and longer retention.

## **4.5. Conclusion**

This study has proven that NSAIDs and oleic acid-based o/w emulsion coated with POLY-A5 or POLY-B5 could potentially provide an effective delivery system for OA drugs due to the electrostatic forces of attraction between the negatively charged GAGs in articular cartilage and the positively charged POLY-A5 and POLY-B5 polymer emulsion coating. The aim of this work was to develop a practical and novel DDS that targets OA; this goal has been achieved as it has been demonstrated that the DDS is functional because there is proof of uptake of NSAIDs in both untreated and GAG-depleted cartilage (mimicking early stages of OA) from bovine joints. With an appropriate combination of NSAIDs o/w emulsion and POLY-A5 or POLY-B5, it is expected that a polymer saturated emulsion-based therapy could be used for OA patients in order to raise both drug uptake

and retention in cartilage, and thus it could be used for specifically targeted drug delivery. Moreover, the stability of o/w emulsion was improved by coating it with PBAEs. The results showed that adding PBAEs prolonged the emulsion's stability, as evidenced by a decrease in droplet size and no phase separation over seven days. These findings have important implications for developing emulsion formulations as drug delivery systems. A future study may explore the optimal conditions for enhancing emulsion stability and investigate the mechanisms underlying the stabilizing effects of the PBAE, as well as add an emulsifier to optimize emulsion stability and reduce the possibility of emulsion instability. Overall, this study highlights the potential of PBAEs as a promising candidate for improving emulsion system stability. A successful DDS would not only reduce the risks associated with repeated intra-articular injections but would also decrease the costs associated with conventional OA therapies.

## 5. Chapter 5: Assessing POLY-A5 coated ketorolac emulsion as drug delivery for post-traumatic osteoarthritis (PTOA)

### 5.1. Introduction:

PTOA develops after direct joint injury or trauma, and is responsible for about 12% of all osteoarthritis cases (Furman *et al.*, 2014; Kar *et al.*, 2016). Levels of pro-inflammatory cytokines, such as interleukin 1 $\alpha$  (IL-1 $\alpha$ ) and tumour necrosis factor alpha (TNF- $\alpha$ ), are elevated in synovial fluid following joint injury, which can diffuse into cartilage and rapidly induce proteolysis and loss of cartilage matrix, leading to OA (Kapoor *et al.*, 2011; Furman *et al.*, 2014; Kar *et al.*, 2016; Punzi *et al.*, 2016). IL-1 $\alpha$  plays a crucial role in the acute inflammatory stage of joint injuries and PTOA production (Furman *et al.*, 2014). Therefore, it is important to intervene early to inhibit the effects of inflammatory cytokines in inducing PTOA following joint injury, in order to prevent OA development in the injured region. PTOA in vivo and ex vivo models have been developed to study the effects of drugs in PTOA treatment. Ex vivo models are developed either by mechanically induced pressure to create cartilage injury when the cartilage is attached to subchondral bone, or by treatment with high doses of pro-inflammatory cytokines as levels are elevated immediately after injury (Bajpayee *et al.*, 2014; Grodzinsky *et al.*, 2017). Generally, an ex vivo model (such as bovine ex-vivo cartilage model) uses normal intact joints from animals to mimic joint injuries and study the effects of drugs in OA treatment. On the other hand, in vivo models using live animals are essential to understanding the development of PTOA and assessing treatment effectiveness. Different animals can be used as in vivo models, such as mice, rats, rabbits, cats, dogs, guinea pigs, sheep, goats, and pigs (Kuyinu *et al.*, 2016; Punzi *et al.*, 2016). PTOA is induced by surgical intervention or by causing a physical trauma directly to the joint. The rapid induction of OA using in vivo animal models ensures that studies can be undertaken in a short period of time (Kuyinu *et al.*, 2016; Punzi *et al.*, 2016).

In this chapter, an ex vivo PTOA bovine cartilage model was used to study the efficacy of the developed drug delivery system. Bovine cartilage extract was cultured in an appropriate medium to be able to be assessed and tested using the DDS. Cartilage tissue must be maintained in the appropriate physiological environment with an adequate oxygen and nutrient exchange system, with a requirement to harvest replicate samples at given time intervals for analysis. The release of sGAG and collagen into a conditioned medium was used to assess articular cartilage explant cultures and to detect/quantify tissue degradation in the present study. DMMB and hydroxyproline assays were used to detect sGAG and collagen levels (as discussed in chapter 3).

## **Aim and objective of chapter 5:**

The aim and objective of this chapter are

- 1) Develop a drug delivery system (DDS) consisting of ketorolac (as a model NSAIDs) emulsion coated with POLY-A5. Based on the results of the NSAIDs testing in chapter four, ketorolac was selected as a model NSAID as it exhibits higher uptake and longer retention period compared to other NSAIDs as well as P and E controls (Figure 4-16 & 4-24).
- 2) Test the hypothesis that the developed DDS can alleviate the catabolic effects in IL-1 $\alpha$  treated cartilage relevant to PTOA using an ex vivo bovine model.

## **5.2. Materials and methods:**

Details of the assay are provided in chapter 2.

## **5.3. Results**

### **5.3.1. Glycosaminoglycan (GAG) loss measurement**

To test the efficacy of the developed drug delivery system in inhibiting IL-1 $\alpha$  induced GAG loss in bovine cartilage, sulphated glycosaminoglycans (sGAG) were quantified using the DMMB assay. DMMB assay is used mainly to estimate the amount of proteoglycan by measuring sGAG in the samples (Warren, 2000). Cartilage explants were treated for 2-3 weeks with Ket emulsion coated with POLY-A5 with/without IL-1 $\alpha$  and different types of controls (as mentioned previously in chapter 2, section 2.6.3.).

The loss of sGAG from the IL-1 $\alpha$  treated cartilage was twice as fast as the controls during the first week of incubation (Figure 5-1). During the period of 24-96 hours, there was a 50 % decrease in sGAG content compared to the controls which reached 60% after 1 week of culture. After that, sGAG loss slightly increased by around 5% to reach 65% at the end of the incubation period (14 days), but the loss was still significantly higher than the controls ( $p < 0.01$ ). Overall, treatment of cartilage extract with IL-1 $\alpha$  caused a significant sGAG loss to the media ( $66.5 \pm 3\%$ ) by day 14 compared to the controls ( $25.4 \pm 3\%$  to  $45.1 \pm 0.12\%$ ) ( $p < 0.01$ ) (figure 5-1). The percentage of sGAG loss was 3 to 5 times higher in IL-1 $\alpha$  treated cartilage compared to the untreated group (in media only).

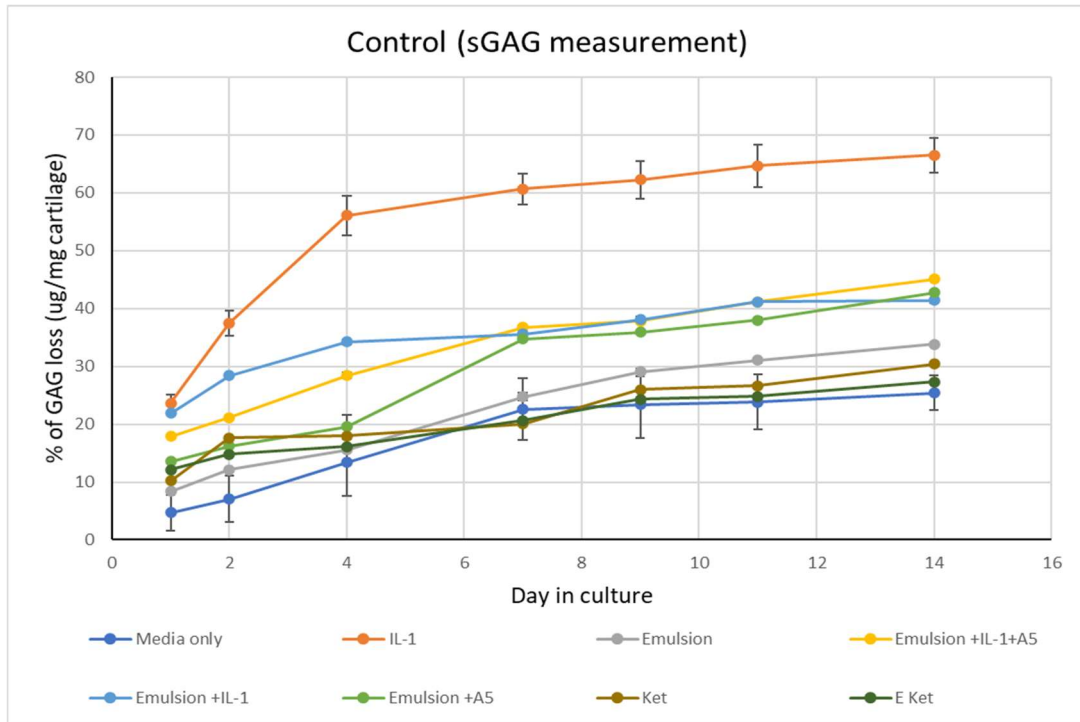
Moreover, when IL-1 $\alpha$  treated, cartilage was exposed to o/w emulsion with/without Ket it led to a remarkably decreased percentage (around 30%) of sGAG loss ( $p < 0.01$ ) compared to the IL-1 $\alpha$  treated group. Using o/w emulsion containing oleic acid (monounsaturated fatty acid) slowed the loss of sGAG, which was significantly different from the loss of sGAG in IL-1 $\alpha$  treated cartilage ( $p < 0.01$ ). Moreover, during the first 24 hours, an approximately equal percentage of sGAG loss was

observed in IL-1 $\alpha$  exposed cartilage with/without emulsion, which was equivalent to 23.6% and 21.8% in IL-1 $\alpha$  and emulsion + IL-1 $\alpha$  treated cartilage, respectively. Then, after 48 hours, sGAG loss was rescued by the anti-inflammatory effects of oleic acid (Sales-Campos et al., 2013; Loef et al., 2019) and decreased significantly more than the IL-1 $\alpha$  treated cartilage ( $p < 0.01$ ). In addition, the same effect of decreasing sGAG loss was found when POLY-A5 was used to coat the emulsion (Figure 5-1 A). Similarly, a study by Bastiaansen-Jenniskens *et al.* (2013) assessed the impact of oleic acid in decreasing the amount of sGAG loss in cartilage explants treated with TNF $\alpha$  and concluded that oleic acid seems to be effective in inhibiting cartilage destruction and inflammation as it lowered sGAG released compared to the control with TNF $\alpha$  alone ( $P = 0.03$ ).

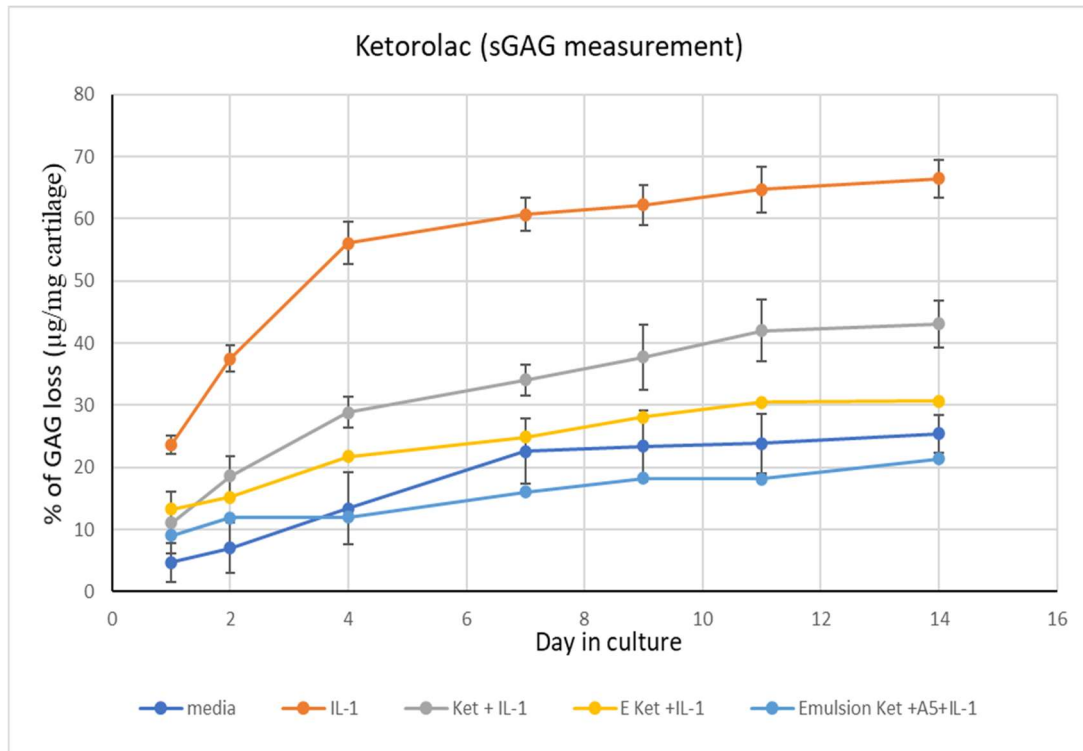
On the other hand, Ket emulsion coated with POLY-A5 (the developed DDS) inhibited sGAG loss even more significantly ( $p < 0.001$ ) than the IL-1 $\alpha$  for up to 14 days. Most of the sGAG loss occurred during the first week of the cartilage culture with the developed drug delivery system, which reached 16% before gradually increasing up to 2 weeks. The loss of sGAG using the developed drug delivery system was comparable with the untreated control, lower than the other control types, and significantly lower than IL-1 $\alpha$  treated cartilage ( $p < 0.001$ ) (Figures 5-1A & 5-1 B). Therefore, Ket emulsion coated with POLY-A5 was efficient in suppressing IL-1 $\alpha$  induced sGAG loss from cartilage.

In addition, dexamethasone (Dex) results show that Dex emulsion coated with POLY-A5 suppressed sGAG loss to the same extent as untreated cartilage, and to a significantly lower extent than IL-1 $\alpha$  treated cartilage ( $p < 0.001$ ) (Figure 5-1 C). Moreover, the developed DDS (Ket emulsion coated with POLY-A5) exhibited the same manner of inhibited sGAG loss as Dex. It is thus clear that coating Ket emulsion with POLY-A5 is an effective method of overcoming the catabolic effect of IL-1 $\alpha$  as an inflammatory cytokine on OA cartilage.

A)



B)



C)

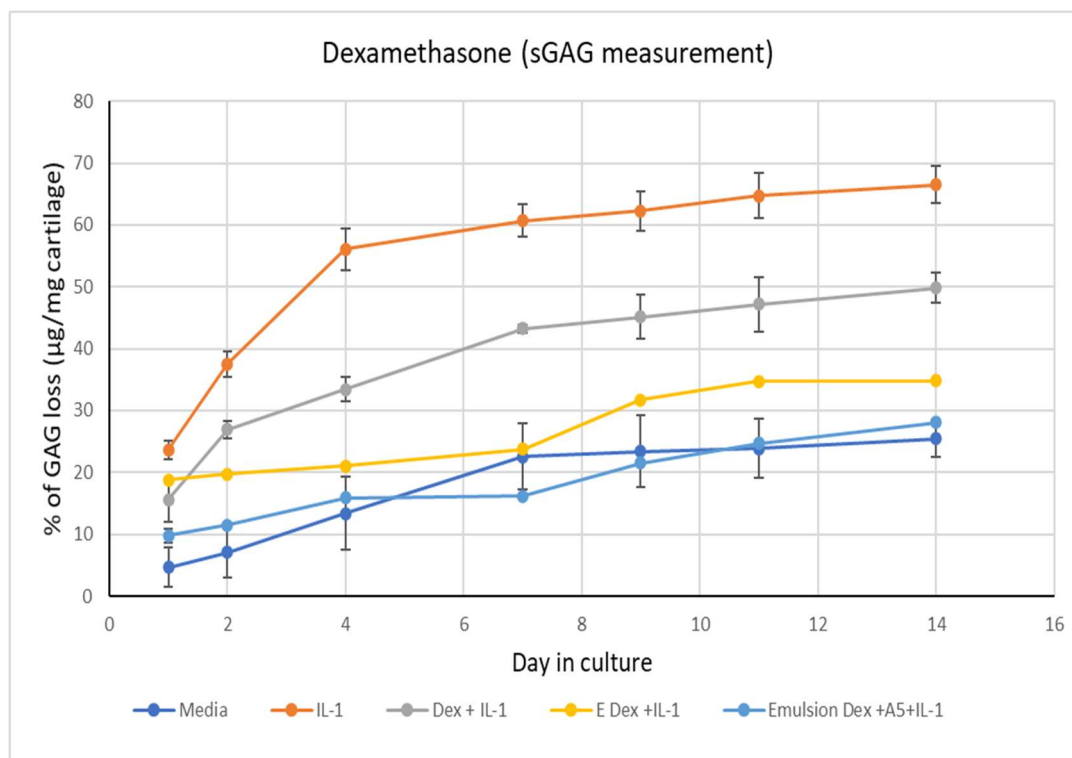


Figure 5-1. Quantification of sGAG in IL-1 $\alpha$  (1 ng/mL) treated cartilage using DMMB assay. Using main samples (untreated (media only) and IL-1  $\alpha$  treated samples) and different types of control (A), Ket emulsion coated with/without POLY-A5(B) and Dex emulsion coated with/without POLY-A5(C), the figures were separated for clarity. The loss of sGAG using Ket and Dex emulsion coated with POLY-A5 was comparable with the untreated control, lower than the other control types and significantly less than IL-1 $\alpha$  treated cartilage ( $p < 0.001$ ).

### 5.3.2. Collagen content determination

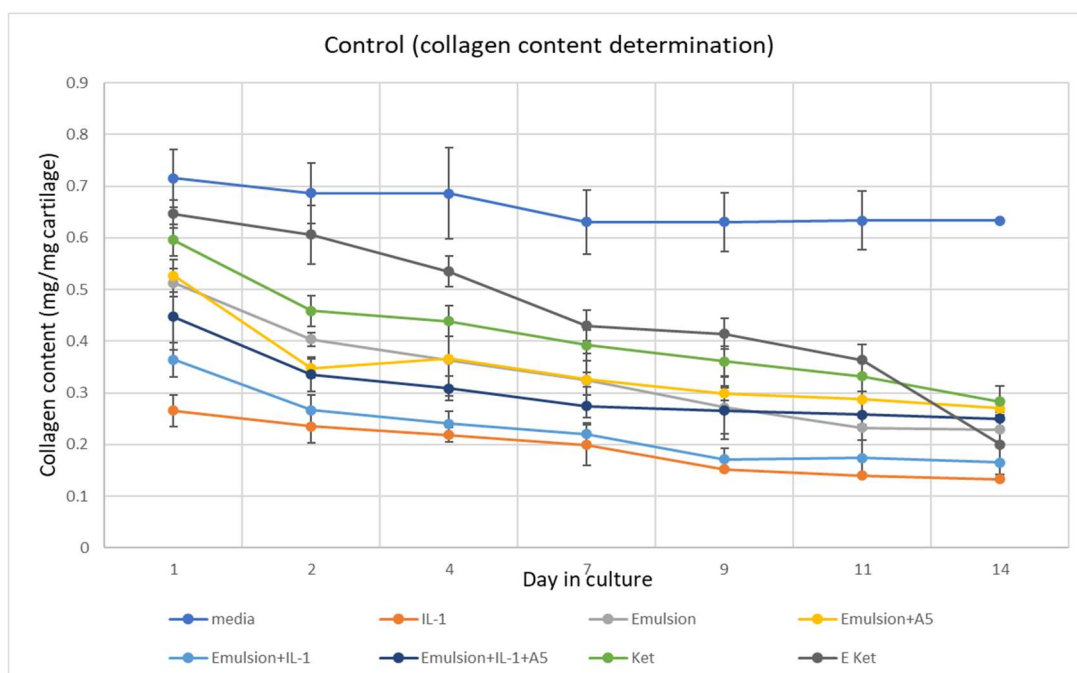
Bovine cartilage explants were incubated with IL-1 $\alpha$  for 14 days, then the extract was digested in papain solution, and the collagen content in the solution was measured using hydroxyproline assay.

Figure 5-2 shows that collagen content dropped to half during the first week after IL-1 $\alpha$  exposure; it then decreased steadily up to the 2-week point ( $0.13 \pm 0.01$  mg), which was significantly lower ( $p < 0.05$ ) than the untreated control ( $0.63 \pm 0.05$  mg). Overall, collagen degradation product was significantly lower following IL-1 $\alpha$  stimulation compared to the controls ( $p < 0.05$ ) (Figure 5-2 A).

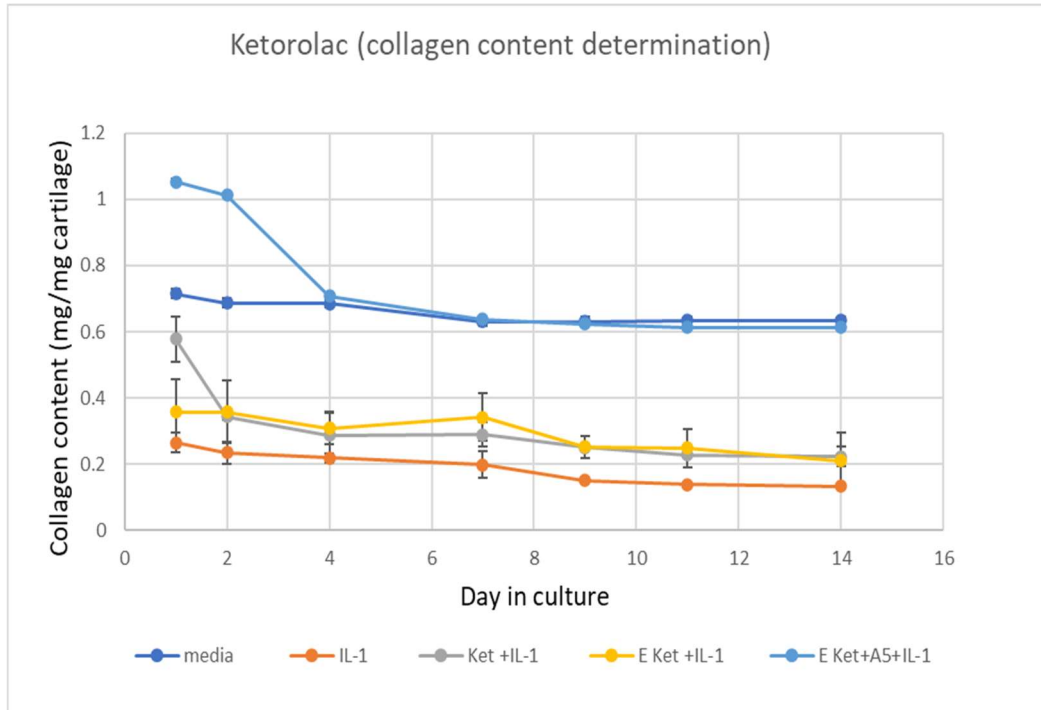
In addition, the anti-inflammatory effect of oleic acid as a type of omega-9 fatty acid helped to protect the collagen content quantity compared with IL-1 $\alpha$  treated cartilage, but the difference was not statistically significant ( $p > 0.05$ ). However, coating the emulsion with POLY-A5 significantly decreased the loss of collagen content during the culture time ( $p < 0.001$ ). Adding Ket with/without o/w emulsion to the media that was exposed to IL-1 $\alpha$  helped to double the decreased amount of collagen loss in the media compared to the IL-1 $\alpha$  treated samples (Figure 5-2 A).

Treating cartilage explants with Ket emulsion coated with POLY-A5 was significantly effective in increasing the amount of collagen synthesis in cartilage to the same level as the untreated control, and above the level of the IL-1 $\alpha$  treated cartilage ( $p < 0.0001$ ) (Figure 5-2 B). After 2 days of the culture, the amount of collagen using the DDS dropped from 1.1 mg to 0.7 mg, which then halved on day 7 (0.6 mg). After that, it stabilised until the termination of the culture. Moreover, using Dex emulsion coated with POLY-A5 resulted in a reduced amount of collagen loss in the media ( $p < 0.0001$ ) (Figure 5-2 C). The developed DDS using Ket as a module for NSAIDs showed promising results, such as the effectiveness of Dex treatment in increasing the amount of collagen in the cartilage tissue exposed to inflammatory cytokine. Dex, a well-known type of steroidal intra-articular injection for OA treatment, showed an increase in collagen content in this work, which was at the same level as Ket emulsion coated with POLY-A5 (Figure 5-2 B&C).

A)



B)



C)

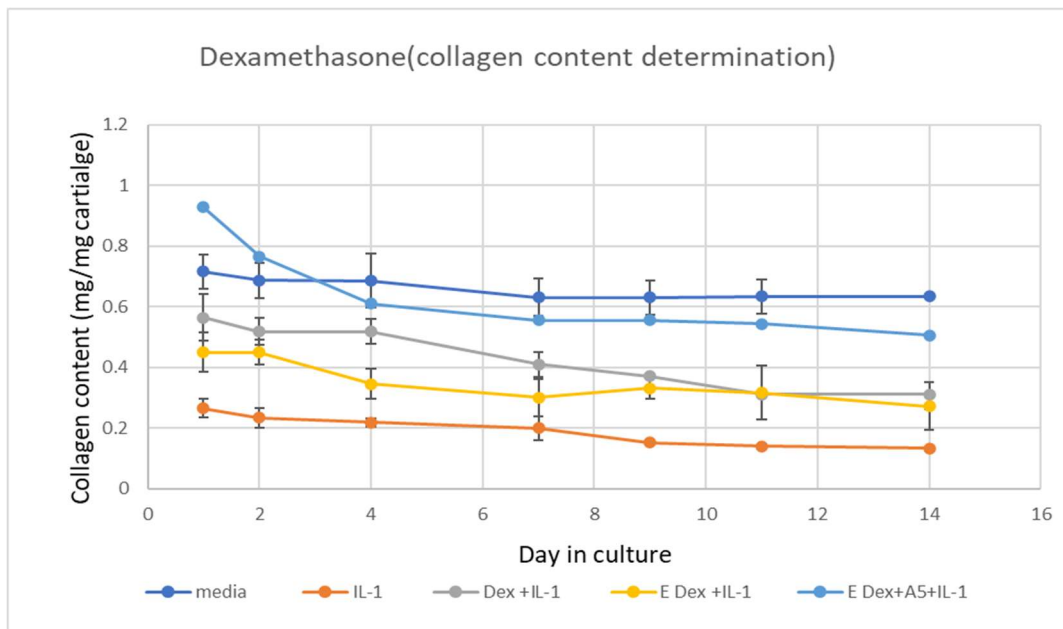


Figure 5-2. Collagen content determination on IL-1 $\alpha$  treated cartilage using hydroxyproline assay. Using main samples (untreated (media only) and IL-1 $\alpha$  treated sample) and different types of control (A), emulsion Ket coated with/without POLY-A5(B) and Dex emulsion coated with/without POLY-A5(C), the figures was separated for clarity. Ket and Dex emulsion coated with POLY-A5 was significantly effective in the increased amount of collagen synthesis in cartilage to the same level as the untreated control and more the IL-1 $\alpha$  treated cartilage ( $p < 0.0001$ ).

### **5.3.3. Live/dead viability imaging:**

The cytotoxicity of Ket emulsion coated with POLY-A5 was evaluated by assessing chondrocyte viability in bovine cartilage explants using a live/dead assay. In this thesis, the images for day 1, 2, 7 and 14 are presented, as there were no differences in appearance of the live/dead cells after the first week.

Initially, treatment of cartilage with IL-1 $\alpha$  led to a clearly observed decrease in cell viability compared with the untreated control, to around 70% (Figure 5-3 to 5-14). This was comparable with the sGAG and collagen determination results, as the amount of the loss was higher in IL-1 $\alpha$  treated samples. In addition, compared to the controls and the DDS, the viability of chondrocytes was much suppressed by IL-1 $\alpha$  treatment in the cartilage explants after 24 hours (Figure 5-3). The illustrative images from cartilage discs at 24 and 48 hours (Figures 5-7&5-8) show no cell death in cartilage treated with the developed DDS, which was similar to the untreated control. Some cell death in the superficial cartilage zone was observed, which may be related to the effect of using a scalpel for cartilage sections, exposure to the air, and drying out of the cartilage surface during preparation (Redman et al., 2004; Bajpayee et al., 2016). Ket emulsion coated with POLY-A5 rescued chondrocyte viability in the presence of IL-1 $\alpha$ , especially in the first week of culture as the number of live cells observed was more apparent in the first 7 days. Similarly, the content of sGAG and collagen loss was higher during the first week than the second week of the culture.

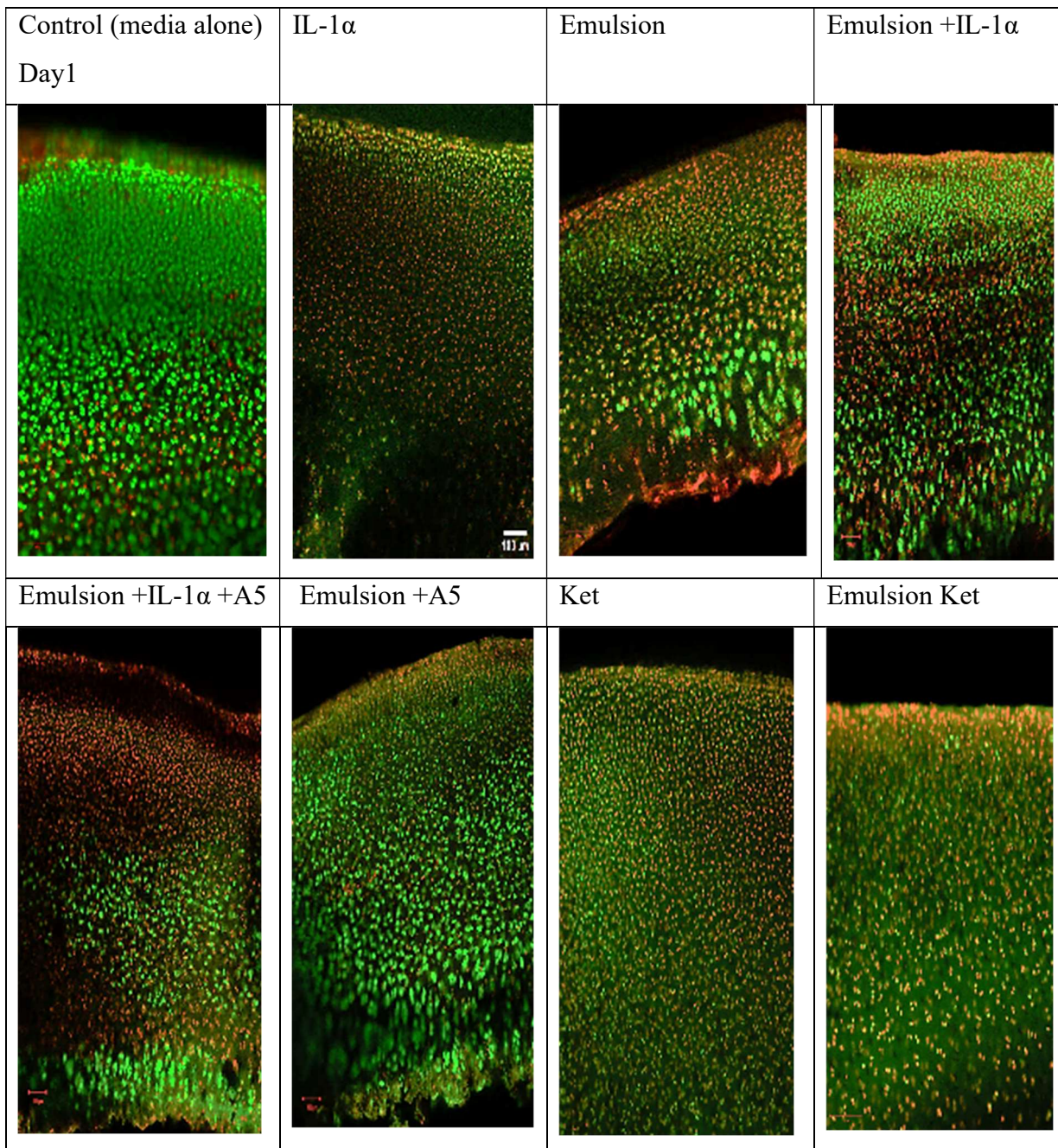


Figure 5-3. Examples of images of live/dead fluorescently stained bovine explants exposed to IL-1 $\alpha$  (1ng/mL) to evaluate chondrocyte viability on day 1. The cartilage explants were incubated with controls (pure media, IL-1 $\alpha$ , Ket, oleic acid emulsion with/without IL-1 $\alpha$  and POLY-A5). Live cells were stained green by calcein and dead cells were stained red by ethidium homodimer. Ket and oleic acid emulsion were reduced cell death induced by IL-1 $\alpha$ . Scale bar 100 $\mu$ m.

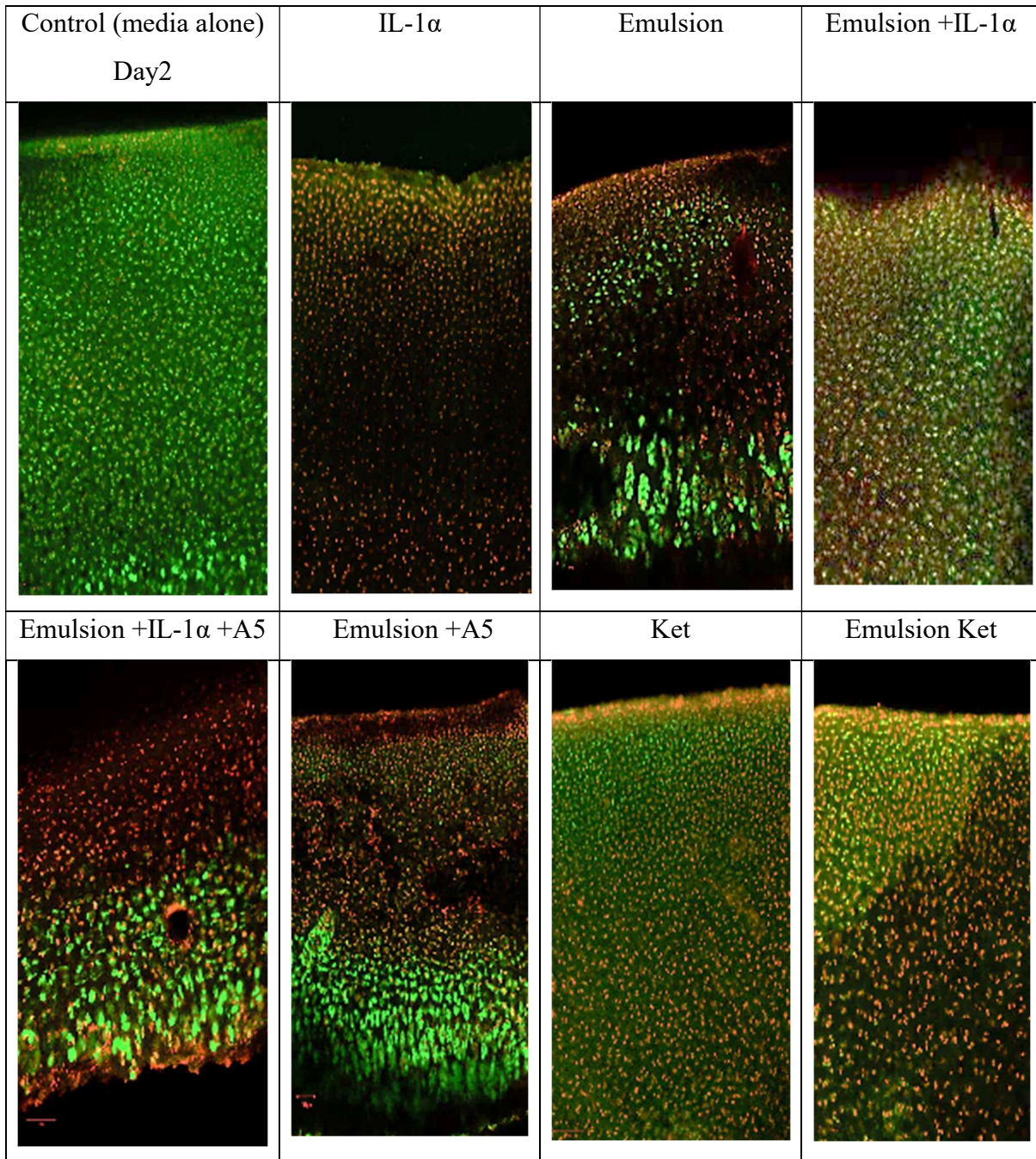


Figure 5-4. Examples of images of live/dead fluorescently stained bovine explants exposed to IL-1 $\alpha$  (1 ng/mL) to evaluate chondrocyte viability on day 2. The cartilage explants were incubated with controls (pure media, IL-1 $\alpha$ , Ket, oleic acid emulsion with/without IL-1 $\alpha$  and POLY-A5). Live cells were stained green by calcein and dead cells were stained red by ethidium homodimer. Ket and oleic acid emulsion were reduced cell death induced by IL-1 $\alpha$ . Scale bar 100 $\mu$ m.

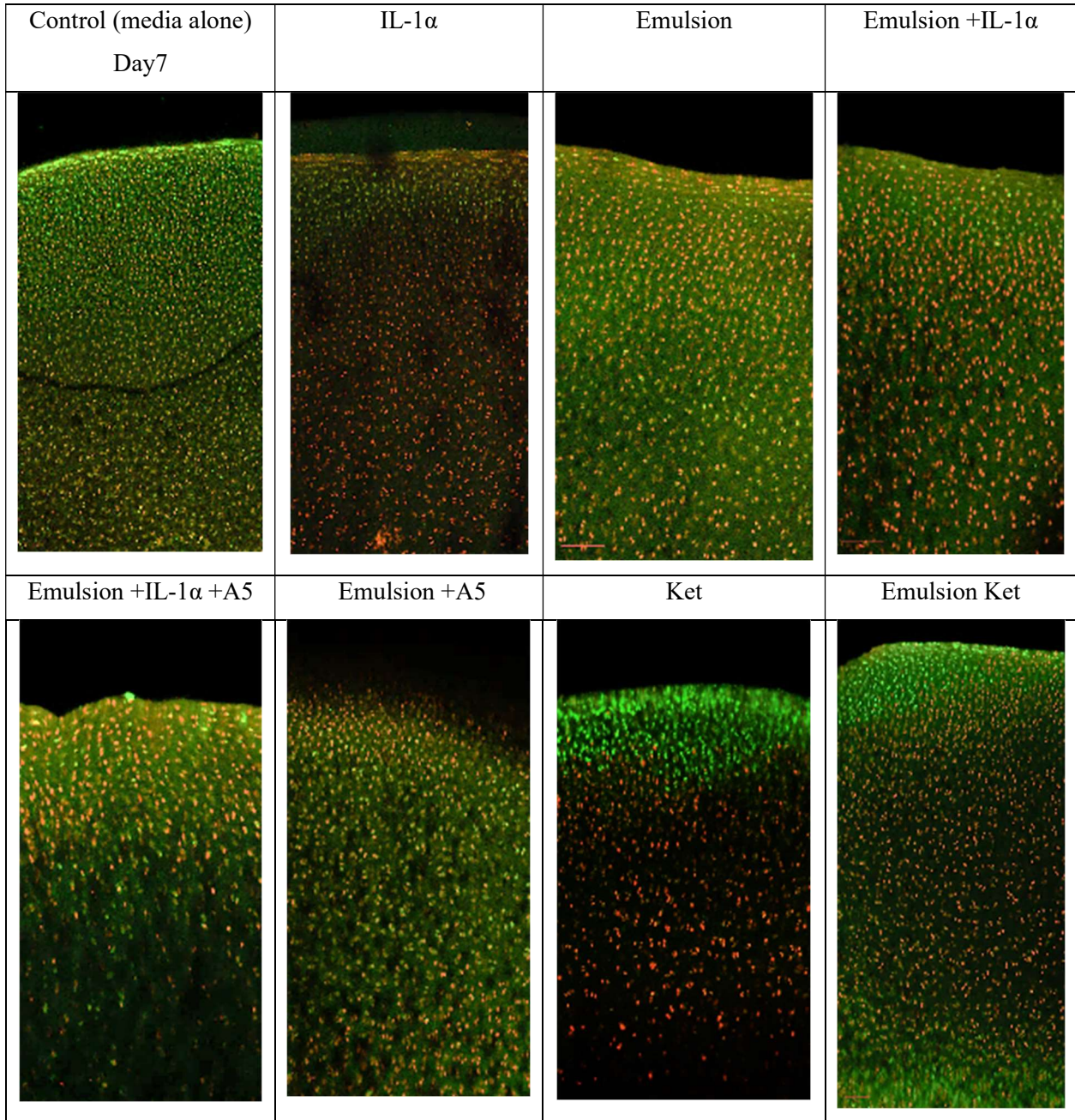


Figure 5-5. Examples of images of live/dead fluorescently stained bovine explants exposed to IL-1 $\alpha$  (1 ng/mL) to evaluate chondrocyte viability on day 7. The cartilage explants were incubated with controls (pure media, IL-1 $\alpha$ , Ket, oleic acid emulsion with/without IL-1 $\alpha$  and POLY-A5). Live cells were stained green by calcein and dead cells were stained red by ethidium homodimer. Ket and oleic acid emulsion were reduced cell death induced by IL-1 $\alpha$ . Scale bar 100 $\mu$ m.

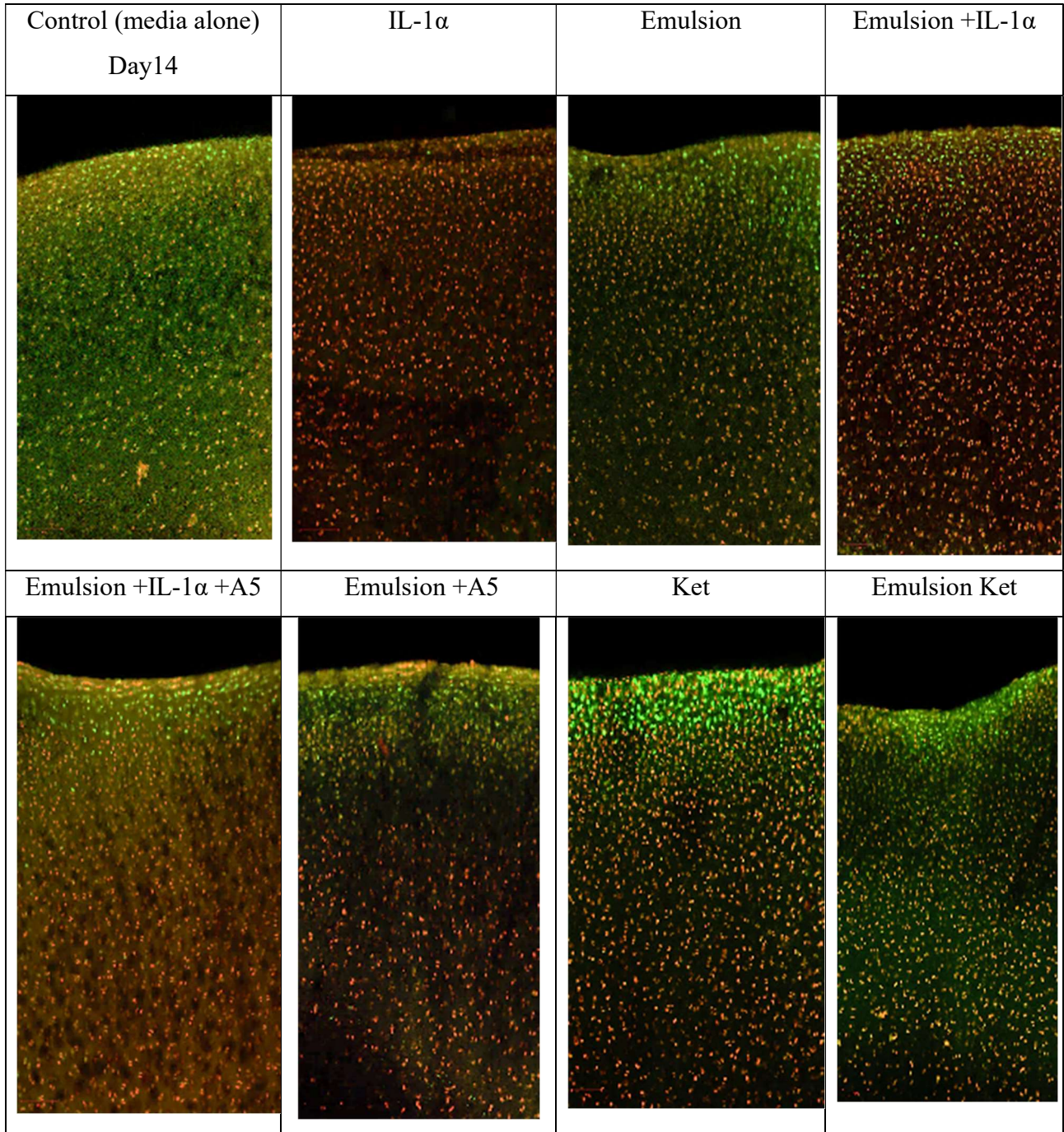


Figure 5-6. Examples of images of live/dead fluorescently stained bovine explants exposed to IL-1 $\alpha$  (1 ng/mL) to evaluate chondrocyte viability on day 14. The cartilage explants were incubated with controls (pure media, IL-1 $\alpha$ , Ket, oleic acid emulsion with/without IL-1 $\alpha$  and POLY-A5). Live cells were stained green by calcein and dead cells were stained red by ethidium homodimer. Ket and oleic acid emulsion were reduced cell death induced by IL-1 $\alpha$ . Scale bar 100 $\mu$ m.

Interestingly, the anti-inflammatory effect of the oleic acid, which promotes the production of an anti-inflammatory mediator such as IL-10 (Sales-Campos et al., 2013; Janke, Bennett and Tieleman, 2014), mostly increased the viability of chondrocytes during the first 48 hours compared to IL-1 $\alpha$  treated explants (Figures 5-3&5-4). Subsequently, a dramatic increase in cell death was observed by day 7 after treatment of the cartilage explants with Ket and Ket emulsion alone in the presence of IL-1 $\alpha$  or the controls (Figure 5-5). It has been shown that oleic acid is not cytotoxic to chondrocyte cells and has anti-inflammatory and anti-destructive effects on cartilage tissue (Bastiaansen-Jenniskens et al., 2013; Pérez-Martínez, Hernández, Rodríguez-Espinosa, Arce-Paredes, Rojas-Espinosa et al., 2016). In contrast, coated Ket emulsion with POLY-A5 successfully prevented cell death induced by IL-1 $\alpha$  by day 14 (Figure 5-10), as it caused a reduction in sGAG and collagen loss during the culture period.

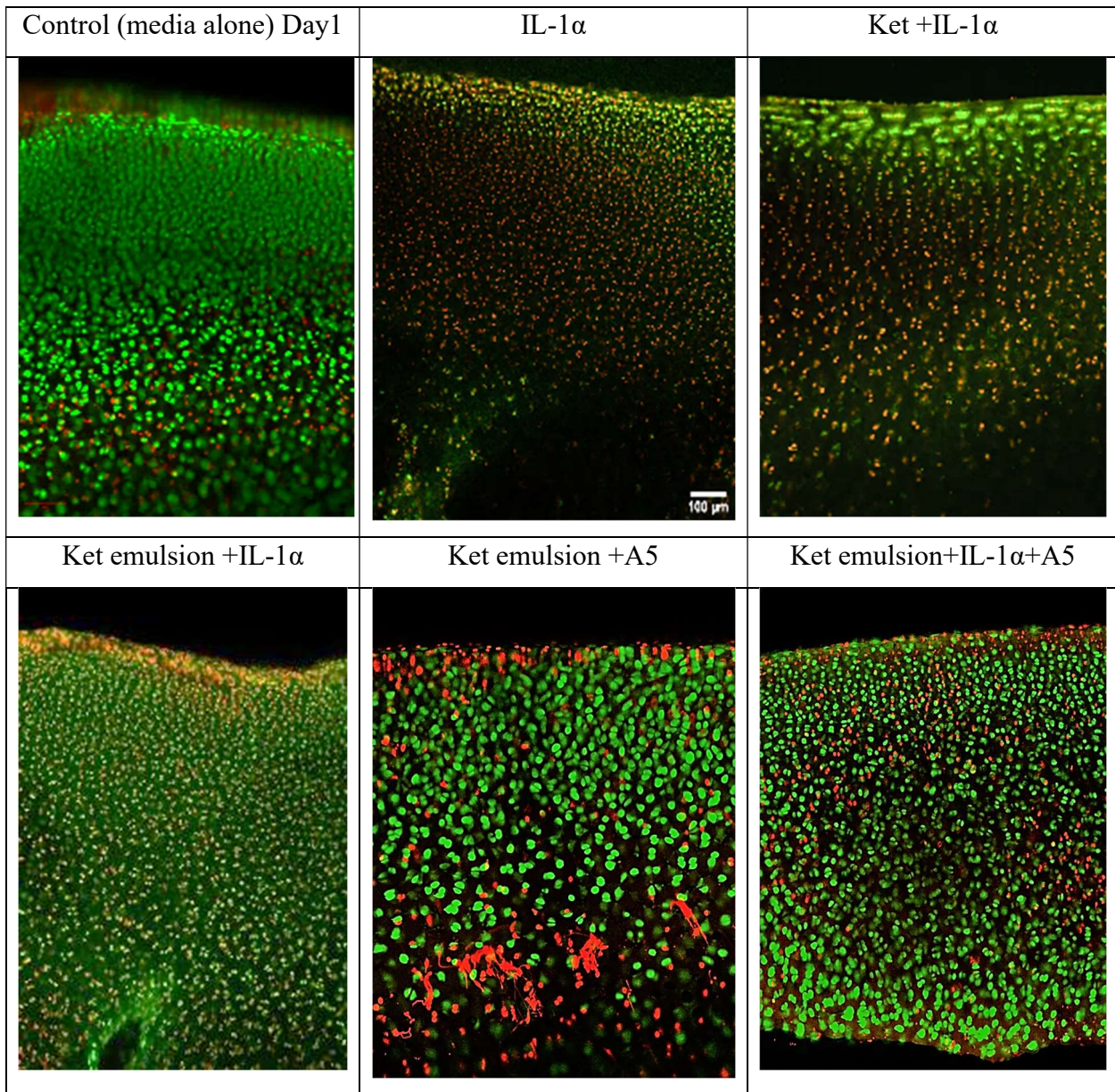


Figure 5-7. Examples of images of live/dead fluorescently stained bovine explants exposed to IL-1 $\alpha$  (1 ng/mL) to evaluate chondrocyte viability on day 1. The cartilage explants were incubated with controls (pure media, IL-1 $\alpha$ , Ket emulsion with without IL-1 $\alpha$  and POLY-A5). Live cells were stained green by calcein and dead cells were stained red by ethidium homodimer. Ket emulsion coated with POLY-A5 was successfully prevented cell death induced by IL-1 $\alpha$ . Scale bar 100 $\mu$ m.

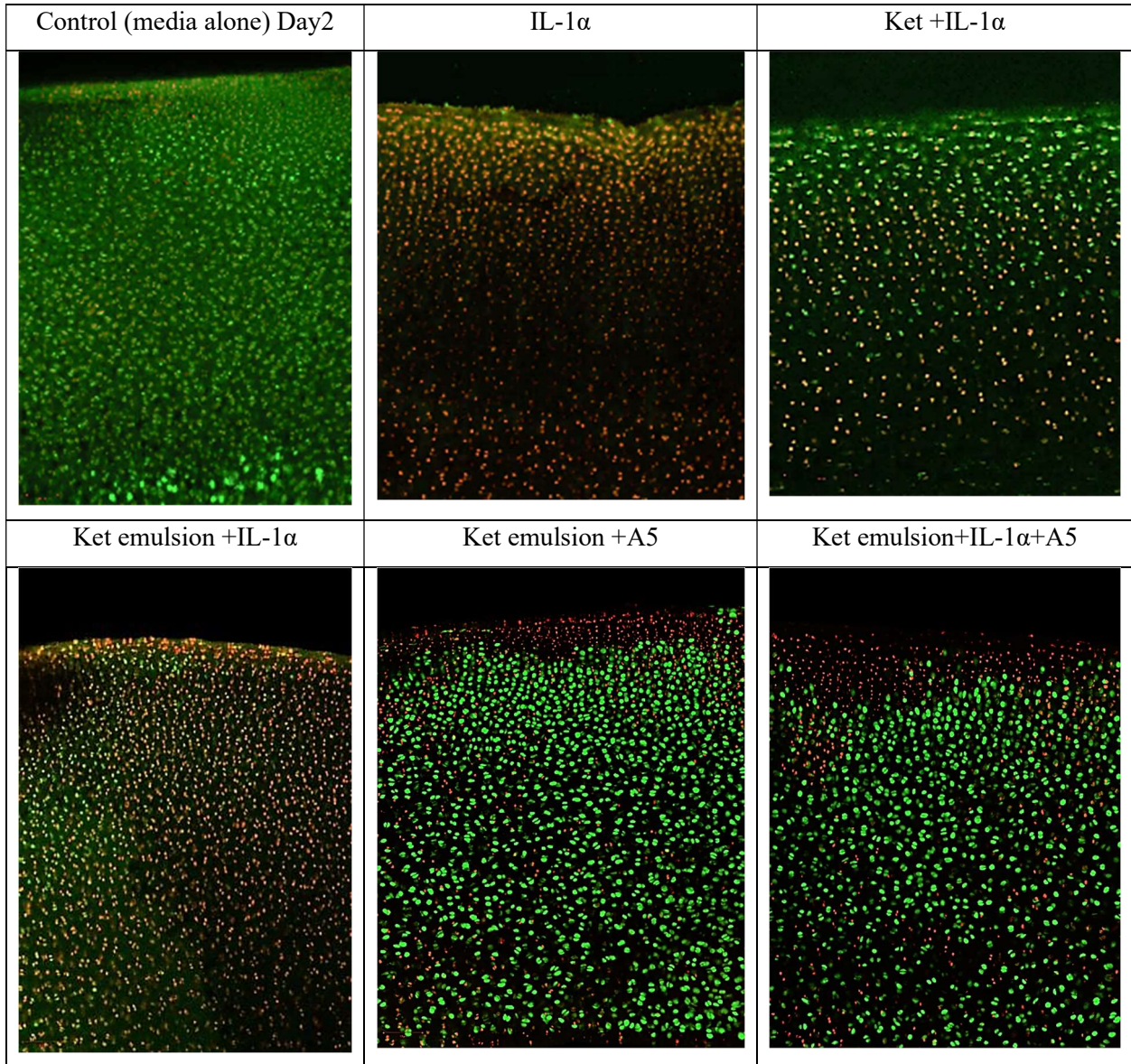


Figure 5-8. Examples of images of live/dead fluorescently stained bovine explants exposed to IL-1 $\alpha$  (1 ng/mL) to evaluate chondrocyte viability on day 2. The cartilage explants were incubated with controls (pure media, IL-1 $\alpha$ , Ket emulsion with or without IL-1 $\alpha$  and POLY-A5). Live cells were stained green by calcein and dead cells were stained red by ethidium homodimer. Ket emulsion coated with POLY-A5 was successfully prevented cell death induced by IL-1 $\alpha$ . Scale bar 100 $\mu$ m.

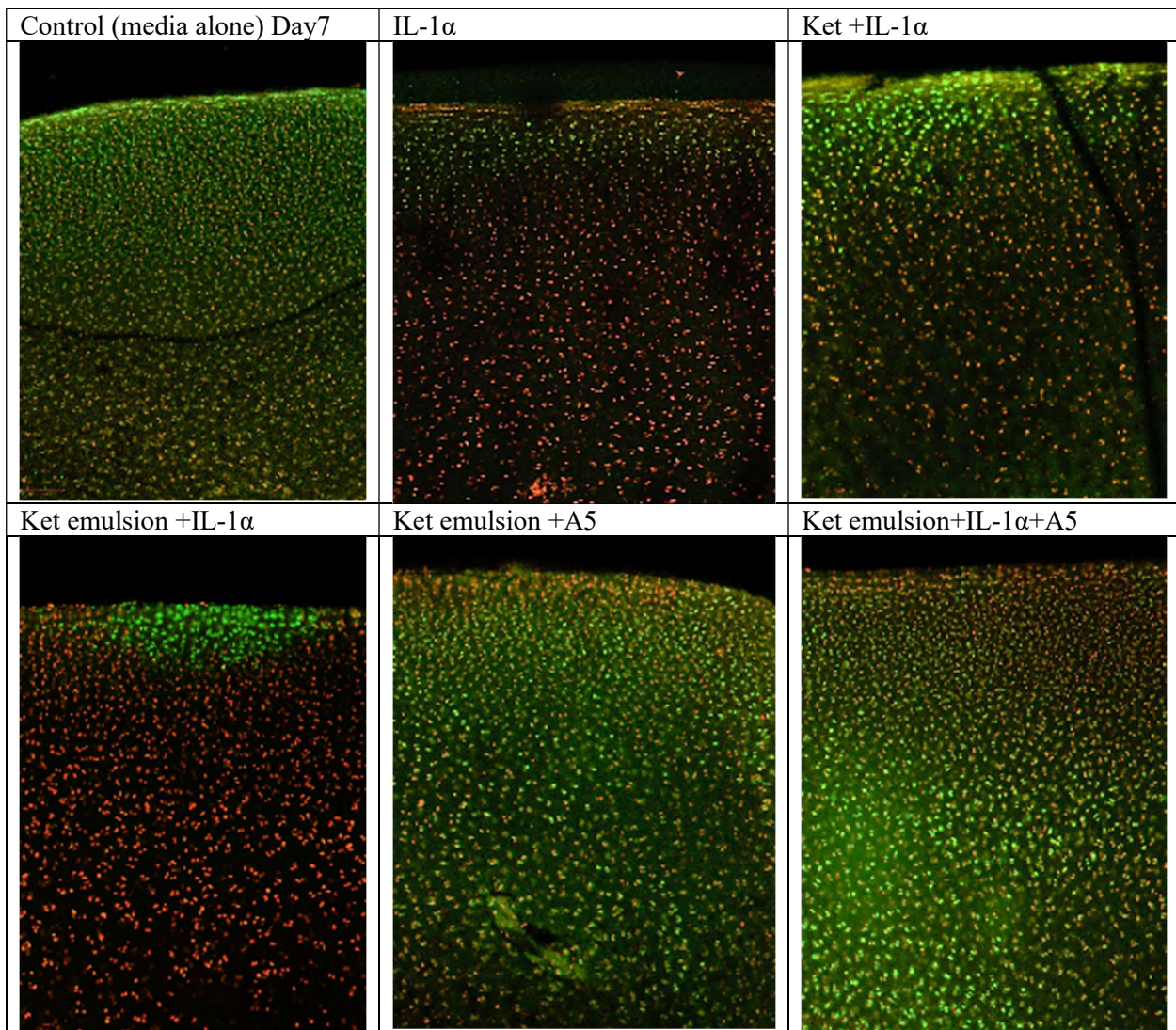


Figure 5-9. Examples of images of live/dead fluorescently stained bovine explants exposed to IL-1 $\alpha$  (1 ng/mL) to evaluate chondrocyte viability on day 7. The cartilage explants were incubated with controls (pure media, IL-1 $\alpha$ , Ket emulsion with or without IL-1 $\alpha$  and POLY-A5). Live cells were stained green by calcein and dead cells were stained red by ethidium homodimer. Ket emulsion coated with POLY-A5 successfully prevented cell death induced by IL-1 $\alpha$ . Scale bar 100 $\mu$ m.

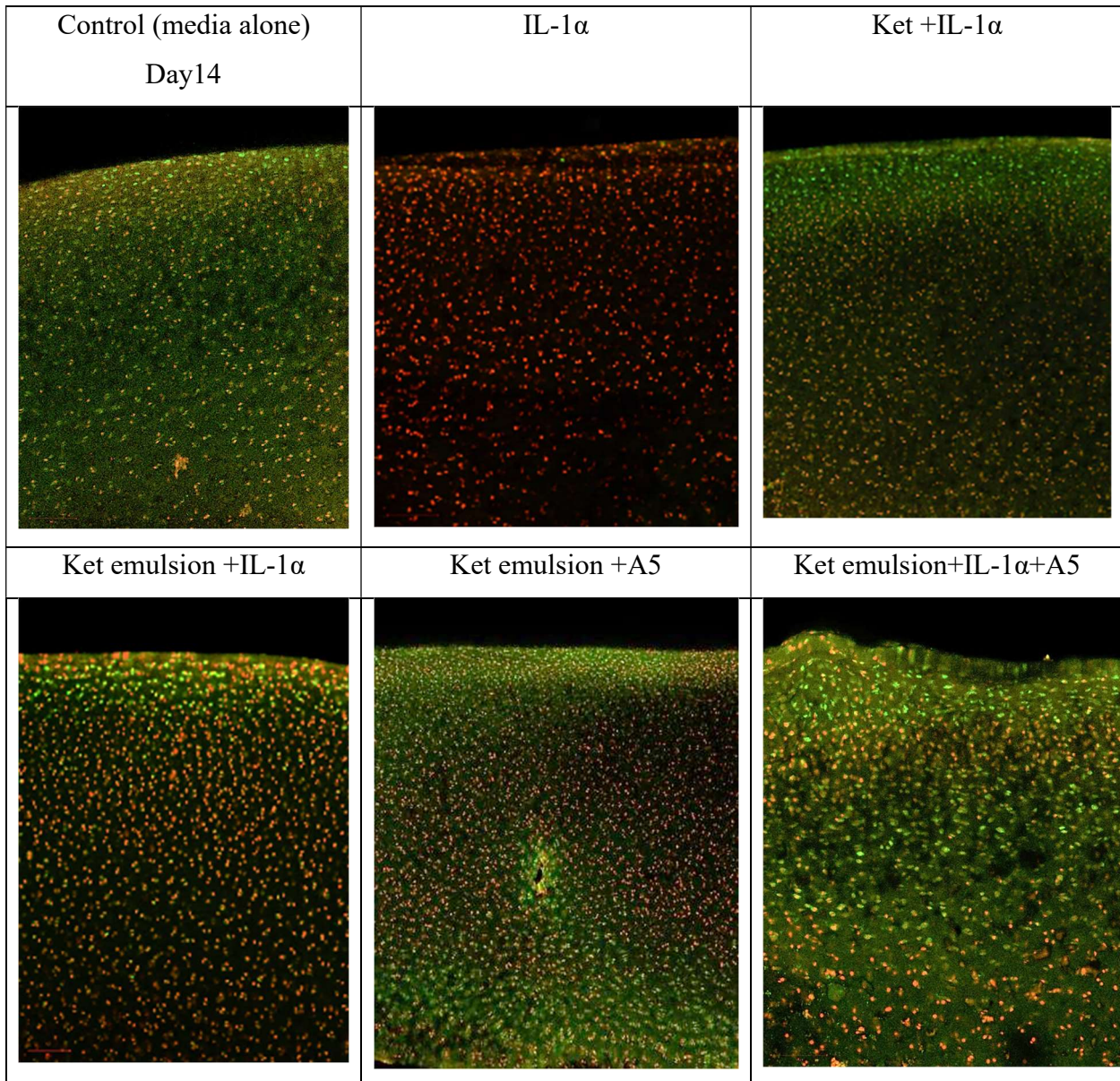


Figure 5-10. Examples of images of live/dead fluorescently stained bovine explants exposed to IL-1 $\alpha$  (1 ng/mL) to evaluate chondrocyte viability on day 14. The cartilage explants were incubated with controls (pure media, IL-1 $\alpha$ , Ket emulsion with or without IL-1 $\alpha$  and POLY-A5). Live cells were stained green by calcein and dead cells were stained red by ethidium homodimer. Ket emulsion coated with POLY-A5 was successfully reduced cell death induced by IL-1 $\alpha$ . Scale bar 100 $\mu$ m.

Moreover, using Dex emulsion coated with POLY-A5 was similar to Ket emulsion + POLY-A5 in protecting chondrocyte cells from destruction when treated with IL-1 $\alpha$  (Figures 5-11 to 5-14). Overall, based on the viability staining images, there was no significant cell death at the end of the culture (14 days) using the DDS and most of the chondrocytes were still viable.

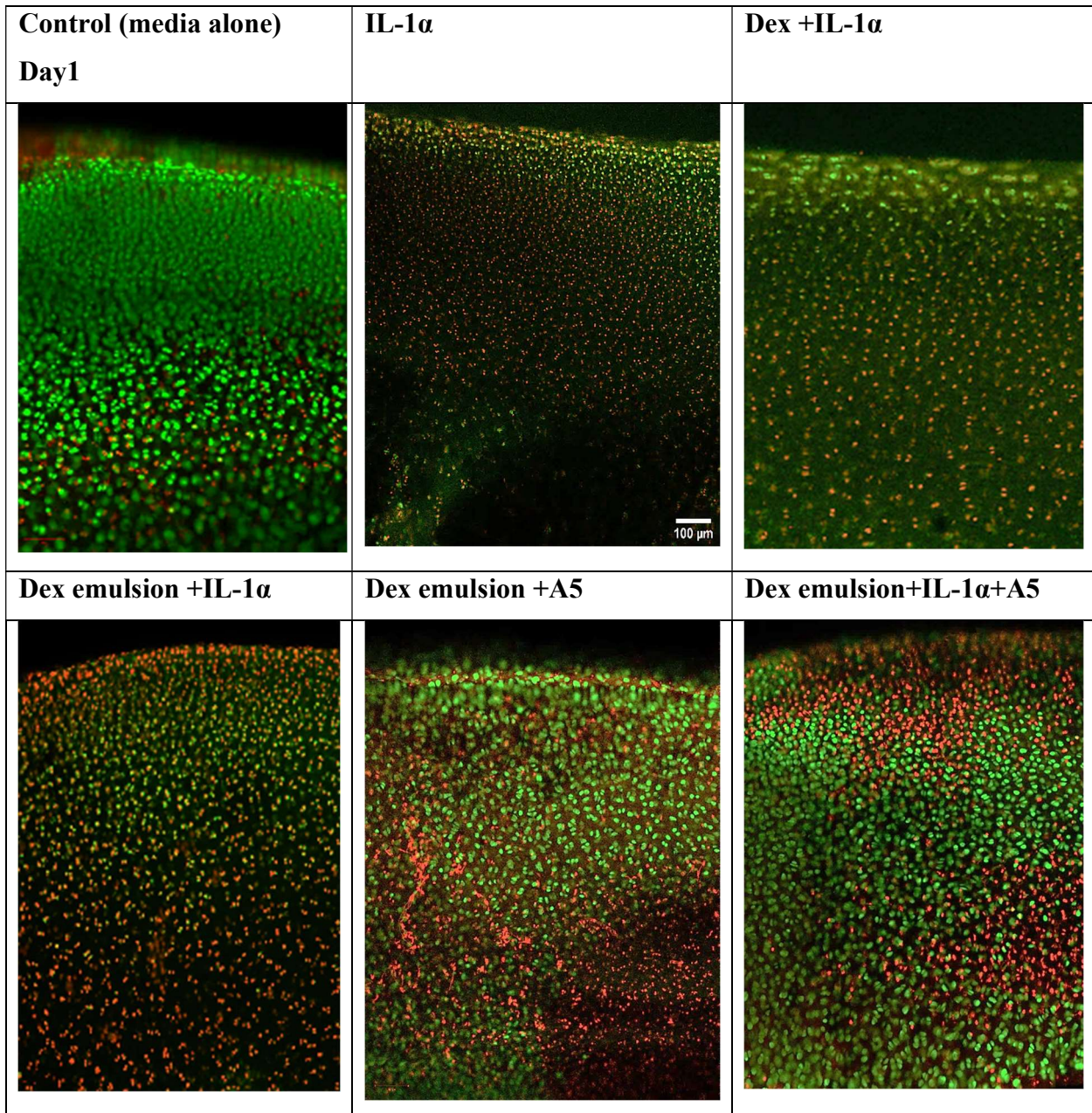


Figure 5-11. Examples of images of live/dead fluorescently stained bovine explants exposed to IL-1 $\alpha$  (1 ng/mL) to evaluate chondrocyte viability on day 1. The cartilage explants were incubated with controls (pure media, IL-1 $\alpha$ , Dex emulsion with or without IL-1 $\alpha$  and POLY-A5). Live cells were stained green by calcein and dead cells were stained red by ethidium homodimer. Dex emulsion coated with POLY-A5 successfully prevented cell death induced by IL-1 $\alpha$ . Scale bar 100 $\mu$ m.

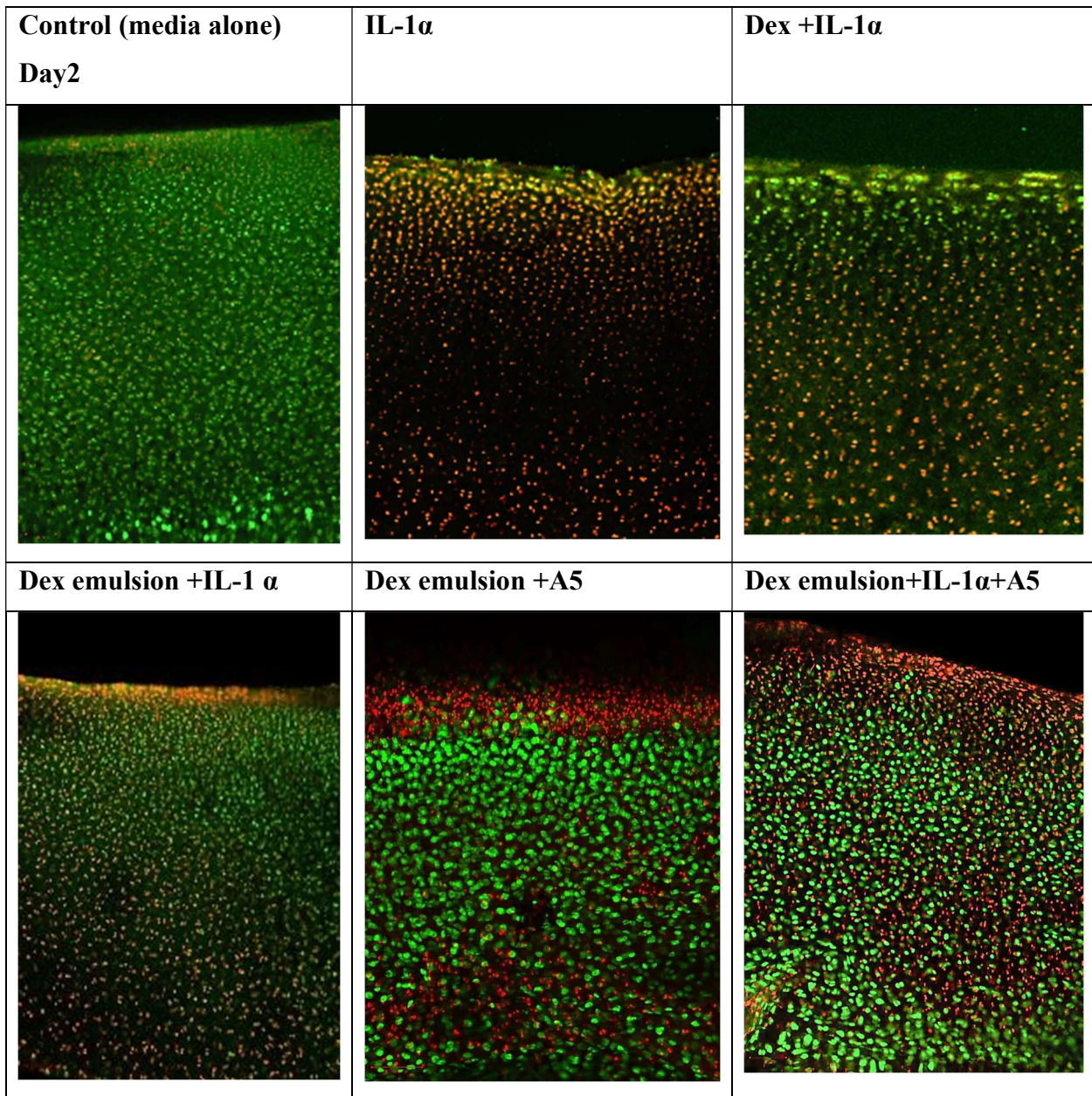


Figure 5-12. Examples of images of live/dead fluorescently stained bovine explants exposed to IL-1 $\alpha$  (1 ng/mL) to evaluate chondrocyte viability on day 2. The cartilage explants were incubated with controls (pure media, IL-1 $\alpha$ , Dex emulsion with or without IL-1 $\alpha$  and POLY-A5). Live cells were stained green by calcein and dead cells were stained red by ethidium homodimer. Dex emulsion coated with POLY-A5 was successfully reduced cell death induced by IL-1 $\alpha$ . Scale bar 100 $\mu$ m.

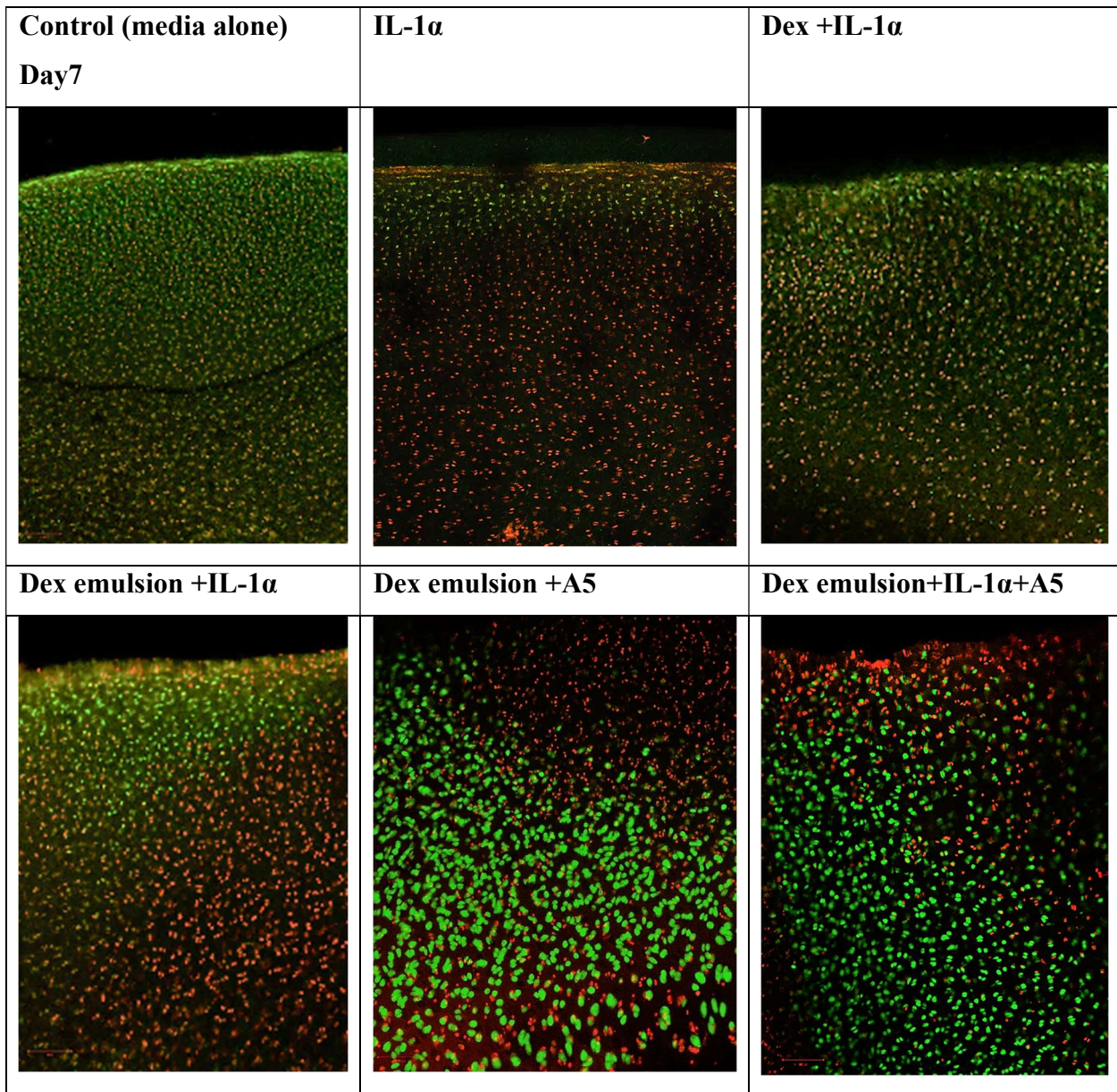


Figure 5-13. Examples of images of live/dead fluorescently stained bovine explants exposed to IL-1 $\alpha$  (1 ng/mL) to evaluate chondrocyte viability on day 7. The cartilage explants were incubated with controls (pure media, IL-1 $\alpha$ , Dex emulsion with or without IL-1 $\alpha$  and POLY-A5). Live cells were stained green by calcein and dead cells were stained red by ethidium homodimer. Dex emulsion coated with POLY-A5 was successfully reduced cell death induced by IL-1 $\alpha$ . Scale bar 100 $\mu$ m.

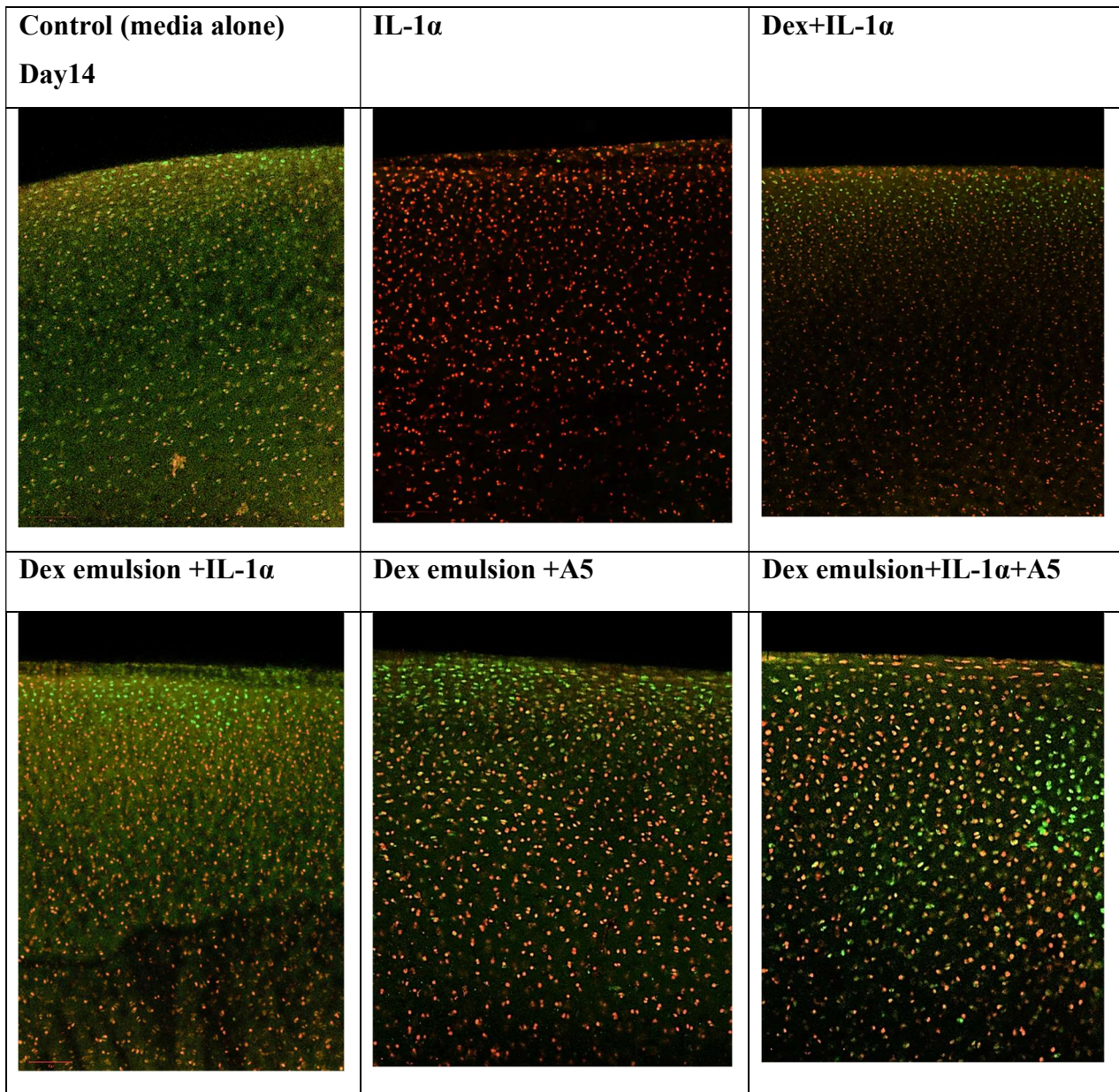


Figure 5-14. Examples of images of live/dead fluorescently stained bovine explants exposed to IL-1 $\alpha$  (1 ng/mL) to evaluate chondrocyte viability on day 14. The cartilage explants were incubated with controls (pure media, IL-1 $\alpha$ , Dex emulsion with or without IL-1 $\alpha$  and POLY-A5). Live cells were stained green by calcein, and dead cells were stained red by ethidium homodimer. Dex emulsion coated with POLY-A5 was successfully reduced cell death induced by IL-1 $\alpha$ . Scale bar 100 $\mu$ m.

#### **5.3.4. Histological analysis of cartilage explants**

Images of sections of the cartilage tissue from the cartilage cultures stained with safranin O are shown in Figure 5-15. Images of control tissue (pure media, untreated sample) sections stained with safranin O revealed high staining intensity, which was around 97% for GAG on day 14. A semi-quantitative scoring system is often used to estimate the percentage of safranin O staining intensity in the results (Mankin *et al.*, 1971). Staining intensity is graded visually on a scale of 0 to 4, where 0 represents no staining and 4 represents the strongest staining. In order to calculate the staining intensity percentage, the total score is divided by the maximum possible score and multiplied by 100. Moreover, in the cartilage tissue treated with IL-1 $\alpha$ , there was a significant reduction (around 50%) in staining intensity compared to the untreated tissue sample on day 14 indicating a massive loss of GAG from the tissue, as illustrated in sGAG loss experiments. In addition, there was an apparent reduction (around 60%) in safranin O intensity when Ket or Ket o/w emulsion alone were added to the cartilage sample compared to the untreated tissue (pure media), but GAG was still present in the tissue. Treating the cartilage section that was exposed to IL-1 $\alpha$  with the Ket emulsion coated with POLY-A5 led to maintaining GAG content and reducing its loss, as the GAG staining intensity appeared strong and bright which is similar to the observations of cartilage culture in pure media (Figure 5-15).

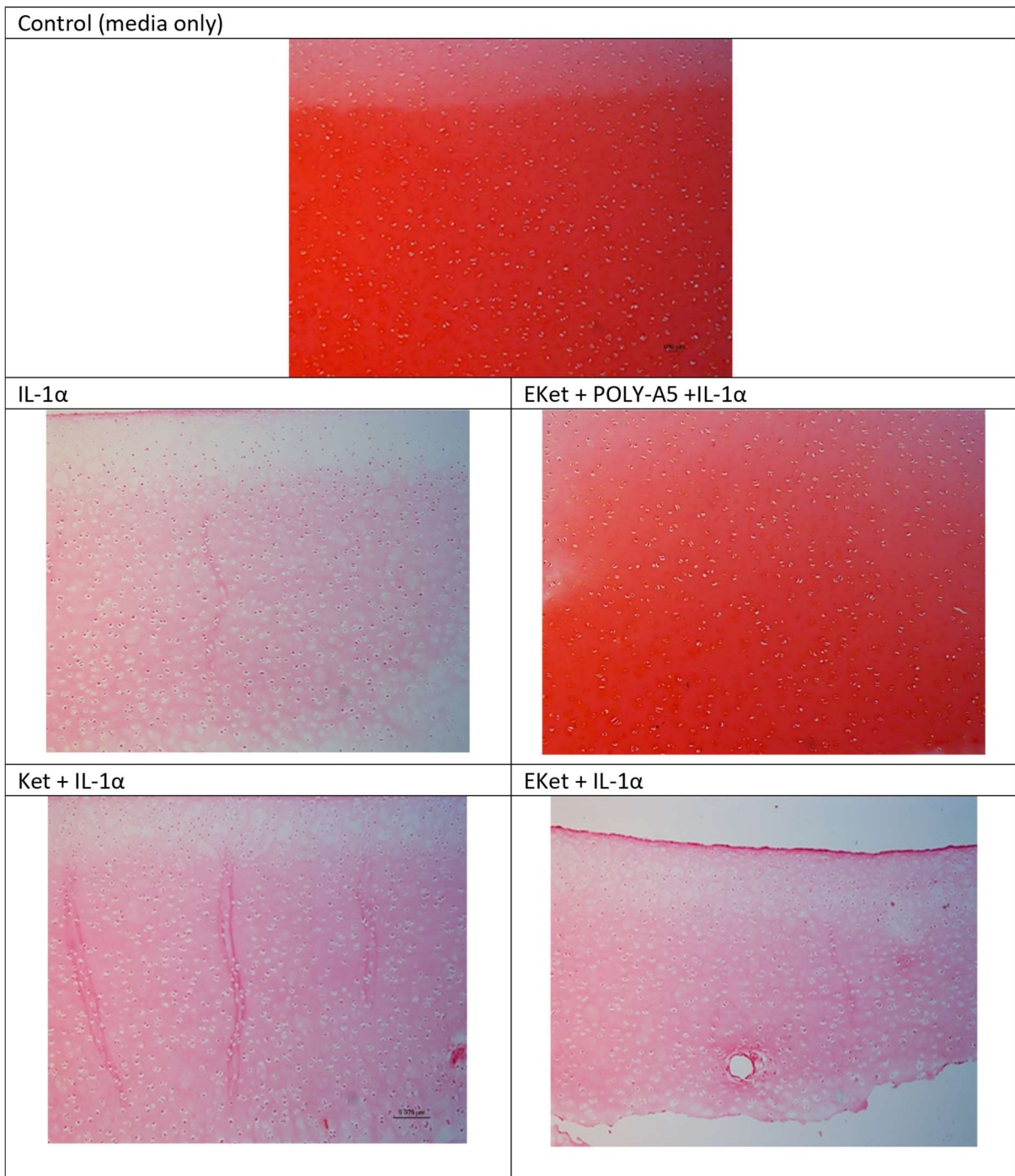


Figure 5-15. Histology sections of cartilage tissue stained with safranin O on day 14 that exposed to pure media, IL-1 $\alpha$  (1 ng/mL), Ket emulsion coated with POLY-A5, Ket o/w emulsion +IL-1 $\alpha$  and Ket+IL-1 $\alpha$ . The reddish orange colour intensity indicates the amount of GAG in the sample. Ket emulsion coated with POLY-A5 maintaining the GAG content and reduced its loss as the GAG staining intensity appeared strong and bright similar to those observed for cartilage culture in pure media. Scale bar 100 $\mu$ m.

### 5.3.5. XTT assay

The XTT assay is based on the cleavage of the yellow tetrazolium salt XTT forming an orange water soluble formazan product by dehydrogenase activity in the active mitochondria (Glasebrook, 1991; Elson et al., 2015). In the current work, a decrease in the number of living cartilage cells resulted in a decrease in the activity of mitochondrial dehydrogenases in the sample. This decrease directly corresponded to the decreased conversion of yellow tetrazolium salt XTT to orange formazan, as monitored by the absorbance. The XTT assay of the cartilage tissue viability results indicated that the cartilage tissue showed reduced XTT conversion or mitochondrial activity from days 0 to 20 when treated with IL-1 $\alpha$  ( $p < 0.01$ ), compared to the untreated control. Treating the cartilage tissue with IL-1 $\alpha$  led to a fourfold decrease in cartilage cell viability during the culture period (days 0-20). After 2 days of incubation of cartilage sections with IL-1 $\alpha$ , cell viability decreased by 50%, meaning a cumulative decrease of around 80% from day 4 to day 20 (Figure 5-16). Moreover, adding Ket with/without emulsion led to a slight increase in cell viability compared to samples treated with IL-1 $\alpha$  alone, as cell viability decreased by 40% after 2 days to around 30% on days 14 and 20 (Figure 5-16). In contrast, treating the cartilage samples with the developed formulation (Ket emulsion + POLY-A5) led to a significant increase in cell proliferation ( $p < 0.01$ ) at a level similar to the untreated cartilage samples (Figure 5-16). XTT assay showed that only about 20% of cartilage degradation occurred using Ket emulsion coated with POLY-A5 at day 2, reaching 50% at day 7. On day 20, the cell viability and mitochondrial activity of the cartilage tissue increased 2 times when treated with the formulation, in comparison to samples treated with IL-1 $\alpha$  alone. Therefore, Ket emulsion + POLY-A5 can be regarded as effective in maintaining cell viability and metabolic activity in the post-traumatic OA cartilage model.

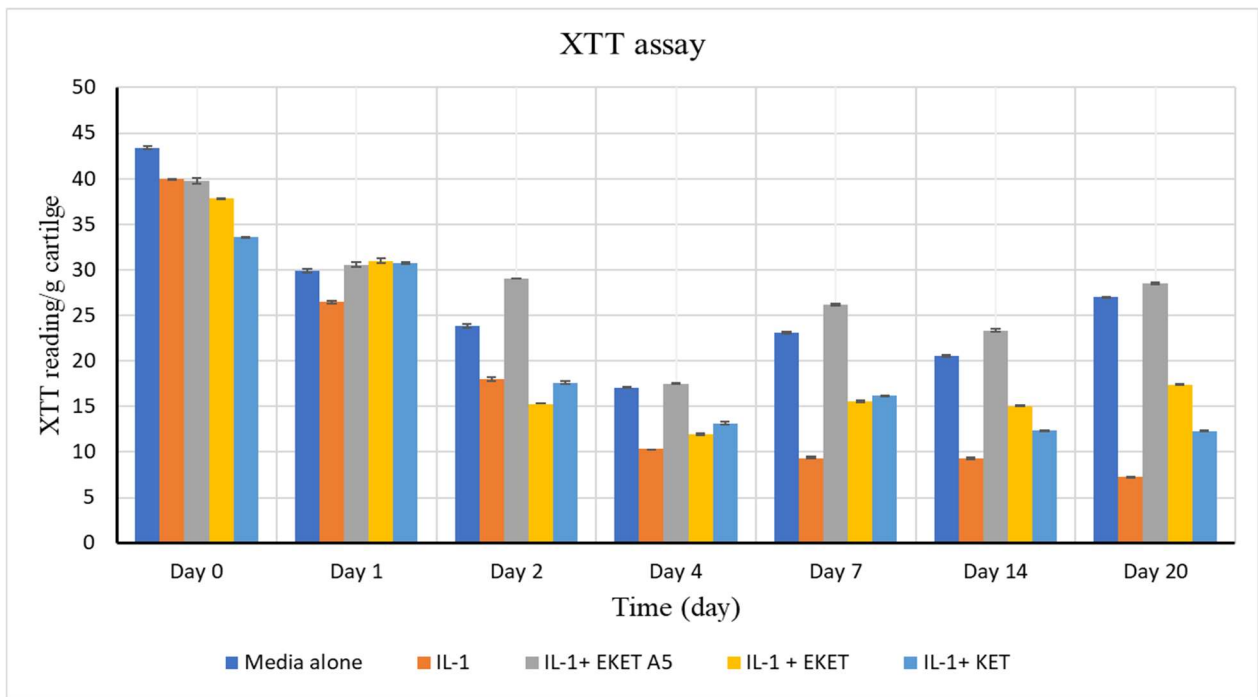


Figure 5-16. Viability assessment of cartilage tissues over 20 days. XTT assay was used to assess the effects of Ket emulsion coated with/without POLY-A5 on cartilage samples that exposed to IL-1 $\alpha$ . The figure showed 80% reduced in XTT results from day 0 to 20 on cartilage that treated with IL-1 $\alpha$ . Conversely, cartilage treated with Ket emulsion coated with POLY-A5 exhibited approximately 20% reduced in XTT results up to day 20.

## 5.4. Discussion

The developed drug delivery system exhibits advantages for targeted intra-cartilage drug delivery: its small size and optimal positive charge enables rapid penetration through full-thickness cartilage and electrostatic binding interactions. Carriers with these characteristics result in weak and irreversible binding between the carrier and cartilage ECM, which provides advantages in terms of allowing the drug to penetrate rapidly and be retained inside cartilage tissue (Bajpayee and Grodzinsky, 2017). Here the coated Ket emulsion (using oleic acid as an oil phase) with POLY-A5 was used to test the hypothesis that it can ameliorate catabolic effects in cytokine-challenged cartilage relevant to post-traumatic OA. Ket is a type of non-steroidal anti-inflammatory drug used as a treatment option for OA; oleic acid has anti-inflammatory properties and acts as a penetration enhancer; and POLY-A5 is a type of cationic PBAEs which can bind electrostatically with the negatively charged cartilage proteoglycan. This drug delivery system allowed the drug to penetrate inside the cartilage tissue and counteract the inflammatory effect of IL-1 $\alpha$ , enabling better treatment of cartilage diseases.

### 5.4.1. Effect of the drug delivery system on the biochemical properties of the cartilage explants treated with IL-1 $\alpha$

The objective of this chapter is to demonstrate the impact of the developed drug delivery system (Ket emulsion coated with POLY-A5) on the loss of sGAG, collagen and chondrocyte viability induced

by IL-1 $\alpha$  inside the cartilage. IL-1 $\alpha$  is the classical inducer of catabolic responses in chondrocytes, and prostaglandin synthesis in human chondrocytes (Hauser, 2010). Moreover, IL-1 $\alpha$  is one of the inflammatory cytokines that play an essential role in PTOA progression this is because as its levels increase at the early ( 0.043 ng/mL) and late stages (0.288 ng/mL) of OA ,which is not normally present at detectable levels in healthy joints, causes GAG and collagen loss by enhancing and stimulating matrix metalloproteinases (MMP) production (enzymes that can degrade all components of the extracellular matrix such as collagen and proteoglycan), and inhibiting cartilage anabolism (Van den Berg, 1999; Jayasuriya, 2013; McNulty *et al.*, 2013; Wojdasiewicz, Poniatowski and Szukiewicz, 2014; Mehana, Khafaga and El-Blehi, 2019). Generally, IL-  $\alpha$  level increase in OA as a results of cartilage damage and inflammation that lead to the activation of the immune system and release of pro-inflammatory molecules by the affected cells (Van den Berg, 1999; Jayasuriya, 2013; McNulty *et al.*, 2013; Wojdasiewicz, Poniatowski and Szukiewicz, 2014; Mehana, Khafaga and El-Blehi, 2019). Prostaglandins are also released in inflamed joints due to IL-1 $\alpha$  stimulation (Warren, 2000). PGs are an inflammatory mediator which play a significant role in the inflammation of OA joints by increasing the production of MMPs in chondrocytes leading to the degradation of the cartilage tissues (Lippiello, 1981; Attur *et al.*, 2008; Berenbaum, 2013). Generally, NSAIDs inhibit the COX enzyme, which is responsible for the conversion of arachidonic acid to PGs (Figure 1-8). Therefore, use of NSAIDs decreases the catabolic process in OA by inhibiting PG synthesis which contributes articular cartilage degeneration.

Furthermore, NSAIDs were used in this study in the form of o/w emulsion containing oleic acid. Using this types of emulsion has an advantage as oleic acid's anti-inflammatory properties can also treat inflammation in affected joints. Oleic acid delivers an anti-inflammatory effect by promoting the production of anti-inflammatory mediators such as IL-10 (Sales-Campos et al., 2013; Janke, Bennett and Tieleman, 2014). Additionally, it has an impact on the immune system which could explain its anti-inflammatory activity observed in the present study. Oleic acid inhibits the lymphoproliferative response and decreases neutrophil migration and accumulation at the site of inflammation, which highlights its potential role in reducing inflammation and alleviating the symptoms of osteoarthritis (Sales-Campos et al., 2013; Janke, Bennett and Tieleman, 2014). Moreover, it acts as a penetration enhancer when used as part of a drug delivery system. Consequently, both oleic acid and NSAIDs have a synergistic effect on treating OA. Based upon XTT and live/dead assays results, there were no toxic effects from using such a combination as the chondrocyte did not suffer negatively. Otherwise, they potentiated anti-inflammatory effects by preventing the catabolic effect of the inflammatory cytokine (IL-1 $\alpha$ ), and formation of NSAIDs emulsion using oleic acid as a penetration enhancer potentiated NSAIDs penetration inside the

cartilage tissue, which could explain the increased uptake of the drug there (Figures 4-11 to 4-18). Furthermore, it is now accepted that multiple delivery systems and drug combinations may be useful for disease treatment and modification (Bajpayee 2016). Therefore, combinations involving PBAEs, oleic acid and NSAIDs are promising for OA treatment. PBAEs and oleic acid act as the DDS while oleic acid and NSAIDs provide anti-inflammatory therapeutic treatment. In this chapter, ketorolac (to exemplify NSAIDs) in oleic acid o/w emulsion was used and coated with positively charged POLY-A5 as a module for OA and PTOA treatment.

The sGAG and collagen content were measured in this project because they are directly proportional to the ability of cartilage to tolerate compressive forces. In fact, cartilage extracellular matrix is rich in collagen macromolecule, which makes up about 60% of dry cartilage weight. Collagen structure consists of three polypeptide chains ( $\alpha$ -chains) folded into a triple helix (Figures 1-5 & 1-6). Glycine and proline are the primary amino acid composition of polypeptide chains, with hydroxyproline providing stability via hydrogen bonds along the length of the molecule. The triple helix structure provides important shear and tensile properties to the articular cartilage, helping to stabilise the matrix (Sophia Fox, Bedi and Rodeo, 2009; Carballo *et al.*, 2017). In addition, glycosaminoglycan is one of the main components of proteoglycans in cartilage ECM. GAGs are negatively charged carbohydrates with sulfation levels of repeating disaccharide units. They maintain the biomechanical properties of cartilage tissue by controlling hydration and swelling pressure, allowing tissue to absorb compressional forces (Sophia Fox, Bedi and Rodeo, 2009; Silva *et al.*, 2019). Therefore, measuring sGAG and collagen levels are essential to determining tissue repair properties (Warren, 2000).

The results for DMMB and hydroxyproline assays show that, by using the developed DDS, sGAG and collagen content in cartilage explants treated with IL-1 $\alpha$  can be successfully maintained for at least 2 weeks. Initially, it was found that stimulation of cartilage with IL-1 $\alpha$  caused significantly more (3 to 5 times) sGAG and collagen loss compared to the untreated control for the 14 days. In fact, a similar effect was shown in a study by Bajpayee *et al.* (2016) as IL-1 $\alpha$  treatment caused high (5 to 6 times) loss of sGAG compared to untreated control. Furthermore, Ket emulsion coated with POLY-A5 provides a significant increase ( $p < 0.01$ ) in sGAG and collagen content during the culture time compared to IL-1 $\alpha$  treated cartilage and are similar to the untreated control (Figures 5-1 & 5-2). In addition, Dex emulsion coated with POLY-A5 delivered similar results and protected the cartilage from the catabolic effect of IL-1 $\alpha$  (Figures 5-1 & 5-2). Other studies show that Dex is necessary for maintaining cartilage functional properties during long term culture (4 weeks) (Liming Bian *et al.*, 2010; Lu, Evans and Grodzinsky, 2011). Avidin-Dex has been found to significantly suppress loss of sGAG induced by cytokine for 14 days (Bajpayee *et al.*, 2016). Moreover, the developed DDS (consisting of Ket) demonstrated the ability to rescue chondrocytes from the deleterious effects of

cytokines, which are known to induce a decrease in chondrocyte viability. Notably, the rescue effect was found to be comparable to that of Dex emulsion (Figures 5-7 to 5-14) and Avidin-Dex (Bajpayee *et al.*, 2016). POLY-A5 facilitates Ket emulsion diffusion inside the cartilage zone to protect chondrocyte cells. Thus, the results support this study's hypothesis that using oleic acid to increase NSAIDs solubility and coating emulsion with POLY-A5 as a DDS is an effective way to deliver NSAIDs to OA cartilage and rescue cells from the catabolic effect of IL-1 $\alpha$ .

Dexamethasone was used as a positive control in this study. It is widely used as an intra-injection drug for OA treatment and has been utilised by researchers to investigate the effects of DDSs. For example, Avidin was conjugated with Dex to investigate its efficacy in ameliorating catabolic effects in cytokine-challenged OA cartilage (Bajpayee *et al.*, 2016). This led to strongly reduced cell death induced by IL-1 $\alpha$  for 8 days using a fluorescent staining assay (Bajpayee *et al.*, 2016). Moreover, the anti-inflammatory effects of intra-articular dexamethasone have been demonstrated to maintain the viability of chondrocytes treated with IL-1 $\alpha$  for 24 days (Grodzinsky *et al.*, 2017). In addition, Dex has been conjugated with A1 and A2 PBAEs polymers to test DDS effectiveness for increasing uptake and retention time inside cartilage tissue (Perni and Prokopovich, 2017). Therefore, it was used in the present study to assess its effect and compare it with Ket in the developed drug delivery system. The results appear promising, as it showed similar results by decreasing sGAG loss, maintaining collagen content, and preserving the viability of cartilage cells as it was able to protect chondrocyte cells from destruction when treated with IL-1 $\alpha$ , and did not suffer negatively or induced cell death for 14 days of culture (Figures 5-7 to 5-14).

It has been shown that using NSAIDs can accelerate degeneration of articular cartilage; Hauser R (2010) found evidence that NSAIDs can reduce the percentage of sGAG synthesis in cartilage by inhibition of prostaglandin E2 (PGE2), as it has a growth stimulatory effect on chondrocytes. However, the roles of prostaglandins and PGE2 in decreasing proteoglycan synthesis and enhancing degradation of both aggrecan and type II collagen has been addressed in various studies (Lippiello, 1981; Attur *et al.*, 2008; Berenbaum, 2013). These effects are associated with the upregulation of MMP and ADAMTS, two proteases which impact OA disease progression by increasing degradation of ECM components (Lippiello, 1981). Additionally, the results of this project highlight the effectiveness of NSAIDs in protecting cartilage proteoglycans from the inflammatory and inhibitory roles of IL-1 $\alpha$ . This work used 4 mg/mL of NSAIDs; despite that, the percentage of sGAG synthesis was higher than IL-1 $\alpha$  treated cartilage (similar to the untreated control). This is mainly because POLY-A5 was used as a delivery system which can penetrate through cartilage tissue via electrostatic interaction and be hydrolysed within the tissue resulting in an effective DDS to deliver anti-inflammatory drugs inside cartilage. In addition, using NSAIDs as an emulsion with oleic acid would

potentiate the anti-inflammatory effects and inhibit the catabolic role of cytokines (Pérez-Martínez *et al.*, 2016).

#### **5.4.2. Viability of cartilage tissue over 20 days**

It was found that the cartilage explant cultures required a period of up to 4-6 days to equilibrate to the *in vitro* environment following harvesting. During this initial period of culture, there was a significant reduction in XTT conversion or mitochondrial activity in cartilage tissue. This was followed by consistent values for XTT conversion by the untreated control sample, for up to 20 days of culture. The day 20 XTT results revealed that IL-1 $\alpha$  treatment of the cartilage tissue resulted in the loss of most cartilage cell viability, clearly showing that treated cartilage samples with IL-1 $\alpha$  cause significant cell death within cartilage tissue. The day 20 results for safranin O cell-stained cartilage tissue slices that had been treated with IL-1 $\alpha$  were in agreement with the XTT data as the staining intensity decreased in the IL-1 $\alpha$  treated sample. Adding Ket emulsion coated with POLY-A5 significantly maintained cell viability for the 20 days of the tissue culture (Figures 5-15 & 5-16).

The levels of sGAG were reduced in IL-1 $\alpha$  treated samples compared to untreated cartilage, indicating the loss of sGAG from the tissue as cartilage is degraded; this which was clearly visible in the safranin O staining results. The staining intensity was reduced in IL-1 $\alpha$  treated cartilage, signifying reduction in sGAG content in the samples (Figure 5-15). Generally, glycosaminoglycan is not homogeneously distributed in cartilage, and safranin O staining also allows the investigation of its spatial distribution; thus, this work was able to determine that the recovery observed with NSAIDs also restored the necessary GAG distribution.

The cartilage tissue treated with IL-1 $\alpha$  showed an increase in GAG release into the medium, which might have been due to the wash-out of proteoglycans from the ECM as a result of interruption of the non-covalent interactions between aggrecan and long chain hyaluronic acid molecules in the cartilage (Elson *et al.*, 2015). Moreover, there was no increase in GAG release in the cartilage tissue cultures treated with the developed DDS, indicating its effectiveness in maintaining cartilage tissue integrity compatible with that detected in control cultures.

Finally, *ex vivo* pre-clinical studies of novel therapies are important initial steps in the clinical translation pathway (Anz *et al.*, 2014). Many therapies will not progress beyond this initial phase of development, and therefore efficient pre-clinical test methods are essential. The measurement of cell viability, GAG, collagen, and cell integrity in tissue culture are important steps in confirming therapy efficacy and reducing costs before undertaken in *in vivo* studies.

## **5.5. Conclusion:**

This work has proven that NSAIDs and oleic acid-based o/w emulsion coated with PBAEs is an effective delivery system for cartilage due to the electrostatic forces of attraction between the negatively charged GAGs in the tissue and the positively charged PBAEs. The data presented has demonstrated that IL- $\alpha$  induced loss of tissue viability in bovine cartilage tissue culture models, but viability was maintained after adding the developed DDS that contained ketorolac (model NSAIDs) and oleic acid-based emulsion coated with POLY-A5; this was equivalent to untreated control cultures without impacting chondrocyte viability and metabolic activity. The drug delivery system is effective in both untreated and GAG depleted cartilage in reducing the percentage of sGAG loss and maintaining collagen content. In addition, there was no observed effect on chondrocyte viability using the live/dead and XTT assays compared to the samples that were treated with Ket alone or cytokine (IL-1 $\alpha$ ). Moreover, Ket effect was similar to dexamethasone, which was used as a positive control in this study. Therefore, the developed drug delivery system is effective, and the approach presented here could provide substantial improvements to therapeutic treatments of OA and thus to patient outcomes.

## **6. Chapter 6: Effect of different types of PBAEs on the efficacy of emulsion-based drug delivery system containing Ketorolac**

### **6.1. Introduction**

As previously discussed, PBAEs are able to penetrate into cartilage tissue and act as carriers for NSAIDs, due to electrostatic attraction between negatively charged components of the cartilage extracellular matrix and positively charged PBAEs (Perni and Prokopovich, 2017; Saeedi and Prokopovich, 2021). In this chapter, a large library of PBAEs is synthesised and used as a vehicle for transporting ketorolac into cartilage tissue to screen the ability of PBAEs to deliver ketorolac to cartilage tissue effectively and to develop a novel approach for treating osteoarthritis (OA). As a result, it is hypothesized that the drug may be able to target the site of inflammation within cartilage tissue, thereby minimizing systemic exposure and adverse effects.

#### **Aims of chapter 6:**

- 1) Design and synthesise a novel DDS composed of oleic acid (oil) in water Ket (model NSAIDs) emulsion and then coated with 15 different types of PBAEs: POLY-A1, POLY-B1, POLY-D1, POLY-E1, POLY-F1, POLY-A3, POLY-B3, POLY-D3, POLY-E3, POLY-F3, POLY-A5, POLY-B5, POLY-D5, POLY-E5, and POLY-F5.
- 2) Examine polymer characterisation in term of size and charge using Zetasizer Nano ZS apparatus.
- 3) Measure levels of Ket uptake and retention inside untreated and GAG depleted cartilage tissue when coated with the developed DDS.
- 4) Measure polymer effect on cartilage tissue proliferation using XTT assay.
- 5) Identify promising PBAE and measure their effects on reducing the amounts of sGAG and collagen released from cartilage tissue while exposed to IL-1 $\alpha$  using DMMB, collagen content measurement, live/dead assay and histological evaluation of cartilage tissue using safranin O staining methods.

### **6.2. Materials and methods**

Cartilage was extracted from bovine as an ex vivo model for OA treatment to build both cartilage models (as discussed in chapter 3). A novel drug delivery system was then developed, composed of 10% emulsion with oleic acid coated with 15 types of PBAEs that encapsulated Ket as a model for NSAIDs. The details assay method is provided in chapter 2.

## 6.3. Results

The results of the particle characterisation using zeta potential and size measurement are presented in this section, together with cartilage uptake and retention experiment results, sGAG and collagen content determination, and XTT, live/dead and safranin O staining imaging.

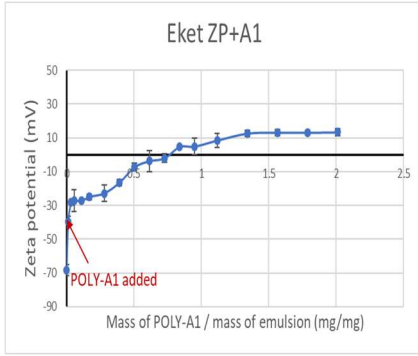
### 6.3.1. Zeta potential measurement

Zeta potential (mV) was calculated to predict the amount of each polymer required to coat the Ket emulsion completely (Table 6-1), and also to measure polymer charges and to determine interaction between the positively charged POLY-X polymers and the negatively charged Ket o/w emulsion. As shown in Figure 6-1, each polymer interacted differently with Ket o/w emulsion in terms of amount required for complete coating. For example, 1800  $\mu\text{l}$  of POLY-F1 was required to completely coat Ket emulsion and to change its negative charge from -73.9mV to +23.1 mV, while only 80  $\mu\text{l}$  of POLY-B5 was needed to convert it to +20 mV. This could be due to differences in polymer net charges, which are dependent on acrylates and amine structure. In these experiments, a relatively high amount of acrylate F was typically required to fully coat Ket emulsion, compared to the other acrylates bound with the same amine group. For example, 1800  $\mu\text{l}$  of POLY-F1 was needed to coat Ket emulsion and change its charge to +23.1mV, whereas only 1000-1500  $\mu\text{l}$  of POLY-X1 was required for this (Table 6-1).

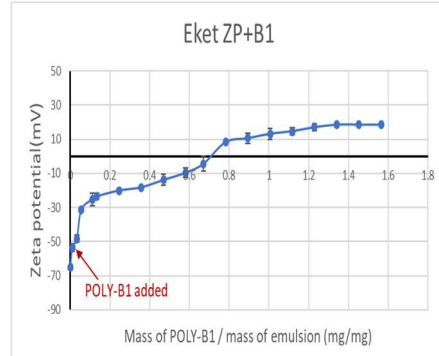
Table 6-1 Characterisation of coated emulsion – zeta potential (mV) values for Ket emulsion before and after coating with POLY-X and the amount of each POLY-X which required to coat Ket emulsion completely ( $\mu\text{L}$ ).

Poly beta amino ester polymers	ZP (mV) for the polymer alone	ZP (mV) for Ket emulsion + POLY-X	Amount of POLY-X (2 mg/mL) added ( $\mu\text{L}$ )
Ket o/w emulsion	-73.9 $\pm$ 0.5		
POLY-A1	+12.3 $\pm$ 3.5	+13.3 $\pm$ 2.3	1500
POLY-B1	+11.4 $\pm$ 1.4	+18.4 $\pm$ 0.8	1300
POLY-D1	+14.1 $\pm$ 1.6	+5.7 $\pm$ 1.3	1000
POLY-E1	+13.8 $\pm$ 3.8	+12.6 $\pm$ 0.7	1500
POLY-F1	+13.9 $\pm$ 8.5	+23.1 $\pm$ 0.5	1800
POLY-A3	+15.4 $\pm$ 1.5	+33.3 $\pm$ 1.9	360
POLY-B3	+16.8 $\pm$ 2.9	+31.8 $\pm$ 2.6	650
POLY-D3	+17.1 $\pm$ 1.4	+39.2 $\pm$ 3.9	600
POLY-E3	+11.3 $\pm$ 0.7	+42.2 $\pm$ 1.6	650
POLY-F3	+19.0 $\pm$ 5.5	+39.6 $\pm$ 2.3	650
POLY-A5	+12.6 $\pm$ 0.4	+17.1 $\pm$ 1.9	160
POLY-B5	+18.7 $\pm$ 0.9	+20.2 $\pm$ 3.6	80
POLY-D5	+9.7 $\pm$ 0.4	+9.3 $\pm$ 0.7	180
POLY-E5	+7.3 $\pm$ 0.7	+8.6 $\pm$ 1.4	500
POLY-F5	+12.9 $\pm$ 0.3	+18 $\pm$ 4.3	500

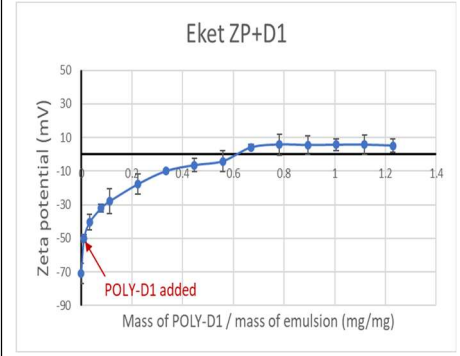
### POLY-A1



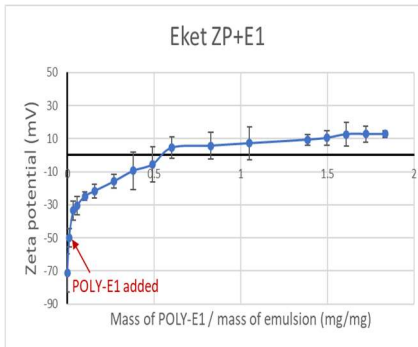
### POLY-B1



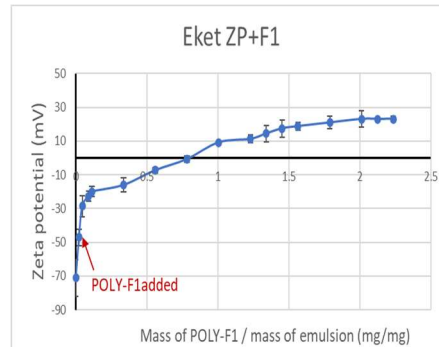
### POLY-D1



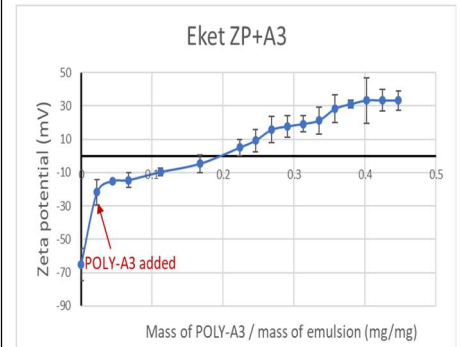
### POLY-E1



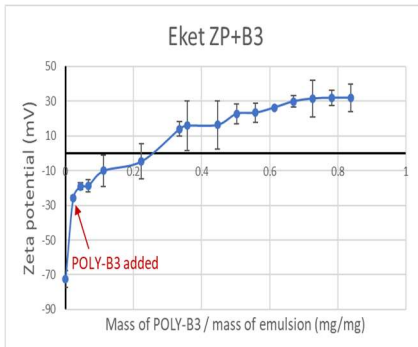
### POLY-F1



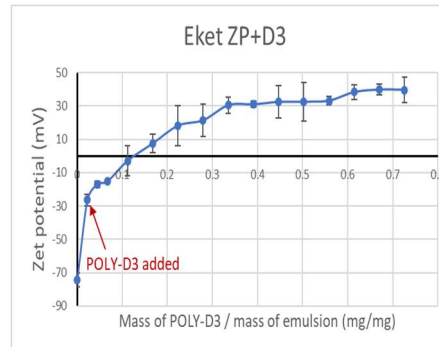
### POLY-A3



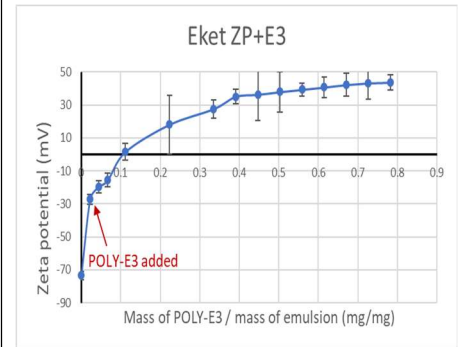
### POLY-B3



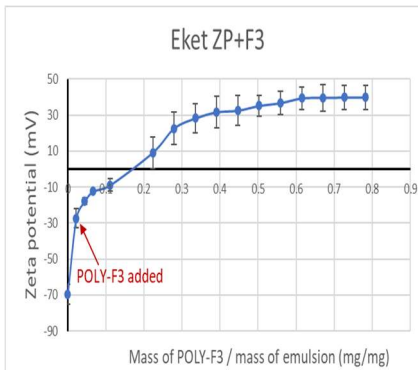
### POLY-D3



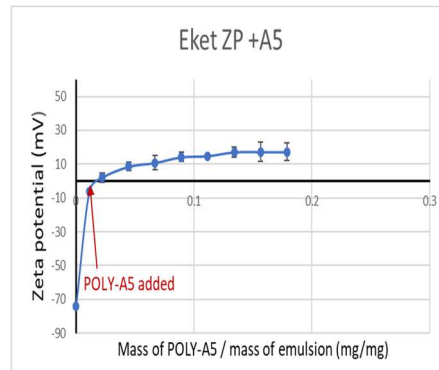
### POLY-E3



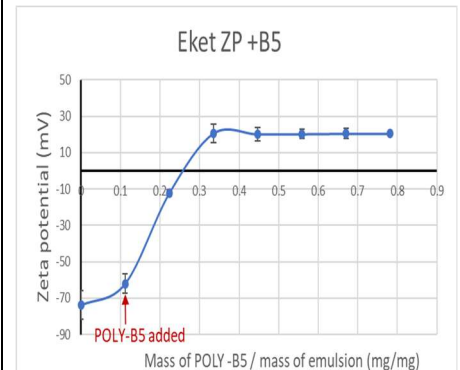
### POLY-F3



### POLY-A5



### POLY-B5



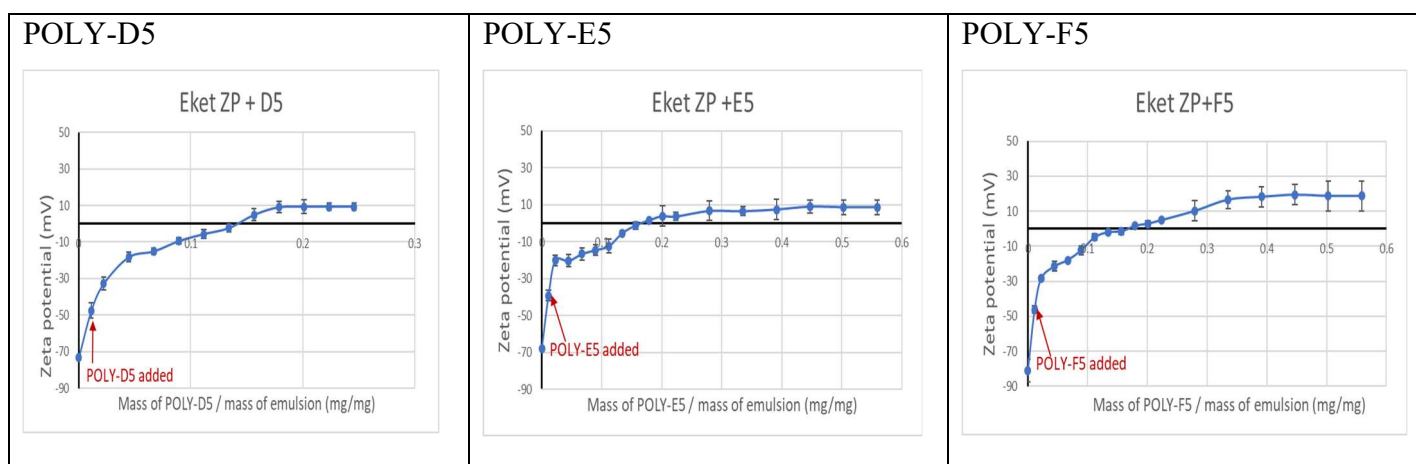


Figure 6-1. Zeta potential (mV) value of Ket emulsions during coating with 14 types of poly-beta amino ester polymers until reach the saturation (1  $\mu$ l of Ket emulsion +10  $\mu$ l of POLY-X) and change the emulsion charge to positive.

### 6.3.2. Size

The size distributions of Ket o/w emulsion and POLY-X coated Ket o/w emulsion were measured using DLS, as shown in Table 6-2. The initial particle size of Ket o/w emulsion was measured, it brings equal to  $0.09 \pm 0.02 \mu\text{m}$ . Then, the size was measured again after the exact amount of the POLY-X needed to completely coat the emulsion was added. As shown in Table 6-2, coating Ket o/w emulsion with POLY-A1, POLY-B1, and POLY-F5 led to tenfold increase in Ket particle size, while the increase was 20 times when coated with POLY-E1, POLY-B3, POLY-A5, and POLY-B5. In contrast, using POLY-F1 and POLY-E5 to coat Ket emulsion led to its size increasing 4 times with the difference being statistically significant ( $p > 0.05$ ). The reason for this variance in particle size among the polymers could be due to differences in electrostatic forces of attraction between the oil droplets and POLY-X making the particles interact in variable manners, thereby leading to different sizes. Overall, coating Ket emulsion with POLY-X polymers led to considerable increased in Ket particle sizes (Table 6-2).

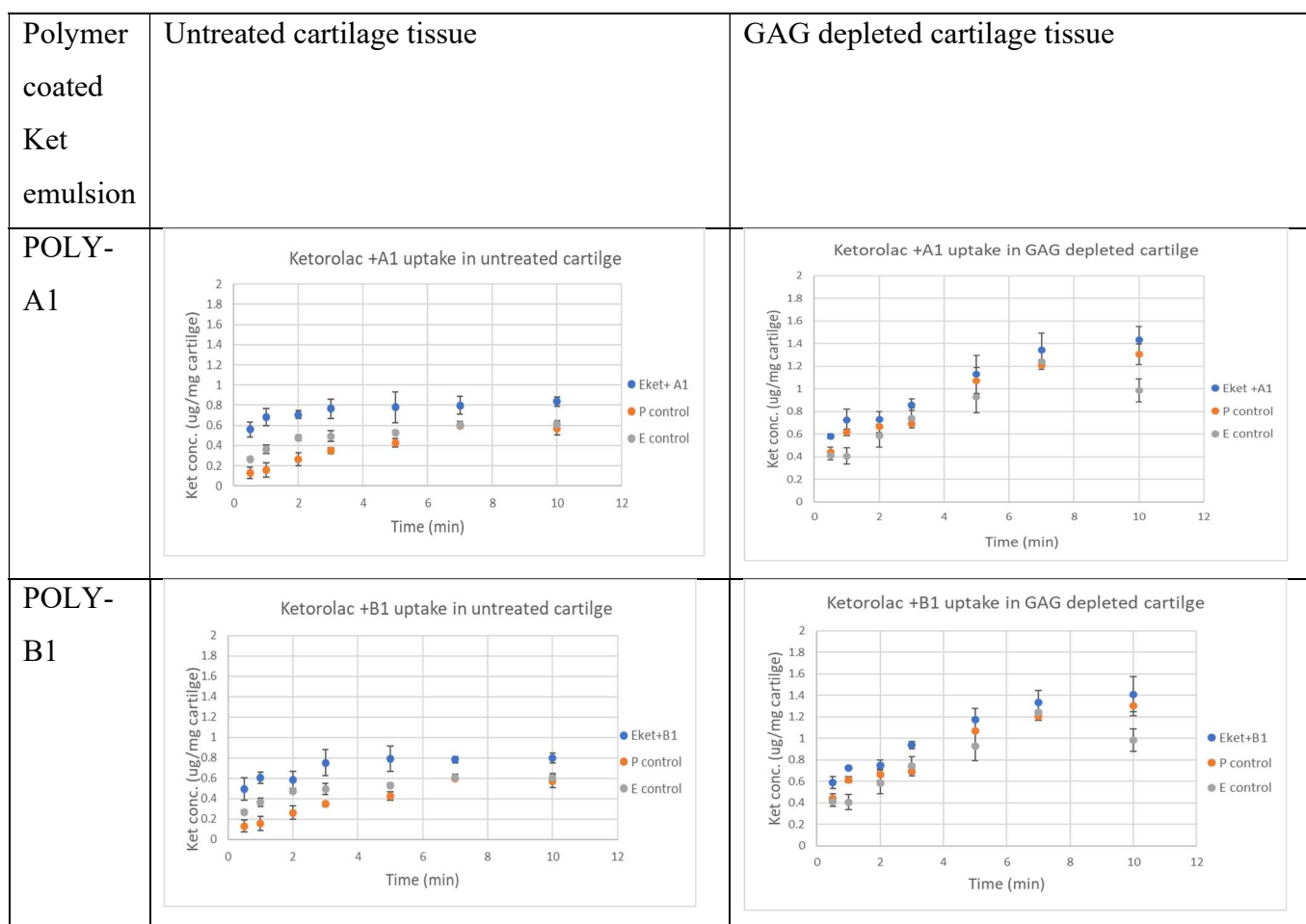
Table 6-2 Size measurements ( $\mu\text{m}$ ) for Ket emulsions coated with 14 different types of poly-beta amino ester polymers. The results show variations in size measurements of the coated emulsions among the different types of poly-beta amino ester polymers used.

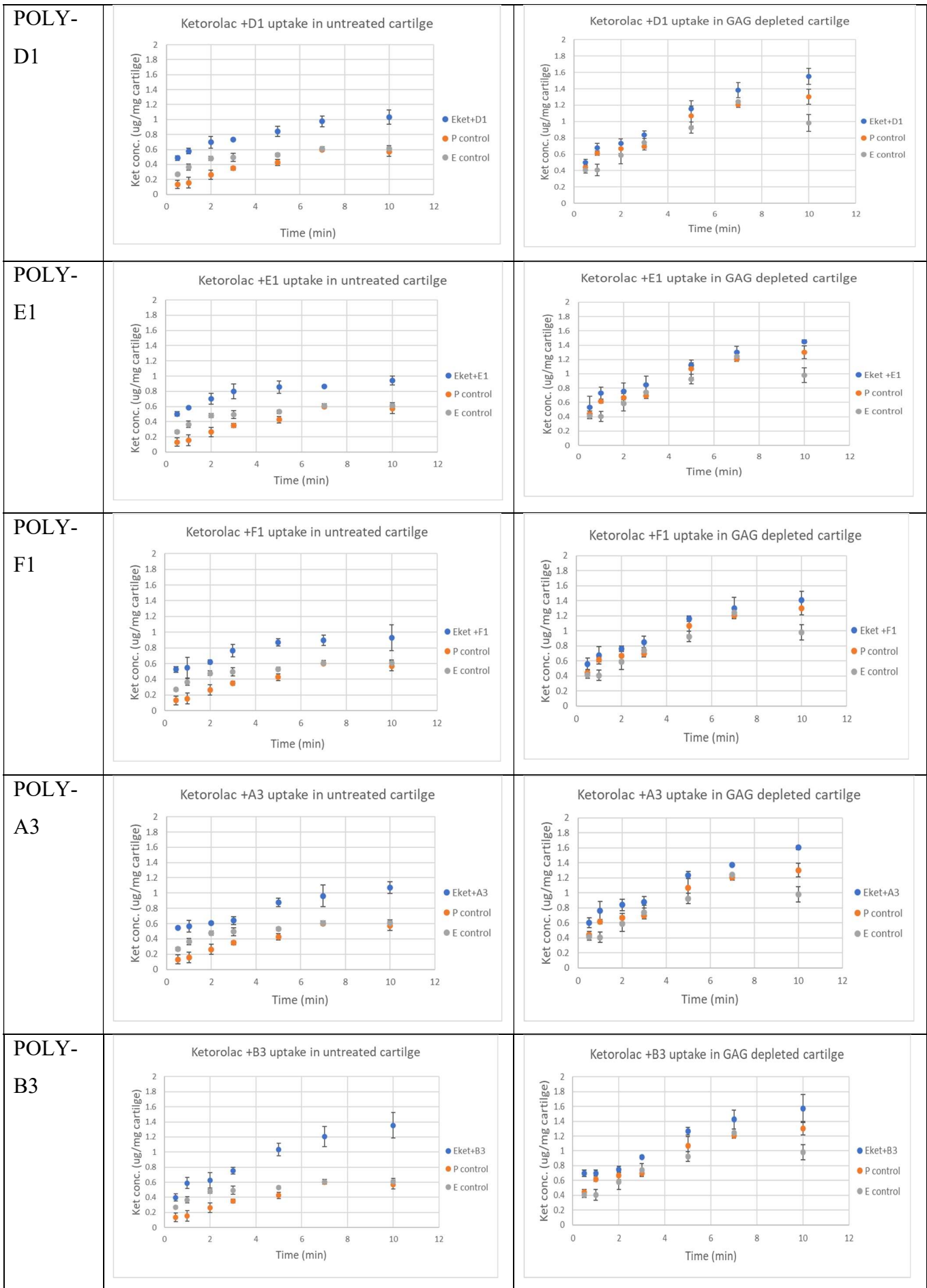
Polymer name	Size diameter ( $\mu\text{m}$ ) after polymer added (the amount is in table 6-1)
POLY-A1	2.13 $\pm$ 0.20
POLY-B1	2.92 $\pm$ 0.19
POLY-D1	3.46 $\pm$ 0.57
POLY-E1	4.53 $\pm$ 0.31
POLY-F1	0.7 $\pm$ 0.06
POLY-A3	1.03 $\pm$ 0.08
POLY-B3	4.01 $\pm$ 0.19
POLY-D3	1.53 $\pm$ 0.15
POLY-E3	1.46 $\pm$ 0.06
POLY-F3	1.85 $\pm$ 0.18
POLY-A5	2.00 $\pm$ 0.08
POLY-B5	2.30 $\pm$ 0.40
POLY-D5	3.23 $\pm$ 0.90
POLY-E5	0.72 $\pm$ 0.09
POLY-F5	2.24 $\pm$ 0.30
Size of Ket emulsion alone	1.50 $\pm$ 0.02

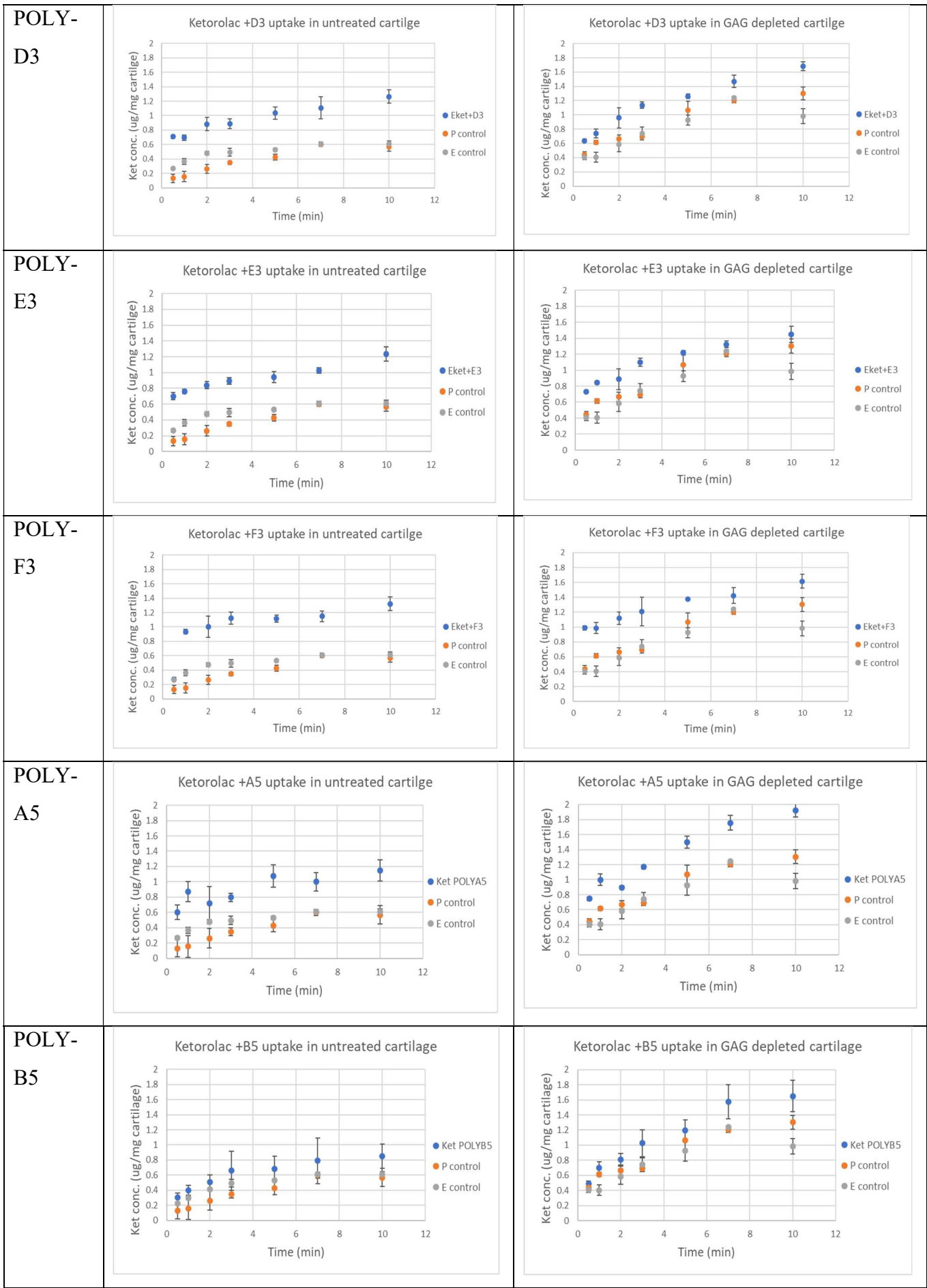
### 6.3.3. Drug uptake measurement

Figure 6-2 shows cartilage uptake for 10 min of Ket after using POLY-X coated Ket o/w emulsion compared to Ket alone and Ket o/w emulsion. It is clear that the amount of Ket cartilage penetration increased over the course of that time. Coating Ket o/w emulsion with POLY-X generally induced an increase in Ket uptake duration delivered through POLY-X compared to the commercial formulations of Ket (P control) and Ket o/w emulsion (E control), with the difference being statistically significant ( $p < 0.001$ ). When GAG depleted samples were used, it was found that despite relying on the negative charges of GAG molecules to deliver to the cartilage, POLY-X was more effective in relation to GAG depleted cartilage, exhibited about 50% of the untreated tissues. The overall effect was higher in GAG depleted compared to untreated cartilage (Figure 6-2).

The amine constituents of the polymer back-bone had an effect on the amounts obtained, the most effective being N, N-bis 3-(methylamino) propyl methylamine (compound 3), followed by 3-(dimethylamino)-propylamine (compound 5), and piperazine (compound 1). Generally, the presence of extra nitrogen in the amines is capable of increasing the positive charges of the polymer chain, leading to an increase in electrostatic attraction between the negatively charged polymers and the extracellular cartilage matrix. When cartilage was exposed to the same concentration of Ket (either the commercial formulation of Ket, Ket o/w emulsion, or the coated form with POLY-X), the Ket o/w emulsion coated with POLY-X resulted in a higher amount of the drug in the cartilage even after a very short time (1 min) (Figure 6-2). Overall, all 15 types of POLY-X examined were similarly effective in increasing Ket uptake inside the cartilage tissue, especially in GAG depleted samples and in comparison, to the controls. The results demonstrate that Ket could be delivered into cartilage more easily and effectively using PBAE polymers in emulsion form.







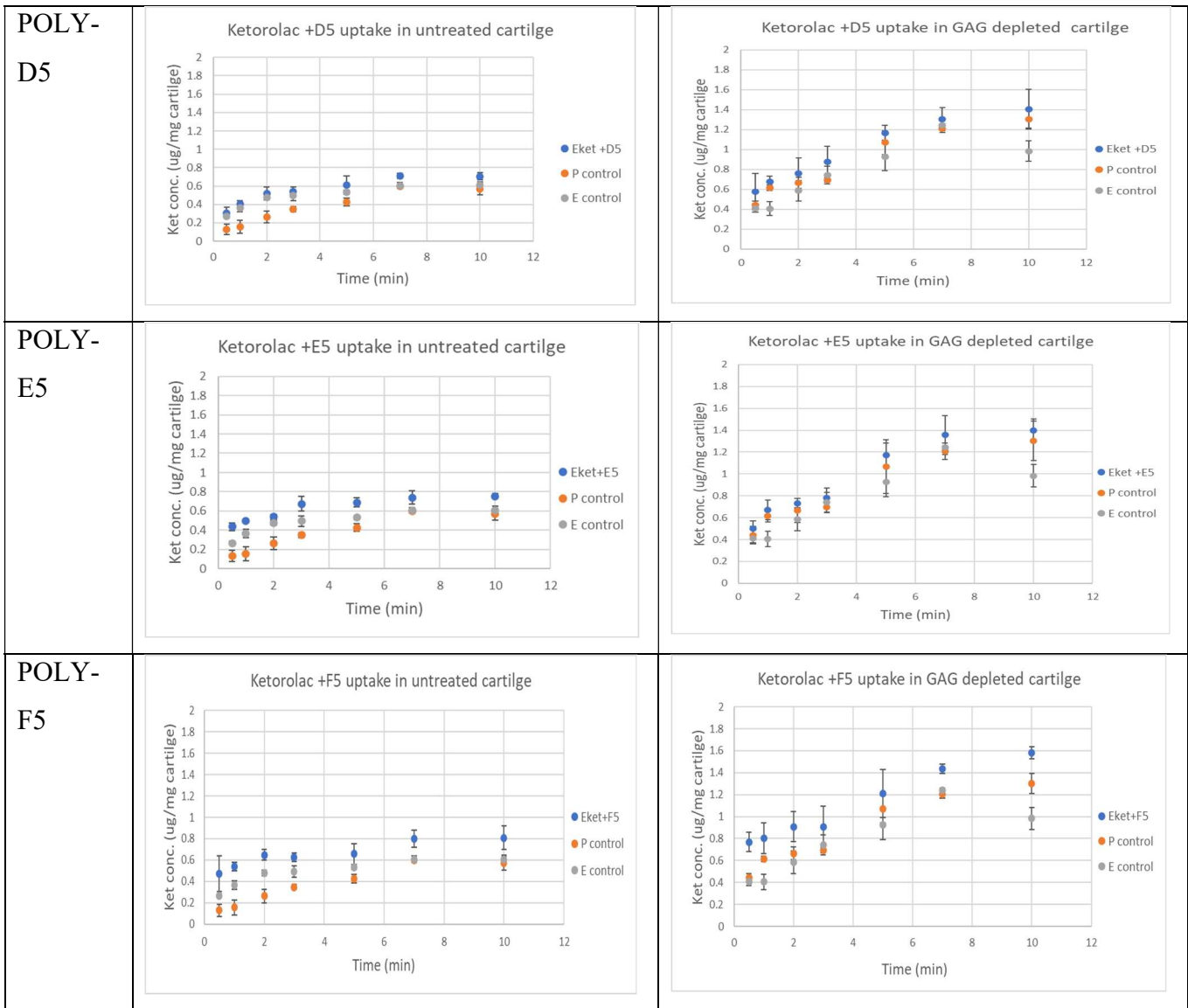
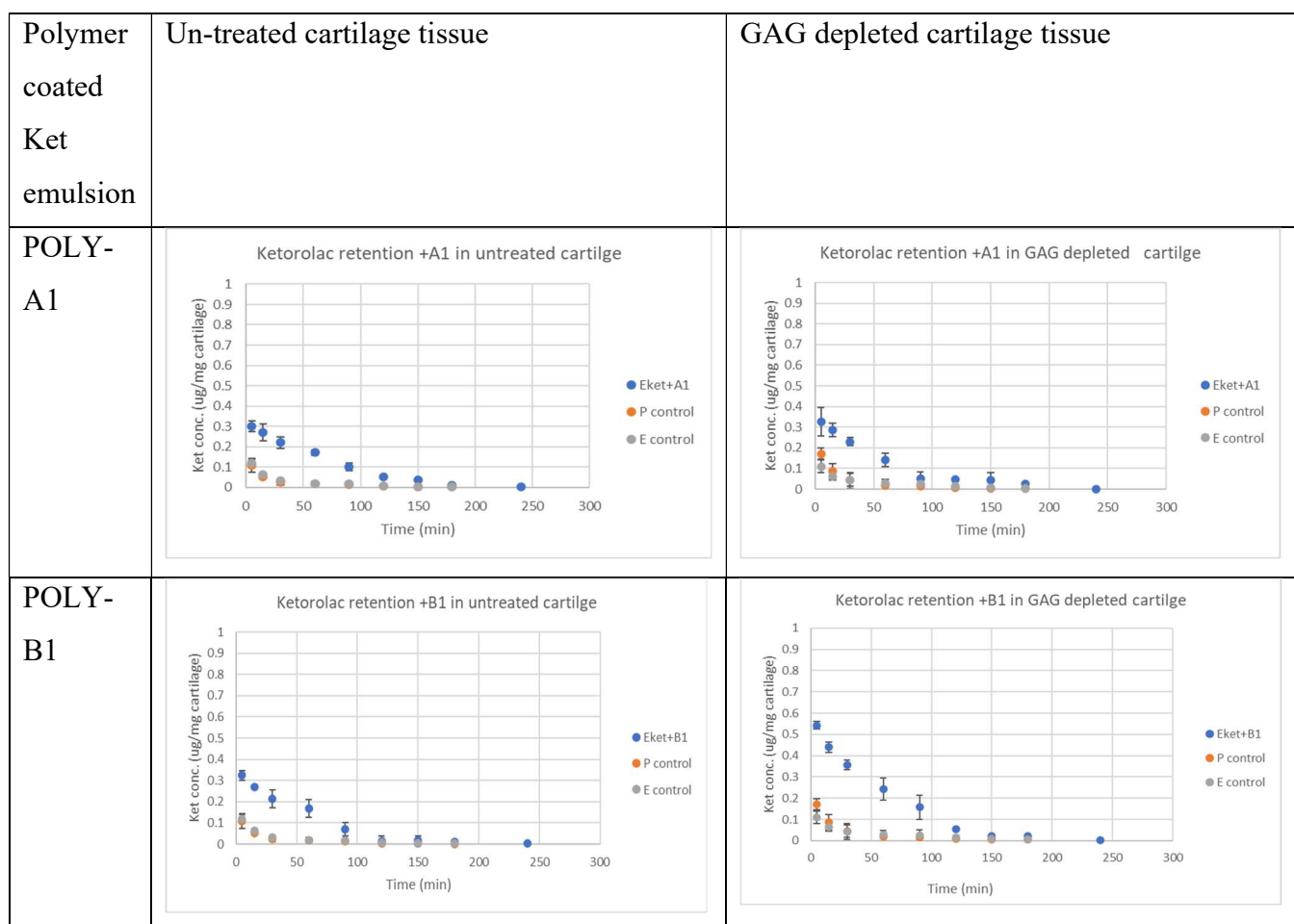
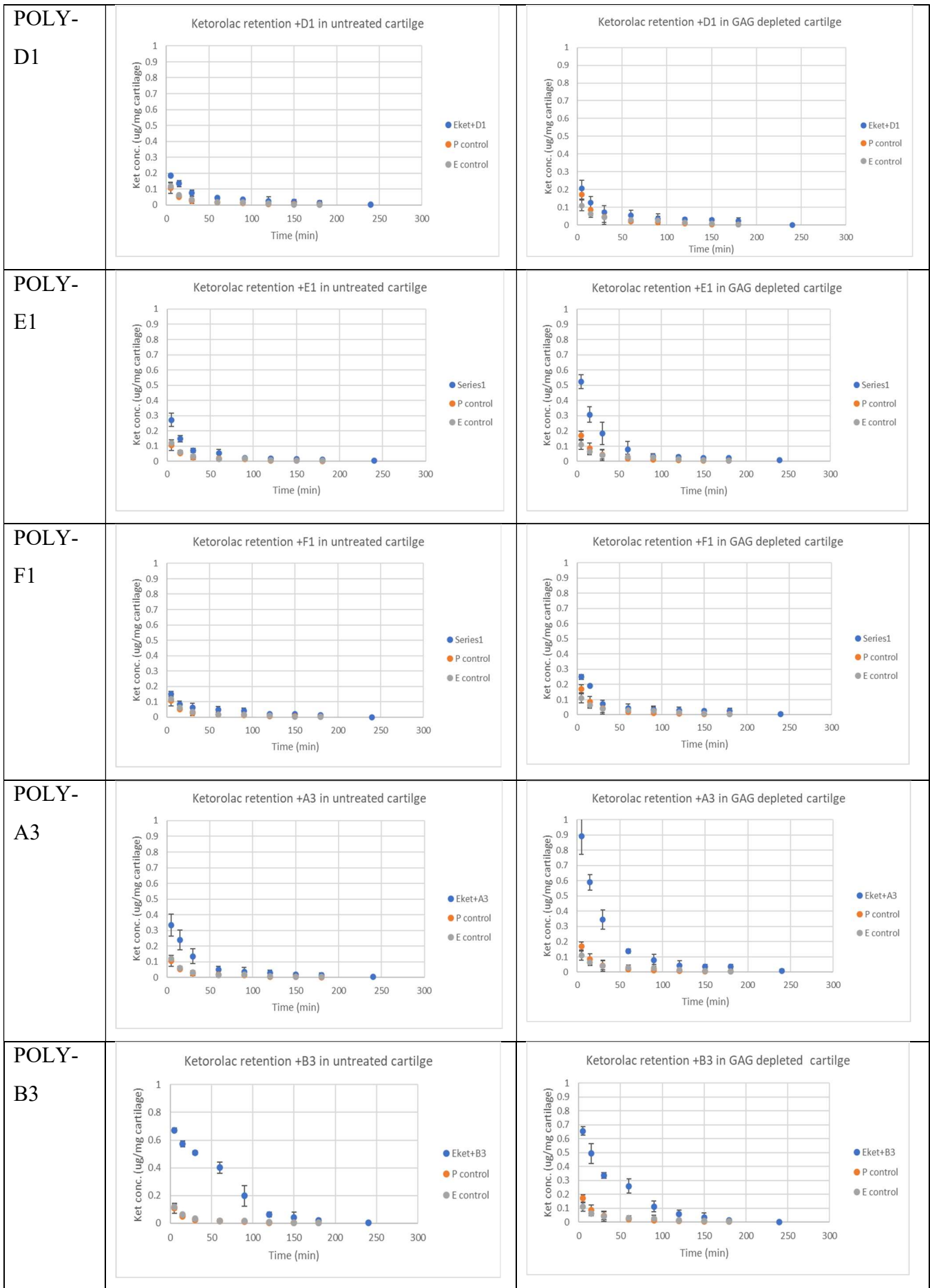


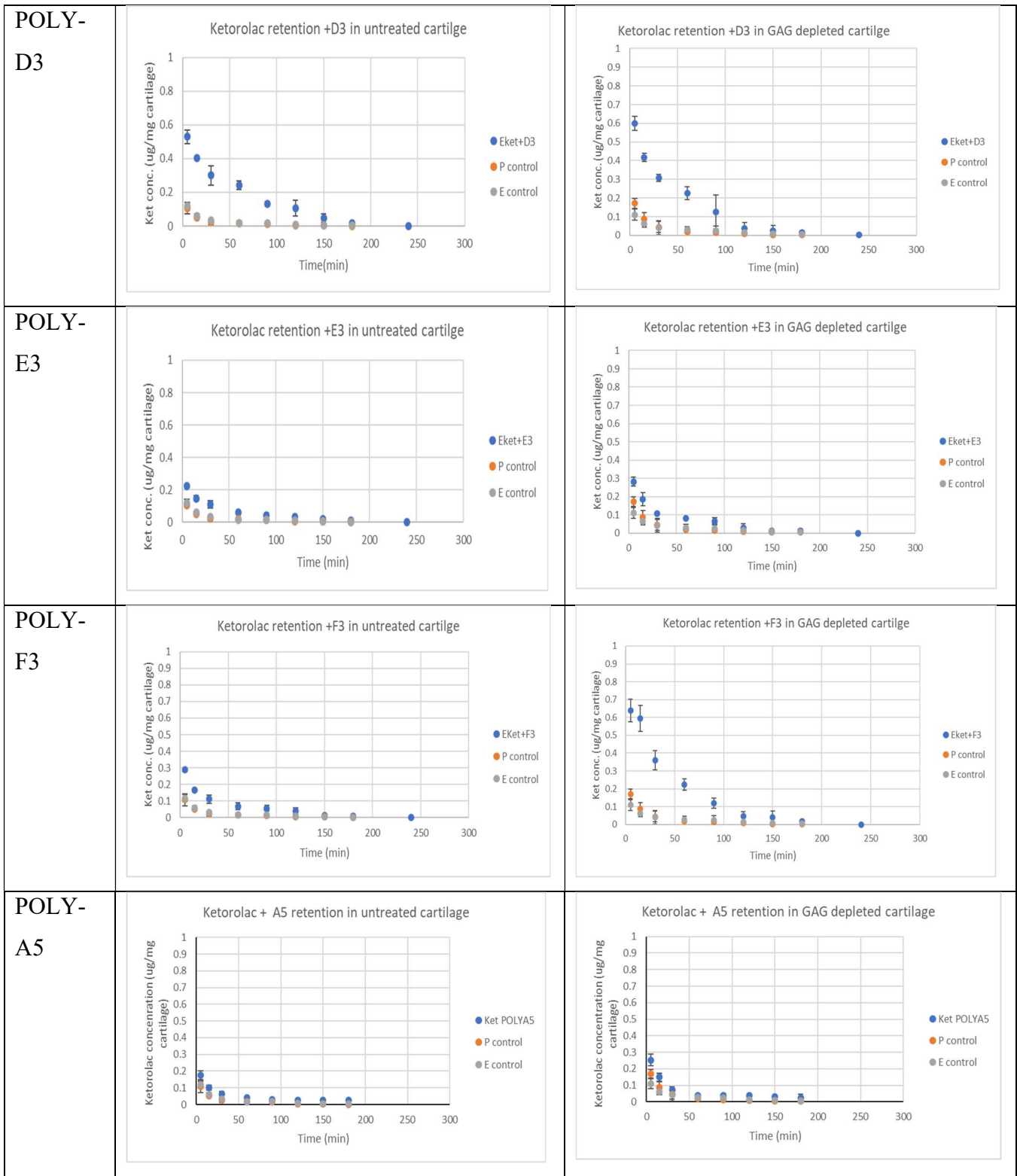
Figure 6-2. Comparison of Ket uptake into cartilage for 10 min using P control (Ket in PBS), E control (Ket o/w emulsion) and Ket o/w emulsion saturated with POLY-X in both untreated and GAG depleted cartilage. The concentration of Ket that has penetrated the cartilage is expressed in  $\mu\text{g}$  per mg cartilage. Ket uptake was higher in GAG depleted cartilage than the untreated cartilage samples.

### 6.3.4. Drug retention duration measurement

Figure 6-3 shows a comparison between Ket retention duration inside of untreated cartilage and GAG depleted cartilage using the aforementioned 15 types of PBAE polymers. Ket was released quickly from the cartilage in the untreated sample, while Ket concentration fell below the detection limit after about 2 hours in the case of the controls. However, when POLY-X was used to coat the emulsion droplet, Ket was still detectable in the cartilage even after 3 hours. In GAG depleted cartilage, release was slower than in the untreated samples, yet the amount of Ket left in the tissue when Ket o/w emulsion coated with POLY-X was used was always higher than for the controls. Coated Ket o/w emulsion with POLY-B5 saw a prolonged retention duration inside the cartilage tissue (6 hours), whereas the emulsions coated with other examined types of POLY-X retained the drug for around 4 hours inside the cartilage tissue. Overall, all 15 types of POLY-X considered effective in increasing Ket retention time inside the cartilage tissue compared to either of the controls (P and E), which was successfully prolonging it from 2 hours to 4-6 hours (Figure 6-3).







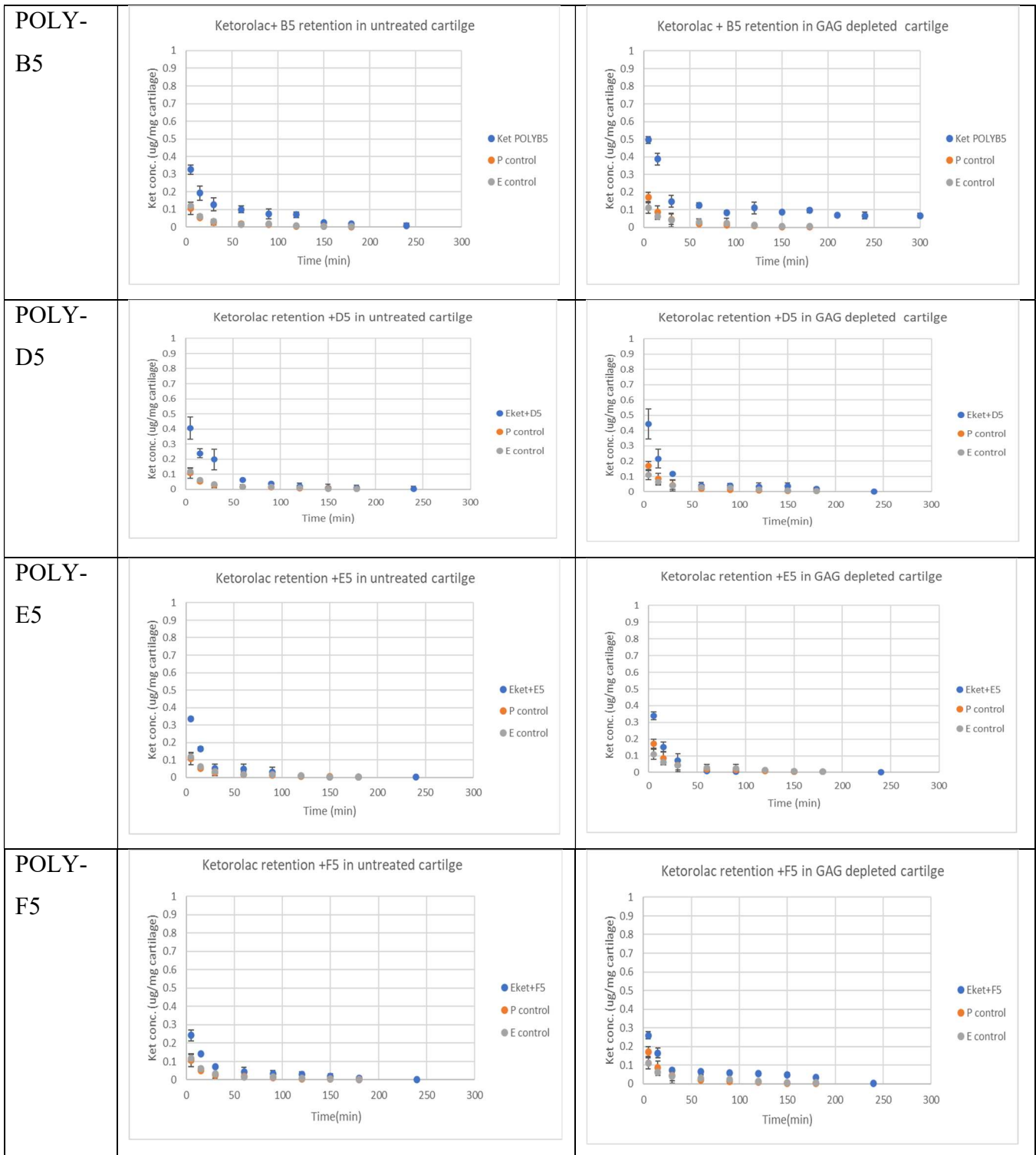


Figure 6-3. Comparison of Ket retention into cartilage for 300 min (5 hours) using P control (Ket in PBS), E control (Ket o/w emulsion) and Ket o/w emulsion saturated with POLY-X in untreated and GAG depleted cartilage samples. The concentration of Ket that has penetrated the cartilage is expressed in  $\mu\text{g}$  per mg cartilage. Ket retention time was prolonged (4-6 hours) using Ket o/w emulsion coated with POLY-X compared to P and E controls.

### 6.3.5. XTT

Use of the XTT assay for assessing cartilage tissue viability indicated that it showed reduced XTT conversion from day 0 to 20 when treated with IL-1 $\alpha$  ( $p < 0.01$ ), compared to the untreated control. Adding POLY-X to the cartilage media-maintained cell viability compared to samples treated with IL-1 $\alpha$  alone (Figure 6-4). These results show that POLY-X are not toxic to cartilage tissue as it maintained its viability compared to IL-1  $\alpha$  treated samples. Moreover, the viability of chondrocytes was not affected by the presence of POLY-X in the media, which is essential for medical applications so as to exclude any cytotoxicity. POLY-A5, POLY-B5, POLY-E1, POLY-F3, and POLY-E5 were most effective in preserving high amounts of XTT in cartilage samples, indicating cartilage cell viability similar to the untreated control over 20 days (Figure 6-4). PBAEs are known to be cytocompatible, but this is the first time that they have been shown in chondrocytes, thereby proving their safety in cartilage tissue.

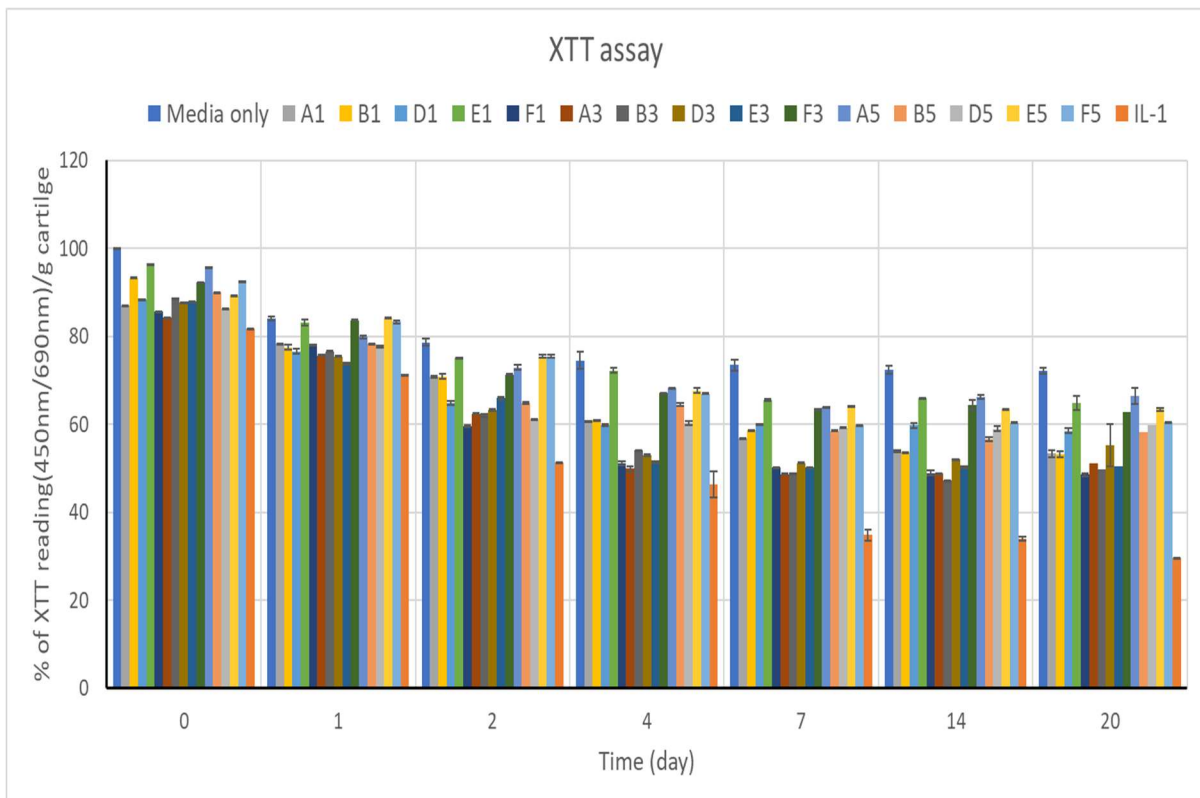


Figure 6-4. Viability assessment of cartilage tissues treated with POLY-X over 20 days in culture. Cartilage cell was not affected by the presence of POLY-X on media compared to samples that were treated with IL-1 $\alpha$ .

## **Bovine ex vivo model**

Based on the previous experiments using the 15 different types of PBAE polymers and after balancing all of the assay parameters (XTT results, uptake, and retention measurement), POLY-B5 and POLY-F3 were chosen for efficacy testing using an IL-1 $\alpha$  exposure ex vivo model. The loss of sGAG was measured, the collagen content was determined, an imaging analysis of live/dead cells was performed, along with a safranin O staining imaging.

### **6.3.6. Glycosaminoglycan (GAG) loss measurement**

To test the efficacy of the developed drug delivery system in inhibiting IL-1 $\alpha$  induced GAG loss in bovine cartilage, sGAG quantities was measured using DMMB assay. Cartilage explants were treated with Ket o/w emulsion coated with POLY-B5 and POLY-F3 with/without IL-1 $\alpha$  and different types of controls for 20 days (as shown in Figures 6-5).

Cartilage samples cultured in media showed a slight decrease in sGAG content loss over a period of 20 days ( $18.6 \pm 10\%$ ) (Figure 6-5). When IL-1 $\alpha$  was added to the media, progressive ECM degradation was observed and more than 50% of the initial sGAG was lost after 72 hours. The simple addition of Ket o/w emulsion coated with POLY-B5 or POLY-F3 to the media containing IL-1 $\alpha$  reduced the inhibitory activity of IL-1 $\alpha$ , with the difference being statistically significant ( $p < 0.001$ ). After 20 days, the untreated cartilage samples had lost around 17% of sGAG content, compared to 66% from IL-1 $\alpha$  treated cartilage. Moreover, when the IL-1 $\alpha$  treated cartilage was exposed to POLY-B5 and POLY-F3 with/without Ket it led to a remarkable decrease in sGAG loss percentage ( $p < 0.001$ ). The percentage of sGAG loss was 3 to 5 times higher in IL-1 $\alpha$  treated cartilage, compared with the untreated group (in media only) and the Ket o/w emulsion coated with POLY-B5 or POLY-F3 treated group ( $p < 0.001$ ) (Figure 6-5). Therefore, Ket emulsion coated with POLY-B5 or POLY-F3 was sufficient to suppress IL-1 $\alpha$  induced sGAG loss from cartilage, making it an effective means of overcoming the catabolic effect of IL-1 $\alpha$  on OA cartilage as an inflammatory cytokine.

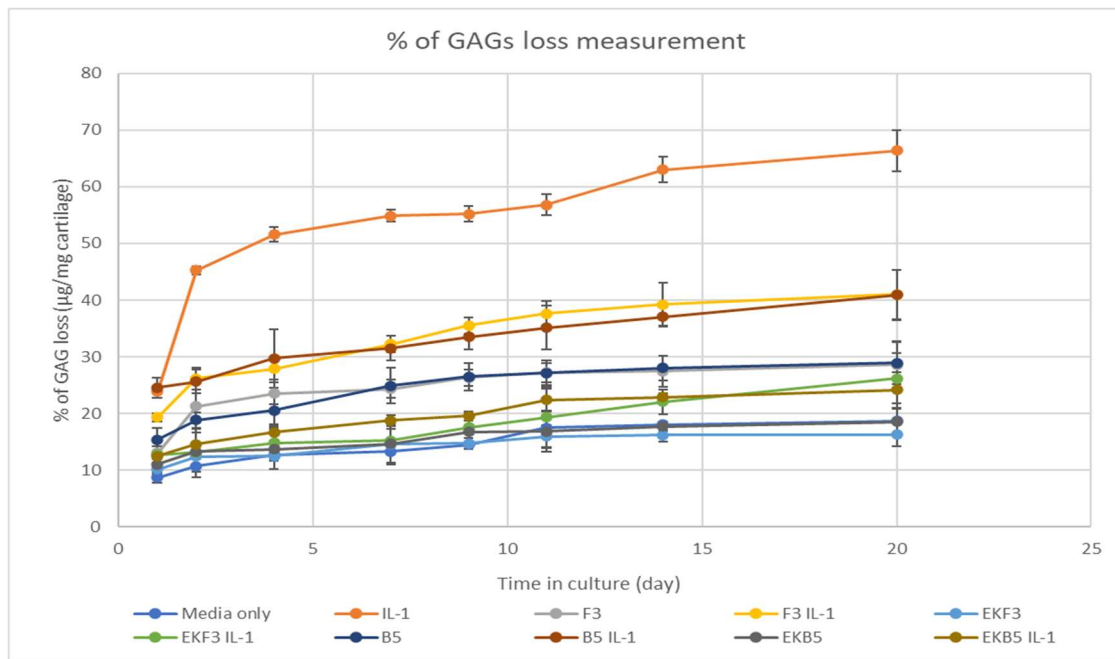


Figure 6-5. Quantification of sGAG in IL-1 $\alpha$  treated cartilage using DMMB assay for 20 days. Using emulsion Ket coated with POLY-B5 and POLY-F3, IL-1 $\alpha$ , POLY-B5 and POLY-F3 with/without IL-1 $\alpha$ . The percentage of sGAG loss was 3-5times higher in IL-1 $\alpha$  treated cartilage compared to the untreated group and Ket emulsion coated with POLY-B5 or POLY-F3 treated group ( $p < 0.001$ ).

### 6.3.7. Collagen content determination

Cartilage sample cultures in media containing IL-1 $\alpha$  showed a 50% drop in collagen content during the first week. This was followed by a steady decrease up to the 2-week point ( $0.1 \pm 0.01$  mg), which was significantly lower ( $p < 0.01$ ) than untreated cultured samples ( $0.5 \pm 0.05$  mg). Overall, collagen degradation product was significantly lower following IL-1 $\alpha$  stimulation than any of the controls ( $p < 0.01$ ) (Figure 6-6).

Treating cartilage explants with the developed DDS was significantly more effective in increasing collagen synthesis to the same level as the untreated control and compared to the IL-1 $\alpha$  treated cartilage ( $p < 0.01$ ) over 20 days (Figure 6-6). The developed DDS using Ket as a module for NSAIDs showed promising results in increasing the amount of collagen in the cartilage tissue exposed to the inflammatory cytokines.

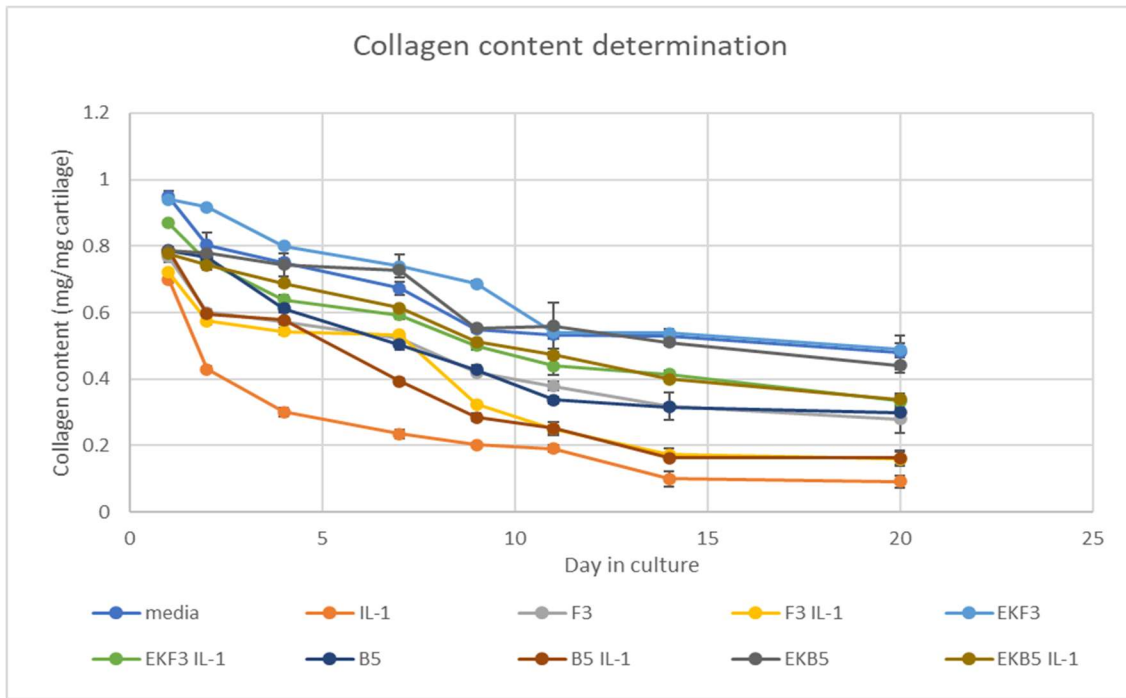


Figure 6-6. Collagen content determination on IL-1 $\alpha$  treated cartilage using hydroxyproline assay for 20 days. Using emulsion Ket coated with POLY-B5 and POLY-F3, IL-1 $\alpha$ , POLY-B5 and POLY-F3 with/without IL-1 $\alpha$ . Ket emulsion coated with POLY-B5 and POLY-F3 was significantly effective in the increased amount of collagen synthesis to the same level as the untreated control and compared to the IL-1 $\alpha$  treated cartilage ( $p < 0.01$ ).

### 6.3.8. Live/dead viability assay

Fluorescent images of the untreated cartilage sample showed viable chondrocytes (green) without appearance of dead cells (red); only the addition of IL-1 $\alpha$  resulted in dead cells clearly being observed close to the interface between cartilage and fluid after first day of the incubation (Figures 6-7 & 6-8). At day 1, most of the chondrocytes in the tissue were viable and the image showed a lot of green fluorescence, indicating live cells. However, a few dead cells were also present when IL-1 $\alpha$  was added to the sample, which would show up as red fluorescence (Figure 6-7). By day 2, some changes have occurred in the tissue samples subjected to IL-1 $\alpha$  that could affect their viability. The image showed a mixture of green and red fluorescence, with a substantially higher proportion of red fluorescence compared to day 1 (Figure 6-8).

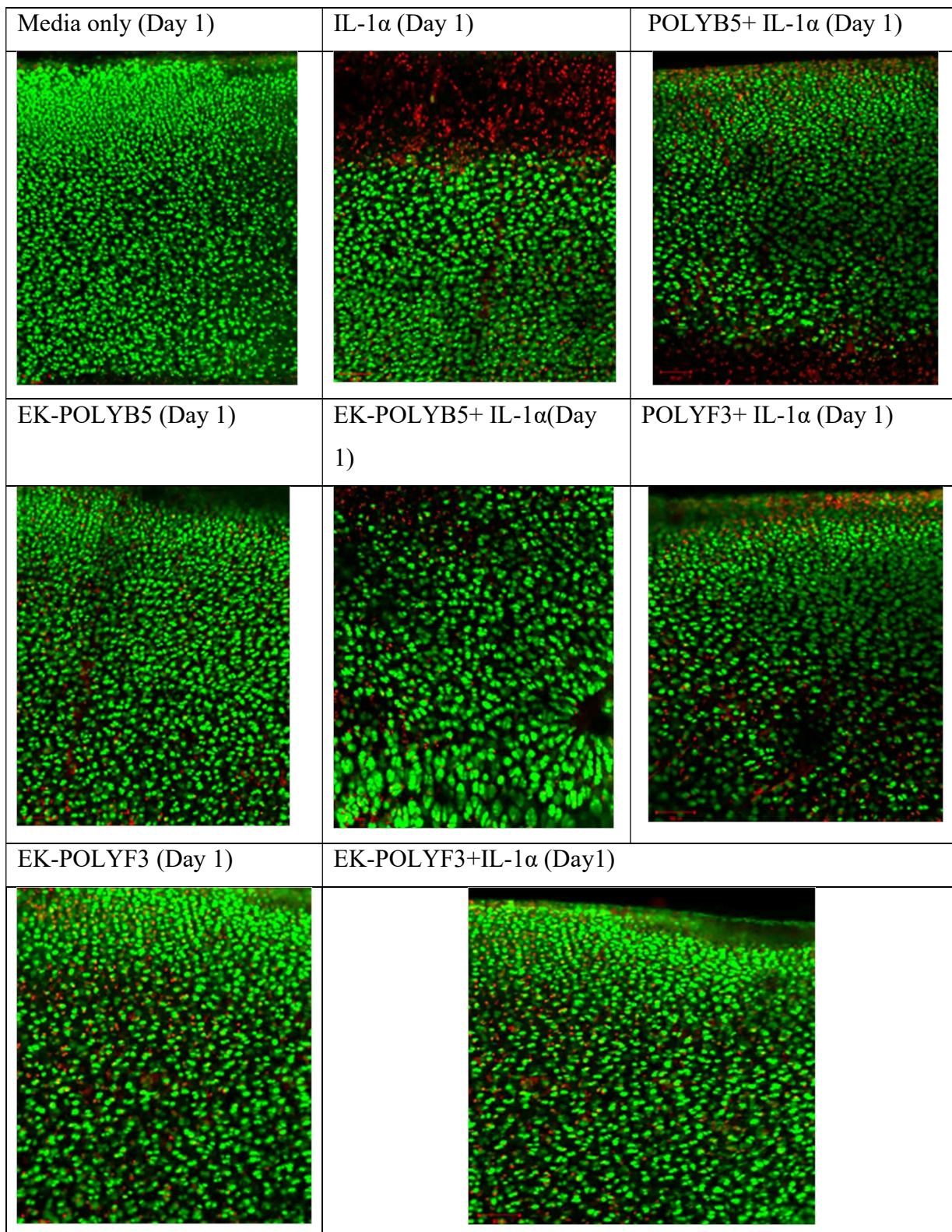


Figure 6-7. Examples of images of live/dead fluorescently stained bovine explants exposed to IL-1 $\alpha$  (1ng/mL) to evaluate chondrocyte viability on day 1. The cartilage explants were incubated with controls (pure media, IL-1 $\alpha$ , oleic acid emulsion with/without IL-1 $\alpha$ , POLY-B5 and POLY-F3). Live cells were stained green by calcein, and dead cells were stained red by ethidium homodimer. Ket emulsion coated with POLY-B5 and POLY-F3 was successfully prevented cell death induced by IL-1 $\alpha$ . Scale bar 100 $\mu$ m.

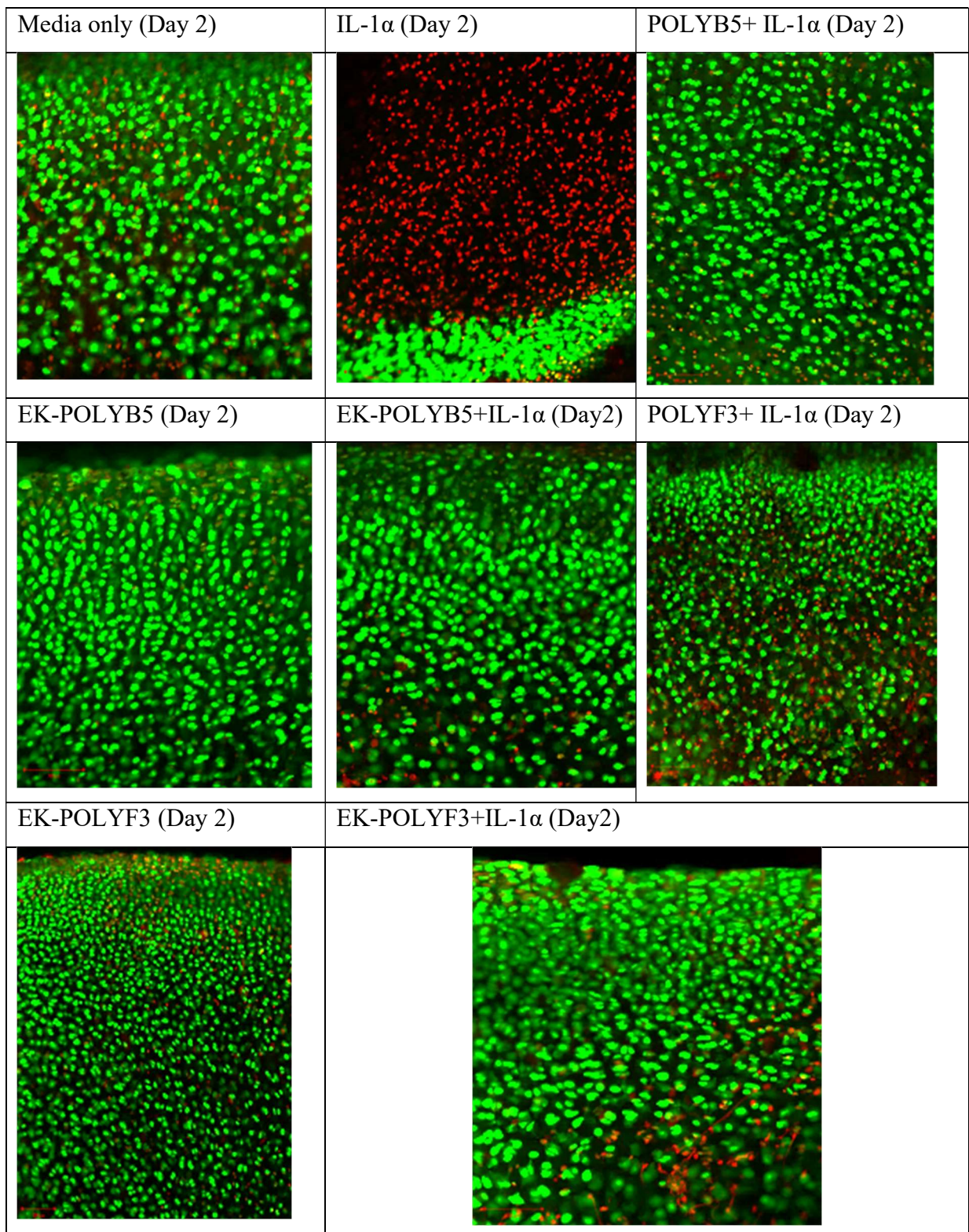


Figure 6-8. Examples of images of live/dead fluorescently stained bovine explants exposed to IL-1 $\alpha$  (1ng/mL) to evaluate chondrocyte viability on day 2. The cartilage explants were incubated with controls (pure media, IL-1 $\alpha$ , oleic acid emulsion with/without IL-1 $\alpha$ , POLY-B5 and POLY-F3). Live cells were stained green by calcein, and dead cells were stained red by ethidium homodimer. Ket emulsion coated with POLY-B5 and POLY-F3 was successfully prevented cell death induced by IL-1 $\alpha$ . Scale bar 100 $\mu$ m.

After 7 days of incubation, dead cells were also visible further away from the superficial area where almost all the cells appeared red in sample treated with IL-1 $\alpha$  (Figures 6-9). However, the chondrocytes have continued to thrive using the developed drug delivery system, which showed a more green fluorescence overall than red fluorescence. By day 14, the tissue had undergone significant changes as most of the IL-1  $\alpha$  treated sample had died by this time, resulting in the predominant red fluorescence of the image (Figures 6-10). The addition of Ket o/w emulsion coated with POLY-B5 or POLY-F3 maintained chondrocyte viability for 14 days of the incubation period. Chondrocyte viability was rescued by Ket emulsion coated with POLY-B5 or POLY-F3 even in the presence of IL-1 $\alpha$ , as the images show viable chondrocytes in green across the 2 weeks.

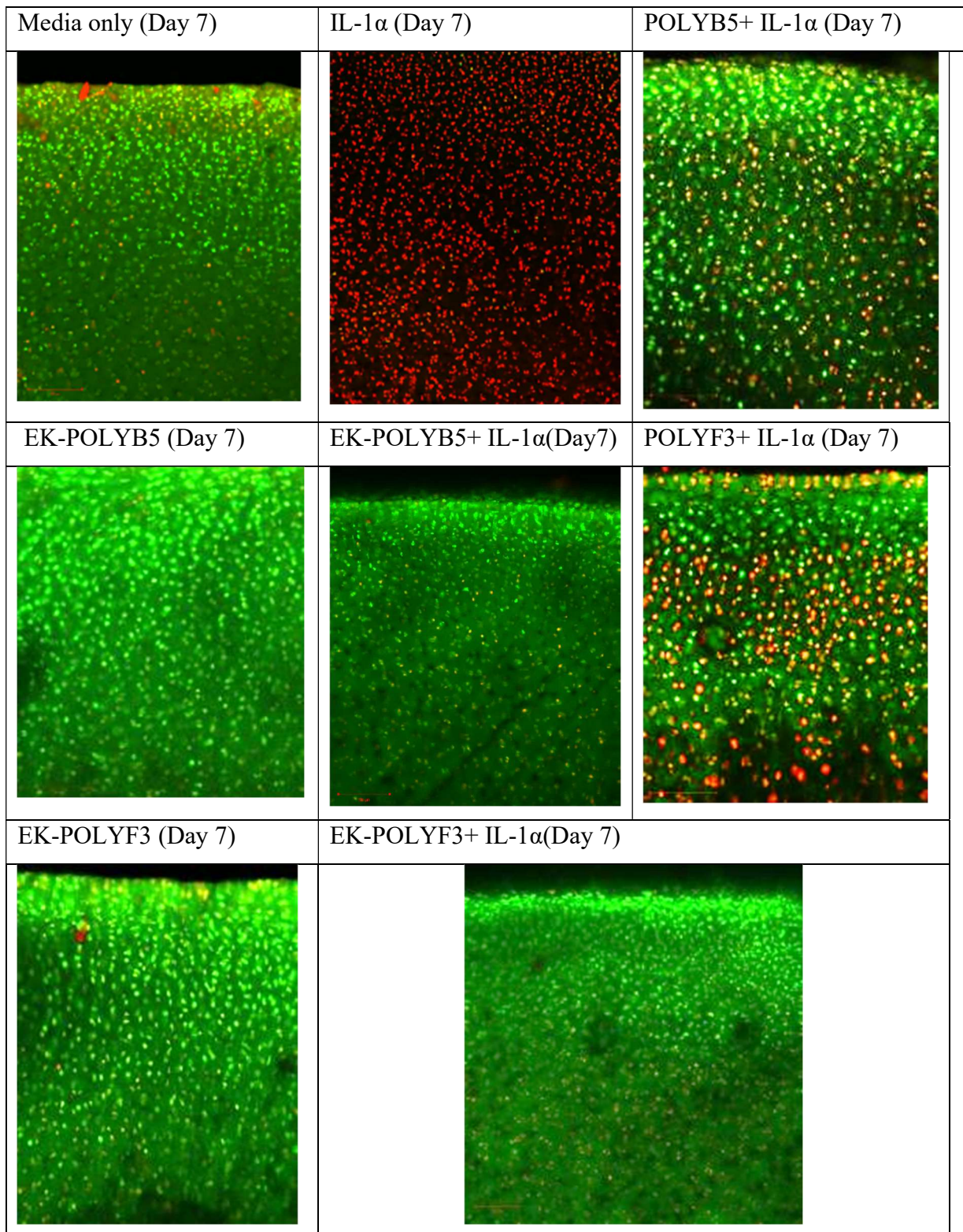


Figure 6-9. Examples of images of live/dead fluorescently stained bovine explants exposed to IL-1 $\alpha$  (1ng/mL) to evaluate chondrocyte viability on day 7. The cartilage explants were incubated with controls (pure media, IL-1 $\alpha$ , oleic acid emulsion with/without IL-1 $\alpha$ , POLY-B5 and POLY-F3). Live cells were stained green by calcein, and dead cells were stained red by ethidium homodimer. Ket emulsion coated with POLY-B5 and POLY-F3 was successfully prevented cell death induced by IL-1 $\alpha$ . Scale bar 100 $\mu$ m.

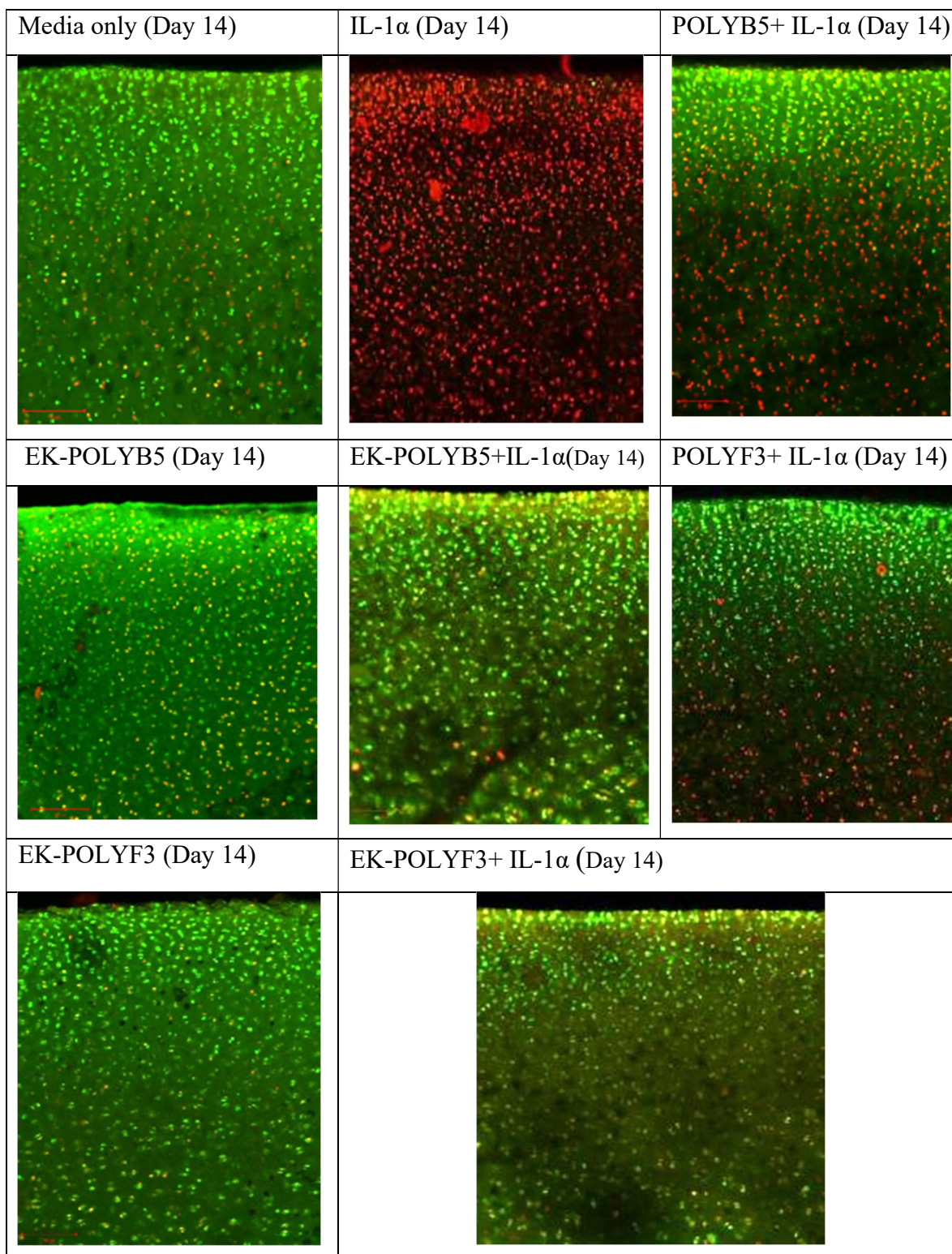
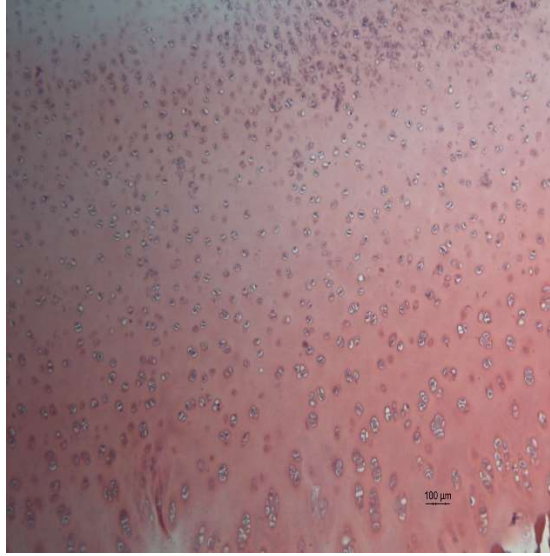


Figure 6-10. Examples of images of live/dead fluorescently stained bovine explants exposed to IL-1 $\alpha$  (1ng/mL) to evaluate chondrocyte viability on day 14. The cartilage explants were incubated with controls (pure media, IL-1 $\alpha$ , oleic acid emulsion with/without IL-1 $\alpha$ , POLY-B5 and POLY-F3). Live cells were stained green by calcein, and dead cells were stained red by ethidium homodimer. Ket emulsion coated with POLY-B5 and POLY-F3 was successfully prevented cell death induced by IL-1 $\alpha$ . Scale bar 100 $\mu$ m.

### **6.3.9. Histological analysis of cartilage explants**

Images of sections of the tissue from the cartilage cultures stained with safranin O are shown in Figure 6-11. Images of untreated (media only) tissue sections stained with safranin O revealed high GAG staining intensity on day 20. In the cartilage tissue treated with IL-1 $\alpha$ , there was a significant reduction in staining intensity compared to the untreated tissue at day 20, indicating a massive loss of GAG from the tissue, as illustrated in sGAG loss experiments (Figure 6-5). Treating the IL-1 $\alpha$  exposed cartilage section with the developed formulation containing POLY-B5 or POLY-F3 led to maintaining GAG content nearly similar to the untreated cartilage samples, in that the GAG staining intensity appeared to be strong and bright which was not unlike the observations of cartilage culture in pure media (untreated samples) (Figure 6-11).

Media only (Day 20)



IL-1α (Day 20)



POLYB5 (Day 20)



POLYB5+ IL-1α (Day 20)



EK-POLYB5 (Day 20)



EK-POLYB5+ IL-1α (Day 20)



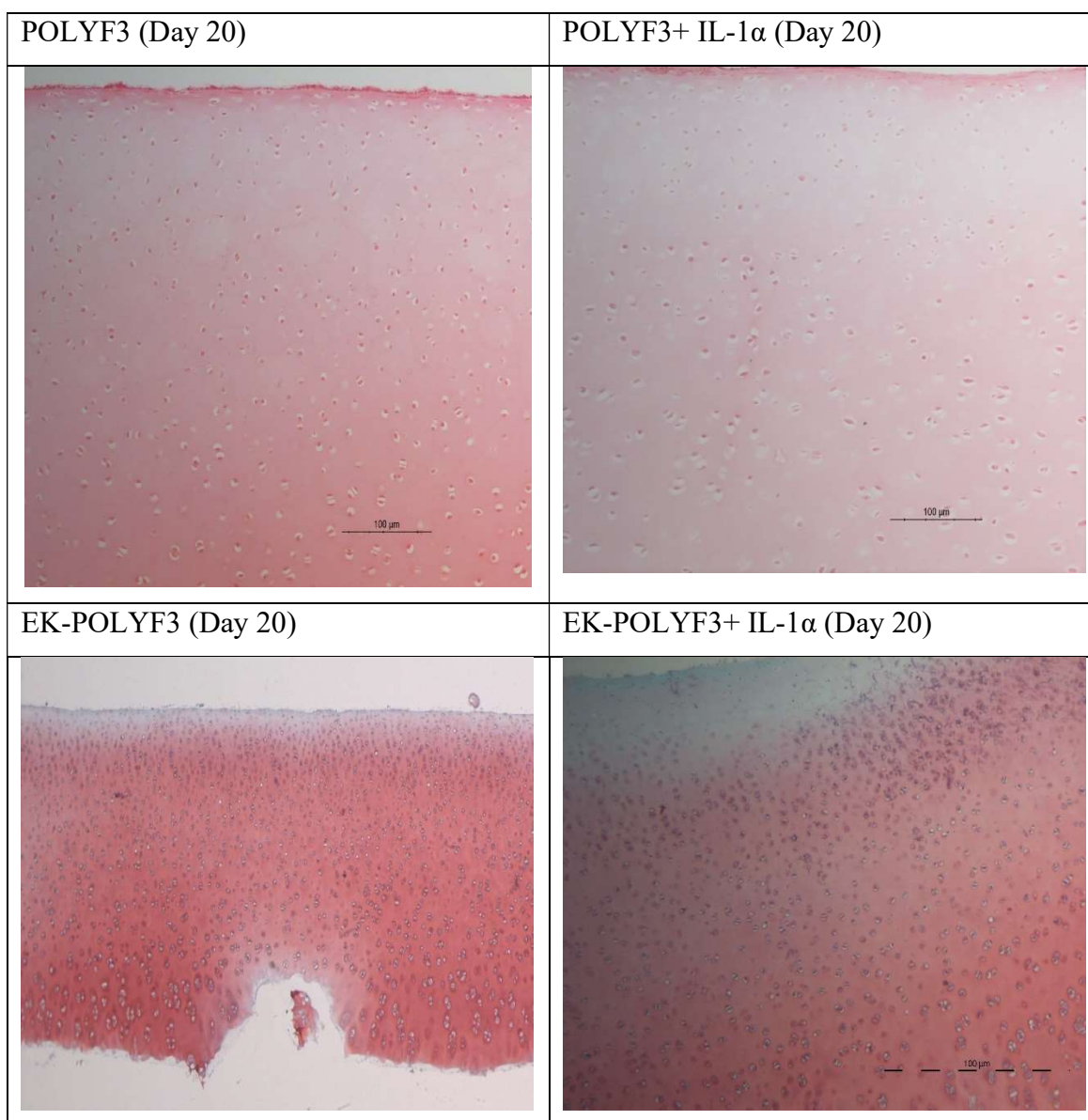


Figure 6-11. Histology sections of cartilage tissue stained with safranin O on day 20 that exposed to pure media, IL-1 $\alpha$  (1 ng/mL), Ket o/w emulsion coated with POLY-B5 and POLY-F3. The reddish orange colour intensity indicates the amount of GAG in the sample. Ket emulsion contained POLY-B5 or POLYF3 maintaining the GAG content nearly similar to the untreated cartilage samples as the GAG staining intensity was appeared strong and bright similar to those observed for cartilage culture in pure media (untreated samples) and compared to IL-1  $\alpha$  treated cartilage. Scale bar 100 $\mu$ m.

## 6.4. Discussion

PBAEs have an amenable biodegradable and hydrophilic nature, which makes them superior to other polycationic polymers and thus suitable for widespread use as drug delivery systems (Perni and Prokopovich, 2017; Iqbal *et al.*, 2020; Saeedi and Prokopovich, 2021). In this work, the rational design of PBAEs has been shown to be a critical step in improving the effectiveness of OA drugs in treating joint disease. In addition, coating Ket o/w emulsion with positively charged PBAEs results in augmenting electrostatic interactions with negatively charged GAG chains in cartilage ECM. It is, therefore, reasonable to expect that such a mechanism would also impact the ability of Ket to diffuse

through cartilage. Indeed, supported by the experimentally observed higher drug uptake and prolonged retention time of Ket coated with different types of PBAEs (Figures 6-2 & 6-3), using different amine and acrylate components to create various cationic polymers (Table 2-2). Thus, the results have proven not only that coating drugs with PBAEs is a necessary step to allowing electrostatic attraction between polymer chain and cartilage, but also that drug uptake and retention time can be increased by using PBAEs as a drug delivery system inside cartilage tissue.

#### **6.4.1. Structure-function activity relationship of PBAEs**

The structure of PBAEs is designed to enhance uptake, retention, and efficacy of OA drugs via multiple steps. PBAE was prepared in an acidic buffer (pH 5) in such a way as to facilitate its secondary and tertiary amines in gaining more positive charges to promote efficacy in binding to negatively charged cartilage ECM (Ishihara *et al.*, 2010; Al Thaher *et al.*, 2018; Iqbal *et al.*, 2020). As in Table 2-3, compounds 3 and 5 had tertiary amine while compound 1 had secondary amine. All gained a high positive charge (7 to 19 mV) (Table 6-1) and demonstrated effective drug uptake and retention time inside the cartilage tissue (figures 6-2 & 6-3). POLY-D5 and POLY-E5 had the least positive charges (+9.7 and + 7.3, respectively), thus providing low uptake and retention time of Ket inside the cartilage tissue.

Ion-pairing interactions are one of the most important noncovalent interactions and result from electrostatic attraction between two groups of opposite charges (Gillespie, Fanourakis and Phipps, 2022). In this project, an ion pair was formed between the positively charged amine end of the PBAE polymer (cation) which coated the emulsion droplet and the negatively charged sulphate group in cartilage sGAG to be temporarily bonded together by electrostatic forces of attraction. Such ion pairs can play a role in the mechanical and biological properties of the cartilage-polymer system. For example, this ionic interaction can increase emulsion stability, forming a stable structure and increasing the resistance to system breakage. In addition, such ionic interaction is critical as it needs to be not so strong as to cause a poor release of drug into the tissue. The developed drug delivery system is dependent on charge based electrostatic interaction, sufficiently weak and reversible, that it can easily and effectively release the drug into the cartilage tissue to help tissue repair and regeneration.

#### **6.4.2. Uptake and retention of Ket inside the cartilage tissue:**

In this work, PBAEs of sizes 0.2-5.0  $\mu\text{m}$  with positive zeta potential of 10 –19 mV has been found to provide an effective delivery system for OA. It is notable that these sizes and charges differ somewhat from other types of delivery systems. For example, PBAE-NPs as plasmid carriers are effective with sizes of 0.07–0.150  $\mu\text{m}$  and positive charges between 5–10 mV (Iqbal *et al.*, 2020). Meanwhile,

Avidin carrier sized  $>0.01\mu\text{m}$  (10 nm) is considered to be ideal for OA drug delivery (Bajpayee *et al.*, 2014).

All of the examined POLY-X polymers exhibited positive charges (Table 6-1), which supports the expectation that POLY-X is a polycation type that protonates amine ends ( $\text{R-NH}_3^+$ ) at appropriate pH level and gains a positive charge (Perni and Prokopovich, 2017). In addition, it has been shown that drugs injected intra-articularly experience joint space clearance in 1 hour; therefore, 10 min was chosen as the longest uptake end-point (Perni and Prokopovich, 2017). Moreover, drug uptake was significantly higher in Ket o/w emulsion coated with PBAEs than in either type of control (P and E). Changing the types of amines or acrylates in the polymer types did not affect polymer efficacy. Accordingly, it can be clearly stated that these polymers were effective not only in untreated cartilage but also in GAG depleted cartilage (Figure 6-2). Moreover, reducing the amount of GAG in the samples did not prevent the uptake of the drug into the cartilage samples.

Another potential aspect to consider is Ket retention in cartilage tissue after uptake. Coating Ket o/w emulsion with PBAEs allowed Ket to be retained in the cartilage explants for almost 4 hours, compared to about 2 hours for the controls (Figure 6-3). Therefore, POLY-X effectively retained Ket inside the cartilage tissue for longer, which is expected to allow the drug to both deliver its effects and reduce clearance time from the cartilage. Overall, improving drug uptake and retention time inside the cartilage tissue is considered to be the first step towards studying the ability of the DDS to be effective in delivering the drug there.

### 6.4.3. XTT

As described above, XTT assay was carried out to examine the cytotoxicity of all 15 types of PBAE polymers (POLY-X) on cartilage tissue, untreated control and  $\text{IL-1}\alpha$  treated samples were selected as controls. The results (see Figure 6-4) reveal that chondrocytes, which are cells present in cartilage, did not suffer negatively from exposure to POLY-X for 20 days. XTT enzyme assays gave nearly the same viability in samples exposed to the untreated control and in samples exposed to POLY-X, but both of these were higher than the samples treated with  $\text{IL-1}\alpha$ . Overall, POLY-X displayed similar satisfactory cell viability to the untreated control. These results confirm that POLY-X, as a type of PBAE polymer, is a non-toxic product; this is consistent with other studies which have shown that PBAEs are considerably less toxic than currently available cationic polymers such as poly (ethyleneimine) and poly L-lysine (Lynn and Langer, 2000; Al Thaher *et al.*, 2018; Liu *et al.*, 2019; Iqbal *et al.*, 2020). Therefore, they are safe to use as DDSs to deliver NSAIDs inside cartilage tissue for OA treatment.

#### 6.4.4. IL-1 $\alpha$ assays

Drug uptake does not guarantee biological activity; for example, once Ket interacts with the delivery system its anti-inflammatory activity could be reduced which could in turn lower its availability. Therefore, the ability of PBAEs to deliver Ket to counteract cartilage GAG degradation induced by IL-1 $\alpha$  was tested in an experimental setting similar to that used by Bajpayee *et al.* (2016) using DMMB. The efficacy of delivering Ket into the cartilage ex vivo model was tested using only Ket o/w emulsion coated with POLY-B5 and POLY-F3 as these polymers were the most effective of those examined in this chapter (aside from POLY-X). The observed sGAG content progressively declined in the samples exposed to IL-1 $\alpha$ , with ECM rescued from the culture in the presence of Ket (Figure 6-5). The results show a decrease in sGAG loss over 20 days for explants cultured under basal conditions (serum-free medium + 1% ITS) which is similar to Bajpayee *et al.*'s. (2016) findings which showed a gradual loss of sGAG over time in young bovine explants cultured ex vivo that treated with Avidin-Dex.

The PBAEs -based delivery system developed in this work was as effective as the untreated control, demonstrating that Ket remained active when delivered through the proposed system. Furthermore, its effectiveness in increasing collagen content when IL-1 $\alpha$  was added to the culture media (Figure 6-6) serves to further highlight the improved drug localisation achieved through the presented delivery system. This outcome could be attributed to the ability of the polymer to diffuse Ket through the tissue to prevent the cytokine effect and to deliver its benefits.

Levels of sGAG were reduced in the OA cartilage (IL-1 $\alpha$  treated samples) compared to the untreated cartilage, indicating that GAG is lost from the tissue as cartilage is degraded; this is clearly evident in the safranin O staining results, (Figure 6-11). The cartilage tissue treated with IL-1 $\alpha$  showed an increase in GAG release into the medium, which might have been due to wash-out of proteoglycans from the ECM as a result of interruption of non-covalent interactions between aggrecan and long-chain hyaluronic acid molecules in the cartilage (Elson *et al.*, 2015). Moreover, there was no increase in GAG release in the cartilage tissue cultures treated with the developed DDS using POLY-B5 or POLY-F3 indicating that it is effective in maintaining cartilage tissue integrity compatible with that detected in the untreated cartilage samples. Overall, measuring cell viability, sGAG, collagen and cell integrity in tissue culture is an important step to confirming therapy efficacy and reducing costs before undertaking in vivo clinical studies.

## 6.5. Conclusion

PBAE polymers with different kinetic profiles, sizes and charges could easily be synthesised by using various amines, and acrylates to fulfil the various requirements of different applications, such as DDSs for OA. PBAEs possess many desirable properties (Scheme 1-1) from the perspective of the NSAIDs delivery system to OA cartilage such as required positive charges to interact electrostatically with cartilage ECM, non-toxicity, readily degradable linkages to deliver the drug easily inside the cartilage tissue, and the ability to maintain the viability of the chondrocyte cells.

Using drug delivery technologies to treat OA disease is the focus of future observations, which could permit local, controlled release of OA drugs and avoid the problems associated with frequent injection and high doses (Gerwin, Hops and Lucke, 2006; Huang and Zhang, 2012; Janssen *et al.*, 2014). The developed drug delivery system needs to be tested in the future in human cartilage, as well as, in vivo using animal models before it can be tested directly on the joints of patients. This study's findings are relevant and can be taken into consideration to promote maintenance of cartilage ECM components and achieve a decrease in OA disease progression.

## **Study limitation:**

The limitations of this research point toward topics to be addressed in the future.

- I. Ex-vivo bovine models are challenging to produce in large volumes and maintain cell viability over extended periods. Maintaining cell viability for more than three weeks is difficult as the cells become unhealthy in the culture media.
- II. Cell death often occurs at the explant edge due to using the scalpel, which may affect the study results as it causes death to some of the tissue cells.
- III. Experiments were performed using a culture medium without synovial fluid (SF). Hyaluronic acid and other negatively charged molecules in SF could decrease the penetration of the drugs into cartilage. Therefore, drug penetration using the drug delivery system may alter or decrease when tested in in vivo models.
- IV. The stability of emulsions can be further improved by adding emulsifiers (such as surfactant) that can be used to modify the properties of the protective layer around the droplets, resulting in increased stability, ensure long-term viability and resistance to external forces such as temperature change. Further research may provide valuable insights into optimizing the emulsion stability to improve the therapeutic outcome of drug formulations.
- V. Lack of access to testing human cartilage samples due to COVID-19 issues. It was more helpful to test the drug delivery system using human samples to investigate its efficacy as there are some differences between human and animal cartilage tissue.

## **Future perspectives.**

Rapid advances in biomedical and biotechnological sectors can improve the field of drug discovery and lead to the appearance of new and efficient drug delivery systems that can effectively target drug candidates. In conjunction with effective and safe drug delivery systems, potent therapeutics can relieve pain and reduce inflammation targeting the cartilage and bone conditions. Therefore, current and future research on arthritis diseases together with novel therapeutics and drug delivery systems tested in pre-clinical and clinical trials, will lead to new treatment strategies that can fulfil the joint disorder needs to improve patient quality of life and compliance. Currently, many kinds of research on different drugs are reported for managing arthritis, but a limited number of formulations entered clinical trials.

The field still requires to be tested using human cartilage explants OA sample to investigate the efficacy and safety profile of the DDS. Additionally, the in vivo animal studies have to be used to determine a starting, safe dose for first in human study and assess the potential toxicity of the developed drug delivery system to be able to use it in the clinic successfully.

## References:

1. Adamczak, M. *et al.* (2012) ‘Polyelectrolyte multilayer capsules with quantum dots for biomedical applications’, *Colloids and Surfaces B: Biointerfaces*. doi: 10.1016/j.colsurfb.2011.10.028.
2. Adamczak, M. *et al.* (2013) ‘Linseed oil based nanocapsules as delivery system for hydrophobic quantum dots’, *Colloids and Surfaces B: Biointerfaces*. doi: 10.1016/j.colsurfb.2013.04.014.
3. Aigner, T. and Schmitz, N. (2011) *173 - Pathogenesis and pathology of osteoarthritis*. Fifth Edit, *Rheumatology*. Fifth Edit. Elsevier Inc. doi: 10.1016/B978-0-323-06551-1.00173-1.
4. Anderson, D. G., Lynn, D. M. and Langer, R. (2003) ‘Semi-automated synthesis and screening of a large library of degradable cationic polymers for gene delivery’, *Angewandte Chemie - International Edition*. doi: 10.1002/anie.200351244.
5. Anz, A. W. *et al.* (2014) ‘Application of biologics in the treatment of the rotator cuff, meniscus, cartilage, and osteoarthritis’, *Journal of the American Academy of Orthopaedic Surgeons*. doi: 10.5435/JAAOS-22-02-68.
6. Arthritis Research UK (2018) ‘State of Musculoskeletal Health 2018’, *Arthritisresearchuk*, p. 30. doi: 10.2214/AJR.16.17742.
7. Ashkavand, Z., Malekinejad, H. and Vishwanath, B. S. (2013) ‘The pathophysiology of osteoarthritis’, *Journal of Pharmacy Research*. Elsevier Ltd, 7(1), pp. 132–138. doi: 10.1016/j.jopr.2013.01.008.
8. Attur, M. *et al.* (2008) ‘Prostaglandin E 2 Exerts Catabolic Effects in Osteoarthritis Cartilage: Evidence for Signaling via the EP4 Receptor’, *The Journal of Immunology*, 181(7), pp. 5082–5088. doi: 10.4049/jimmunol.181.7.5082.
9. Ayhan, E. (2014) ‘Intraarticular injections (corticosteroid, hyaluronic acid, platelet rich plasma) for the knee osteoarthritis’, *World Journal of Orthopedics*. doi: 10.5312/wjo.v5.i3.351.
10. Bajpayee, A. G. *et al.* (2014) ‘Avidin as a model for charge driven transport into cartilage and drug delivery for treating early stage post-traumatic osteoarthritis’, *Biomaterials*. doi: 10.1016/j.biomaterials.2013.09.091.
11. Bajpayee, A. G. *et al.* (2016) ‘Charge based intra-cartilage delivery of single dose dexamethasone using Avidin nano-carriers suppresses cytokine-induced catabolism long term’, *Osteoarthritis and Cartilage*, 24(1), pp. 71–81. doi: 10.1016/j.joca.2015.07.010.
12. Bajpayee, A. G. and Grodzinsky, A. J. (2017) ‘Cartilage-targeting drug delivery: Can electrostatic interactions help?’, *Nature Reviews Rheumatology*. Nature Publishing Group, 13(3), pp. 183–193. doi: 10.1038/nrrheum.2016.210.
13. Balazs, E. and Denlinger, J. . (1993) ‘Viscosupplementation: a new concept in the treatment of osteoarthritis’, *The journal of rheumatology . supplement*, 39, pp. 3–9.
14. Barré-Sinoussi, F. and Montagutelli, X. (2015) ‘Animal models are essential to biological research: Issues and perspectives’, *Future Science OA*, 1(4), pp. 4–6. doi: 10.4155/fso.15.63.
15. Bauer, S. *et al.* (2012) ‘Knee joint preservation with combined neutralising High Tibial Osteotomy (HTO) and Matrix-induced Autologous Chondrocyte Implantation (MACI) in younger patients with medial knee osteoarthritis: A case series with prospective clinical and MRI follow-up ove’, *Knee*. doi: 10.1016/j.knee.2011.06.005.
16. Bédouet, L. *et al.* (2013) ‘Intra-articular fate of degradable poly(ethyleneglycol)-hydrogel microspheres as carriers for sustained drug delivery’, *International Journal of Pharmaceutics*. doi: 10.1016/j.ijpharm.2013.08.016.
17. Berenbaum, F. (2013) ‘Osteoarthritis as an inflammatory disease (osteoarthritis is not osteoarthrosis!)’, *Osteoarthritis and Cartilage*, pp. 16–21. doi: 10.1016/j.joca.2012.11.012.
18. Van den Berg, W. B. (1999) ‘The role of cytokines and growth factors in cartilage destruction in osteoarthritis and rheumatoid arthritisVan den Berg, W. B. (1999) “The role of cytokines

- and growth factors in cartilage destruction in osteoarthritis and rheumatoid arthritis”, in *Zeits*’, in *Zeitschrift für Rheumatologie*, pp. 136–141. doi: 10.1007/s003930050163.
19. Beri, R. G., Hacche, L. S. and Martin, C. F. (2000) ‘Gel permeation chromatography’, in *HPLC: Practical and Industrial Applications, Second Edition*. doi: 10.1201/9781420042665.
  20. Bertrand, J. and Held, A. (2017) ‘Role of proteoglycans in osteoarthritis’, in *Cartilage: Volume 2: Pathophysiology*. doi: 10.1007/978-3-319-45803-8\_4.
  21. Bijlsma, J. W. J., Berenbaum, F. and Lafeber, F. P. J. G. (2011) ‘Osteoarthritis: An update with relevance for clinical practice’, *The Lancet*, 377(9783), pp. 2115–2126. doi: 10.1016/S0140-6736(11)60243-2.
  22. Bjordal, J. M. *et al.* (2007) ‘Short-term efficacy of physical interventions in osteoarthritic knee pain. A systematic review and meta-analysis of randomised placebo-controlled trials’, *BMC Musculoskeletal Disorders*, 8, pp. 1–14. doi: 10.1186/1471-2474-8-51.
  23. Blanco, F. J. and Ruiz-Romero, C. (2013) ‘New targets for disease modifying osteoarthritis drugs: Chondrogenesis and Runx1’, *Annals of the Rheumatic Diseases*. doi: 10.1136/annrheumdis-2012-202652.
  24. Bliddal, H., Leeds, A. R. and Christensen, R. (2014) ‘Osteoarthritis, obesity and weight loss: Evidence, hypotheses and horizons - a scoping review’, *Obesity Reviews*, 15(7), pp. 578–586. doi: 10.1111/obr.12173.
  25. Blood-Smyth, J. (2015) *Osteoarthritis, local physio*. Available at: <https://www.local-physio.co.uk/articles/osteoarthritis>.
  26. Bowman, S. *et al.* (2018) ‘Recent advances in hyaluronic acid based therapy for osteoarthritis’, *Clinical and Translational Medicine*. doi: 10.1186/s40169-017-0180-3.
  27. Burke, J. *et al.* (2016) ‘Therapeutic potential of mesenchymal stem cell based therapy for osteoarthritis’, *Clinical and Translational Medicine*. doi: 10.1186/s40169-016-0112-7.
  28. Buyuk, A. F. *et al.* (2017) ‘COMPARED EFFICACY OF INTRA-ARTICULAR INJECTION OF METHYLPREDNISOLONE AND TRIAMCINOLONE.’, *Acta ortopedica brasileira*. doi: 10.1590/1413-785220172505172581.
  29. Carballo, C. B. *et al.* (2017) ‘Basic Science of Articular Cartilage’, *Clinics in Sports Medicine*. doi: 10.1016/j.csm.2017.02.001.
  30. Carbone, L. D. *et al.* (2013) ‘Assistive Walking Device Use and Knee Osteoarthritis: the Health, Aging, and Body Composition Study (Health ABC Study)’, *Arch Phys Med Rehabil.*, 94(2), pp. 332–339. doi: 10.1016/j.apmr.2012.09.021.Assistive.
  31. Cetin, M., Atila, A. and Kadioglu, Y. (2010) ‘Formulation and In vitro Characterization of Eudragit® L100 and Eudragit® L100-PLGA Nanoparticles Containing Diclofenac Sodium’, *AAPS PharmSciTech*. doi: 10.1208/s12249-010-9489-6.
  32. Chen, A. *et al.* (2012) ‘The Global Economic Cost of Osteoarthritis: How the UK Compares’, *Arthritis*, 2012, pp. 1–6. doi: 10.1155/2012/698709.
  33. Chen, G., Deng, C. and Li, Y. P. (2012) ‘TGF- $\beta$  and BMP signaling in osteoblast differentiation and bone formation’, *International Journal of Biological Sciences*. doi: 10.7150/ijbs.2929.
  34. Chen, J. *et al.* (2007) ‘Synthesis and degradation of poly(beta-aminoester) with pendant primary amine’, *Polymer*, 48(3), pp. 675–681. doi: 10.1016/j.polymer.2006.12.008.
  35. Chevalier, X. (2010) ‘Intraarticular treatments for osteoarthritis: new perspectives.’, *Current drug targets*, 11(5), pp. 546–60. doi: 10.2174/138945010791011866.
  36. Cho, J. *et al.* (2017) ‘A phase III clinical results of INVOSSA™(TissueGene C): A clues for the potential disease modifying OA drug’, *Cytotherapy the journal of cell therapy*, 19(5), p. S148. doi: <https://doi.org/10.1016/j.jcyt.2017.02.221>.
  37. Christensen, R. *et al.* (2007) ‘Effect of weight reduction in obese patients diagnosed with knee osteoarthritis: A systematic review and meta-analysis’, *Annals of the Rheumatic Diseases*, pp. 433–439. doi: 10.1136/ard.2006.065904.
  38. Cissell, D. D. *et al.* (2017) ‘A Modified Hydroxyproline Assay Based on Hydrochloric Acid in Ehrlich’s Solution Accurately Measures Tissue Collagen Content’, *Tissue Engineering -*

- Part C: Methods*, 23(4), pp. 243–250. doi: 10.1089/ten.tec.2017.0018.
39. Coglitore, D. *et al.* (2017) ‘Transition from fractional to classical Stokes-Einstein behaviour in simple fluids’, *Royal Society Open Science*, 4(12), pp. 1–9. doi: 10.1098/rsos.170507.
  40. Collins, J. A. *et al.* (2013) ‘Oxygen and pH-sensitivity of human osteoarthritic chondrocytes in 3-D alginate bead culture system’, *Osteoarthritis and Cartilage*, 21(11), pp. 1790–1798. doi: 10.1016/j.joca.2013.06.028.
  41. Cope, P. J. *et al.* (2019) ‘Models of osteoarthritis: the good, the bad and the promising’, *Osteoarthritis and Cartilage*. doi: 10.1016/j.joca.2018.09.016.
  42. Corzo-León, D. E., Munro, C. A. and MacCallum, D. M. (2019) ‘An ex vivo human skin model to study superficial fungal infections’, *Frontiers in Microbiology*. doi: 10.3389/fmicb.2019.01172.
  43. Crivelli, B. *et al.* (2019) ‘Silk fibroin nanoparticles for celecoxib and curcumin delivery: ROS-scavenging and anti-inflammatory activities in an in vitro model of osteoarthritis’, *European Journal of Pharmaceutics and Biopharmaceutics*. doi: 10.1016/j.ejpb.2019.02.008.
  44. Cross, M. *et al.* (2014) ‘The global burden of hip and knee osteoarthritis: Estimates from the Global Burden of Disease 2010 study’, *Annals of the Rheumatic Diseases*, 73(7), pp. 1323–1330. doi: 10.1136/annrheumdis-2013-204763.
  45. D., P. *et al.* (2013) ‘A novel in vitro bovine cartilage punch model for assessing the regeneration of focal cartilage defects with biocompatible bacterial nanocellulose’, *Arthritis Research and Therapy*, 15(3). Available at: <http://www.embase.com/search/results?subaction=viewrecord&from=export&id=L52585272%5Cnhttp://arthritis-research.com/content/15/3/R59%5Cnhttp://dx.doi.org/10.1186/ar4231%5Cnhttp://sfx.library.uu.nl/utrecht?sid=EMBASE&issn=14786354&id=doi:10.1186/ar4231&ati>.
  46. Damiano, J. and Bardin, T. (2010) *Synovial fluid*. Third Edit, *EMC-Rhumatologie-Orthopedie*. Third Edit. Elsevier Limited. doi: 10.1016/j.emcrho.2003.11.002.
  47. Davies, P. S. E. *et al.* (2013) ‘Disease-modifying osteoarthritis drugs: in vitro and in vivo data on the development of DMOADs under investigation.’, *Expert opinion on investigational drugs*, 22(4), pp. 423–41. doi: 10.1517/13543784.2013.770837.
  48. DECKER, B. *et al.* (1959) ‘Concentration of hyaluronic acid in synovial fluid.’, *Clinical chemistry*.
  49. Dunlap Burton *et al.* (2021) ‘Vitamin C supplementation for the treatment of osteoarthritis: perspectives on the past, present, and future’, *Therapeutic Advances in Vaccines*, 12, pp. 1–11. doi: 10.1177/https.
  50. Edwards, S. H. R. (2011) ‘Intra-articular drug delivery: The challenge to extend drug residence time within the joint’, *Veterinary Journal*. Elsevier Ltd, 190(1), pp. 15–21. doi: 10.1016/j.tvjl.2010.09.019.
  51. Elsaid, K. A. *et al.* (2013) ‘Pharmaceutical nanocarrier association with chondrocytes and cartilage explants: Influence of surface modification and extracellular matrix depletion’, *Osteoarthritis and Cartilage*. doi: 10.1016/j.joca.2012.11.011.
  52. Elson, K. M. *et al.* (2015) ‘Non-destructive monitoring of viability in an ex vivo organ culture model of osteochondral tissue’, *European Cells and Materials*, 29(0), pp. 356–369. doi: 10.22203/eCM.v029a27.
  53. Evans, C. H. (2016) ‘Drug delivery to chondrocytes’, *Osteoarthritis and Cartilage*. doi: 10.1016/j.joca.2015.08.012.
  54. Factors, I. R. (2000) ‘NIH Conference Osteoarthritis : New Insights AND I TS’, *Annals of Internal Medicine*, 133(8), pp. 637–639. doi: 10.7326/0003-4819-133-8-200010170-00016.
  55. Fardale, R. W., Buttle, D. J. and Barrett, A. J. (1986) ‘Improved quantitation and discrimination of sulphated glycosaminoglycans by use of dimethylmethylene blue’, *BBA - General Subjects*, 883(2), pp. 173–177. doi: 10.1016/0304-4165(86)90306-5.
  56. Felson, D. T. (2010) ‘Arthroscopy as a treatment for knee osteoarthritis’, *Best Practice & Research Clinical Rheumatology*, 24(1), pp. 47–50. doi: 10.1016/j.berh.2009.08.002.

57. Fendrick, A. M. and Greenberg, B. (2009) 'A review of the benefits and risks of nonsteroidal anti-inflammatory drugs in the management of mild-to-moderate osteoarthritis', *Osteopathic Medicine and Primary Care*, 3(1), p. 1. Available at: <http://www.om-pc.com/content/3/1/1>.
58. Fini, A., Fazio, G. and Feroci, G. (1995) 'Solubility and solubilization properties of non-steroidal anti-inflammatory drugs', *International Journal of Pharmaceutics*. doi: 10.1016/0378-5173(95)04102-8.
59. Fioravanti, A. *et al.* (2009) 'Treatment of erosive osteoarthritis of the hands by intra-articular infliximab injections: A pilot study', *Rheumatology International*. doi: 10.1007/s00296-009-0872-0.
60. Firestein, G. S. (2013) 'Pathogenesis of rheumatoid arthritis Pathogenesis of rheumatoid arthritis', pp. 1–28.
61. Fortier, L. A. *et al.* (2011) 'The role of growth factors in cartilage repair', in *Clinical Orthopaedics and Related Research*. doi: 10.1007/s11999-011-1857-3.
62. Foster, Z. J. *et al.* (2015) 'Corticosteroid injections for common musculoskeletal conditions', *American Family Physician*. doi: 10.1016/S0002-838X(15)30302-6.
63. Fransen, M. *et al.* (2015) 'Glucosamine and chondroitin for knee osteoarthritis: A double-blind randomised placebo-controlled clinical trial evaluating single and combination regimens', *Annals of the Rheumatic Diseases*, 74(5), pp. 851–858. doi: 10.1136/annrheumdis-2013-203954.
64. Furman, B. D. *et al.* (2014) 'Targeting pro-inflammatory cytokines following joint injury: Acute intra-articular inhibition of interleukin-1 following knee injury prevents post-traumatic arthritis', *Arthritis Research and Therapy*, 16(3), pp. 1–15. doi: 10.1186/ar4591.
65. Gaur, K. *et al.* (2009) 'Licofelone- novel analgesic and anti-inflammatory agent for osteoarthritis: An overview', *Journal of Young Pharmacists*. doi: 10.4103/0975-1483.51884.
66. Geiger, B. C., Grodzinsky, A. J. and Hammond, P. (2018) 'Designing drug delivery systems for articular joints', *Chemical Engineering Progress*.
67. Gerwin, N., Hops, C. and Lucke, A. (2006) 'Intraarticular drug delivery in osteoarthritis', *Advanced Drug Delivery Reviews*. doi: 10.1016/j.addr.2006.01.018.
68. Geusens, P. *et al.* (1994) 'Long-term effect of omega-3 fatty acid supplementation in active rheumatoid arthritis. A 12-month, double-blind, controlled study.', *Arthritis and rheumatism*. doi: 10.1002/art.1780370608.
69. Gillespie, J. E., Fanourakis, A. and Phipps, R. J. (2022) 'Strategies That Utilize Ion Pairing Interactions to Exert Selectivity Control in the Functionalization of C-H Bonds', *Journal of the American Chemical Society*, 144(40), pp. 18195–18211. doi: 10.1021/jacs.2c08752.
70. Goldberg, M., Mahon, K. and Anderson, D. (2008) 'Combinatorial and rational approaches to polymer synthesis for medicine', *Advanced Drug Delivery Reviews*. doi: 10.1016/j.addr.2008.02.005.
71. Goldberg, V. M. and Buckwalter, J. A. (2005) 'Hyaluronans in the treatment of osteoarthritis of the knee: Evidence for disease-modifying activity', *Osteoarthritis and Cartilage*, 13(3), pp. 216–224. doi: 10.1016/j.joca.2004.11.010.
72. Goldberg, V. M. and Goldberg, L. (2010) 'Intra-articular hyaluronans: the treatment of knee pain in osteoarthritis.', *Journal of pain research*, 3, pp. 51–56. doi: 10.2147/JPR.S4733.
73. Grässel, S. and Aszódi, A. (2017) 'Cartilage volume 2: Pathophysiology', *Cartilage: Volume 2: Pathophysiology*, pp. 27–40. doi: 10.1007/978-3-319-45803-8.
74. Grässel, S. and Lorenz, J. (2014) 'Tissue-Engineering Strategies to Repair Chondral and Osteochondral Tissue in Osteoarthritis: Use of Mesenchymal Stem Cells', *Current Rheumatology Reports*, 16(10), pp. 1–16. doi: 10.1007/s11926-014-0452-5.
75. Green, J. J. *et al.* (2006) 'Biodegradable polymeric vectors for gene delivery to human endothelial cells', *Bioconjugate Chemistry*. doi: 10.1021/bc0600968.
76. Grigsby, E. *et al.* (2021) 'XT-150- A novel immunomodulatory gene therapy for osteoarthritis pain in phase 2b development', *Osteoarthritis and Cartilage*. Elsevier Ltd, 29(2021), p. S12. doi: 10.1016/j.joca.2021.05.023.

77. Grodzinsky, A. J. *et al.* (2017) 'Intra-articular dexamethasone to inhibit the development of post-traumatic osteoarthritis', *Journal of Orthopaedic Research*. doi: 10.1002/jor.23295.
78. Grogan, S. P. *et al.* (2001) 'Rapid Evaluation Of Cell Viability AND APOPTOSIS IN INTACT CARTILAGE VIA CONFOCAL MICROSCOPY', *Sun*, 11, p. 9925. Available at: <http://www.ors.org/Transactions/47/0034.pdf>.
79. Hajjalilo, M. *et al.* (2016) 'A double-blind randomized comparative study of triamcinolone hexacetonide and dexamethasone intra-articular injection for the treatment of knee joint arthritis in rheumatoid arthritis', *Clinical Rheumatology*. doi: 10.1007/s10067-016-3397-4.
80. Hartung, T. (2008) 'Thoughts on limitations of animal models', *Parkinsonism and Related Disorders*, 14(SUPPL.2), pp. 83–85. doi: 10.1016/j.parkreldis.2008.04.003.
81. Hauser, R. (2010) 'The Acceleration of Articular Cartilage Degeneration in Osteoarthritis by Nonsteroidal Anti-inflammatory Drugs', *Journal of Prolotherapy*.
82. Haywood, L. and Walsh, D. A. (2001) 'Vasculature of the normal and arthritic synovial joint', *Histology and Histopathology*, pp. 277–284. doi: 10.14670/HH-16.277.
83. He, Z. *et al.* (2017) 'Colloids and Surfaces B : Biointerfaces An overview of hydrogel-based intra-articular drug delivery for the treatment of osteoarthritis', *Colloids and Surfaces B: Biointerfaces*. Elsevier B.V., 154, pp. 33–39. doi: 10.1016/j.colsurfb.2017.03.003.
84. Hermans, J. *et al.* (2012) 'Productivity costs and medical costs among working patients with knee osteoarthritis', *Arthritis Care and Research*, 64(6), pp. 853–861. doi: 10.1002/acr.21617.
85. Hochberg, M., McAlindon, T. and Felson, D. (2000) 'Osteoarthritis: New Insights. Part 2: Treatment approaches', *Annals of Internal Medicine*, 133(9), pp. 726–729. doi: 10.7326/0003-4819-133-9-200011070-00015.
86. Hoffman, A. S. (2008) 'The origins and evolution of “controlled” drug delivery systems', *J Control Release*. doi: S0168-3659(08)00469-0 [pii]10.1016/j.jconrel.2008.08.012.
87. Holland, K. (2017) 'Stages of Osteoarthritis of the Knee', *health line*. Available at: <https://www.healthline.com/health/osteoarthritis-stages-of-oa-of-the-knee#1>.
88. Huang, G. and Zhang, Z. (2012) 'Micro- and nano-carrier mediated intra-articular drug delivery systems for the treatment of osteoarthritis', *Journal of Nanotechnology*, 2012. doi: 10.1155/2012/748909.
89. Huang, H. *et al.* (2022) 'Intra-articular drug delivery systems for osteoarthritis therapy: shifting from sustained release to enhancing penetration into cartilage', *Drug Delivery*. Taylor & Francis, 29(1), pp. 767–791. doi: 10.1080/10717544.2022.2048130.
90. Huang, Z. *et al.* (2018) 'Current status and future prospects for disease modification in osteoarthritis', *Rheumatology (United Kingdom)*, 57(December 2017), pp. iv108–iv123. doi: 10.1093/rheumatology/kex496.
91. Huebner, K. D., Shrive, N. G. and Frank, C. B. (2014) 'Dexamethasone inhibits inflammation and cartilage damage in a new model of post-traumatic osteoarthritis', *Journal of Orthopaedic Research*. doi: 10.1002/jor.22568.
92. Iqbal, S. *et al.* (2020) 'Poly ( $\beta$ -amino esters) based potential drug delivery and targeting polymer; an overview and perspectives (review)', *European Polymer Journal*. Elsevier, 141(October), p. 110097. doi: 10.1016/j.eurpolymj.2020.110097.
93. Ishihara, T. *et al.* (2010) 'Preparation and characterization of a nanoparticulate formulation composed of PEG-PLA and PLA as anti-inflammatory agents', *International Journal of Pharmaceutics*, 385(1–2), pp. 170–175. doi: 10.1016/j.ijpharm.2009.10.025.
94. Islam, M. R., Islam, A. K. M. . and Hossain, M. . (2018) 'Emulsion-based drug delivery systems: past, present and future', *Journal of Controlled Release*, 260.
95. Janke, J. J., Bennett, W. F. D. and Tieleman, D. P. (2014) 'Oleic acid phase behavior from molecular dynamics simulations', *Langmuir*. doi: 10.1021/la501962n.
96. Janssen, M. *et al.* (2014) 'Drugs and polymers for delivery systems in OA joints: Clinical needs and opportunities', *Polymers*, pp. 799–819. doi: 10.3390/polym6030799.
97. Jayasuriya, C. T. (2013) 'Role of Inflammation in Osteoarthritis', *Rheumatology: Current Research*, 03(02), pp. 3–4. doi: 10.4172/2161-1149.1000121.

98. Jerosch, J. (2011) 'Effects of glucosamine and chondroitin sulfate on cartilage metabolism in OA: Outlook on other nutrient partners especially omega-3 fatty acids', *International Journal of Rheumatology*, 2011. doi: 10.1155/2011/969012.
99. Jo, C. H. *et al.* (2014) 'Intra-articular injection of mesenchymal stem cells for the treatment of osteoarthritis of the knee: A proof-of-concept clinical trial', *Stem Cells*. doi: 10.1002/stem.1634.
100. John, T. *et al.* (2007) 'Interleukin-10 modulates pro-apoptotic effects of TNF- $\alpha$  in human articular chondrocytes in vitro', *Cytokine*, 40(3), pp. 226–234. doi: 10.1016/j.cyto.2007.10.002.
101. Jones, I. and Johnson, M. I. (2009) 'Transcutaneous electrical nerve stimulation', *Continuing Education in Anaesthesia, Critical Care and Pain*, 9(4), pp. 130–135. doi: 10.1093/bjaceaccp/mkp021.
102. Kahar, S. N. S. *et al.* (2021) 'W/O Emulsions: Formulation, Characterization and Destabilization', *Malaysian Applied Biology*, 50(1), pp. 169–179. doi: 10.55230/mabjournal.v50i1.1505.
103. Kang, C. *et al.* (2020) 'Acid-activatable polymeric curcumin nanoparticles as therapeutic agents for osteoarthritis', *Nanomedicine: Nanotechnology, Biology, and Medicine*. Elsevier Inc., 23, p. 102104. doi: 10.1016/j.nano.2019.102104.
104. Kaplan, W. and Laing, R. (2004) 'Priority medicines for Europe and the world', *World Health Organization, Department of Essential Drugs and Medicines Policy*, (November), pp. 1–134. doi: <http://www.who.int/iris/handle/10665/68769>.
105. Kapoor, M. *et al.* (2011) 'Role of proinflammatory cytokines in the pathophysiology of osteoarthritis', *Nature Reviews Rheumatology*. doi: 10.1038/nrrheum.2010.196.
106. Kar, S. *et al.* (2016) 'Systems based study of the therapeutic potential of small charged molecules for the inhibition of IL-1 mediated cartilage degradation', *PLoS ONE*, 11(12), pp. 1–38. doi: 10.1371/journal.pone.0168047.
107. Karlsson, J. *et al.* (2021) 'and opportunities', 17(10), pp. 1395–1410. doi: 10.1080/17425247.2020.1796628.Poly).
108. Kidd, B. (2012) 'Mechanisms of Pain in Osteoarthritis', *HSS Journal*, 8(1), pp. 26–28. doi: 10.1007/s11420-011-9263-7.
109. Kim, J., Sunshine, J. C. and Green, J. J. (2014) 'Differential polymer structure tunes mechanism of cellular uptake and transfection routes of poly( $\beta$ -amino ester) polyplexes in human breast cancer cells', *Bioconjugate Chemistry*, 25(1), pp. 43–51. doi: 10.1021/bc4002322.
110. de Klerk, B. M. *et al.* (2009) 'No clear association between female hormonal aspects and osteoarthritis of the hand, hip and knee: A systematic review', *Rheumatology*. doi: 10.1093/rheumatology/kep194.
111. Kürti, L. *et al.* (2013) 'In vitro and in vivo characterization of meloxicam nanoparticles designed for nasal administration', *European Journal of Pharmaceutical Sciences*. doi: 10.1016/j.ejps.2013.03.012.
112. Kurtz, S. L. and Lawson, L. B. (2019) 'Nanoemulsions Enhance in vitro Transpapillary Diffusion of Model Fluorescent Dye Nile Red', *Scientific Reports*. Springer US, 9(1), pp. 1–11. doi: 10.1038/s41598-019-48144-x.
113. Kuyinu, E. L. *et al.* (2016) 'Animal models of osteoarthritis: Classification, update, and measurement of outcomes', *Journal of Orthopaedic Surgery and Research*. Journal of Orthopaedic Surgery and Research, 11(1), pp. 1–27. doi: 10.1186/s13018-016-0346-5.
114. Li, H. (2003) 'Dithiothreitol (Cleland's Reagent)', *Free Radicals in Biology and Medicine*, 77, pp. 0–11. Available at: <http://www.healthcare.uiowa.edu/CoreFacilities/esr/education/2003/5/ZimmermanMC-paper-5.pdf>.
115. Liggins, R. T. *et al.* (2004) 'Intra-articular treatment of arthritis with microsphere formulations of paclitaxel: Biocompatibility and efficacy determinations in rabbits',

- Inflammation Research*. doi: 10.1007/s00011-004-1273-1.
116. Lim, Y. B., Choi, Y. H. and Park, J. S. (1999) 'A self-destroying polycationic polymer: Biodegradable poly(4-hydroxy-L- proline ester)', *Journal of the American Chemical Society*, 121(24), pp. 5633–5639. doi: 10.1021/ja984012k.
  117. Liming Bian *et al.* (2010) 'Effects of dexamethasone on the functional properties of cartilage explants during long-term culture', *American Journal of Sports Medicine*, 38(1), pp. 78–85. doi: 10.1177/0363546509354197.
  118. Lindsley, C. W. (2014) 'Lipophilicity', *Encyclopedia of Psychopharmacology*, pp. 6–11. doi: 10.1007/978-3-642-27772-6.
  119. Lippiello, L. (1981) 'Prostaglandins and articular cartilage metabolism: Does prostaglandin perturbation perpetuate cartilage destruction?', *Seminars in Arthritis and Rheumatism*, 11(1 SUPPL. 1), pp. 87–88. doi: 10.1016/0049-0172(81)90053-6.
  120. Liu, Y. *et al.* (2019) 'Poly( $\beta$ -Amino Esters): Synthesis, Formulations, and Their Biomedical Applications', *Advanced healthcare materials*, 8(1801359).
  121. Loef, M. *et al.* (2019) 'Fatty acids and osteoarthritis: different types, different effects', *Joint Bone Spine*. Elsevier Masson SAS, 86(4), pp. 451–458. doi: 10.1016/j.jbspin.2018.07.005.
  122. Lotz, M. K. (2010) 'New developments in osteoarthritis. Posttraumatic osteoarthritis: Pathogenesis and pharmacological treatment options', *Arthritis Research and Therapy*, 12(3). doi: 10.1186/ar3046.
  123. Lozano, R. *et al.* (2010) 'Global and regional mortality from 235 causes of death for 20 age groups in 1990 and 2010 : a systematic analysis for the Global Burden of Disease Study 2010', *Lancet*, 380(9859), pp. 2095–2128. doi: 10.1016/S0140-6736(12)61728-0.
  124. Lu, Y. C. S., Evans, C. H. and Grodzinsky, A. J. (2011) 'Effects of short-term glucocorticoid treatment on changes in cartilage matrix degradation and chondrocyte gene expression induced by mechanical injury and inflammatory cytokines', *Arthritis Research and Therapy*. doi: 10.1186/ar3456.
  125. Luyten, F. P. and Vanlauwe, J. (2012) 'Tissue engineering approaches for osteoarthritis', *Bone*. Elsevier Inc., 51(2), pp. 289–296. doi: 10.1016/j.bone.2011.10.007.
  126. Lynn, D. M. and Langer, R. (2000) 'Degradable poly( $\beta$ -amino esters): Synthesis, characterization, and self-assembly with plasmid DNA', *Journal of the American Chemical Society*, 122(44), pp. 10761–10768. doi: 10.1021/ja0015388.
  127. Maeda, T. *et al.* (2017) 'Does transcutaneous electrical nerve stimulation (TENS) simultaneously combined with local heat and cold applications enhance pain relief compared with TENS alone in patients with knee osteoarthritis?', *Journal of Physical Therapy Science*, 29(10), pp. 1860–1864. doi: 10.1589/jpts.29.1860.
  128. Manjanna, K. M., Shivakumar, B. and Kumar, T. M. P. (2010) 'Microencapsulation: An Acclaimed Novel Drug-Delivery System for NSAIDs in Arthritis', *Critical Reviews in Therapeutic Drug Carrier Systems*. doi: 10.1615/CritRevTherDrugCarrierSyst.v27.i6.20.
  129. Mankin, H. J. . *et al.* (1971) 'Biochemical and Metabolic Abnormalities in Articular Cartilage from Osteo-Arthritic Human Hips II. CORRELATION OF MORPHOLOGY WITH BIOCHEMICAL AND METABOLIC DATA', *The Journal of Bone & Joint Surgery*, 53(3), pp. 523–537.
  130. Mao, W. *et al.* (2011) 'Perfusion-cultured bovine anterior segments as an ex vivo model for studying glucocorticoid-induced ocular hypertension and glaucoma', *Investigative Ophthalmology and Visual Science*. doi: 10.1167/iovs.11-8133.
  131. Maradit Kremers, H. *et al.* (2015) 'Prevalence of Total Hip and Knee Replacement in the United States.', *The Journal of bone and joint surgery. American volume*, 97(17), pp. 1386–97. doi: 10.2106/JBJS.N.01141.
  132. Marcacci, M. *et al.* (2005) 'Articular cartilage engineering with Hyalograft® C: 3-Year clinical results', in *Clinical Orthopaedics and Related Research*. doi: 10.1097/01.blo.0000165737.87628.5b.

133. Mathiessen, A. and Conaghan, P. G. (2017) 'Synovitis in osteoarthritis: Current understanding with therapeutic implications', *Arthritis Research and Therapy*. doi: 10.1186/s13075-017-1229-9.
134. Maudens, P. *et al.* (2018) 'Nanocrystal–Polymer Particles: Extended Delivery Carriers for Osteoarthritis Treatment', *Small*, 14(8). doi: 10.1002/smll.201703108.
135. McAlindon, T. E. *et al.* (1996) 'Do antioxidant micronutrients protect against the development and progression of knee osteoarthritis?', *Arthritis and Rheumatism*, 39(4), pp. 648–656. doi: 10.1002/art.1780390417.
136. McAlindon, T. E. *et al.* (2014) 'OARSI guidelines for the non-surgical management of knee osteoarthritis', *Osteoarthritis and Cartilage*. Elsevier Ltd, 22(3), pp. 363–388. doi: 10.1016/j.joca.2014.01.003.
137. McAlindon, T. E. *et al.* (2017) 'Effect of Intra-articular Triamcinolone vs Saline on Knee Cartilage Volume and Pain in Patients With Knee Osteoarthritis: A Randomized Clinical Trial.', *JAMA*, 317(19), pp. 1967–1975. doi: 10.1001/jama.2017.5283.
138. McCoy, A. M. (2015) 'Animal Models of Osteoarthritis: Comparisons and Key Considerations', *Veterinary Pathology*, 52(5), pp. 803–818. doi: 10.1177/0300985815588611.
139. McIlwraith, C. W., Frisbie, D. D. and Kawcak, C. E. (2012) 'The horse as a model of naturally occurring osteoarthritis', *Bone & Joint Research*, 1(11), pp. 297–309. doi: 10.1302/2046-3758.111.2000132.
140. McLawhorn, A. S. and Buller, L. T. (2017) 'Bundled Payments in Total Joint Replacement: Keeping Our Care Affordable and High in Quality', *Current Reviews in Musculoskeletal Medicine*. doi: 10.1007/s12178-017-9423-6.
141. McNulty, A. L. *et al.* (2013) 'Synovial fluid concentrations and relative potency of interleukin-1 alpha and beta in cartilage and meniscus degradation', *Journal of Orthopaedic Research*, 31(7), pp. 1039–1045. doi: 10.1002/jor.22334.
142. Mehana, E. S. E., Khafaga, A. F. and El-Blehi, S. S. (2019) 'The role of matrix metalloproteinases in osteoarthritis pathogenesis: An updated review', *Life Sciences*. Elsevier, 234(June), p. 116786. doi: 10.1016/j.lfs.2019.116786.
143. Miceli-Richard, C. *et al.* (2004) 'Paracetamol in osteoarthritis of the knee', *Annals of the Rheumatic Diseases*. doi: 10.1136/ard.2003.017236.
144. Miguel, O. *et al.* (2012) 'Human Chondrocyte Cultures as Models of Cartilage-Specific Gene Regulation', in *human cell culture protocols*. springer protocols, pp. 302–336.
145. Mobasheri, A. and Batt, M. (2016) 'An update on the pathophysiology of osteoarthritis', *Annals of Physical and Rehabilitation Medicine*. Elsevier Masson SAS, 59(5–6), pp. 333–339. doi: 10.1016/j.rehab.2016.07.004.
146. Molecular-Probes (2005) 'LIVE/DEAD Viability/Cytotoxicity Kit for mammalian cells. Product Information.', p. 7. Available at: <https://tools.thermofisher.com/content/sfs/manuals/mp03224.pdf>.
147. Moody, H. R. *et al.* (2006) 'In vitro degradation of articular cartilage: Does trypsin treatment produce consistent results?', *Journal of Anatomy*, 209(2), pp. 259–267. doi: 10.1111/j.1469-7580.2006.00605.x.
148. Moore, N. *et al.* (2016) 'Does paracetamol still have a future in osteoarthritis?', *The Lancet*, pp. 2065–2066. doi: 10.1016/S0140-6736(15)01170-8.
149. Muller, D. (2018) 'Rheumatoid Arthritis', *Integrative Medicine*, pp. 493-500.e1. doi: 10.1016/B978-0-323-35868-2.00049-9.
150. Narayanan, D. *et al.* (2013) 'Poly-(ethylene glycol) modified gelatin nanoparticles for sustained delivery of the anti-inflammatory drug Ibuprofen-Sodium: An in vitro and in vivo analysis', *Nanomedicine: Nanotechnology, Biology, and Medicine*. doi: 10.1016/j.nano.2013.02.001.
151. National Clinical Guideline Centre (UK). (2014) 'Osteoarthritis: Care and Management in Adults.', *NICE Clinical Guidelines, No. 177*, (February), pp. 104–148. doi:

- nice.org.uk/guidance/cg177.
152. Nazila, K. *et al.* (2016) ‘Degradable Controlled-Release Polymers and Polymeric Nanoparticles: Mechanisms of Controlling Drug Release’, *Chem Rev.*, 116(4), pp. 2602–2663. doi: 10.1021/acs.chemrev.5b00346.Degradable.
  153. Neil, K. M., Caron, J. P. and Orth, M. W. (2005) ‘The role of glucosamine and chondroitin sulfate in treatment for and prevention of osteoarthritis in animals’, *Journal of the American Veterinary Medical Association*. doi: 10.2460/javma.2005.226.1079.
  154. Nia, H. T. *et al.* (2015) ‘High-bandwidth AFM-based rheology is a sensitive indicator of early cartilage aggrecan degradation relevant to mouse models of osteoarthritis’, *Journal of Biomechanics*. doi: 10.1016/j.jbiomech.2014.11.012.
  155. O’Neil, M. J. (2013) *The Merck Index - An Encyclopedia of Chemicals, Drugs, and Biologicals*, Royal Society of Chemistry. doi: 10.1007/s13398-014-0173-7.2.
  156. Osiri, M. *et al.* (2009) ‘Transcutaneous electrical nerve stimulation for knee osteoarthritis ( Review )’, (4).
  157. Palazzo, C. *et al.* (2016) ‘Risk factors and burden of osteoarthritis’, *Annals of Physical and Rehabilitation Medicine*, 59(3), pp. 134–138. doi: 10.1016/j.rehab.2016.01.006.
  158. Patrignani, P. *et al.* (2011) ‘Managing the adverse effects of nonsteroidal anti-inflammatory drugs’, *Expert Review of Clinical Pharmacology*. doi: 10.1586/ecp.11.36.
  159. Patterson-Kane, J. C. and Firth, E. C. (2014) ‘Tendon, ligament, bone, and cartilage: Anatomy, physiology, and adaptations to exercise and training’, *The Athletic Horse: Principles and Practice of Equine Sports Medicine: Second Edition*, pp. 202–242. doi: 10.1016/B978-0-7216-0075-8.00022-8.
  160. Pelletier, J. P. *et al.* (2016) ‘Efficacy and safety of oral NSAIDs and analgesics in the management of osteoarthritis: Evidence from real-life setting trials and surveys’, *Seminars in Arthritis and Rheumatism*, 45(4), pp. S22–S27. doi: 10.1016/j.semarthrit.2015.11.009.
  161. Pelletier, J. P., Martel-Pelletier, J. and Abramson, S. B. (2001) ‘Osteoarthritis, an inflammatory disease: Potential implication for the selection of new therapeutic targets’, *Arthritis and Rheumatism*. doi: 10.1002/1529-0131(200106)44:6<1237::AID-ART214>3.0.CO;2-F.
  162. Pérez-Martínez, P. I. *et al.* (2016) ‘Dietary fatty acids for the treatment of OA, including fish oil’, *Annals of the Rheumatic Diseases*, 12(1), pp. 1–2. doi: 10.4236/mri.2016.53004.
  163. Perkins, C., Whiting, B. and Lee, P. Y. (2017) ‘Steroids and Osteoarthritis’, *Journal of Arthritis*, 06(03). doi: 10.4172/2167-7921.1000e115.
  164. Perni, S. and Prokopovich, P. (2017) ‘Poly-beta-amino-esters nano-vehicles based drug delivery system for cartilage’, *Nanomedicine: Nanotechnology, Biology, and Medicine*. The Authors, 13(2), pp. 539–548. doi: 10.1016/j.nano.2016.10.001.
  165. Poon, C. (2022) ‘Measuring the density and viscosity of culture media for optimized computational fluid dynamics analysis of in vitro devices’, *Journal of the Mechanical Behavior of Biomedical Materials*, 126(i). doi: 10.1016/j.jmbbm.2021.105024.
  166. Pratta, M. A. *et al.* (2003) ‘Aggrecan Protects Cartilage Collagen from Proteolytic Cleavage’, *Journal of Biological Chemistry*, 278(46), pp. 45539–45545. doi: 10.1074/jbc.M303737200.
  167. Proffen, B. *et al.* (2013) ‘Surgical management of osteoarthritis’, *Wiener Medizinische Wochenschrift*, 163(9–10), pp. 243–250. doi: 10.1007/s10354-013-0199-z.
  168. Punzi, L. *et al.* (2016) ‘Post-traumatic arthritis: Overview on pathogenic mechanisms and role of inflammation’, *RMD Open*, 2(2), pp. 1–9. doi: 10.1136/rmdopen-2016-000279.
  169. Van Raaij, T. M. *et al.* (2010) ‘Medial knee osteoarthritis treated by insoles or braces a randomized trial’, *Clinical Orthopaedics and Related Research*, 468(7), pp. 1926–1932. doi: 10.1007/s11999-010-1274-z.
  170. Radin, E. L. and Paul, I. L. (1970) ‘Does cartilage compliance reduce skeletal impact loads?. the relative force-attenuating properties of articular cartilage, synovial fluid,

- periarticular soft tissues and bone', *Arthritis & Rheumatism*, 13(2), pp. 139–144. doi: 10.1002/art.1780130206.
171. Rajaei, E. *et al.* (2015) 'The Effect of Omega-3 Fatty Acids in Patients With Active Rheumatoid Arthritis Receiving DMARDs Therapy: Double-Blind Randomized Controlled Trial', *Global Journal of Health Science*. doi: 10.5539/gjhs.v8n7p18.
  172. Rang, H. *et al.* (2012) *Pharmacology, Rang and Dale's Pharmacology*. Available at: <http://scholar.google.com/scholar?hl=en&btnG=Search&q=intitle:Rang+and+Dale+Pharmacology#1>.
  173. Rannou, F., Pelletier, J. P. and Martel-Pelletier, J. (2016) 'Efficacy and safety of topical NSAIDs in the management of osteoarthritis: Evidence from real-life setting trials and surveys', *Seminars in Arthritis and Rheumatism*, 45(4), pp. S18–S21. doi: 10.1016/j.semarthrit.2015.11.007.
  174. Raynauld, J. P. *et al.* (2009) 'Protective effects of licofelone, a 5-lipoxygenase and cyclo-oxygenase inhibitor, versus naproxen on cartilage loss in knee osteoarthritis: A first multicentre clinical trial using quantitative MRI', *Annals of the Rheumatic Diseases*. doi: 10.1136/ard.2008.088732.
  175. Reinmüller, J. (2003) 'Hyaluronic acid', *Aesthetic Surgery Journal*. doi: 10.1016/S1090-820X(03)00158-4.
  176. Remaut, K. (2019) 'Ex vivo bovine retinal models to study intravitreal mobility and inner limiting membrane penetration of nanomedicines', *Acta Ophthalmologica*. doi: 10.1111/j.1755-3768.2019.8309.
  177. Rivera-Delgado, E. *et al.* (2018) 'Injectable liquid polymers with extended delivery of corticosteroids for the treatment of osteoarthritis', *Journal of Controlled Release*. Elsevier, 284(May), pp. 112–121. doi: 10.1016/j.jconrel.2018.05.037.
  178. Robert, H. (2011) 'Chondral repair of the knee joint using mosaicplasty', *Orthopaedics and Traumatology: Surgery and Research*. doi: 10.1016/j.otsr.2011.04.001.
  179. Roberts, E. *et al.* (2016) 'Paracetamol: Not as safe as we thought? A systematic literature review of observational studies', *Annals of the Rheumatic Diseases*, 75(3), pp. 552–559. doi: 10.1136/annrheumdis-2014-206914.
  180. Roddy, E., Zhang, W. and Doherty, M. (2005) 'Aerobic walking or strengthening exercise for osteoarthritis of the knee? A systematic review', *Annals of the Rheumatic Diseases*, pp. 544–548. doi: 10.1136/ard.2004.028746.
  181. Rodrigo, M., Jofré, C. M. and Minguell, J. J. (2015) 'Cell Therapy and Tissue Engineering Approaches for Cartilage Repair and/or Regeneration', *International Journal of Stem Cells*, 8(1).
  182. Rosenberger, R. E. *et al.* (2008) 'Repair of large chondral defects of the knee with autologous chondrocyte implantation in patients 45 years or older', *American Journal of Sports Medicine*. doi: 10.1177/0363546508322888.
  183. Rumin, J. *et al.* (2015) 'The use of fluorescent Nile red and BODIPY for lipid measurement in microalgae', *Biotechnology for Biofuels*, 8(1), pp. 1–16. doi: 10.1186/s13068-015-0220-4.
  184. Rutjes, A. W. *et al.* (2009) 'Transcutaneous electrostimulation for osteoarthritis of the knee', *Cochrane Database of Systematic Reviews*, (4). doi: 10.1002/14651858.CD002823.pub2.
  185. Saedi, T. and Prokopovich, P. (2021) 'Poly beta amino ester coated emulsions of NSAIDs for cartilage treatment', *Journal of Materials Chemistry B*. doi: 10.1039/d1tb01024g.
  186. Saleh, N. *et al.* (2005) 'Oil-in-water emulsions stabilized by highly charged polyelectrolyte-grafted silica nanoparticles', *Langmuir*, 21(22), pp. 9873–9878. doi: 10.1021/la050654r.
  187. Sales-Campos, H. *et al.* (2013) 'An Overview of the Modulatory Effects of Oleic Acid in Health and Disease', *Mini-Reviews in Medicinal Chemistry*. doi: 10.2174/1389557511313020003.

188. Salgado, C., Jordan, O. and Allémann, E. (2021) 'Osteoarthritis in vitro models: Applications and implications in development of intra-articular drug delivery systems', *Pharmaceutics*, 13(1), pp. 1–23. doi: 10.3390/pharmaceutics13010060.
189. Samimi, S. *et al.* (2018) *Lipid-Based Nanoparticles for Drug Delivery Systems, Characterization and Biology of Nanomaterials for Drug Delivery: Nanoscience and Nanotechnology in Drug Delivery*. Elsevier Inc. doi: 10.1016/B978-0-12-814031-4.00003-9.
190. Samvelyan, H. J. *et al.* (2021) 'Models of Osteoarthritis: Relevance and New Insights', *Calcified Tissue International*. Springer US, 109(3), pp. 243–256. doi: 10.1007/s00223-020-00670-x.
191. Sarker, D. (2005) 'Engineering of Nanoemulsions for Drug Delivery', *Current Drug Delivery*, 2(4), pp. 297–310. doi: 10.2174/156720105774370267.
192. Saunders (2003) *arthritis - definition of arthritis in the Medical dictionary - by the Free Online Medical Dictionary, Thesaurus and Encyclopedia., Miller-Keane Encyclopedia and Dictionary of Medicine, Nursing, and Allied Health, Seventh Edition*.
193. Schrock, J. B. *et al.* (2017) 'A cost-effectiveness analysis of surgical treatment modalities for chondral lesions of the knee: Microfracture, osteochondral autograft transplantation, and autologous chondrocyte implantation', *Orthopaedic Journal of Sports Medicine*. doi: 10.1177/2325967117704634.
194. Sellam, J. and Berenbaum, F. (2010) 'The role of synovitis in pathophysiology and clinical symptoms of osteoarthritis', *Nature Reviews Rheumatology*, 6, pp. 625–635. doi: <https://doi.org/10.1038/nrrheum.2010.159>.
195. Sharma, L. and Berenbaum, F. (2007) *Osteoarthritis Year in Review 2015: Clinical*. First edit. Edited by D. LeMelledo. Kim Murphy.
196. Shen, J., Li, S. and Chen, D. (2014) 'TGF- $\beta$  signaling and the development of osteoarthritis', *Bone Research*. doi: 10.1038/boneres.2014.2.
197. Shuid, A. N. *et al.* (2013) 'Drug delivery systems for prevention and treatment of osteoporotic fracture.', *Current drug targets*, 14(13), pp. 1558–64. doi: 10.2174/1389450114666131108153905.
198. Silva, J. C. *et al.* (2019) 'Compositional and structural analysis of glycosaminoglycans in cell-derived extracellular matrices', *Glycoconjugate Journal*, 36(2), pp. 141–154. doi: 10.1007/s10719-019-09858-2.Compositional.
199. Solheim, E. *et al.* (2013) 'Results at 10 to 14years after osteochondral autografting (mosaicplasty) in articular cartilage defects in the knee', *Knee*. doi: 10.1016/j.knee.2013.01.001.
200. Sophia Fox, A. J., Bedi, A. and Rodeo, S. A. (2009) 'The Basic Science of Articular Cartilage: Structure, Composition, and Function', *Sports Health: A Multidisciplinary Approach*, 1(6), pp. 461–468. doi: 10.1177/1941738109350438.
201. Soussan, E. *et al.* (2009) 'Drug delivery by soft matter: Matrix and vesicular carriers', *Angewandte Chemie - International Edition*, 48(2), pp. 274–288. doi: 10.1002/anie.200802453.
202. Steintraesser, L. *et al.* (2010) 'A novel human skin chamber model to study wound infection ex vivo', *Archives of Dermatological Research*. doi: 10.1007/s00403-009-1009-8.
203. Stoddart, M. *et al.* (2009) 'Cells and biomaterials in cartilage tissue engineering', *Regenerative Medicine*, pp. 81–98. doi: 10.2217/17460751.4.1.81.
204. Storer, A. C. and Ménard, R. (2013) 'Chapter 419 - Papain', in *Handbook of Proteolytic Enzymes*, pp. 1858–1861. doi: <http://dx.doi.org/10.1016/B978-0-12-382219-2.00418-X>.
205. Stott, A. (2017) 'Hyaluronic Acid and Other Conservative Treatment Options for Osteoarthritis of the Ankle', *Orthopaedic Nursing*, pp. 361–362. doi: 10.1097/NOR.0000000000000384.
206. Swain, S. *et al.* (2020) 'Trends in incidence and prevalence of osteoarthritis in the United Kingdom: findings from the Clinical Practice Research Datalink (CPRD)',

- Osteoarthritis and Cartilage*. Elsevier Ltd, 28(6), pp. 792–801. doi: 10.1016/j.joca.2020.03.004.
207. Szczepanowicz, K. *et al.* (2010) ‘Formation of biocompatible nanocapsules with emulsion core and pegylated shell by polyelectrolyte multilayer adsorption’, *Langmuir*, 26(15), pp. 12592–12597. doi: 10.1021/la102061s.
  208. Sze, A. *et al.* (2003) ‘Zeta-potential measurement using the Smoluchowski equation and the slope of the current-time relationship in electroosmotic flow’, *Journal of Colloid and Interface Science*, 261(2), pp. 402–410. doi: 10.1016/S0021-9797(03)00142-5.
  209. T.R., S. *et al.* (2016) ‘INTRA-ARTICULAR DRUG DELIVERY SYSTEMS FOR ARTHRITIC DISEASES: OVERCOMING THE INADEQUACIES OF THERAPY’, *Indo American journal of Pharmaceutical Research*, 6(02).
  210. Tadros, T. (2004) *Application of rheology for assessment and prediction of the long-term physical stability of emulsions*, *Advances in Colloid and Interface Science*. doi: 10.1016/j.cis.2003.10.025.
  211. Takada, Y. *et al.* (2004) ‘Nonsteroidal anti-inflammatory agents differ in their ability to suppress NF- $\kappa$ B activation, inhibition of expression of cyclooxygenase-2 and cyclin D1, and abrogation of tumor cell proliferation’, *Oncogene*. doi: 10.1038/sj.onc.1208169.
  212. Tannenbaum, J. and Bennett, B. T. (2015) ‘Russell and Burch’s 3Rs then and now: The need for clarity in definition and purpose’, *Journal of the American Association for Laboratory Animal Science*, 54(2), pp. 120–132.
  213. Al Thaher, Y. *et al.* (2018) ‘Role of poly-beta-amino-esters hydrolysis and electrostatic attraction in gentamicin release from layer-by-layer coatings’, *Journal of Colloid and Interface Science*, 526, pp. 35–42. doi: 10.1016/j.jcis.2018.04.042.
  214. Thorat, B. and Jangle, R. (2013) ‘Reversed-phase High-performance Liquid Chromatography Method for Analysis of Curcuminoids and Curcuminoid-loaded Liposome Formulation’, *Indian Journal of Pharmaceutical Sciences*. doi: 10.4103/0250-474X.113555.
  215. Tonge, P. J. (2018) ‘Drug-Target Kinetics in Drug Discovery’, *ACS Chemical Neuroscience*. doi: 10.1021/acschemneuro.7b00185.
  216. Torjesen, I. (2016) ‘Paracetamol ineffective in treating osteoarthritis, meta-analysis finds’, *The Pharmaceutical Journal*, 296(7887). Available at: <https://www.pharmaceutical-journal.com/news-and-analysis/paracetamol-ineffective-in-treating-osteoarthritis-meta-analysis-finds/20200897.article?firstPass=false>.
  217. Tunçay, M. *et al.* (2000) ‘In vitro and in vivo evaluation of diclofenac sodium loaded albumin microspheres’, *Journal of Microencapsulation*. doi: 10.1080/026520400288382.
  218. Vasiliadis, H. S. and Tsikopoulos, K. (2017) ‘Glucosamine and chondroitin for the treatment of osteoarthritis’, *World Journal of Orthopedics*, 8(1), p. 1. doi: 10.5312/wjo.v8.i1.1.
  219. Vignon, E. *et al.* (2003) ‘Measurement of radiographic joint space width in the tibiofemoral compartment of the osteoarthritic knee: Comparison of standing anteroposterior and Lyon schuss views’, *Arthritis and Rheumatism*, 48(2), pp. 378–384. doi: 10.1002/art.10773.
  220. Wajid, M. A. *et al.* (2011) ‘Osteochondral grafting of knee joint using mosaicplasty’, *Journal of the College of Physicians and Surgeons Pakistan*. doi: 10.2011/JCPSP.184186.
  221. Wang, B. *et al.* (2021) ‘Metabolism pathways of arachidonic acids: mechanisms and potential therapeutic targets’, *Signal Transduction and Targeted Therapy*. Springer US, 6(1). doi: 10.1038/s41392-020-00443-w.
  222. Wang, M. L. and Peng, Z. X. (2015) ‘Wear in human knees’, *Biosurface and Biotribology*. doi: 10.1016/j.bsbt.2015.06.003.
  223. Warren, S. (2000) *A critical analysis of the 1,9-dimethylene blue assay for sulfated glycosaminoglycans in synovial fluid*. doi: 10.1002/publication/uuid/C195AF85-7730-48E8-A899-73EF32E64685.
  224. Wehling, P. *et al.* (2017) ‘Effectiveness of intra-articular therapies in osteoarthritis: a

- literature review', *Therapeutic Advances in Musculoskeletal Disease*, pp. 183–196. doi: 10.1177/1759720X17712695.
225. Weil, Y. *et al.* (2012) 'Chondrogenic differentiation of induced pluripotent stem cells from osteoarthritic chondrocytes in alginate matrix', *European Cells and Materials*. doi: 10.22203/eCM.v023a01.
226. Wernecke, C., Braun, H. J. and Dragoo, J. L. (2015) 'The effect of intra-articular corticosteroids on articular cartilage: A systematic review', *Orthopaedic Journal of Sports Medicine*, 3(5), pp. 1–7. doi: 10.1177/2325967115581163.
227. WHO (2013) 'Osteoarthritis', *World Health*, 12(Osteoarthritis in Priority Medicines for Europe and the World 2013 Update), pp. 6–8. Available at: [http://www.who.int/medicines/areas/priority\\_medicines/Ch6\\_12Osteo.pdf?ua=1](http://www.who.int/medicines/areas/priority_medicines/Ch6_12Osteo.pdf?ua=1).
228. Wojdasiewicz, P., Poniatowski, Ł. A. and Szukiewicz, D. (2014) 'The role of inflammatory and anti-inflammatory cytokines in the pathogenesis of osteoarthritis', *Mediators of Inflammation*. doi: 10.1155/2014/561459.
229. Wolf, K. and Gilbert, P. A. (1992) 'EDTA-ethylenediaminetetraacetic acid', in *Handbook of Environmental Chemistry*, pp. 243–259. doi: 10.1007/978-3-540-47108-0-7.
230. Wu, B. (2018) 'The stages of osteoarthritis of the knee', *medical news today*. Available at: <https://www.medicalnewstoday.com/kc/stages-osteoarthritis-knee-310579>.
231. Yoo, H. J. *et al.* (2011) 'Contrast-enhanced CT of Articular Cartilage: Experimental Study for Quantification of Glycosaminoglycan Content in Articular Cartilage', *Radiology*, 261(3), pp. 805–812. doi: 10.1148/radiol.11102495.
232. Zachwieja, E., Perez, J. and M, S. (2017) 'Hip and Knee Arthroplasty in Osteoarthritis', *Current Treatment Options in Rheumatology*, 3(2), pp. 75–87. doi: <http://dx.doi.org/10.1007/s40674-017-0063-1>.
233. Zeng, C. *et al.* (2015) 'Effectiveness and safety of Glucosamine, chondroitin, the two in combination, or celecoxib in the treatment of osteoarthritis of the knee', *Scientific Reports*. Nature Publishing Group, 5(August), pp. 1–10. doi: 10.1038/srep16827.
234. Zhang, L., Hu, J. and Athanasiou, K. A. (2009) 'The role of tissue engineering in articular cartilage repair and regeneration.', *Critical reviews in biomedical engineering*, 37(1–2), pp. 1–57. doi: 10.1126/scisignal.3104re1.Basal.
235. Zhang, W. *et al.* (2016) 'Current research on pharmacologic and regenerative therapies for osteoarthritis', *Bone Research*. doi: 10.1038/boneres.2015.40.
236. Zheng, C. H. and Levenston, M. . (2015) 'Fact versus artifact: Avoiding erroneous estimates of sulfated glycosaminoglycan content using the dimethylmethylene blue colorimetric assay for tissue-engineered constructs', *European Cells and Materials*, 29, pp. 224–236.